Physics of liquid crystals of bent-shaped molecules

Antal Jákli, Oleg D. Lavrentovich, and Jonathan V. Selinger

Department of Physics and Chemical Physics Interdisciplinary Program, Liquid Crystal Institute, Kent State University, Kent, Ohio 44242, USA

(published 20 November 2018)

Thermotropic liquid crystals can be formed by various molecular shapes, some discovered over 125 years ago. The simplest and most-studied liquid crystals are made of rod-shaped molecules and led to today's omnipresent liquid crystal displays. While applied scientists and engineers have been perfecting liquid crystal displays, a large group of liquid crystal scientists have become excited about liquid crystals of bent-shaped (banana-shaped) molecules. These compounds were first reported 20 years ago and since then have taken center stage in current liquid crystal science. The "banana mania" is due to the fact that even a small kink in the molecular shape leads to fundamentally new properties and phases. This review summarizes the large variety of novel structures and physical properties and describes the underlying physics. The dependence of macroscopic properties on both the shape of the molecules and the flexibility of the central core is emphasized. Most rigid bent-core molecules form smectic and sometimes columnar structures; only a minority forms nematic phases. By contrast, most flexible bent-core molecules form nanostructured nematic phases, including the twist-bend nematic phase discovered very recently.

DOI: 10.1103/RevModPhys.90.045004

CONTENTS

I. INTRODUCTION

One of the main themes of liquid crystal science is the relationship between the microscopic shape of the molecules and the macroscopic symmetry of the phase. In some cases, the effects of molecular shape can be quite profound. For example, long rodlike (or *calamitic*) molecules can form a nematic phase with orientational order of the molecular axes, while shorter molecules form a disordered, isotropic fluid. Likewise, chiral molecules form a cholesteric phase, with a helical modulation of the molecular orientation, while similar achiral molecules form a uniform nematic phase. In other cases, the effects of molecular shape are much less important. For example, most nematic liquid crystals are formed by molecules that are not exactly rod shaped, but the details of molecular shape average out to give a uniaxial nematic phase.

Over the past two decades, many experimental and theoretical studies have investigated *bent-core liquid crystals*, i.e., liquid crystal phases formed of molecules with a bent

structure, resembling bananas. These studies have shown that the bent shape can indeed have important effects on the macroscopic physics of liquid crystal phases. When bent-core molecules form nematic phases, the molecular shape can produce polar or other order, in addition to the nematic order of the main molecular axes. Furthermore, the uniform nematic phase can become unstable to the formation of a modulated *twist-bend nematic phase*, with a heliconical variation in the molecular orientation, which has recently been recognized as a new type of orientationally ordered fluid. Similarly, when bent-core molecules form smectic layered phases, the molecular shape interacts with other order parameters (including the layer normal and tilt directions) to produce a wide range of phases. In both nematic and smectic cases, the phases can exhibit spontaneous chirality, even when the individual bent-core molecules are not chiral.

The purpose of this article is to review experimental and theoretical research on bent-core liquid crystals. In Sec. II we begin by discussing the theory of bent-core liquid crystals, particularly emphasizing the types of order that can arise as well as the coupling of these types of order to gradients in the main nematic director. Section III is devoted to the review of rigid bent-core molecules, which have been synthesized and investigated since the 1990s. We describe the experimental techniques that have been applied to these materials and the resulting evidence for polar and chiral order. In Sec. IV we move on to flexible bimesogens, which have only been studied more recently. We survey experiments on these liquid crystals and especially concentrate on the discovery and characterization of the twist-bend nematic phase. Finally, we make some conclusions and predictions about future progress.

Overall, the main theme of this review is that bent-core liquid crystals are remarkable materials, which exhibit an unusual variety of orientational, translational, and chiral order parameters. Because of this variety, they are ideal systems to study the interaction of different types of order. We expect that they will continue to give new insight into the fundamental physics of liquid crystals.

II. THEORY OF BENT-CORE LIQUID CRYSTALS

In the theory of bent-core liquid crystals, the key issue is whether bent-core molecules form liquid crystal phases with the same types of order as conventional rodlike molecules or whether they form phases with additional short-range or long-range order. We emphasize that bent-core molecules are *not required* to form phases with additional order. It is quite possible for bent-core molecules to have a random distribution of orientations about their long axes. In that case, on a statistical basis, their properties would be the same as conventional rodlike molecules. Even so, the bent shape of the molecules provides some tendency for the liquid crystal phase to form extra short-range or long-range order. In this section, we consider the types of extra order that can form in bent-core liquid crystals, and we discuss the consequences of such order.

In a conventional nematic phase, there is only one type of order: orientational order of the molecules along the local director $\hat{\boldsymbol{n}}$. This order can be represented by a second-rank, symmetric tensor order parameter. It tends to be uniform as a function of position, although it can vary due to surface anchoring or thermal fluctuations.

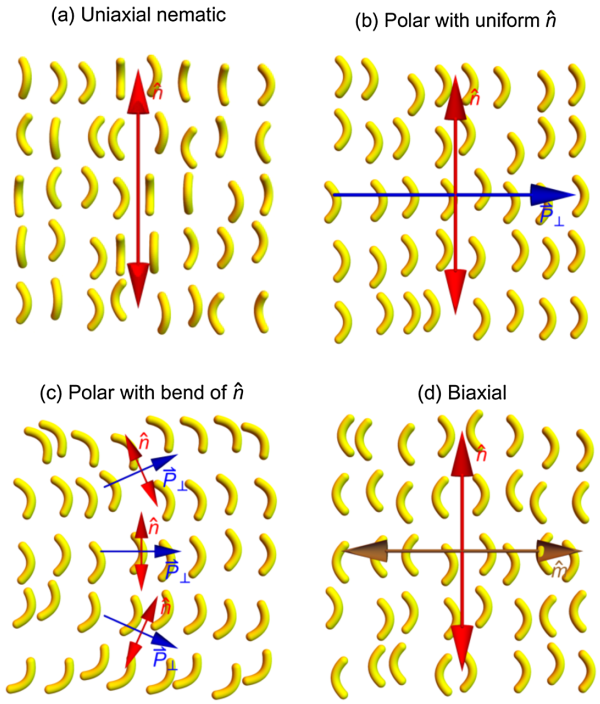

FIG. 1. Phases of bent-core liquid crystals. (a) Uniaxial nematic, (b) polar with uniform $\hat{\boldsymbol{n}}$, (c) polar with bend of $\hat{\boldsymbol{n}}$, and (d) biaxial.

For nematic phases formed by bent-core molecules, we must ask two important questions: First, is there any extra order of the molecules in addition to the primary nematic order parameter? Second, if there is any extra order, does it induce any spatial modulations of $\hat{\boldsymbol{n}}$?

Here we discuss several types of order that can occur in bent-core nematic phases and then consider modulated structures in more detail.

A. Types of order

1. Polar

A conventional uniaxial nematic phase of bent-core molecules is shown schematically in Fig. 1(a). In this structure, the long axes of the molecules are aligned along the local director $\hat{\boldsymbol{n}}$, and the transverse orientations of the molecules are random in the plane perpendicular to $\hat{\boldsymbol{n}}$. By contrast, a nematic phase with polar order is shown in Fig. 1(b). Here the transverse orientations have some net alignment in a specific direction in the plane perpendicular to $\hat{\boldsymbol{n}}$. This polar order can be described by a vector $\boldsymbol{P}_\perp$, the average of the transverse orientations, which is a vector perpendicular to $\hat{\boldsymbol{n}}$.

The concept of polar order in a nematic phase of bent-core molecules was first investigated by Meyer (1969) in the early history of liquid crystal physics. He pointed out that polar order $\boldsymbol{P}_\perp$ is coupled with bend in $\hat{\boldsymbol{n}}$, through a mechanism called the *bend flexoelectric effect*. A simple physical interpretation of this coupling is shown schematically in Fig. 1(c). If the nematic liquid crystal has a bend in $\hat{\boldsymbol{n}}$, this bend creates an anisotropic environment in the plane perpendicular to $\hat{\boldsymbol{n}}$,

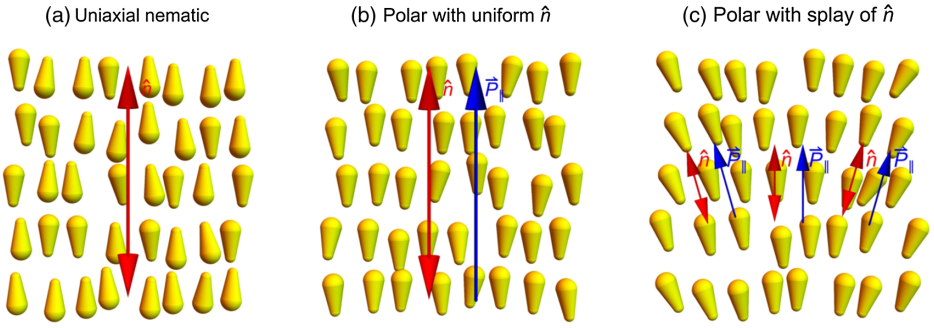

FIG. 2. Phases of pear-shaped liquid crystals. (a) Uniaxial nematic, (b) polar with uniform $\hat{\boldsymbol{n}}$, and (c) polar with splay of $\hat{\boldsymbol{n}}$.

with one special direction, and $\boldsymbol{P}_\perp$ tends to align in that direction. Conversely, if the nematic liquid crystal has polar order $\boldsymbol{P}_\perp$, the most efficient packing of the molecules does not have a uniform director, but rather has a specific bend.

The bend flexoelectric effect can occur in liquid crystals formed by molecules with any arbitrary shape. However, it is likely to be larger in systems of bent-core molecules, because it is highly compatible with the molecular shape.

In addition to polar order perpendicular to $\hat{\boldsymbol{n}}$, the early work of Meyer (1969) also investigated polar order parallel to $\hat{\boldsymbol{n}}$. This phenomenon is likely to occur in systems of pear-shaped molecules, not bent-core molecules, but we mention it here for completeness. In a conventional uniaxial nematic phase of pear-shaped molecules, shown in Fig. 2(a), half of the molecules point upward along $\hat{\boldsymbol{n}}$, and the other half point downward. By contrast, in a nematic phase with polar order, shown in Fig. 2(b), there is some population difference between molecules pointing upward and molecules pointing downward. This polar order can be described by a vector $\boldsymbol{P}_\parallel$ along the average of the pear-shaped molecular orientations, which is a vector parallel to $\hat{\boldsymbol{n}}$.

Polar order $\boldsymbol{P}_\parallel$ is coupled with splay in $\hat{\boldsymbol{n}}$ through a mechanism called the *splay flexoelectric effect*. A physical interpretation of this coupling is shown schematically in Fig. 2(c). If the nematic liquid crystal has a splay in $\hat{\boldsymbol{n}}$, this splay creates an asymmetry between the two directions upward and downward along $\hat{\boldsymbol{n}}$, and $\boldsymbol{P}_\parallel$ tends to align in the direction with lower free energy. Conversely, if the nematic liquid crystal has polar order $\boldsymbol{P}_\parallel$, the most efficient packing of the molecules does not have a uniform director, but rather has a specific splay.

In this discussion, we regard $\boldsymbol{P}_\perp$ and $\boldsymbol{P}_\parallel$ as dimensionless vectors that characterize the statistical order of the molecular orientations perpendicular and parallel to $\hat{\boldsymbol{n}}$, respectively. They are not necessarily components of the electrostatic polarization. However, if the individual molecules have electric dipole moments, then the statistical ordering of the molecular orientations will induce a macroscopic electrostatic polarization. As a result, the total electrostatic polarization arising from the combination of splay and bend effects becomes

$$\boldsymbol{P}_{\text{electrostatic}} = e_1\hat{\boldsymbol{n}}(\boldsymbol{\nabla}\cdot\hat{\boldsymbol{n}}) - e_3\hat{\boldsymbol{n}}\times\boldsymbol{\nabla}\times\hat{\boldsymbol{n}}, \tag{1}$$

where e_1 and e_3 are the splay and bend flexoelectric coefficients, respectively. Over the years, numerous theoretical studies have calculated e_1 and e_3 in specific model systems, beginning with the early work of Helfrich (1971a) and Derzhanski and Petrov (1971). Flexoelectricity in liquid crystals has been reviewed recently by Buka and Éber (2012).

2. Biaxial nematic

Another type of extra order, beyond the conventional uniaxial nematic order, is biaxial nematic. A biaxial nematic phase of bent-core molecules has the structure shown in Fig. 1(d). In this structure, the long axes of the molecules are aligned along the primary nematic director $\hat{\boldsymbol{n}}$, and the transverse directions are aligned back and forth along a secondary director $\hat{\boldsymbol{m}}$. In terms of symmetry, this phase is intermediate between the uniaxial nematic phase [Fig. 1(a)] and the polar phase [Fig. 1(b)]: It has less symmetry than the uniaxial nematic phase but more symmetry than the polar phase. For that reason, it cannot be characterized by a vector order parameter $\boldsymbol{P}$. Instead, it requires a second-rank tensor order parameter to represent the order along $\pm\hat{\boldsymbol{m}}$.

Unlike polar order, biaxial nematic order does not induce gradients in the primary director $\hat{\boldsymbol{n}}$. Physically, we can see this difference from the structure in Fig. 1(d). Even in the presence of biaxial nematic order, the system has no preference for bend in any single direction; bend does not improve the packing efficiency.

3. Octupolar (including tetrahedratic)

Beyond polar and nematic order, a liquid crystal phase of bent-core molecules may have more complex types of orientational order. The set of possible orientational order parameters was classified by Lubensky and Radzihovsky (2002). This classification can be understood as a multipole expansion: The lowest-order type of orientational order is polar (or dipolar) order, represented by a vector (or first-rank tensor) P_i. The next leading type of orientational order is nematic (or quadrupolar) order, represented by a second-rank tensor Q_{ij}. The expansion can continue to octupolar order, represented by a third-rank tensor T_{ijk}. If octupolar order exists by itself, with $P_i = 0$ and $Q_{ij} = 0$, it represents a *tetrahedratic* phase, i.e., a fluid phase with tetrahedral symmetry. Just as a nematic phase has two special directions $\hat{\boldsymbol{n}}$ and $-\hat{\boldsymbol{n}}$, which are equivalent to each other, a tetrahedratic phase has four special directions equivalent to each other. If octupolar order exists together with dipolar or quadrupolar order, it represents a more complex distorted phase. Lubensky and Radzihovsky

(2002) categorized these distorted phases and showed the range of possible phase transitions among them.

It is interesting to consider the optical consequences of octupolar order. In a tetrahedratic phase, because there is no quadrupolar order $Q_{ij} = 0$, the dielectric tensor ϵ_{ij} must be proportional to the identity matrix δ_{ij}. For that reason, a tetrahedratic phase appears optically isotropic, although it is not really isotropic but rather has an orientational order that is more difficult to observe. If one applies an electric field to a tetrahedratic phase, it induces quadrupolar order $Q_{ij} \sim T_{ijk}E_k$, and hence the material becomes optically anisotropic. Hence, one experimental signature of a tetrahedratic phase would be optical anisotropy that is linearly proportional to the applied field (Brand, Pleiner, and Cladis, 2005; Brand and Pleiner, 2010).

If a material has octupolar order in addition to nematic order, the octupolar order parameter T_{ijk} should be coupled with gradients in the director $\hat{\boldsymbol{n}}$ of the form $n_i\partial_j n_k$, through a generalized flexoelectric effect. In particular, octupolar order should favor director gradients, and any imposed director gradients should induce octupolar order. We are not aware of any simple visualization of this coupling.

4. Chiral

One special feature of the combination of order parameters in bent-core liquid crystals is *chiral symmetry breaking*. Even if the individual bent-core molecules are not chiral, the arrangement of the molecules can become spontaneously chiral. The chirality can be either right or left handed, or the system can form domains of right- and left-handed chirality. Mathematically, the spontaneous chirality can be understood through the theory of Lubensky and Radzihovsky (2002) as a combination of quadrupolar and octupolar order parameters. Physically, it can be visualized through the argument of Longa, Pająk, and Wydro (2009) illustrated in Figs. 3(a) and 3(b). In this structure, pairs of bent-core molecules come together, with an oblique angle between the molecular planes to form a chiral dimer. In particular, the dimers in Figs. 3(a) and 3(b) are mirror images of each other, which cannot be superimposed on each other through any proper rotations or translations.

The chiral order parameter is usually expressed as a pseudoscalar ψ [although an interesting alternative formalism, based on a second-rank pseudotensor, was proposed by Efrati and Irvine (2014)]. The pseudoscalar ψ couples with twist of the director field. Physically, this coupling can be understood because one handedness of a dimer is more compatible with one handedness of the twisted environment, compared with the mirror-image dimer.

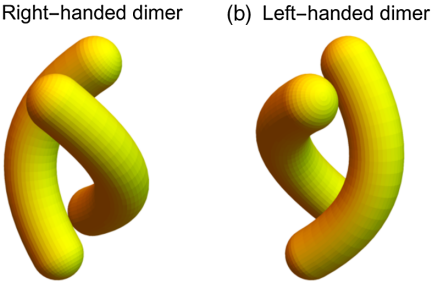

FIG. 3. Chiral symmetry breaking in the formation of right- and left-handed dimers of bent-core molecules. From Longa, Pająk, and Wydro, 2009.

B. Director modulations induced by polar and chiral order

In the previous section, we argued that polar order and chiral order both couple to gradients of the nematic director $\hat{\boldsymbol{n}}$. In this section, we present a detailed discussion of how polarity or chirality can induce a transition from a uniform liquid crystal phase to a modulated phase. This argument is particularly important in the theory of bent-core liquid crystals, because it predicts the formation of the twist-bend nematic phase, which has recently been observed experimentally.

The argument in this section is inspired by the early work of Robert Meyer. In 1973, shortly after his original prediction of flexoelectricity (Meyer, 1969), Meyer presented lectures in Les Houches about "Structural Problems in Liquid Crystal Physics" (Meyer, 1976). Among many other topics, he discussed the possibility of spontaneous polar order leading to spontaneous splay or bend. Here we will discuss Meyer's theoretical approach in detail, because it demonstrates important points about the role of molecular shape in liquid crystal phases. Our discussion is conceptual, not historical. It combines Meyer's own work with much later articles by Selinger and collaborators (Dhakal and Selinger, 2010; Shamid, Dhakal, and Selinger, 2013). When they began their research, they were unaware of Meyer's early work on spontaneous polar order, but they independently developed the same general approach and worked out predictions in more detail.

First, consider the Frank free energy density for elastic distortions in the director field $\hat{\boldsymbol{n}}(\boldsymbol{r})$. For a nonchiral, nonpolar nematic phase, this free energy density is conventionally written as (Frank, 1958)

$$F_{\text{Frank}} = \tfrac{1}{2}K_{11}(\nabla\cdot\hat{\boldsymbol{n}})^2 + \tfrac{1}{2}K_{22}(\hat{\boldsymbol{n}}\cdot\nabla\times\hat{\boldsymbol{n}})^2 + \tfrac{1}{2}K_{33}|\hat{\boldsymbol{n}}\times\nabla\times\hat{\boldsymbol{n}}|^2. \tag{2}$$

The third term can be expressed in terms of the bend vector $\boldsymbol{b} = \hat{\boldsymbol{n}}\times\boldsymbol{\nabla}\times\hat{\boldsymbol{n}}$, which shows the magnitude and direction of the bend in the plane perpendicular to $\hat{\boldsymbol{n}}$. Likewise, the second term can be written in terms of the twist pseudoscalar $t = \hat{\boldsymbol{n}}\cdot\boldsymbol{\nabla}\times\hat{\boldsymbol{n}}$, which represents the magnitude and sign of the twist. In a similar way, one might be tempted to characterize splay by the scalar $\boldsymbol{\nabla}\cdot\hat{\boldsymbol{n}}$. However, that quantity is not uniquely defined, because the director $\hat{\boldsymbol{n}}$ is equivalent to $-\hat{\boldsymbol{n}}$. It would be better to define the splay vector $\boldsymbol{s} = \hat{\boldsymbol{n}}(\boldsymbol{\nabla}\cdot\hat{\boldsymbol{n}})$, parallel to $\hat{\boldsymbol{n}}$, which is even in $\hat{\boldsymbol{n}}$ and hence single valued. The free energy for a nonchiral, nonpolar nematic phase then has the mathematical structure

$$F_{\text{Frank}} = \tfrac{1}{2}K_{11}|\boldsymbol{s}|^2 + \tfrac{1}{2}K_{22}t^2 + \tfrac{1}{2}K_{33}|\boldsymbol{b}|^2. \tag{3}$$

Clearly the minimum of F_{Frank} is the uniform state with zero splay, zero twist, and zero bend.

Now suppose that the liquid crystal is composed of chiral molecules. Of course, this is a very familiar situation in liquid crystal science. In this case, the chirality of the molecules is

characterized by some pseudoscalar t_0, which couples with the twist t. That coupling can be expressed by the free energy

$$F_{\text{Frank}} = \tfrac{1}{2}K_{11}|\boldsymbol{s}|^2 + \tfrac{1}{2}K_{22}(t-t_0)^2 + \tfrac{1}{2}K_{33}|\boldsymbol{b}|^2. \quad (4)$$

The minimum of this free energy is a cholesteric phase with a helical pitch $p = 2\pi/q$, where $q = t_0$. It has zero splay, zero bend, and nonzero twist t_0.

By analogy with the case of favored twist, we can ask: Is it ever possible for a liquid crystal to have favored splay or bend? If so, the free energy could take the form

$$F_{\text{Frank}} = \tfrac{1}{2}K_{11}|\boldsymbol{s}-\boldsymbol{s}_0|^2 + \tfrac{1}{2}K_{22}t^2 + \tfrac{1}{2}K_{33}|\boldsymbol{b}-\boldsymbol{b}_0|^2. \quad (5)$$

Because $\boldsymbol{s}$ is a vector parallel to $\hat{\boldsymbol{n}}$, the only way for $\boldsymbol{s}$ and $\boldsymbol{s}_0$ to have a nonzero coupling is if $\boldsymbol{s}_0$ is also a vector parallel to $\hat{\boldsymbol{n}}$. Likewise, because $\boldsymbol{b}$ is a vector perpendicular to $\hat{\boldsymbol{n}}$, the only way for $\boldsymbol{b}$ and $\boldsymbol{b}_0$ to have a nonzero coupling is if $\boldsymbol{b}_0$ is also a vector perpendicular to $\hat{\boldsymbol{n}}$. Hence, we can write them as the parallel and perpendicular components of a vector $\boldsymbol{P}$, with $\boldsymbol{s}_0 = (\lambda_\parallel/K_{11})\boldsymbol{P}_\parallel$ and $\boldsymbol{b}_0 = (\lambda_\perp/K_{33})\boldsymbol{P}_\perp$. The reason for choosing those coefficients will become clear soon. With those coefficients, the Frank free energy becomes

$$F_{\text{Frank}} = \frac{1}{2}K_{11}\left|\boldsymbol{s} - \frac{\lambda_\parallel}{K_1}\boldsymbol{P}_\parallel\right|^2 + \frac{1}{2}K_{22}t^2 + \frac{1}{2}K_{33}\left|\boldsymbol{b} - \frac{\lambda_\perp}{K_3}\boldsymbol{P}_\perp\right|^2. \quad (6)$$

It is important to note that $\boldsymbol{P}_\parallel$ and $\boldsymbol{P}_\perp$ are vectors with polarity. Unlike the nematic director $\hat{\boldsymbol{n}}$, they are not equivalent to their negatives. Hence, they represent some polar order in the nematic phase, and we will refer to them as polarization. Physically, this polar order may be an electrostatic polarization or it may be a purely steric ordering of the molecular shapes; this physical property is not determined by the symmetry argument.

In addition to the Frank free energy, the system must have additional contributions to represent the free energy cost or benefit for developing polar order. Those additional contributions can be written as a usual Ginzburg-Landau expansion (Dhakal and Selinger, 2010; Shamid, Dhakal, and Selinger, 2013) in powers of $\boldsymbol{P}_\parallel$ and $\boldsymbol{P}_\perp$, giving the combined free energy

$$\begin{aligned} F = {} & \tfrac{1}{2}K_{11}|\boldsymbol{s}|^2 - \lambda_\parallel \boldsymbol{s}\cdot\boldsymbol{P}_\parallel + \tfrac{1}{2}\mu_\parallel|\boldsymbol{P}_\parallel|^2 + \tfrac{1}{2}\nu_\parallel|\boldsymbol{P}_\parallel|^4 \\ & + \tfrac{1}{2}\kappa_\parallel|\boldsymbol{\nabla}\boldsymbol{P}_\parallel|^2 + \cdots \\ & + \tfrac{1}{2}K_{22}t^2 + \tfrac{1}{2}K_{33}|\boldsymbol{b}|^2 - \lambda_\perp \boldsymbol{b}\cdot\boldsymbol{P}_\perp + \tfrac{1}{2}\mu_\perp|\boldsymbol{P}_\perp|^2 \\ & + \tfrac{1}{2}\nu_\perp|\boldsymbol{P}_\perp|^4 + \tfrac{1}{2}\kappa_\perp|\boldsymbol{\nabla}\boldsymbol{P}_\perp|^2 + \cdots. \end{aligned} \quad (7)$$

Based on these theoretical considerations, we can imagine three types of experiments to explore the coupling between director gradients and polar (or chiral) order.

1. Experiment 1: Impose director gradient

For the polar version of this experiment, we impose some fixed splay $\boldsymbol{s}$ or bend $\boldsymbol{b}$ and then measure the resulting polar order of the system. By minimizing the free energy (7) over $\boldsymbol{P}$, assuming $\boldsymbol{P}$ is small and uniform, we obtain

$$\boldsymbol{P} = \frac{\lambda_\parallel}{\mu_\parallel}\boldsymbol{s} + \frac{\lambda_\perp}{\mu_\perp}\boldsymbol{b} = \frac{\lambda_\parallel}{\mu_\parallel}\hat{\boldsymbol{n}}(\boldsymbol{\nabla}\cdot\hat{\boldsymbol{n}}) + \frac{\lambda_\perp}{\mu_\perp}\hat{\boldsymbol{n}}\times\boldsymbol{\nabla}\times\hat{\boldsymbol{n}}. \quad (8)$$

This equation is essentially equivalent to the standard expression for the flexoelectric effect in Eq. (1). The only minor difference is that the statistical order parameter $\boldsymbol{P}$ must be converted to the electrostatic polarization $\boldsymbol{P}_{\text{electrostatic}}$ by factors of the electric dipole moment per molecule and the concentration of molecules per volume. Thus, we see that there is nothing inherently electrical about the flexoelectric effect; a better name might be the "flexopolar effect." It is a manifestation of the inherent coupling of polar order with director splay and bend as required by symmetry.

For a chiral version of this experiment, we impose some fixed twist t and measure the resulting pseudoscalar order parameter. This pseudoscalar might represent a concentration difference between right- and left-handed chiral conformations of the molecules, known as "deracemization." Unlike the flexoelectric experiment, this chiral experiment is not commonly performed, perhaps because it is difficult to measure slight imbalances between chiral conformations in the laboratory. However, this experiment was done in recent work by Basu *et al.* (2011), which found that macroscopic twist induces conformational deracemization, just as macroscopic splay and bend induce polar order.

2. Experiment 2: Impose chiral or polar order

The chiral version of this experiment is something that liquid crystal chemists do every day. They routinely synthesize liquid crystal materials with well-established chiral order, i.e., with a large, permanent population difference between the right- and left-handed chiral conformers. This population difference provides a pseudoscalar order parameter and hence a favored twist t_0. That twist is seen in the helical structure of a cholesteric phase.

The polar version of this experiment is the converse flexoelectric effect. Here experimenters apply an electric field, which couples to the polar order through the free energy $F_{\text{total}} = F - \boldsymbol{E}\cdot\boldsymbol{P}$. Minimizing that free energy over polar order, bend, and splay gives

$$\boldsymbol{P}_\parallel = \frac{K_{11}}{\mu_\parallel K_{11} - \lambda_\parallel^2}\boldsymbol{E}_\parallel, \qquad \boldsymbol{s} = \frac{\lambda_\parallel}{\mu_\parallel K_{11} - \lambda_\parallel^2}\boldsymbol{E}_\parallel, \quad (9)$$

$$\boldsymbol{P}_\perp = \frac{K_{33}}{\mu_\perp K_{33} - \lambda_\perp^2}\boldsymbol{E}_\perp, \qquad \boldsymbol{b} = \frac{\lambda_\perp}{\mu_\perp K_{33} - \lambda_\perp^2}\boldsymbol{E}_\perp. \quad (10)$$

Hence, an applied electric field parallel to the director induces a splay, and an applied electric field perpendicular to the director induces a bend. The ratios $\lambda_\parallel/(\mu_\parallel K_{11} - \lambda_\parallel^2)$ and $\lambda_\perp/(\mu_\perp K_{33} - \lambda_\perp^2)$ are the susceptibilities of splay and bend to the applied field. They are different from the standard definitions of the converse flexoelectric coefficients (which involve the amplitude ratio of $\boldsymbol{s}$ to $\boldsymbol{P}_\parallel$, or $\boldsymbol{b}$ to $\boldsymbol{P}_\perp$), but still they express the same concept.

One should notice that each of these susceptibilities involves a characteristic denominator, and hence the susceptibility diverges when the denominator approaches zero. This divergence might be induced by low polar energy μ, low Frank constant K, or high coupling coefficient λ. In any of those cases, the splay or bend would be extremely sensitive to any slight applied field. If the denominator actually passes through zero, we reach experiment 3.

3. Experiment 3: Spontaneous chiral or polar order

In the context of chirality, spontaneous symmetry breaking has been studied in many liquid crystals and related systems. For example, theoretical research has modeled symmetry breaking in Langmuir monolayers and smectic films (Selinger *et al.*, 1993). Those calculations showed that a domain of right-handed chirality will have one sign of twist in the director field, while a domain of left-handed chirality will have the opposite sign of twist. In some cases, a material can show alternating stripes of right- and left-handed chirality, which are accompanied by alternating twist in the director field. This chiral stripe formation has been observed in freely suspended smectic films (Pang and Clark, 1994).

In the context of polarity, suppose that we have a liquid crystal that forms spontaneous polar order. Such polar order is disfavored by entropy, and it is also disfavored by electrostatic interactions. However, it might be favored by steric packing considerations for molecules with appropriate shape. In particular, pear-shaped molecules might have a tendency to develop polar order parallel to the director. In that case, from the considerations presented, the spontaneous polar order would induce spontaneous splay. Likewise, bent-core molecules might have a tendency to develop polar order perpendicular to the director, and that polar order would induce spontaneous bend.

The key research issue then becomes: How is the spontaneous splay or bend organized in the 3D structure of the phase? Splay and bend are different from twist in an important way: A cholesteric liquid crystal can have pure uniform twist everywhere, but a liquid crystal cannot have pure uniform splay or bend everywhere. Hence, a liquid crystal with spontaneous splay or bend experiences *geometric frustration*: It is not able to form the ideal structure because of geometric constraints. Rather, it must make some compromise between different terms in the free energy.

Let us concentrate on the case of spontaneous bend rather than splay, because spontaneous bend is more relevant to bent-core liquid crystals. Although a liquid crystal cannot fill space with pure uniform bend everywhere, it can fill space with a combination of bend and twist by forming the twist-bend nematic (N_{TB}) phase, with the director field

$$\hat{\boldsymbol{n}}(z) = (\sin\beta\cos qz, \sin\beta\sin qz, \cos\beta), \tag{11}$$

varying in a cone of opening angle β about the z axis. Here the magnitude of bend is $|\boldsymbol{b}| = q\sin\beta\cos\beta$, and the twist is $t = q\sin^2\beta$. The corresponding polar order should be aligned with the bend vector, and hence

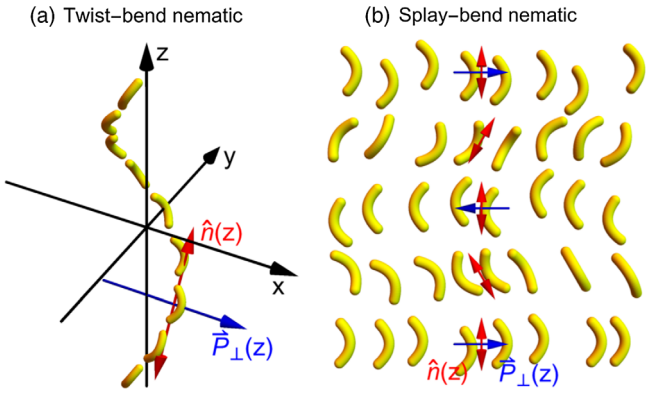

FIG. 4. Modulated nematic phases of bent-core molecules. (a) Twist bend and (b) splay bend.

$$\boldsymbol{P}_{\perp}(z) = (P\sin qz, -P\cos qz, 0), \qquad \boldsymbol{P}_{\parallel}(z) = 0. \tag{12}$$

This structure is shown in Fig. 4(a). We insert these expressions into Eq. (7) to obtain the free energy in terms of three variational parameters β, P, and q. By minimizing over these parameters, we see that the uniform nematic phase (with $\beta = 0$, $P = 0$) becomes unstable to the formation of a heliconical structure (with $\beta \neq 0$, $P \neq 0$) at the critical point when $\mu_{\perp}K_{33} = \lambda_{\perp}^2$. This is the same point where the denominators of Eqs. (9) and (10) vanish and the susceptibilities diverge. If we interpret $\mu_{\perp}$ as a temperature-dependent Landau coefficient, with $\mu_{\perp}(T) = \mu'(T - T_0)$, then the critical temperature is $T_C = T_0 + \lambda_{\perp}^2/(\mu' K_{33})$. Below the critical temperature, the parameters of the N_{TB} phase vary as

$$\beta \propto (T_C - T)^{1/2}, \quad P \propto (T_C - T)^{1}, \quad q \propto (T_C - T)^{1/2}. \tag{13}$$

Note that the predicted pitch ($2\pi/q$) is infinite at T_C, and it decreases (presumably toward the molecular length scale) as the temperature decreases into the N_{TB} phase. This prediction will be discussed further in Sec. II.D on pitch selection.

In addition to the twist-bend phase, another possibility for the liquid crystal is to form the splay-bend phase, shown in Fig. 4(b). In this phase, the director field has the planar form

$$\hat{\boldsymbol{n}}(z) = (\sin\phi(z), 0, \cos\phi(z)), \tag{14}$$

with $\phi(z) = \beta\sin qz$. That structure has alternating domains of splay and bend. The corresponding polar order is aligned with the bend vector, hence

$$\boldsymbol{P}_{\perp}(z) = \left(-P\cos qz\cos^2\phi(z), 0, \tfrac{1}{2}P\cos qz\sin 2\phi(z)\right),$$
$$\boldsymbol{P}_{\parallel}(z) = 0. \tag{15}$$

Following the same steps as in the twist-bend case, the free energy can be expressed in terms of the variational parameters β, P, and q. The transition from uniform nematic to splay-bend phase occurs at the same critical point, and the parameters have the same scaling below the transition. Comparing the free energies of these two structures shows that twist-bend phase is more stable if $K_{11} > 2K_{22}$, while splay-bend phase is more stable if $K_{11} < 2K_{22}$. In addition to

the twist-bend and splay-bend phases, more complex phases have also been predicted (Lorman and Mettout, 2004; Shamid, Allender, and Selinger, 2014; Longa and Pająk, 2016). These phases involve superpositions of different waves in the nematic and polar order parameters. Some of these phases have 1D modulations, similar to the twist-bend and splay-bend structures. Other phases have 2D or 3D modulations and hence require periodic arrays of defects in the nematic and polar order, analogous to blue phases of chiral liquid crystals.

C. Alternative view of director modulations induced by negative bend elastic constant

Meyer's work on flexoelectricity was extremely influential in the field of liquid crystal physics. However, his work on spontaneous polar ordering leading to spontaneous splay or bend passed almost unnoticed, perhaps because there were no known experimental realizations at the time. This subject was not actively studied until a theoretical article by Dozov (2001) drew great interest.

The theoretical work of Dozov was motivated by thinking about the bend elastic constant K_{33} of bent-core liquid crystals, without any consideration of polar order (Dozov, 2001). Dozov proposed that bent-core liquid crystals have an anomalously small value of K_{33}, compared with other nematic liquid crystals. He then asked what would happen if K_{33} actually became negative. In that case, the free energy would need to include higher-order terms in derivatives of the director field in order to be thermodynamically stable. The competition between the negative K_{33} term and the positive higher-order terms would favor a certain spontaneous bend. Because it is impossible to have pure bend everywhere, the liquid crystal could form either a twist-bend phase (with a heliconical structure) or a splay-bend phase (with alternating domains).

Quantitatively, Dozov's theory predicts that the uniform nematic phase becomes unstable to the formation of a twist-bend or splay-bend phase at the critical point $K_{33} = 0$. If we interpret K_{33} as a temperature-dependent coefficient, with $K_{33}(T) = K'_{33}(T - T_C)$, then the transition occurs at the temperature T_C. At that transition, the system enters the twist-bend phase if $K_{11} > 2K_{22}$, or the splay-bend phase if $K_{11} < 2K_{22}$. Below the critical temperature, the angle β and wave vector q vary as

$$\beta \propto (T_C - T)^{1/2}, \qquad q \propto (T_C - T)^{1/2}. \tag{16}$$

These results are consistent with the results of the polarization theory in Eq. (14) [and indeed they were made *before* Eq. (14) was derived by Shamid, Dhakal, and Selinger (2013)].

The theory of Dozov was especially influential because it suggested that the spontaneous formation of the twist-bend helix is related to molecular shape. For that reason, it inspired experimenters to search for highly bent liquid crystal molecules that would form the twist-bend phase in the laboratory. This work led to the experimental discovery of the twist-bend phase, as discussed in Sec. IV.

One might ask how is the negative-K_{33} theory related to the polarization theory? To answer that question, we should point out that the polarization theory is slightly more microscopic, because it describes the liquid crystal in terms of polar order $\boldsymbol{P}$ and director $\hat{\boldsymbol{n}}$, while the negative-K_{33} theory is slightly more macroscopic, because it describes the liquid crystal in terms of only $\hat{\boldsymbol{n}}$. There is a well-established mathematical procedure to go from microscopic theories to macroscopic theories: One minimizes the microscopic free energy over the microscopic variables to obtain an effective free energy in terms of only the macroscopic variables. Applying this procedure to the polarization free energy of Eq. (7), we minimize over $\boldsymbol{P}_\parallel$ and $\boldsymbol{P}_\perp$ (assuming these variables are small and slowly varying so that the ν and κ terms are negligible) and obtain the effective macroscopic free energy

$$F_{\text{eff}} = \frac{1}{2}\left(K_{11} - \frac{\lambda_\parallel^2}{\mu_\parallel}\right)|S|^2 + \frac{1}{2}K_{22}t^2 + \frac{1}{2}\left(K_{33} - \frac{\lambda_\perp^2}{\mu_\perp}\right)|B|^2 + \cdots. \tag{17}$$

This macroscopic free energy is the usual Frank free energy for director gradients, with the effective, renormalized Frank constants

$$K_{11}^R = K_{11} - \frac{\lambda_\parallel^2}{\mu_\parallel}, \qquad K_{33}^R = K_{33} - \frac{\lambda_\perp^2}{\mu_\perp}. \tag{18}$$

There is an important physical distinction between the bare constant K_{33} and the renormalized constant K_{33}^R: K_{33} gives the energy cost of a bend if we constrain $\boldsymbol{P}_\perp = 0$ during the bend, while K_{33}^R gives the energy cost of a bend if we allow $\boldsymbol{P}_\perp$ to relax to its optimum value during the bend. Likewise, the same is true for K_{11} and $\boldsymbol{P}_\parallel$—as well as for K_{22} and the chiral order parameter, as discussed by Srigengan *et al.* (2018). Of course, any realistic experiment to measure elastic constants does not put constraints on polar or chiral order, but rather allows them to relax. Hence, K_{11}^R, K_{22}^R, and K_{33}^R are the relevant elastic constants whenever we do not think about polar order.

In bent-core liquid crystals, it is reasonable to suppose that the coupling $\lambda_\perp$ between bend and polar order is particularly large, and the free energy cost $\mu_\perp$ of polar order is anomalously small. Hence, the polarization theory provides an explanation of why the effective bend constant K_{33}^R should be anomalously small. Indeed, if $\lambda_\perp$ becomes large enough and $\mu_\perp$ becomes small enough, the polarization theory provides an explanation of why the effective bend constant might be driven negative. Hence, there is no contradiction between the polarization theory and the negative-K_{33} theory; they can be different ways of looking at the same transition with or without considering polar order.

Could there be some different explanation of the negative bend elastic constant, which does not involve polar order? In principle, the answer is yes. There can always be a range of different microscopic theories that all correspond to the same macroscopic theory. For example, bent-core liquid crystals might have octupolar order, represented by a tensor T_{ijk}, even without polar (i.e., dipolar) order P_i. It is conceivable that the energy penalty for T_{ijk} might be small, but the energy penalty for P_i might be large. In that case, the effective bend elastic constant would mainly be driven negative by interactions with T_{ijk} rather than with P_i. However, we do not see any reason to

think that this type of explanation is necessary in realistic twist-bend phases. The presence of polar order provides the simplest explanation for negative bend elastic constant and for the formation of the twist-bend phase. Hence, we believe it is plausible to use the polarization approach as a more microscopic theory and the negative-K_{33} approach as an equivalent but more macroscopic theory.

D. Pitch selection

As discussed in Sec. IV, experiments have found that the pitch of the heliconical structure in the N_{TB} phase is about 10 nm. This is a remarkably small length scale, close to the molecular scale. It is much smaller than the typical pitch of a cholesteric liquid crystal, which is usually about 1 μm. Two approaches for explaining this length scale have been discussed in the community.

One approach is to reverse the question and ask why is the pitch of a cholesteric liquid crystal so large? From this point of view, the natural length scale for any modulated structure is of the order of the molecular length, and the much greater pitch of a cholesteric helix needs to be explained. The pitch of a cholesteric phase was investigated by Harris, Kamien, and Lubensky (1997, 1999). In that theory, they considered chiral intermolecular interactions, which they model as the sum of pairwise central-force interactions between the atoms. They showed that such interactions can generate a chiral twist only if there are at least short-range biaxial correlations in the molecular orientations. In other words, if each molecule is free to spin about its long axis, independently of the other molecules, then all of the chiral interactions are washed out and there will be no chiral twist. Hence, their explanation for the long pitch of a cholesteric phase is that the molecules are almost free to spin about their long axes, and hence the chiral interactions are almost washed out. Only a small chiral interaction remains, and this small interaction leads to a very large pitch.

Based on this concept, one might argue that in bent-core liquid crystals, the molecules are not at all free to spin about their long axes, because the molecular shape creates large energy barriers to inhibit such rotation. Indeed, the N_{TB} phase has polar order, which is even more ordered (i.e., less symmetric) than the biaxial order discussed by Harris, Kamien, and Lubensky (1997, 1999). In bent-core liquid crystals, we cannot make the argument about interactions being washed out by uncorrelated rotation. Hence, the pitch of the N_{TB} phase is not increased by this mechanism. Instead, it should take the natural length scale, which is comparable to the molecular length.

This argument seems plausible as an explanation for why the pitch is so small inside the N_{TB} phase, far from any phase transitions. However, it is not clear whether this argument can explain the behavior near the transition from N_{TB} to the conventional nematic phase. As discussed, both the polarization theory and the negative-K_{33} theory predict that the pitch should diverge at this transition. We do not see any reason why the argument about rotational correlations would change this divergence. Hence, we should consider an alternative approach to explain the behavior near the transition as well as deep inside the N_{TB} phase.

An alternative approach is based on an analogy with the theory of crystallization or the theory of the nematic–smectic-A transition. One version of this approach, based on separating low- and high-wave-vector components of the director field, was done by Kats and Lebedev (2014). Another version of this approach, based on a modified free energy for director and polarization, was suggested by Radzihovsky and Clark (2016), although they have not yet published the details. Here we present our interpretation of this type of theory.

In the process of crystallization, the high-temperature liquid phase has enhanced fluctuations at a characteristic wave vector q_0, and these fluctuations can be seen as diffuse peaks in the x-ray scattering. As the temperature is reduced, a density wave condenses at that peak wave vector q_0, which becomes the characteristic wave vector of the crystalline lattice. Similarly, at the nematic–smectic-A transition, the high-temperature nematic phase has local short-range order in cybotactic groups with a characteristic wave vector q_0, which appears as diffuse peaks in x-ray scattering. These local density fluctuations condense into a density wave with the same wave vector q_0 in the low-temperature smectic-A phase.

For the nematic-N_{TB} transition, neither the polarization theory nor the negative-K_3 theory includes the concept of a characteristic wave vector for fluctuations in the high-temperature phase. Rather both of these theories assume that the $q = 0$ mode is the first mode to become ordered. Perhaps we should modify the theories to include the concept of a characteristic wave vector.

For this modification, let us first consider the polarization theory. In the free energy of Eq. (7), the spectrum of fluctuations in P is controlled by the term $+(1/2)\kappa|\nabla \boldsymbol{P}|^2$, which favors fluctuations at $q = 0$ compared with other wave vectors. If we want to model enhanced fluctuations at a nonzero wave vector, which is parallel to the director $\hat{\boldsymbol{n}}$, we should add a term of the form $-(1/2)(\kappa + \delta\kappa)|(\hat{\boldsymbol{n}} \cdot \nabla)\boldsymbol{P}|^2$. Physically this negative term implies that the polarization vector tends to rotate as one moves along the director axis. This term becomes unstable at short length scales, and hence it must be stabilized by a higher derivative term, such as $+(1/2)\gamma|\nabla^2 \boldsymbol{P}|^2$.

By adding these two extra terms to the theory of the nematic-N_{TB} transition, we see several new results. First, the heliconical structure forms at a characteristic wave vector $q_0 = \sqrt{\delta\kappa/(2\gamma)}$, which is presumably at a molecular length scale, not at $q = 0$. For temperatures just below the transition, the parameters of the N_{TB} phase vary as

$$\beta \propto (T_C - T)^{1/2}, \quad P \propto (T_C - T)^{1/2}, \quad q \propto (T_C - T)^0. \tag{19}$$

In the nematic phase, for temperatures just above the transition, the renormalized bend elastic constant $K_{33}^R(T, q)$ now becomes wave vector dependent with a minimum at the same wave vector q_0. In other words, it should be easier to bend the director field at the nanometer length scale $2\pi/q_0$ than at macroscopic length scales. Because optical experiments probe macroscopic length scales, they would not be able to observe this wave vector dependence; rather they would measure the long-wavelength limit $K_{33}^R(T, 0)$, which would be the same as calculated in Eq. (9).

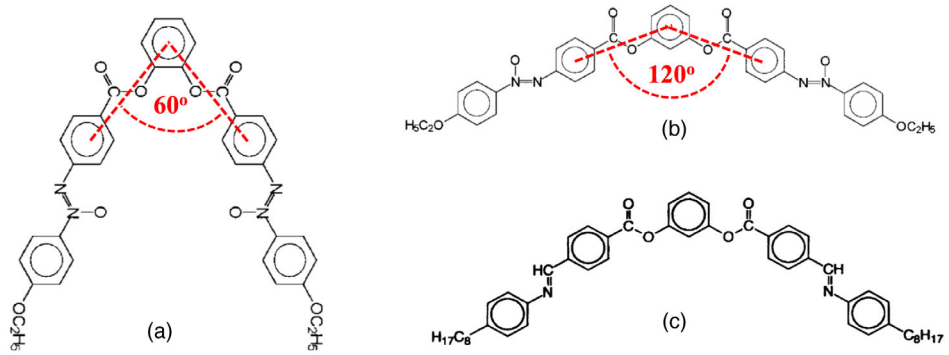

FIG. 5. Historic bent-shaped liquid crystal molecules with opening angles (a) about 60°, (b) 120°, and (c) 120°. The compound (a), synthesized by Vorländer and Apel in 1932, has an isotropic—nematic—crystal (I 219 °C N 171 °C Cr) phase sequence on cooling. The compound (b), synthesized by Vorländer in 1929, shows an isotropic—smectic—crystal (I 224°C *Sm* 186°C Cr) phase sequence on cooling. The compound (c), synthesized by Watanabe in 1996, has an isotropic—smectic 1—smectic 2—crystal (I 158°C *Sm*1 140°C *Sm*2 72°C Cr) phase sequence on cooling.

The same results can be translated into the language of the negative-K_{33} theory. With this modification, the nematic-N_{TB} transition would occur at $K_{33}^R(T, q_0) = 0$, i.e., the uniform nematic phase would become unstable at the wave vector q_0. At that transition temperature, the long-wavelength limit $K_{33}^R(T, 0)$ would still be positive. Hence, optical measurements of the bend elastic constant would see it decrease toward zero, but it would not decrease all the way to zero, as the nematic phase is cooled toward the N_{TB} phase.

Within mean-field theory, the nematic-N_{TB} transition may be either continuous or first order, depending on the phenomenological parameters in the free energy. Kats and Lebedev (2014) considered fluctuation corrections to mean-field theory and argued that fluctuations drive the transition to be first order, which is consistent with most experiments.

These modified predictions, based on the concept of a characteristic wave vector q_0, seem generally plausible. We understand that Radzihovsky and Clark (2016) are currently comparing this concept with resonant x-ray diffraction studies, and it should certainly be compared with the full range of experiments on the nematic-N_{TB} transition.

III. RIGID CORE BENT-SHAPED LIQUID CRYSTALS

Just 10 years after Reinitzer (1888) discovered liquid crystals Daniel Vorländer started his long career while he synthesized over 4000 liquid crystal compounds. During his work he concluded that the liquid crystalline state is best promoted by linear (rod) shaped molecules (Demus, 1989). This rule has proved to be valid until now and is represented by the over 100-billion-dollar liquid crystal display industry that uses rod-shaped liquid crystals almost exclusively. Strangely enough Vorländer was also the first to synthesize bent-shaped liquid crystal compounds (Pelzl, Wirth, and Weissflog, 2001), where the central aromatic core links two-ring mesogenic units in the orto and meta (1 and 2) positions (Vorländer and Apel, 1932) and in the orto and para (1 and 3) positions (Vorländer, 1929). Their mesogenic arms had 60° and 120° opening angles [see Figs. 5(a) and 5(b)] and had nematic and smectic phases, respectively.

The dominance of the rod-shaped liquid crystals was so overwhelming that we had to wait 60 years for the synthesis of more bent-core molecules when chemists at the University of Sapporo in Japan synthesized a number of bent-shaped molecules with 60° (Kuboshita, Matsunaga, and Matsuzaki, 1991; Matsuzaki and Matsunaga, 1993) and 120° (Matsunaga and Miyamoto, 1993; Akutagawa, Matsunaga, and Yasuhara, 1994) opening angles. The significance of the bent shape in liquid crystal molecules was noticed at the Tokyo Institute of Technology led by Hideo Takezoe in 1996 (Niori *et al.*, 1996), who found that a bent-core material with 120° opening angle [Fig. 5(c)] becomes ferroelectric in the smectic phase.

In the paper describing the ferroelectricity of bent-core molecules, the material was referred to as banana-shaped liquid crystals, which triggered the banana mania that led to the observation of over 50 more new liquid crystal phases, the understanding of layer chirality without chiral molecules, and many other seminal observations and possible new applications.

In the following section we will not review the chemical structures (Pelzl, Diele, and Weissflog, 1999; Hird, 2005; Pelzl and Weissflog, 2007) and their structure-property relations (Takezoe and Eremin, 2017), but will concentrate only on their physical properties in nematic, smectic, and columnar phases.

A. Nematic phases

The examples in Fig. 5 show bent-core molecules with acute and obtuse opening angles. Generally it is found that the obtuse angle bent-core liquid crystals that form nematic phases have an opening angle larger than 130° (Jákli, 2013) either due to some bulky substitution in their central phenyl ring, or they have oxadiazoles [for an example, see Fig. 8(a)] in their center, or they are asymmetric. Such a large opening angle suppresses locking into layers with long-range positional order, thus forming a smectic phase instead of a nematic phase.

In spite of this, a nanostructure of bent-core nematic (BCN) materials is much more complex than that of a rod-shaped nematic as they usually consist of smectic nanoclusters in the

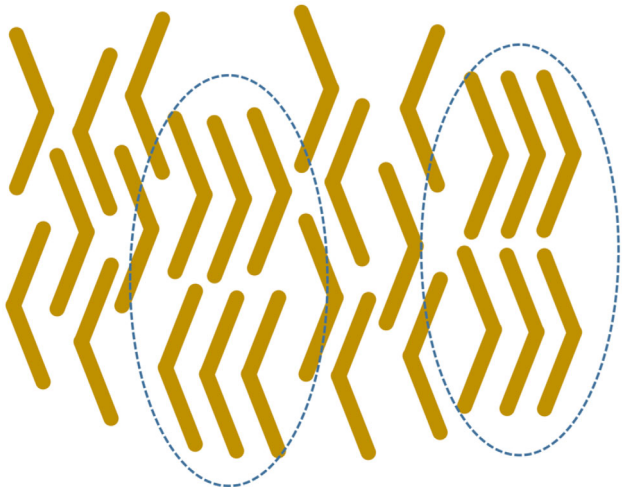

FIG. 6. Sketch of hypothetical nematic phase of bent-core liquid crystals illustrating the smectic clusters enclosed in dotted lines.

entire nematic range, which make their macroscopic (rheological, magnetic, and electric) properties quite different from conventional nematic materials.

1. Nanostructure

Short-range positional order in bent-core nematic liquid crystals has been found first by dynamic light scattering (DLS) measurements of Stojadinovic *et al.* (2002) and then in nuclear magnetic resonance (^{2}H NMR) studies by Dong *et al.* (2004), Domenici, Veracini, and Zalar (2005), and Cinacchi and Domenici (2006). The occurrence of positional order can be qualitatively understood by the frustrated translational symmetry of bent-shaped molecules in the nematic phase. As schematically illustrated in Fig. 6, this frustration leads to local and temporary locking of molecules into layered clusters, thus allowing the nematic order only on a length scale much larger than the size of the clusters.

In calamitic liquid crystals such "cybotactic" (Vries, 1970) smectic order is only pretransitional and restricted only near the vicinity of an underlying smectic phase. As the illustration in Fig. 6 indicates, there can be several different types of molecular packing in the smectic clusters. The arms in the neighbor layers can point in the same direction, i.e., the clusters can be polar (ferroelectric order), or they can point in the opposite direction, i.e., the polarities of the adjacent nanosize layers cancel each other (antiferroelectric order). Additionally, the director can be tilted (*SmCP*-type) or orthogonal (*SmA*-type) to the layers. These clusters have been studied by small-angle x-ray scattering (SAXS) (Vaupotič, Pociecha *et al.*, 2009; Francescangeli and Samulski, 2010; Hong *et al.*, 2010; Keith *et al.*, 2010; Chakraborty *et al.*, 2013; Francescangeli, Vita, and Samulski, 2014), electro-optical investigations (Shanker *et al.*, 2014), and cryogenic transmission electron microscopy (cryo-TEM) (Zhang, Gao *et al.*, 2012; Gao *et al.*, 2014). It was found that typically these clusters have a size between 10 and 100 nm, which only weakly depends on temperature. The four-lobe SAXS patterns indicate short-range tilted (smectic-C-like) layer correlations comprising a few hundred molecules. Such observation is consistent with direct cryo-TEM results obtained on a three-ring BCN material (Zhang, Gao *et al.*, 2012) showing direct evidence of smectic clusters on length scales of 30–50 nm as seen in Fig. 7(a). Domains with molecular layering extending a few tens of nanometers along the layer direction (length) and containing 3–7 layers are clearly seen. Interestingly, the shorter clusters show fairly straight layers; however, in the longer ones observed (length$>3\times$ width), we see bent layers with curvature $\sim 0.01\ \mathrm{nm}^{-1}$. The overlapping layered domains show that the depth of the field exceeds the layer depth in a single cluster. Although polarized optical microscopy (POM) observations showed that the director is uniform over the μm range, the direction of the layers in separate clusters—even in one spot, but at different heights—varies by nearly as much as 90°. This is because layers can be tilted with respect to the director by $\pm\theta$, so the maximum deviation of the layers can be 2θ. Cryo-TEM experiments therefore show the tilt angle is about 45°, which indeed is in agreement with SAXS results that show a four-lobe pattern with layer tilt being about 45° [see Fig. 7(b)].

2. Hypothetical biaxial nematic phase.

Current liquid crystal electro-optics and display applications use mostly thermotropic uniaxial nematics (N_U)

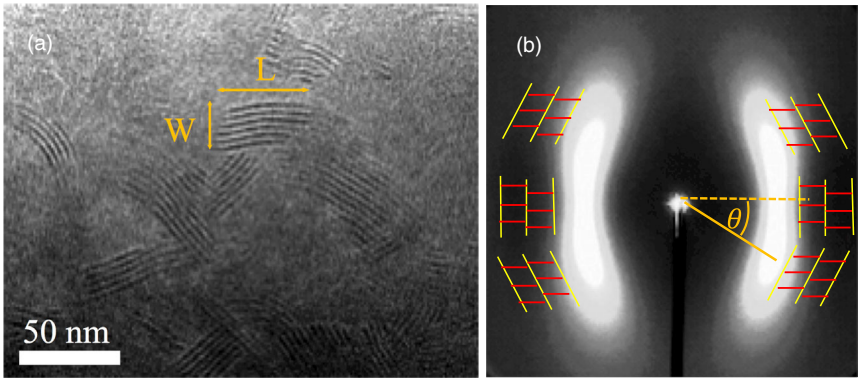

FIG. 7. Experimental proof of the smectic clusters in bent-core nematic liquid crystals. (a) Representative cryo-TEM pattern of a three-ring bent-core liquid crystal material in the nematic phase. (b) Corresponding small-angle x-ray scattering results with the illustration of the smectic layers in clusters.

showing anisotropy of physical properties with two principal directions, along and perpendicular to the director $\hat{\boldsymbol{n}} \equiv -\hat{\boldsymbol{n}}$. For a long time, attention has been drawn to a hypothetical biaxial nematic N_B on the ground of fundamental interest and the promise of faster switching times in display applications (Luckhurst, 2001; Berardi, Muccioli, and Zannoni, 2008). The N_B phase was theoretically described by Freiser (1970) as being of orthorhombic symmetry with physical properties different along three mutually perpendicular directors $\hat{\boldsymbol{n}} \equiv -\hat{\boldsymbol{n}}$, $\hat{\boldsymbol{m}} \equiv -\hat{\boldsymbol{m}}$, and $\hat{\boldsymbol{l}} \equiv -\hat{\boldsymbol{l}}$. The existence of N_B was first shown in lyotropic liquid crystals (Yu and Saupe, 1980), but in thermotropic systems, N_B remained elusive, despite the intense search.

The current focus of the search is on materials with molecules of unusual shape. First, Li *et al.* (1994) demonstrated the N_B phase in the nematic material formed by cyclic (ringlike) molecules. The search expanded to the bent-core molecules after Niori *et al.* (1996) showed that they can form a biaxial smectic phase.

It is important to note that the four-lobe SAXS pattern often found in the nematic phase of bent-core compounds, such as shown in Fig. 8, was originally interpreted as a combined result of the form factor of the bent-shaped molecules and the macroscopic biaxial order where, in addition to the primary director $\hat{\boldsymbol{n}}$ describing the average alignment of long molecular axes, there are also secondary directors $\hat{\boldsymbol{m}}$ and $\hat{\boldsymbol{l}}$ (Acharya, Primak, and Kumar, 2004).

As discussed and illustrated in Fig. 7, by now it is clear that the four-lobe SAXS pattern is caused by smectic clusters rather than by a long-range biaxial order. However, the shape of individual BCN molecules is indeed biaxial, since the directions parallel to the "wing span" (the director $\hat{\boldsymbol{n}}$), the axis along the kink direction ($\hat{\boldsymbol{p}}$ or $\hat{\boldsymbol{l}}$), and the axis $\hat{\boldsymbol{m}}$ perpendicular to the molecular plane are all different (Luckhurst, 2001, 2004). Indeed, over the last decade there have been a large number of reports of a N_B phase in bent-core liquid crystals (Acharya *et al.*, 2003; Madsen *et al.*, 2004; Dong and Marini, 2009; Jang *et al.*, 2009; Xiang *et al.*, 2009; Lehmann, 2011; Seltmann *et al.*, 2011; Yoon *et al.*, 2011; To, Sluckin and Luckhurst, 2013; Jákli, 2016). There have also been a number of papers that demonstrate that the observed features do not correspond to the long-range biaxial order but reflect various facets of uniaxial nematics that mimic the N_B behavior (Olivares *et al.*, 2003; Van Le *et al.*, 2009; Vaupotič, Pociecha *et al.*, 2009; Senyuk *et al.*, 2010; Ostapenko *et al.*, 2011; Senyuk *et al.*, 2011; Young-Ki Kim *et al.*, 2012, 2014, 2015, 2016). Since the existence of the biaxial nematic phase is an issue of fundamental importance, next we discuss the main approaches to identify the biaxial nematic phase and also the main effects that produce apparent biaxial features in uniaxial nematic samples.

The most popular approach to identify the biaxial nematic phase is optical conoscopy in which the sample is observed under a polarizing microscope with a cone of converging rays of light (Scharf, 2007). When the sample represents a homeotropic cell of a uniaxial nematic N_U, the converging rays observed simultaneously produce a conoscopic pattern with a Maltese cross, formed by two pairs of mutually perpendicular extinction brushes, called isogyres; see Fig. 9(a). The center of the cross, called a melatope, corresponds to the optic axis. Many research groups observed that when a homeotropic N_U sample is cooled down, this pattern changes, as the isogyres split by some distance $2a$. The splitting can be interpreted as a result of a N_U-N_B phase transition with the occurrence of the in-plane orientational order and thus two optic axes. For an N_B with three refractive indices $n_1 < n_2 < n_3$, the splitting of isogyres provides a direct measure of the in-plane birefringence $\Delta n_{12} = n_2 - n_1$,

$$\frac{2a}{2R} = \frac{\bar{n}}{\mathrm{NA}} \frac{n_3}{n_2} \left(\frac{n_2^2 - n_1^2}{n_3^2 - n_1^2} \right)^{1/2},$$

where R is the radius of the field of view [Fig. 9(b)], NA is the numerical aperture of the objective, and $\bar{n}$ is the average refractive index (Wahlstrom, 1969; Senyuk *et al.*, 2010). Experiments show that the in-plane birefringence Δn_{12} of potential N_B candidates is very weak, on the order of 10^{-4}. More important, however, is the fact that this in-plane birefringence has been demonstrated to originate in a specific behavior of the uniaxial N_U phase rather than in the appearance of N_B. The molecular structures of such materials, initially considered to be the prime examples of N_B, are shown in Fig. 8. These are 4, 4′ (1,3,4-oxadiazole-2,5-diyl) di-*p*-heptylbenzoate (ODBP-Ph-C_7) or C7, 4, 4′ (1,3,4-oxadiazole-2,5-diyl) di-*p*-dodecyloxybenzoate (ODBP-Ph-O-C_{12}) or C12 (Senyuk *et al.*, 2011) and 4-((4-dodecylphenyl)

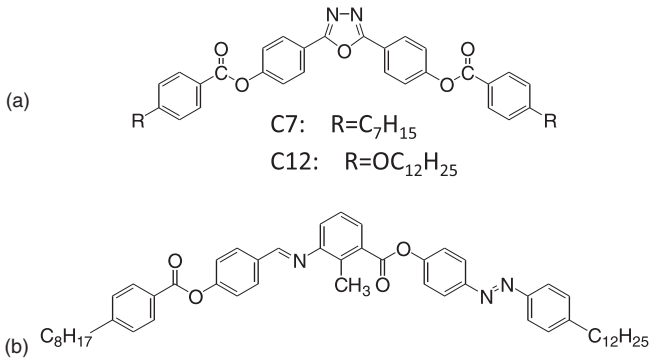

FIG. 8. Molecular structure of bent-core nematics (a) C7, C12 and (b) A131. The length of the C7 molecule is about 3.8 nm, and the width is 0.8 nm.

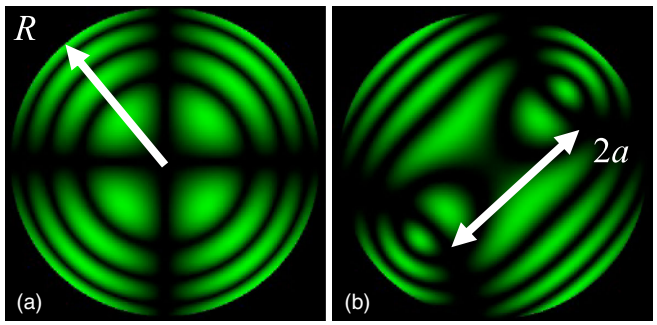

FIG. 9. Conoscopic images of a homeotropic sample in (a) N_U and (b) hypothetical N_B phases. The splitting of isogyres shown in (b) can be observed in the N_U phase when the director varies along the direction of observation.

diazenyl) phenyl 2-methyl-3-(4-(4-octylbenzoyloxy) benzyle-deneamino) benzoate abbreviated A131 (Van Le *et al.*, 2009; Senyuk *et al.*, 2010). In some cases, the proof of uniaxial order is rather easy to obtain. For example, if the material is of a positive dielectric anisotropy, $\Delta\varepsilon > 0$, one can measure how the split distance depends on the applied voltage. Van Le *et al.* (2009) and Senyuk *et al.* (2010) demonstrated that in A131, with $\Delta\varepsilon > 0$, the split of isogyres vanishes as the applied voltage is raised to a relatively modest value of 20 V. It means that when the electric field aligns the principal director $\hat{\boldsymbol{n}}$, there is no orientational order in the planes perpendicular to $\hat{\boldsymbol{n}}$, which contradicts the idea of N_B. In a similar way, biaxiality has been ruled out in a organo-siloxane tetrapode material (Young-Ki Kim *et al.*, 2014).

There are few mechanisms other than the N_U-N_B transition that explain the appearance of in-plane birefringence when a homeotropic N_U sample is cooled down. The most obvious reason is a surface anchoring transition, when the director changes its orientation from homeotropic to tilted (Van Le *et al.*, 2009; Senyuk *et al.*, 2010; Kim *et al.*, 2015). These temperature-triggered transitions are well documented for various nematic materials, including the rodlike mesogens (Volovik and Lavrentovich, 1983; Patel and Yokoyama., 1993). Surface anchoring transitions do not necessarily cause the splitting of isogyres. A uniform tilt of the director produces a mere shift of the Maltese cross (Scharf, 2007; Senyuk *et al.*, 2010). However, when the director tilt is spatially varying along the direction of observation, then the anchoring transition in an N_U cell mimics the appearance of N_B by splitting the isogyres (Senyuk *et al.*, 2010, 2011; Kim *et al.*, 2012; Kim, Senyuk, and Lavrentovich, 2012). A spatially varying director tilt $\theta(z)$ along the axis z normal to the bounding plates causes a split

$$\frac{2a}{2R} = \frac{\bar{n}}{\mathrm{NA}}\left(\frac{1}{d}\int_0^h [\bar{\theta} - \theta(z)]^2 dz\right)^{1/2}.$$

Here

$$\bar{\theta} = \frac{1}{h}\int_0^h \theta(z) dz$$

and h is the cell thickness (Senyuk *et al.*, 2010, 2011). Exploring the role of the director deformations in conoscopic patterns, Senyuk *et al.* (2010, 2011) and Young-Ki Kim *et al.* (2012, 2014) demonstrated that the materials such as A131, C7, C12, J35/DT6Py6E6, and organo-siloxane tetrapodes, previously claimed to be N_B, are in fact N_U since they exhibit isogyre splitting that depends on the cell thickness, which means that the effect is caused by an anchoring transition with a nonuniform director field in the N_U cell rather than by the biaxial macroscopic order. Determining whether the splitting of isogyres changes with the cell thickness is an especially important test for uniaxiality of materials with negative dielectric anisotropy, such as BCN oxadiazole derivatives C7 and C12 shown in Fig. 8, since in this case the electric field cannot align the director uniaxially. Dependence on the cell thickness signals that the splitting of isogyres is caused by a nonuniform director along the direction of light propagation rather than by the presence of two optical axes. (Senyuk *et al.*, 2011) An independent small-angle diffuse x-ray diffraction (XRD) at C7 and C12 samples by Francescangeli *et al.* (2011) led to the conclusion that "the XRD data does not provide any direct support of the existence of a molecular biaxial nematic phase."

Especially subtle N_B-mimicking behavior of N_U cells was reported by Kim *et al.* (2012) and Kim, Senyuk, and Lavrentovich (2012) for a simple cooling or heating of the material when there is no anchoring transition; see Fig. 10.

The temperature change causes thermal expansion or contraction of the liquid crystals. As a result, the material flows. Coupling of the flow to the director causes a bipolar director tilt, which results in the splitting of isogyres; see Fig. 10(a). In some cases, the transient nature of the deformation and splitting is not obvious as relaxation to the ground state is very slow. From a theoretical point of view, the director distortion caused by thermal expansion represents a rare case when the condition of incompressibility routinely used in solving hydrodynamic problems, including those in anisotropic fluids, is clearly invalid. Kim, Senyuk, and Lavrentovich (2012) proposed a simple analytical model of the observed thermomechanic and thermo-optical effects that is described below.

Consider a homeotropic N_U cell with a uniform director written in Cartesian coordinates as $\hat{\boldsymbol{n}} = (0, 0, 1)$; see Fig. 10(b). The z axis is perpendicular to the bounding plates located at $z = 0, h$. The material is subject to a changing temperature. For simplicity, we consider only expansion along the horizontal x axis; see Fig. 10(c). The mechanism of thermally induced flow is clear from the mass conservation equation $\partial\rho/\partial t = -\rho\nabla \cdot \boldsymbol{v}$, which connects the time derivative of the

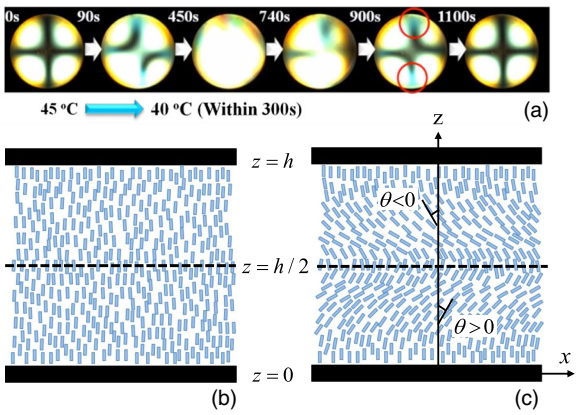

FIG. 10. Biaxiality-mimicking effect of thermal contraction and expansion in homeotropic cells of N_U. (a) Cooling of the N_U phase of nonsymmetrically substituted thiadiazole abbreviated J35 or DT6Py6E6 results in transient but long-lived splitting of isogyres that mimic biaxial order (Young-Ki Kim *et al.*, 2012), (b) equilibrium director in the homeotropic cell, and (c) director deformations in a homeotropic cell caused by thermal contraction and expansion that produce split isogyres in conoscopic patterns of a deformed N_U.

fluid density ρ to the spatial gradients of its velocity. The density of the N_U slab thermally expanding or shrinking can be presented as $\rho(t) = \rho_0(1 - \beta\xi t)$, where $\rho_0 = \rho(T = T_0)$ is the initial density, ξ is the temperature change rate, and β is the coefficient of thermal expansion. The mass conservation equation then immediately yields $v_x \propto \beta\xi x$, that is, a nonzero velocity along the axis x that depends linearly on the distance from the geometrical center $x = 0$. The experimental conditions in typical liquid crystal (LC) cells of a thickness $h \approx 10\ \mu$m correspond to a low Reynolds number $\mathrm{Re} \ll 1$, thus the velocity should satisfy the Stokes equation $\nabla p = \mu\nabla^2 \boldsymbol{v}$ (here ∇p is the pressure gradient and μ is the dynamic viscosity), as well as a no-slip condition $v_x = 0$ and no-penetration condition at the bounding walls. The solution for v_x is then

$$v_x \approx 6\beta\xi x \frac{z}{h}\left(1 - \frac{z}{h}\right).$$

The flow along the x axis realigns $\hat{\boldsymbol{n}}$ toward the x axis. The viscous reorienting torque $\alpha_2(\partial v_x/\partial z)$, where α_2 is the anisotropic viscosity of N_U in the geometry under consideration, is proportional to the shear rate $\partial v_x/\partial z$ that is vanishing at the walls and at the middle plane $z = h/2$. The viscous torque is opposed by the elastic torque $K_{33}\partial^2\theta/\partial z^2$ that tends to keep $\hat{\boldsymbol{n}}$ along the z axis; here K_{33} is the Frank elastic constant of bend. The balance of the two torques for small angles $\theta(z)$ between $\hat{\boldsymbol{n}}$ and the vertical z axis determines the flow-induced director profile

$$\theta(z) = \beta\xi x z \frac{|\alpha_2|}{K_{33}}\left(1 - \frac{z}{h}\right)\left(1 - \frac{2z}{h}\right),$$

schematically illustrated in Fig. 10(c). This tilt produces a transient splitting of isogyres in conoscopic observations

$$\frac{2a}{2R} = |\alpha_2|\beta\xi \frac{\bar{n}|x|h}{\sqrt{210}K_{33}\mathrm{NA}}.$$

The splitting increases with the viscosity $|\alpha_2|$ of the material, rate of temperature change ξ, and thermal expansion coefficient β. Note that the splitting of isogyres produced by thermal expansion does not depend on the thermal history of the sample in the sense that after thermal equilibration at a fixed temperature, the same temperature rate change ξ would result in the same evolution of the optical response [unless the prolonged heating causes irreversible degradation as reported for oxadiazole materials C7 and C12 by Senyuk *et al.* (2011)]. Although the effect can trigger a noticeable splitting of isogyres or other optical effects at any temperature (depending on the cell geometry and ξ), if the experiments are performed with a fixed rate ξ, the apparent temperature of optical response mimicking the appearance of biaxiality would be reproducible, thus further masking the effect of thermal expansion as the phase transition. By reducing ξ to a very small value, one could distinguish the thermal expansion effect from a true phase transition. Both the theory and the experiments (Kim, Senyuk, and Lavrentovich, 2012) yield thermally induced velocities of the N_U flows on the order of 10 μm/s for typical $|\alpha_2| = 0.3\ \mathrm{kg\,m^{-1}\,s^{-1}}$, $\beta = 10^{-3}/\mathrm{K}$, $\xi = 0.5\ \mathrm{K/s}$, and $h = 50\ \mu$m.

The described effect of thermal expansion-induced director deformations can be observed in any thermotropic or lyotropic LC (Kim, Senyuk, and Lavrentovich, 2012). In most materials, such as 5CB, the deformations relax to the ground state relatively quickly, within seconds. However, many bent-core nematics are of a high viscosity (Dorjgotov *et al.*, 2008) and in these cases the deformations could persist for tens of minutes and even hours, thus leading to potential misinterpretation of the effect as the appearance of N_B during cooling or heating.

This consideration illustrates limitations of optical and x-ray testing of the macroscopic biaxial order in the nematic materials, since these approaches provide information that is integrated over the pathway of the testing beam. Similar limitations are characteristic for other techniques that rely on bulk response, such as NMR. An alternative robust approach to test the long-range biaxial order is through topological defects, especially those that correspond to the ground state of the nematic phase in confined geometries. N_U and N_B exhibit different sets of topological defects, i.e., configurations of the phase of the order parameter ($\hat{\boldsymbol{n}}$ in the case of N_U and a triad $\hat{\boldsymbol{n}}$, $\hat{\boldsymbol{m}}$, $\hat{\boldsymbol{l}}$ in N_B) that cannot be continuously transformed into a uniform state (Toulouse, 1977; Kleman and Lavrentovich, 2009). Let us recall the main features of point (hedgehogs and boojums) and line (disclinations) defects. In the N_U bulk, topologically stable defects are disclination lines of strength $|s| = 1/2$; s is defined as a number of director turns by 2π when one circumnavigates the defect core once. Disclinations of strength $|s| = 1$ are not topologically stable (Cladis and Kléman, 1972; Meyer, 1976). Even if the configuration with $|s| = 1$ is enforced by boundary conditions, for example, by confining N_U into a circular capillary, $\hat{\boldsymbol{n}}$ would realign along the axis of the capillary (Cladis and Kléman, 1972; Meyer, 1976), a process called by Robert Meyer an "escape into the third dimension" (Meyer, 1976). Besides the disclinations, the N_U phase exhibits two different types of topological point defects (Volovik and Mineyev, 1977; Volovik and Lavrentovich, 1983), (i) the so-called hedgehogs that can exist in the N_U bulk or at its surfaces and (ii) the so-called boojums that exist only at the surface of N_U; see Fig. 11 (Volovik and Lavrentovich, 1983).

In N_B, the line disclinations are stable when the corresponding strength is $\pm 1/2$, but also when $|s| = 1$: the escape of one director does not remove the defect core, as the two other directors restore the singularity (Toulouse, 1977). One of the most fascinating features of these disclinations predicted by Toulouse (1977) is that crossing of two disclinations of strength $|s| = 1/2$ can result in the appearance of an $|s| = 1$ disclination that connects these two. Since the elastic energy of disclinations is proportional to their length, the interaction of crossing disclinations is similar to the behavior of quarks. In N_U, disclinations cross each other freely (Toulouse and Kleman, 1976). Observation of the nontrivial crossing would be an ultimate test of N_B existence, but, unfortunately, its experimental realization is difficult. Crossing of disclinations has been so far studied only for N_U (Ishikawa and Lavrentovich, 1998).

Isolated point defects cannot exist in N_B. For example, a radial configuration of one director implies that the two other directors are defined at a spherical surface and thus should

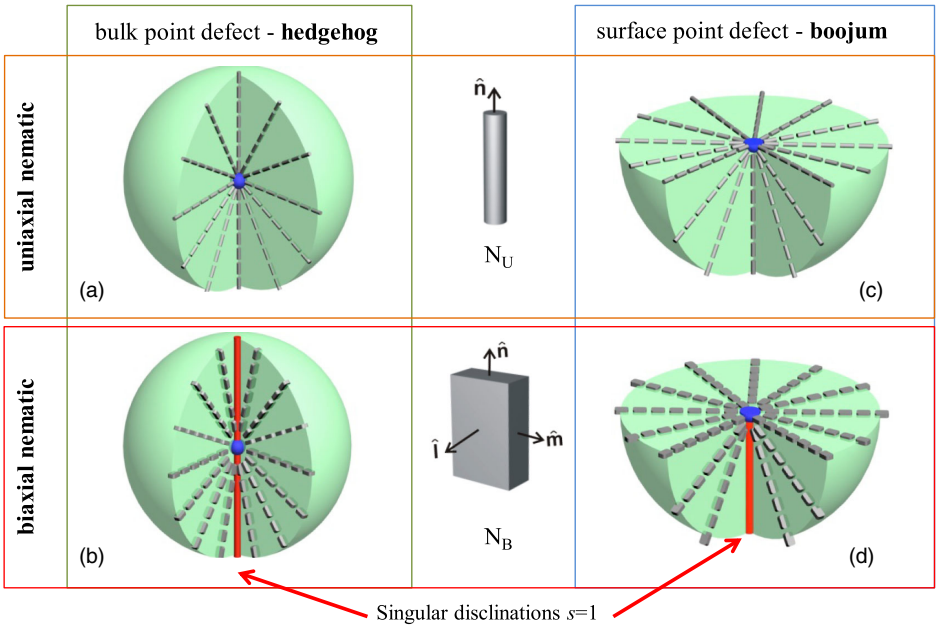

FIG. 11. Bulk point defects: hedgehogs in (a) N_U and (b) N_B. Surface point defects: boojums in (c) N_U and (d) N_B. Note that the point defects in N_B are always connected to singular disclinations. Point defects provide another opportunity for an experimental test of bulk biaxial order. Schemes courtesy of Bohdan Senyuk.

form additional singularities emanating from the center of the defect, similar to the "Dirac monopole" structure with a radial magnetic field and vector-potential perpendicular to it; see Fig. 11(b) (Kleman and Lavrentovich, 2009). Surface point defect boojums of strength $|s_b| = 1$ also cannot exist, as they must be connected to a singular bulk disclination of the same strength $|s| = 1$, and thus represent the ends of these disclinations rather than isolated points; see Fig. 11(d).

This consideration suggests a number of relatively simple tests of the existence of a biaxial N_B phase. These tests rely on confined geometries such as cylindrical capillaries, freely suspended droplets, and liquid crystal slabs containing spherical colloidal particles.

Cylindrical capillaries with normal director orientation should exhibit a nonsingular texture of an "escape into the third dimension" in N_U and a singular disclination $s = 1$ in N_B. Experimental studies of nematics such as A131 (Senyuk *et al.*, 2010), C7 and C12 (Senyuk *et al.*, 2011), and tetrapods (Young-Ki Kim *et al.*, 2014) show that the director $\hat{\boldsymbol{n}}$ realigns along the capillary axis as expected for the N_U phase in all these materials in the entire range of the nematic phase. Since the two possible directions of the escape are of equal probability, director escape often results in a number of point defects, hedgehogs, Fig. 11(a), separating the zones of opposite directions of escape. In the explored N_B candidates, these defects remain isolated, free of any disclinations, which contradicts the topological restrictions imposed by the biaxial order, Fig. 11(b), and thus confirms that the studied materials exhibit only an N_U phase (Senyuk *et al.*, 2010, 2011; Young-Ki Kim *et al.*, 2014).

Spherical colloidal inclusions placed in an otherwise uniformly aligned nematic slab can also be used for biaxiality tests (Senyuk *et al.*, 2010, 2011; Avci *et al.*, 2013; Young-Ki Kim *et al.*, 2014, 2016). Next we describe an example of a sphere with tangential anchoring (Senyuk *et al.*, 2010, 2011; Avci *et al.*, 2013; Young-Ki Kim *et al.*, 2014, 2016). Normally anchored spherical colloids (Senyuk *et al.*, 2011; Young-Ki Kim *et al.*, 2014) as well as the case of an inverse geometry, nematic droplets (Avci *et al.*, 2013; Young-Ki Kim *et al.*, 2014), can be considered in a similar way.

Colloidal spheres with tangential anchoring produce N_U textures with quadrupolar symmetry of the director field $\hat{\boldsymbol{n}}$ and two point defects boojums located at the poles of the sphere, along the axis that is parallel to the uniform far field $\hat{\boldsymbol{n}}_0 = \text{const}$. Their existence is dictated by the topological requirement: a director field tangential to the surface of a sphere should contain singularities with the total strength equal to the Euler characteristic of the sphere, which is 2: $\sum_i s_{b,i} = 2$ (Kleman and Lavrentovich, 2009). The texture with two isolated boojums at the poles is allowed in N_U but not in N_B. In N_B, the relationship $\sum_i s_{b,i} = 2$ is still valid, but the isolated boojums of strength $s_b = 1$ cannot exist, as they should represent the ends of disclination lines of strength $s = 1$ terminating at the surface of the spherical particle. Experiments with the biaxial candidates (Senyuk *et al.*, 2010, 2011; Avci *et al.*, 2013; Young-Ki Kim *et al.*, 2014, 2016) show that the boojums remain isolated and do not produce disclination lines; see Fig. 12. When a few tangentially anchored spheres cluster in N_U, they attract each other along a line that makes a large angle, ~30°–60° with $\hat{\boldsymbol{n}}_0$ (Smalyukh *et al.*, 2005); see Fig. 12(b). If the material were N_B, there should be disclinations terminating at the boojums. The disclinations would rearrange the colloidal chain, aligning it along $\hat{\boldsymbol{n}}_0$, in order to shorten their length. Such

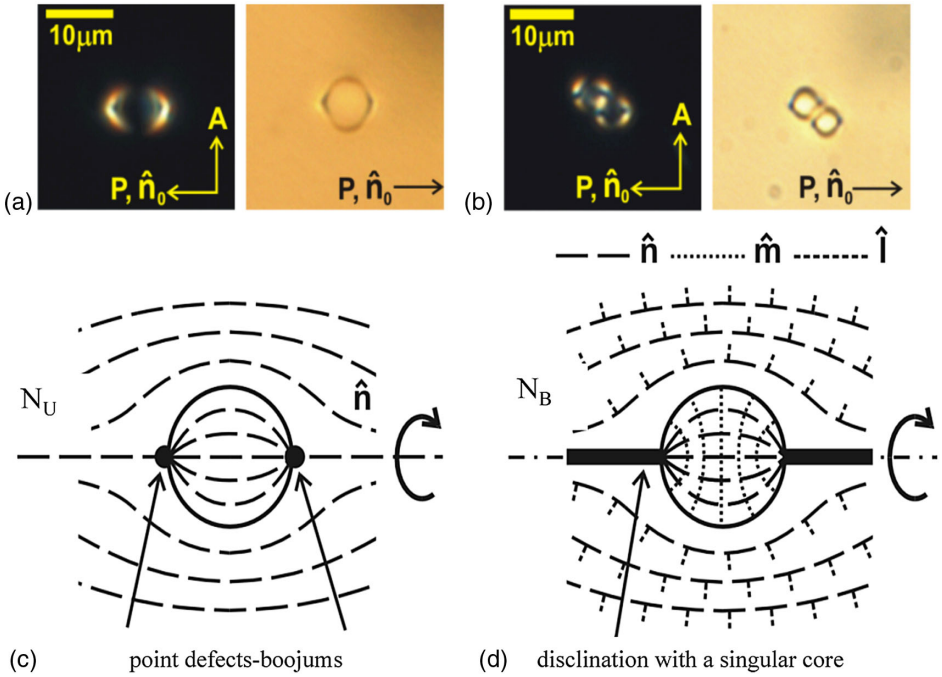

FIG. 12. Colloidal polystyrene spheres in the planar cells ($h = 25$ μm) of (a) C12, sphere diameter 8 μm; (b) C7, diameter 5 μm; (c) scheme of director configuration with boojums around the sphere in N_U; (d) a hypothetical scheme of director configuration around the sphere in N_B. The singular lines shown in (d) are not observed experimentally in the studied biaxial candidate materials. From Senyuk *et al.*, 2011.

rearrangements of colloids should be detectable even if the core of the disclinations is invisible under the microscope, but they are not observed; see Fig. 12(b). The experimentally observed configurations correspond to the expected symmetry of N_U, Fig. 12(c), but not N_B, Fig. 12(d).

Despite the lack of evidence of the existence of the N_B phase in bent-core materials, DLS (Stojadinovic *et al.*, 2002) and x-ray studies often reveal strong fluctuations attributable to local biaxial ordering. Assuming a Landau-type expansion of the orientational free energy, it was estimated for a three-ring bent-core material (Zhang, Gao *et al.*, 2012) that the correlation length associated with these fluctuations is about 100 nm (Stojadinovic *et al.*, 2002). These biaxial fluctuations again can be attributed to the presence of tilted smectic clusters that are inherently biaxial. It appears that the biaxial shapes of individual molecules is not enough to produce measurable phase biaxiality (biaxial order over the visible wave range), or if it exists, it should be less than $\delta n \leq 2 \times 10^{-5}$ (Jákli, 2013).

The absence of unequivocal experimental evidence of the existence of N_B poses the question of what are the factors preventing such a phase? Numerical simulations are well suited to explore the various parameters contributing to the stability of biaxial nematics and competing structures. A Monte Carlo study of elongated particles interacting through an attractive-repulsive biaxial Gay-Berne potential demonstrates that the most dangerous rival of N_B is smectic ordering (Berardi and Zannoni, 2000; Berardi *et al.*, 2008). Namely, Berardi and Zannoni (2000) demonstrated that an enhancement of shape and interaction potential biaxialities promoted not only biaxial orientational order but also smectic stacking. Peláez and Wilson (2006) performed molecular dynamics simulations of an atomistic model of C7 shown in Fig. 8(a) and demonstrated that the simulated nematic phase is biaxial but that the degree of biaxiality is small. The simulations also showed the formation of ferroelectric domains in the nematic associated with the alignment of central dipole moments. Removal of electrostatic interactions in the model destabilized both the N_B and the ferroelectric domains, which stresses a fine balance of molecular forces responsible for the potential N_B ordering. It was suggested that asymmetric placement of electric dipoles within the molecules might disrupt the tendency to smectic order and thus enhance the stability of N_B (Querciagrossa, Berardi, and Zannoni, 2018). The most recent simulations by Dijkstra's group (Dussi *et al.*, 2018) stress an important role of a strong shape asymmetry. The study focused on an entropy-driven colloidal suspension comprised of hard biaxial particles, characterized by long (L), medium (M), and short (S) particle axes. The stable N_B was observed close to the so-called dual shape $M = \sqrt{LS}$ but only when the particles were strongly anisometric, with the ratio L/S exceeding a rather steep threshold that varies from 9 to 23, depending on the concrete geometry that ranged from rhombi to prisms and cuboids. Weaker shape anisotropy produced positionally ordered states such as smectic and columnar phases. If one risks applying these results for colloidal suspensions to thermotropic molecules with a typical $S \approx 0.34$ nm and assumes a cuboid shape, then the minimum value of L should be about 7.8 nm, with $M \approx 1.6$ nm. These shape anisotropies significantly exceed the ranges explored for bent-core molecules so far. For example, C7 shows $M \approx 0.8$ nm and $L \approx 3.8$ nm (Kim *et al.*, 2015), which do not satisfy the criteria $M = \sqrt{LS}$ and $L/S > 23$. One can safely

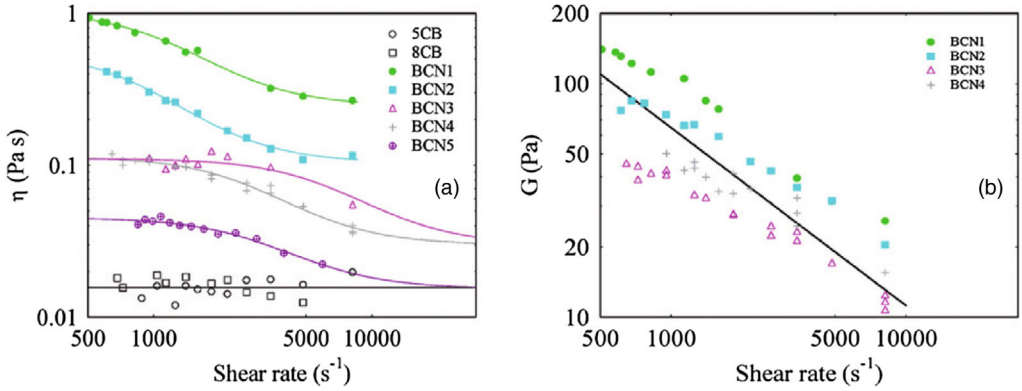

FIG. 13. Rheological properties of several bent-core nematogens. (a) Shear rate dependences of the viscosities in the isotropic phases 10 °C above the *I-N* transition. In comparison the viscosities of two rod-shaped materials 5CB and 8CB are also shown. (b) Shear rate dependences of the elastic modulus in the isotropic phases 10 °C above the *I-N* transition. The shear moduli for 5CB and 8CB are not shown because they are within the experimental error of ∼5 Pa. From Bailey *et al.*, 2009.

conclude that the topic of biaxial nematics will intrigue researchers for years to come.

In addition to the spontaneous phase biaxiality, field-induced biaxiality is also of interest, especially because it could provide linear phase modulation or displays with excellent gray scale. In fact, measurements of the splitting of the ordinary refractive index in a Fabry-Perot cell of a BCN material with oxazole center indicated (Olivares *et al.*, 2003) electric field-induced biaxiality of $\delta n = 2 \times 10^{-3}$ at $E = 6.7\ \mathrm{V}/\mu\mathrm{m}$, which is about 1 order of magnitude larger than the induced biaxiality observed previously in calamitic liquid crystals (Dunmur, Szumilin, and Waterworth, 1987). Borshch *et al.* (2014) demonstrated that the electric field-induced biaxial order can be used to determine how close the N_U phase is to forming N_B in the absence of an electric field.

Although the induced biaxial state usually relaxes back to the uniaxial ground state after field removal, in one case the field-induced biaxial state was found to be metastable (Stannarius *et al.*, 2007).

3. Rheological properties

An inherent property of nematic liquid crystals is that shear flow and the director fields are coupled: the gradient of the velocity field leads to an inhomogeneous rotation of the director (flow alignment), and an inhomogeneous director rotation results in an inhomogeneous flow (backflow effect) (Leslie, 1968). The flow alignment angle of most nematic liquid crystals of low molecular weight rod-shaped molecules is independent of the shear rate. Consequently, nematic liquid crystals in bulk behave as Newtonian fluids with no observable dependence of the flow viscosity on the shear rate and little measurable shear modulus. Smectic liquid crystals however appear as soft solids (storage modulus in the range of 1 MPa) for flow normal to the layers. Strong flow can realign the layers parallel to the flow, thus rendering them strongly shear thinning (Larson, 1999).

The viscoelastic properties of BCN materials are observed by dynamic light scattering (Stojadinovic *et al.*, 2002; Niori, Yamamoto, and Yokoyama, 2004), the analysis of Fredericks transitions (Panov *et al.*, 2010; Paladugu Sathyanarayana *et al.*, 2010, 2012), electrorotation (Dorjgotov *et al.*, 2008), nanoliter rheometry (Bailey *et al.*, 2009), and NMR (Domenici, 2011). All of these measurements provide estimates of the rotational viscosity, which range on the order of 0.1–3 Pa s. The observations in which the shear flow viscosities are greatly amplified compared to the twist viscosity indicate that the smectic clusters create a steric barrier to shear flow.

The flow rate dependences of the viscosity and elastic moduli for several BCN materials are shown in Fig. 13. It can be seen in Fig. 13(a) that rod-shaped nematics are practically Newtonian with shear rate independent viscosity in the range of 20 mPa s (20 cP) and shear modulus less than 5 Pa. BCNs however show non-Newtonian behavior with shear thinning at or above $10^3\ \mathrm{s}^{-1}$ shear rates. The measured data could be well fit to a relaxation relationship valid for suspensions of soft or compliant spheres with typical radius of 10–20 nm. These deformable nanoparticles can be attributed to the smectic clusters we discussed in Sec. III.A.1.

4. Frank elastic constants

Measurements of elastic constants K_{11}, K_{22}, and K_{33} describing the energy costs of the splay, twist, and bend director distortions, respectively, are important parameters to obtain information about the nanostructure of the LC materials. For rod-shaped liquid crystals typically $K_{33} > K_{11} > K_{22}$, but all are in the 1–10 pN range. Concerning the ratio of the bend and splay elastic constant, de Jeu (1980) showed that $K_{33}/K_{11} \propto L/D$, where L and D are the length and width of the molecule. One would expect K_{33}/K_{11} to increase as the molecular chain increases (i.e., for higher homologs in a series of compounds), although this was found to not be true due to the increasing number of conformations of flexible chains that increase the effective width of the molecules (de Jeu and Claassen, 1977). In the case of bent-core molecules the effective width increases with increasing bend angle, and one might expect typically smaller K_{33}/K_{11} than in rod-shaped molecules; see Fig. 14.

Theoretically the effect of the molecular shape on the Frank elastic constants of nematic liquid crystals was first studied by Gruler (1974) and Helfrich (1974). Helfrich argued that for bent-shaped molecules the strain in the bend distortion can be partly relieved by rotation around the long axis of the

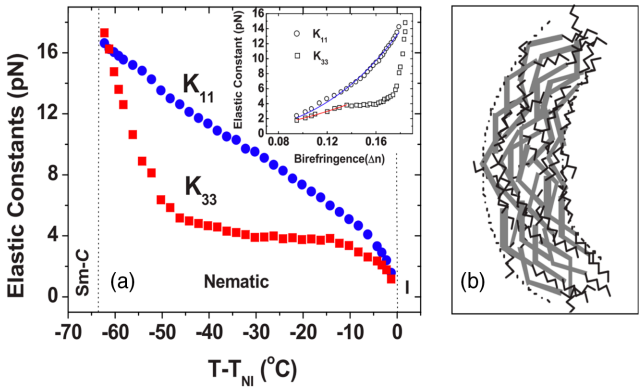

FIG. 14. (a) Variation of splay (K_{11}) and bend (K_{33}) elastic constants as a function of reduced temperature of a bent-core material with a broad range of nematic phase. The inset shows K_{11} and K_{33} at the function of birefringence (Δn). (b) Schematic of the biasing of the kink directions by rotation around the long axis to relieve bend elastic energy. From P. Sathyanarayana *et al.*, 2010.

individual molecules so that more molecules have bend orientation toward the externally imposed bend as discussed in the theoretical Sec. II.A.3. Specifically, he predicted a decrease in the bend constant K_{33} for bent-shaped mesogens given by

$$K_{33} = \frac{\tilde{K}_{33}}{1 + \beta^2 N^{-1/3} \tilde{K}_{33}/(2k_B T)}, \tag{20}$$

where β is the molecular bend angle, $\tilde{K}_{33}$ is the bend elastic constant when $\beta = 0$ (as for a rodlike molecule), and N is the molecular number density. Taking $\beta \sim 1$ rad, $N \sim 10^{27}$ m^{-3}, $T = 350$ K, and $\tilde{K}_{33} \sim 10$ pN, we get $K_{33} \approx \tilde{K}_{33}/2$. This model did not take into account internal field corrections for elongated molecular shape or the degree of order that was taken into account by Gruler, who obtained a larger decrease of K_{33} than Helfrich.

Experimentally several groups found that K_{33} is indeed significantly smaller than K_{11} for BCN materials (Görtz *et al.*, 2009; P. Sathyanarayana *et al.*, 2010; Tadapatri *et al.*, 2010b; Majumdar *et al.*, 2011; Salter *et al.*, 2011; Kaur *et al.*, 2012; Srigengan *et al.*, 2018) or in mixtures of bent-core and rod-shaped molecules (Kundu, Pratibha, and Madhusudana, 2007; Sathyanarayana and Dhara, 2013), often by a factor of 3–5. Such a dramatic reduction of K_{33} as compared to rodlike mesogens cannot be easily reconciled with Eq. (20). Instead, as noticed by Kaur *et al.* (2012), a much better prediction of the bend and splay moduli is provided by a mean-field formula derived by Berreman and Meiboom (1984),

$$\frac{K_{ii}}{S^2} = K_i^{(2)} + K_i^{(3)} S + K_i^{(4)} \left(\frac{S}{1-S}\right)^2,$$

where $K_i^{(2)}$ are fitting parameters that might be temperature dependent. Recent numerical calculations by Kaur *et al.* (2012) and theory (Srigengan *et al.*, 2018) similar to what we presented in Sec. II could find good agreement with experiment.

In the theories discussed neither the splay constant K_{11} nor the twist constant K_{22} is affected by the molecular bend; however, experiments in rigid bent-core nematic liquid crystals found approximately 1 order of magnitude decrease of K_{22} compared to K_{11} (Majumdar *et al.*, 2011; Salamon *et al.*, 2012) For example, 2 °C below the isotropic-nematic transition of a bent-core nematic material the elastic constants of splay, twist, and bend director deformations, respectively, were found to be $K_{11} = 3.1$ pN, $K_{22} = 0.31$ pN, and $K_{33} = 0.88$ pN. The order of magnitude reduction of the twist elastic constant was attributed to the nanoscale tilted smectic clusters we described in Sec. II.1.a. It was argued that *SmCP*-type clusters are chiral (as we will show in the next section) and therefore are acting as dopants and may selectively soften K_{22} (Majumdar *et al.*, 2011).

5. Dielectric properties

Dielectric spectroscopy is a useful technique to obtain important information about the magnitude and dynamics of dipole moments of certain linkage groups of the molecules and have been studied on BCNs as well (Salamon *et al.*, 2010; Tadapatri *et al.*, 2010b; Jang *et al.*, 2011; Gleeson *et al.*, 2014; Srivastava *et al.*, 2017).

Figure 15 shows a summary of the most important features of the dielectric behavior of a BCN with one chlorine atom in the central ring, which has a negative dielectric anisotropy. Two dispersions can clearly be identified in the parallel and one in the perpendicular component (and one more has to be present at higher frequencies in each component). This implies that the BCNs exhibit more dispersions than

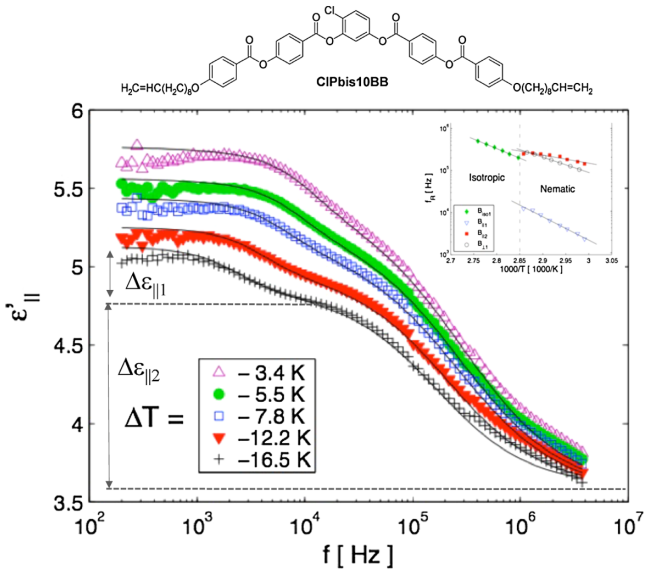

FIG. 15. Summary of dielectric measurements on a bent-core nematic material. Top: Molecular structure and abbreviated name of the material. Main panel: Frequency dependence of the real part of the dielectric constant parallel to the director at selected temperatures below the *I*-*N* transition. Upper inset: Temperature dependence of the relaxation frequencies in the isotropic and nematic phases. From Salamon *et al.*, 2010.

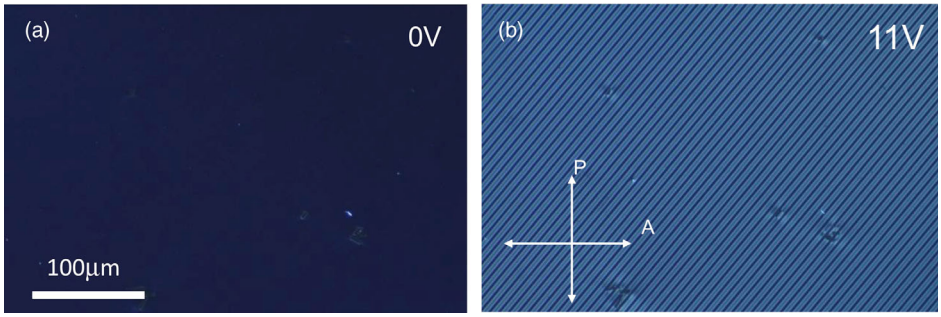

FIG. 16. Textures of the BPIII phase of a BCN doped with 2 wt % chiral dopant (BDH1281) in 10 μm film with in-plane electrodes. The texture is black at (a) zero electric fields and becomes birefringent when (b) 11 V in-plane voltage is applied. From Jákli, 2013.

rod-shaped materials. In addition, the relaxation frequencies are found to be substantially lower; the lowest one in the parallel component falls at a few kHz range. It is unclear whether the low frequency relaxation can be associated with dynamics of individual molecules or it should be the consequence of a collective mode of the smectic clusters.

An even slower and stronger relaxation mode in $\varepsilon'_{\|}$ have been seen in the cyanoresorcynol based BCN with an azoxy terminal chain (Tadapatri, Krishnamurthy, and Weissflog, 2010). Recent dielectric measurements on a bent-core liquid crystal with undisclosed structure found a relaxation response between 10 and 20 Hz with a susceptibility of a few hundred (Marino *et al.*, 2012), which suggests the presence of ferroelectric clusters. In fact, Francescangeli *et al.* (2009) reported a ferroelectric-type electric current response on a BCN with oxadiazole center at a very high-temperature range of the nematic phase and at low frequencies (1–2 Hz). However, one needs to be careful interpreting the current peak as a sign for polarization reversal as at such low frequencies one can observe very similar current peaks even in simply dielectric liquid crystals, such as 5CB due to ionic impurities (Eremin and Jákli, 2013).

6. Bent molecular shape and macroscopic chirality

Polarized optical microscopy (POM) observations in several cases showed regions with different optical properties. Starting from the crossed position of the polarizers and rotating one polarizer slightly (<20°) clockwise, one observes that the texture is comprised of dark and light domains. Rotating the polarizer counterclockwise by the same angle causes the transmitted light intensity to be reversed, i.e., the previously dark domains now appear light and vice versa (Hird *et al.*, 2001; Pelzl *et al.*, 2002; Niori, Yamamoto, and Yokoyama, 2004; Görtz and Goodby, 2005; Takezoe and Takanishi, 2006; Jang *et al.*, 2012). These domains can also be distinguished by illuminating the cell with left or right circularly polarized light in the reflection mode of the microscope. The formation of regions with opposite handedness can be attributed to a macroscopic twist. This twist is usually attributed to a spontaneous chirality breaking, although in some cases the phenomenon was found only after several heating-cooling cycles between the nematic and crystalline states (Liao, Stojadinovic *et al.*, 2005) indicating a possible role of surface memory effect as well. One explanation for the chiral symmetry breaking could be a conformational or "axial" chirality of the bent-shaped molecules. Recent computational studies showed that chiral superstructures could also form by a temperature-driven self-assembly (Hird *et al.*, 2001; Memmer, 2002).

Another example showing the intricate connection between bent-shaped molecules and chirality is the observation that bent-core liquid crystal molecules lead to a decrease of the pitch of a cholesteric LC when they are added as dopants (Thisayukta *et al.*, 2002). Even more, Nakata *et al.* (2003) found the induction of blue phases (BPs), when ordinary chiral nematic (N^*) LCs were doped with achiral bent-core molecules. This apparent increase of the helical twisting power by achiral molecules could (at least partially) be related to a decrease of the twist elastic constant (P. Sathyanarayana *et al.*, 2010; Majumdar *et al.*, 2011) or to the conformational (axial) chirality of the molecules as previously discussed. Achiral bent-core units covalently linked with a chiral cholesterol in one end group through a flexible spacer showed a BPIII phase over a 20 °C range (Yelamaggad *et al.*, 2006) suggesting that the biaxial shape of the molecules is responsible for the stabilization of BPIII. Recent experiments also reported an induction of a BPIII by simply doping achiral BCNs with chiral dopants, finding a wide temperature range (Taushanoff *et al.*, 2010; Van Le *et al.*, 2011) extending to near room temperature. Electro-optical responses (see Fig. 16) showed switching between optically isotropic and birefringence textures in a few tens of milliseconds. It is expected that, by suitable mixtures, polymer stabilization, or by nanoparticle doping, practically viable wide and low-temperature range blue phases can be achieved by using bent-core liquid crystals. These observations may set out new display as well as optoelectronic device applications exploiting the "blue-fog" BPIII.

7. Electrohydrodynamic convections (EHCs)

Application of an electric field to a weakly conducting liquid (such as BCN materials) often results in a convection driven by the Coulomb force acting on space charges (Ramos *et al.*, 1998). Nematic liquid crystals exhibit exceptional richness of EHC phenomena, such as Williams domains (Williams, 1963), and Carr-Helfrich and chevron instabilities (Carr, 1969; Helfrich, 1969, 1971b). In analyzing the electroconvection (EC) features (Éber, Salamon, and Buka, 2016) it is usual to classify four possible combinations: $(--)$, $(+-)$, $(-+)$, and $(++)$, where the first symbol represents the sign of

the dielectric anisotropy $\Delta\varepsilon$ and the second symbol the sign of the conductivity anisotropy $\Delta\sigma$ (Kramer and Pesch, 1996).

In BCN liquid crystals EHC was first studied on the BCN material shown in Fig. 15. It has a negative dielectric anisotropy and very weak conductivity anisotropy that changes sign at two frequencies (Wiant *et al.*, 2005). In samples with initially planar alignment, three nonstandard EC regimes were found in decreasing frequencies (see Fig. 17): "prewavy 1," "prewavy 2," and "parallel stripes." Between the two prewavy states there exists an "empty region" where no instability can be observed. None of these ac field-induced patterns could be explained within the framework of the standard model (Éber, Salamon, and Buka, 2016b) of EHC instabilities. Below 50 Hz at increasing voltages above the parallel stripes regime, first a turbulent state appears, which, however, becomes optically isotropic above 100 V indicating that the periodicity becomes less than the visible light wavelength. Interestingly, however, at even higher voltages the sample becomes birefringent again, which is not yet understood.

Subsequent EHC studies on other BCNs were carried out by a number of research groups (Stannarius *et al.*, 2007; Tanaka *et al.*, 2009; Xiang *et al.*, 2009; Tadapatri, Krishnamurthy, and Weissflog, 2010; Tadapatri *et al.*, 2010a). Studies on a (+ −) material (Heuer *et al.*, 2008) revealed transition between longitudinal and normal rolls. Xiang *et al.* (2009) and Kaur *et al.* (2011) studied an oxadiazole centered BCN with a negative dielectric anisotropy and found a profound change of electrohydrodynamic patterns as the temperature was varied within the nematic phase. The change was interpreted as a result of a uniaxial to biaxial transition, when the relevant anisotropy of electric conductivity changes sign. The observed change in the electrohydrodynamic patterns might well be connected to the appearance of the biaxial order, but one should not rule out other possibilities such as the formation of cybotactic clusters and surface anchoring transitions. The studied material is very similar to C7 and C12, Fig. 8(a), representing a hybrid of the two, featuring the same central bent core and different terminal groups, one with seven carbons, and another with an oxygen and 12 carbons. As already indicated, independent XRD (Francescangeli *et al.*, 2011) and optical (Senyuk *et al.*, 2011) studies of C7 and C12 concluded that these materials are in fact uniaxial and the difference in properties at the low- and high-temperature ends of the nematic range are caused by effects such as the formation of cybotactic clusters (Francescangeli *et al.*, 2011), surface anchoring transitions (Senyuk *et al.*, 2011), and director nonuniformity along the normal to the bounding plates. Since the oxadiazole materials are of a negative dielectric anisotropy, further tests of biaxiality could be based on the study of conoscopic patterns in cells of different thickness and exploration of topological defects as described in Sec. III.A.2.

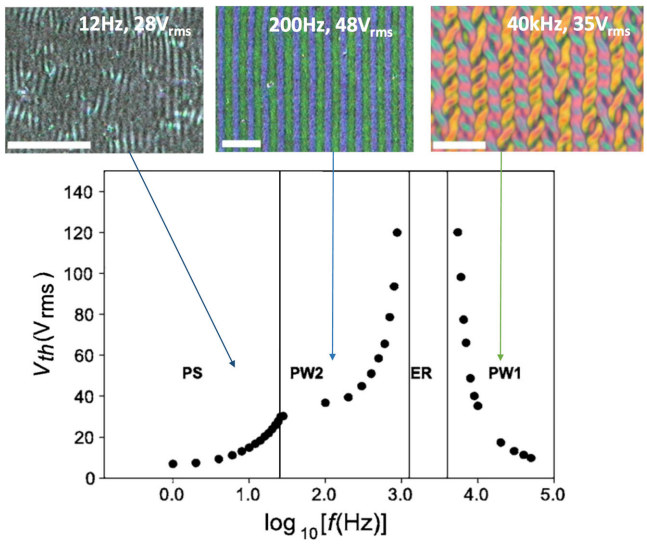

FIG. 17. Summary of the EC patterns in a 15 μm thick BCN film (molecular structure shown in Fig. 15) in planar alignment. PS: parallel stripes; PW: prewavy; ER: empty region. The length scale represents 100 μm in each picture. The rubbing direction is vertical for PS and horizontal for the others. From Wiant *et al.*, 2005.

8. Electromechanical effects

Linear electromechanical effects have been mainly studied in ferroelectric liquid crystals (Jákli, 2010). They are related to piezoelectricity and are due to the lack of inversion symmetry of $N*$, $SmA*$, and $SmC*$ phases of rodlike molecules, and $SmCP$ and SmC_G phases of bent-core molecules. Another linear electromechanical phenomenon, flexoelectricity, connects mechanical flexing and electricity (see Sec. II.A.1).

Measurements on rod-shaped liquid crystals are based on bend or splay director distortions of samples with rigid substrates, induced by the interaction of the flexoelectric polarization with the external electric field-induced bending or splay deformation of samples with rigid substrates. Such measurements typically give $|e_1{-}e_3| \sim 10$ pC/m (Buka and Éber, 2012).

Similar to rod-shaped liquid crystals, most of the flexoelectric measurements in bent-core nematics are also based on measuring linear electro-optical signals due to external electric fields. Converse flexoelectric measurements on calamitic nematics doped by less than 10 wt % BCN molecules found strong (up to sixfold) enhancement of the bend flexoelectric coefficients (Wild *et al.*, 2005; Kundu *et al.*, 2009), indicating 1–2 orders of magnitudes larger bend flexoelectric coefficients of BCNs than for calamitics, in agreement with the larger bend angle of the BCN molecules. On the other hand, $e_3 < 20$ pC/m values were obtained on several pure BCN materials under $E \ll 1$ V/μm dc (Kumar *et al.*, 2009; Van Le *et al.*, 2009) or at high frequency fields (Salter *et al.*, 2011). Measurements on pure BCNs based on the classical hybrid alignment technique (Barbero *et al.*, 1986), where the alignment varies between planar and homeotropic from one substrate to the other, turned out to be unsuccessful, because BCNs fail to form hybrid alignments, but only either planar or homeotropic in case of negative or positive dielectric anisotropies, respectively (Kundu, 2009).

In addition to the conventional techniques that measure the converse flexoelectric effect via field-induced director deformations, a direct method that measures the electric current flowing through a periodically bent BCN liquid crystal film was carried out by Harden *et al.* (2006). This method is based

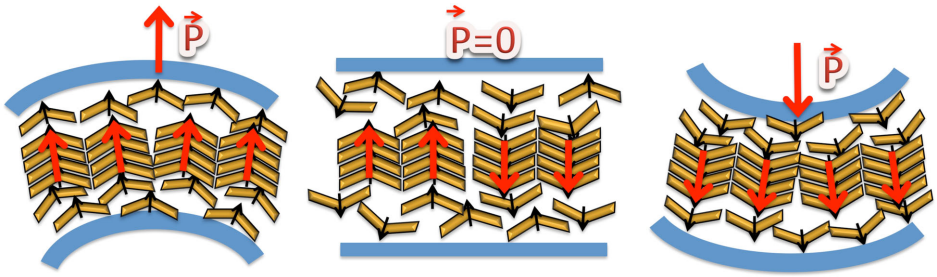

FIG. 18. Schematic of the ferroelectric cluster mechanism proposed to explain the "giant" flexoelectricity. From Harden *et al.*, 2006.

on Meyer's original demonstration of the flexoelectricity and does not require knowledge about the Frank elastic constants, dielectric anisotropy, and birefringence. It was found that the flexing-induced current has the same frequency as the bending (a necessary condition for the flexoelectricity), although the current is not a linear function of the bending amplitude, and it decreases sharply above 10 Hz. Calculating the apparent bend flexoelectric coefficient from the current values below 10 Hz and at high bending values, $e_3 \sim 80$ nC/m was deduced for the BCN shown in Fig. 15. This value is 3 orders of magnitudes larger than measured by Van Le *et al.* (2009) and Kumar *et al.* (2009) with electro-optical method at low fields ($E \ll 1$ V μm^{-1}). By measuring the flexing of a film when an electric field is applied (converse flexoelectric effect) (Harden *et al.*, 2008) basically no flexing was detected below a critical electric field of $E \sim 1$ V μm^{-1}; however, from the bending under $E \gg 1$ V μm^{-1} electric fields, $e_3 \sim$ 60 nC/m was obtained, which is a similar magnitude to e_3 measured by the direct flexing method. These observations indicate a novel linear electromechanical effect above a threshold and at low frequencies, providing orders of magnitude larger effective flexoelectric constant than Meyer's dipolar mechanism.

Concerning the physical mechanism of this apparent "giant" flexoelectricity, Kumar *et al.* (2009) proposed that it could be associated with a quadrupolar contribution of apolar smectic clusters. In this model the flexoelectric coefficients are expected to scale linearly with the number of molecules in a cluster, if a sufficiently large external mechanical distortion could reorient them. In contrast to this, Harden *et al.* (2006) attributed this effect to polar smectic clusters. According to this "polar cluster model" (see Fig. 18), bending biases the dipoles of the bent-core molecules outside the smectic clusters according to the dipolar mechanism. Through the steric interaction between the molecules outside and inside the clusters this effect leads to flipping of the polarization of the clusters above a threshold and at sufficiently low frequencies. This mechanism relies on the ferroelectricity of the clusters and can explain why the effect was observed only at large thresholds and low frequencies, two conditions that were present only in measurements of Harden *et al.* (2006, 2008). Since there are still discussions about the interpretation of the giant flexoelectricity (Castles, Morris, and Coles, 2011, 2013; Palffy-Muhoray, 2013; Addis *et al.*, 2016), further studies needed to fully exploit these effects both for theoretical and practical points of view.

B. Bent-core smectics

Smectic phases of bent-core molecules were discussed in a review by Eremin and Jákli (2013). In a typical smectic phase of rodlike molecules, there are two types of order: orientational order and layer order. For smectic phases formed by bent-core molecules, we must ask whether the molecular shape leads to any additional order. There are many possible combinations of order parameters as we discuss in this section.

As discussed in Sec. III.A the formation of a nematic phase usually requires either an acute opening angle with $\theta \leq 60°$ or an obtuse angle with $\theta \geq 130°$. When the opening angle is as large as 160°, the material may form nonpolar (rodlike) smectic phases, such as *SmA* or *SmC*, which at even lower temperatures as the opening angle decreases, may form polar smectic phases (Eremin *et al.*, 2004). Generally, if the opening angle is between 110° and 130°, the molecules form to superparaelectric, ferroelectric, and antiferroelectric smectic phases directly below the isotropic phase.

1. Orthogonal smectic phases

For rod-shaped LC materials there is only one smectic phase with fluid in-layer order, where in each layer the average director $\hat{\boldsymbol{n}}$ is orthogonal to the smectic layers, i.e., parallel to the smectic layer normal $\hat{\boldsymbol{k}}$ and is called an *SmA* phase. In bent-core materials, such a nonpolar *SmA* phase [see Fig. 19(a)] is usually found for molecules with larger than 160° opening angle. When the opening angle is smaller than ~160°, the transverse molecular directions may be aligned with some net polar order $\boldsymbol{P}$ within each layer. The layer polarization $\boldsymbol{P}$ is due to long-range order of the molecular bend direction inside a layer. Depending on the interlayer sequence of the polar order, a number of different *SmAP*-type phases can appear. The structures of the three most often observed phases are schematically illustrated in Figs. 19(b)–19(d).

In the $SmAP_R$ phase [Fig. 19(b)] a random sequence of the layer polarization appears in subsequent layers. When the polarity of strong enough electric fields applied across the electrodes is quickly reversed, they produce single polarization current peaks similar to macroscopically ferroelectric phases, but no residual polarization remains after field removal. In homeotropically aligned samples (layers are parallel to the film surface) the texture appears dark between crossed polarizers. In-plane electric fields induce birefringence that disappears at zero field (Shimbo, Takanishi *et al.*, 2006; Shimbo, Gorecka *et al.*, 2006). The phase is also characterized by a large dielectric constant ($\varepsilon' \sim 40$), and a strong field-induced second harmonic signal (SHG). Based on these, it was suggested they

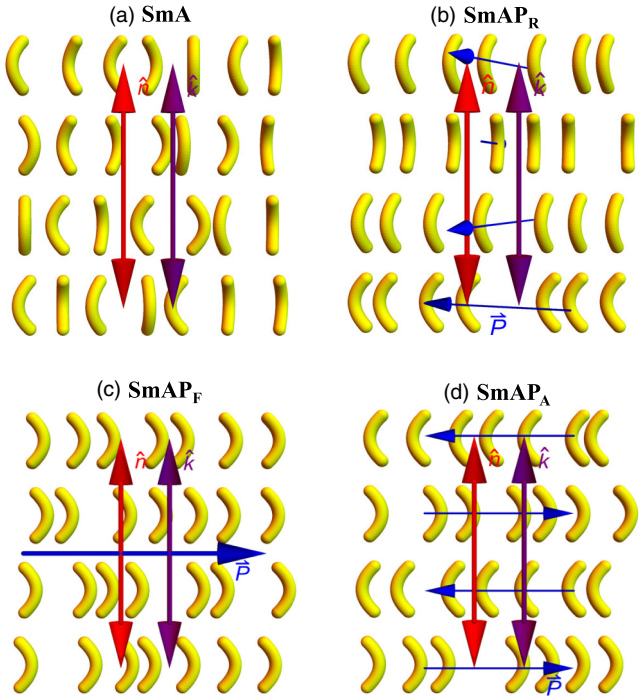

FIG. 19. Smectic-*A* (*SmA*) phases of bent-core molecules. (a) *SmA*, (b) $SmAP_R$, (c) $SmAP_F$, and (d) $SmAP_A$.

have a random interlayer order (Shimbo, Takanishi *et al.*, 2006). Later, such $SmAP_R$ phases were observed in a number of materials (Panarin *et al.*, 2010, 2011; Guo, Gomola *et al.*, 2011; Shanker *et al.*, 2011). A randomized polar smectic phase showing antiferroelectric-type switching (two current peaks in each half period of ac fields) was also observed by Gomola *et al.* (2010) and can be called $SmAP_{AR}$. They probably consist of randomly aligned clusters with antiferroelectric order. All these materials have at least one long (with more than 12 carbons) terminal chain which is responsible for decoupling the in-layer polar order between subsequent layers.

If the polarization vectors are aligned from layer to layer, as in Fig. 19(c), then the material forms a *ferroelectric* phase. It is labeled as a $SmAP_F$ phase, with the letter *A* indicating that $\hat{\boldsymbol{n}}$ is parallel to $\hat{\boldsymbol{k}}$, and the P_F indicating that the polar order is ferroelectric.

The ferroelectric $SmAP_F$ phase corresponds to the structure proposed originally by Sekine, Niori *et al.* (1997a), but observed only recently by Reddy *et al.* (2011) and Guo *et al.* (2011). This phase is rarely observed, because it requires the stabilization of anticlinic packing of adjacent layers. An anticlinic arrangement of the arms in neighbor layers suppresses the out-of-layer fluctuations, i.e., decreases the entropy of the system. Molecules that favor $SmAP_F$ can be obtained with only a single alkyl tail to provide more space for the tails and thus forcing the rigid rods to occupy larger volumes by packing them orthogonally (Reddy and Sadashiva, 2002; Sadashiva *et al.*, 2002), and reducing the tendency for antiferroelectric layer ordering by terminating the tail with a carbosilane group to suppress the interpenetration of tails in adjacent layers (Robinson *et al.*, 1998). Films in a $SmAP_F$ phase with smectic layer along the film surface have only four brush ($s = 1$) defects, which indicate polar order.

Electro-optic responses of $SmAP_F$ in a sandwich cell show thresholdless (V-shaped) switching as a consequence of complete screening of the applied field by the net polarization;

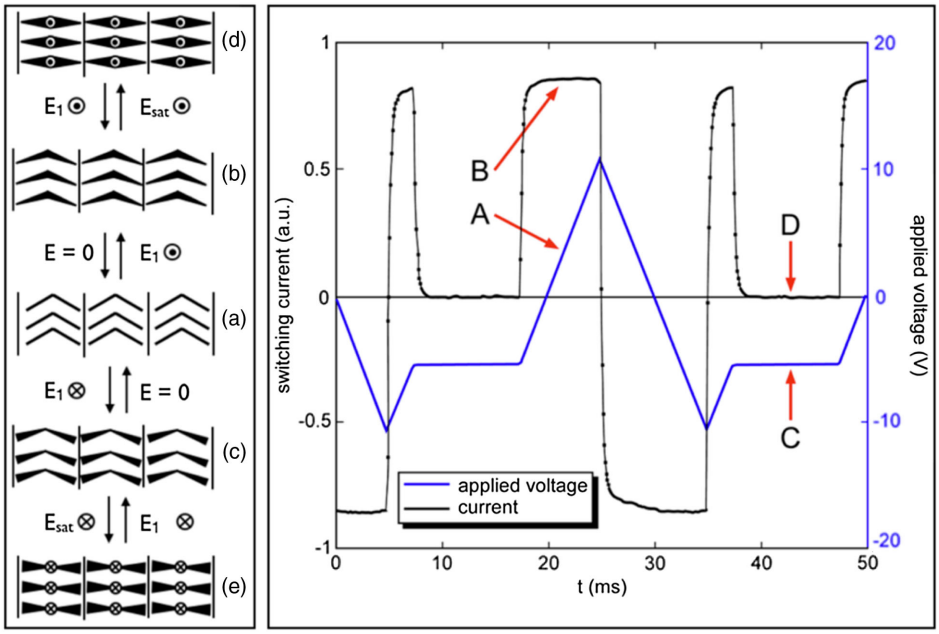

FIG. 20. Illustration of the V-shaped electro-optic switching in the $SmAP_F$ phase. (Left) Cartoon showing the reorientation of the polar axis in a bookshelf-aligned cell (substrates parallel to the page) in response to applied electric fields. (a) Bookshelf layer structure with *P* parallel to the substrates at $E = 0$; (b), (c) partial reorientation of *P* with applied field E_1 (subsaturation); (d), (e) at E_{sat} (saturation) with *P* along *E*. (Right) Electrostatic V-shaped switching with optical latching. *A*: Applied voltage (blue) changing with time; *B*: current response (black) to voltage ramp (constant current); *C*: constant applied voltage results in *D*: no current and essentially no energy dissipation (latching). From Korblova *et al.*, 2017.

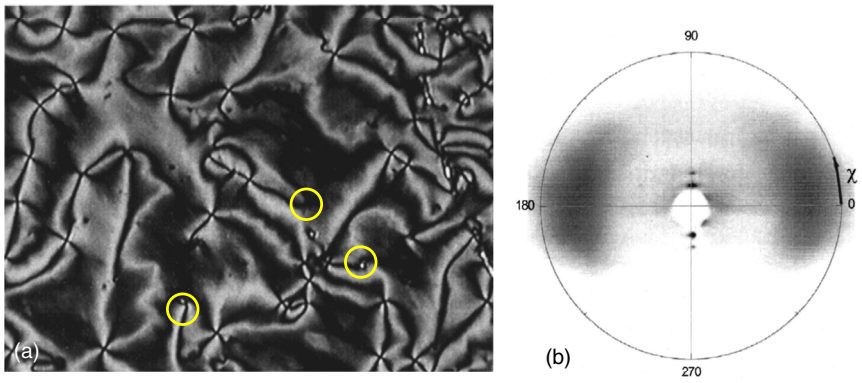

FIG. 21. Evidence of the existence of the $SmAP_A$ phase. (a) Schlieren texture of the $SmAP_A$ phase with smectic layers parallel to the substrates. The existence of two brush defects (shown by yellow circles). (b) X-ray pattern of a sample with director oriented vertically. The small-angle peaks in the vertical direction are proof of the orthogonal smectic structure. From Eremin *et al.*, 2001.

see Fig. 20 (Shen *et al.*, 2011; Korblova *et al.*, 2017). In films with rubbed polyimide-coated glass plates, the layers orient perpendicular to the substrates, with the ferroelectric polarization P parallel to the plates. Application of increasing electric field across the substrates causes a smooth analog change in birefringence without any rotation of the optic axis until saturation, where the polarization is oriented normal to the plates, along the field (Fig. 20, left). This is an example of electrostatic V-shaped switching, as first reported for rod-shaped (calamitic) ferroelectric $SmC*$ materials with high polarization (Rudquist *et al.*, 1999; Korblova *et al.*, 2017). This V-shaped switching gives uniform, phase-only modulation of incident polarized light with no rotation of the optic axis, which is a potentially useful effect, because no power is required to maintain the optical state. $SmAP_F$ materials also show a large dielectric constant (>1000) and SHG activity, which are also potentially useful (Guo, Gomola *et al.*, 2011).

When the polarization vectors alternate in sign from layer to layer, as in Fig. 19(d), then the material forms an *antiferroelectric* phase. It is labeled as a $SmAP_A$, with the P_A indicating that the polar order is antiferroelectric. The first example of the orthogonal antiferroelectric $SmAP_A$ phase was found by Eremin *et al.* (2001) using x-ray and electro-optical techniques on a BC material with a cyano-resorcinol center and fluorinated outer rings. It shows double hysteresis and two current peaks in each half period of triangular wave electric fields, features that are characteristic to antiferroelectric materials. It is also biaxial and shows the so-called Schlieren texture in homeotropic alignment. Such texture is characteristic to tilted smectic such as the SmC phase, but there only four brush ($s = 1$) defects can exist, since the projection of the director to the layers (c director) is a real vector, so its rotation by 180° would not be identical to the original structure, excluding $s = 1/2$ defects. As indicated by yellow circles in Fig. 21(a), the Schlieren texture of the $SmAP_A$ has two brush ($s = 1/2$) defects, which are compatible only with anticlinic structures, where the c director cancels in molecular scale. Although this could still be compatible with a SmC_A-type structure, x-ray scattering measurements [see Fig. 21(b)] show proof of the orthogonal phase. Additionally, it was found that the layer spacing has weaker temperature dependence and more defined layer structure [higher-order peaks in the small angle, as seen in Fig. 21(b)] than of a conventional SmA phase. The existence of the $SmAP_A$ phase has been shown with other cyano-resorcinol centers (Weissflog *et al.*, 2005; Shanker *et al.*, 2011) and acetophenone units (Guo, Gomola *et al.*, 2011).

In addition to the three $SmAP$-type phases discussed above, there are two other $SmAP$ phases with uniform in-plane director order. They are (i) the short-pitch helical $SmAP_\alpha$ phase, which is uniaxial and can be stabilized by long-range interactions (Pociecha *et al.*, 2003), and experimentally observed by Panarin *et al.* (2011); and (ii) the biaxial bilayer $SmAP_2$ phase observed experimentally below the $SmAP_\alpha$ phase of a cyano-resorcinol bent-core compound (Panarin *et al.*, 2011).

2. Tilted smectic phases

Phases in which the director $\hat{\boldsymbol{n}}$ is tilted with respect to the smectic layer normal $\hat{\boldsymbol{k}}$ have some anisotropy within the smectic layer plane, and this anisotropy tends to align the transverse molecular directions. We can then classify the phases based on the relationship among the $\hat{\boldsymbol{n}}$, $\hat{\boldsymbol{k}}$, and $\boldsymbol{P}$ directions.

a. SmCP phases

One common situation is that $\boldsymbol{P}$ is perpendicular to both $\hat{\boldsymbol{n}}$ and $\hat{\boldsymbol{k}}$, as in all the structures shown in Fig. 22. These structures are normally called *tilted*, and they are labeled as $SmCP$. In this notation, the letter C indicates tilt as in the conventional SmC phase (perhaps standing for *clinic*), and the letter P indicates polar order. This was the second bent-core or "banana" phase and was originally labeled as the B_2 phase (Pelzl, Diele, and Weissflog, 1999). The phases can then be further classified based on the relationship between the tilt and polarization directions from layer to layer. If the tilt is in the same direction from layer to layer, the phase is called *synclinic* and is labeled C_S. By contrast, if the tilt alternates in a direction from layer to layer, the phase is called *anticlinic* and is labeled C_A. Likewise, if the polarization vectors are the same from layer to layer, the phase is ferroelectric (P_F); if the polarization vectors alternate from layer to layer, the phase is antiferroelectric (P_A). Hence, there are four distinct tilted polar phases (SmC_sP_F, SmC_aP_F, SmC_sP_A, and SmC_aP_A) as shown in Figs. 22(a)–22(d).

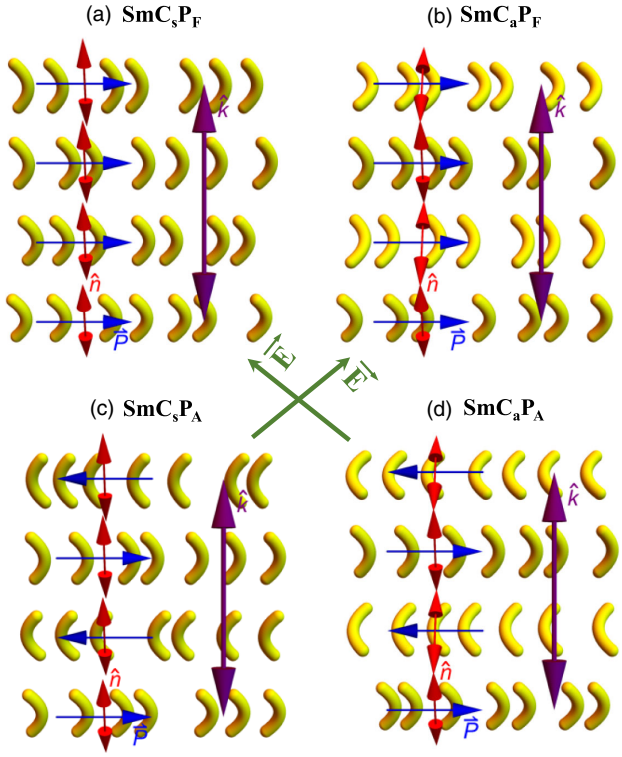

FIG. 22. Tilted, polar smectic phases of bent-core molecules. (a) SmC_sP_F, (b) SmC_aP_F, (c) SmC_sP_A, and (d) SmC_aP_A.

As pointed out by Link *et al.* (1997), the relationship among the $\hat{\boldsymbol{n}}$, $\hat{\boldsymbol{k}}$, and $\boldsymbol{P}$ directions in *SmCP* phases implies that the smectic layers are chiral. This chirality is spontaneous; i.e., it occurs randomly in a right- or left-handed sense, even if the individual molecules are not chiral. It can be characterized by a chiral order parameter (Xu *et al.*, 2001)

$$\chi = 2[(\hat{\boldsymbol{k}} \times \hat{\boldsymbol{n}}) \cdot \hat{\boldsymbol{p}}](\hat{\boldsymbol{k}} \cdot \hat{\boldsymbol{n}}), \tag{21}$$

which is a pseudoscalar between -1 and 1. Here $\chi = 0$ indicates no chirality, while $\chi = \pm 1$ is the maximum chirality in the two mirror-image senses. In a SmC_sP_F or a SmC_aP_a phase, the chirality is the same from one layer to the next, and hence the material becomes homochiral. By contrast, in a SmC_aP_F or SmC_sP_A phase, the chirality alternates in sign from one layer to the next. This structure is normally called *racemic* [although Selinger (2003) argued that *antichiral* would better describe the rigid alternation between successive layers].

The majority of the bent-core smectic materials are tilted for several possible reasons. First, the rigid bent-core molecules include several benzene rings (typically 4–6), which create steric bumps, and these bumps provide better packing when the molecules are tilted by about 30° (the classic cannonball problem). Second, the long flexible alkyl or alkyl-oxy tails at both ends are wider than the rigid core, which therefore should tilt to provide tighter packing.

SmCP phases typically show antiferroelectric ground states (Link *et al.*, 1997; Jákli *et al.*, 1998, 1999), as usually they have large layer polarizations ($P > 2$ mC/m^2), which favor antiferroelectric arrangement due to strong dipole-dipole interactions. Textures of the synclinic (s) antiferroelectric (A) SmC_sP_A phase usually consist of fan-shaped domains decorated with a few micron wide stripes, attributed to oppositely tilted synclinic domains (Link *et al.*, 1997). In the anticlinic (a) antiferroelectric (A) SmC_aP_A phase the optical axis is parallel to the layer normal. Because of the achiral nature of the molecules, in SmC_aP_A there are equal volumes of left and right domains. The antiferroelectric ground state can be reversibly switched to ferroelectric (F) by applying sufficiently strong (typically larger than 3–5 V/μm) and slow ($f < 10$ kHz) external electric fields. During the A-F switching the polarization has to be reversed only in every other layer, which can happen by rotating the director around the tilt cone by 180°. This way an originally anticlinic state becomes synclinic, and a synclinic ground state becomes anticlinic, corresponding to $SmC_sP_A \rightarrow SmC_aP_F$ and $SmC_aP_A \rightarrow SmC_sP_F$. Such electric field-induced transitions are indicated by green arrows in Fig. 22. The optic axis does not change when racemic ferroelectric states are switched to opposite directions, whereas the optic axis rotates by twice the tilt angle in homochiral ferroelectric states (Link *et al.*, 1997; Jákli *et al.*, 1998).

All states shown in Fig. 22 are uniform, i.e., optically clear. Experiments, however, showed that the synclinic structures (the racemic SmC_sP_A and the chiral SmC_sP_F) scatter light, whereas the anticlinic structures (the chiral SmC_aP_A and the racemic SmC_aP_F) are transparent (Jakli *et al.*, 2002; Etxebarria *et al.*, 2003). This effect is related to the achiral nature of the molecules and disappears when a chiral dopant is added to the achiral bent-core molecules (Jakli *et al.*, 2002). In the absence of chiral dopants in the racemic synclinic state there is equal probability of left and right tilts, and in the homochiral state there is equal probability of left and right homochiral domains, which correspond to oppositely tilted ferroelectric states. Depending on the cooling rate, the size of oppositely tilted domains can be in the several micrometer range. As these differently tilted micron-size domains are separated by defects with smaller refractive index, they scatter white light. The switching is reversible and may be fast (well below 100 μs) (Jákli, Chien, Kruerke, Rauch *et al.*, 2003) and can be observed without polarizers, thus offering polarizer free scattering-type displays. In the racemic SmC_sP_A phase the switching takes place between the opaque OFF state, and the transparent SmC_aP_F ON states. For the homochiral SmC_aP_A phase the OFF state is transparent and the SmC_sP_F ON state is opaque. The scattering efficiency of bent-core smectics shows only weak thickness dependence in the 2–10 μm range. Thinner films have better transmission and require smaller driving voltages (~10–15 V for the 2 μm film), so they are attractive for applications such as privacy windows, projectors, and 3D-TV goggles that require shutters.

In addition to these promising light scattering properties, anticlinic and synclinic domains also differ in their birefringence. Since the *SmCP* phase generally appears directly below the isotropic phase, the tilt angle is $\theta > 30°$ and anticlinic domains have small birefringence ($\Delta n_a < 0.05$) (Macdonald *et al.*, 1998). By contrast, synclinic domains have a birefringence comparable to calamitic molecules ($\Delta n_s > 0.1$). In fact, in materials with large tilt angle ($\theta \sim 45°$) and small opening

angle ($\Phi \sim 109°$) it was observed that the anticlinic state was optically isotropic ($\Delta n = 0$) (Jákli and Fodor-Csorba, 2003; Nair *et al.*, 2008). Notably, such an optically isotropic phase is chiral even without chiral molecules (Link *et al.*, 1997) and spontaneously splits into optically active domains of opposite handedness (Jákli, Huang *et al.*, 2003). These antiferroelectric LCs can be reversibly switched between optically isotropic and birefringent states (Shreenivasa and Sadashiva, 2002; Kang and Kim, 2013). Recently wide temperature range optically isotropic SmC_aP_A mixtures have been obtained in wide temperature range down to below −20°C (Bergquist *et al.*, 2017; Wang *et al.*, 2018), which makes promising the future applications of bent-core smectic (BCS) materials as transparent and reflective liquid crystal displays as well as switchable windows (Jákli, 2002).

Even though the majority of BCS materials conserve their chirality during electric field-induced switching, for moderately long ($12 < n < 16$ carbon atoms) terminal chains the layer chirality changes after over 1000 voltage cycles. Racemic domains can be rendered chiral by surface interactions too (A. Jákli *et al.*, 2001; Bault *et al.*, 2002). As pointed out by Lansac *et al.* (2003) the synclinic SmC_sP_A structure enables out-of-plane fluctuations, thus increasing the entropy and decreasing the free energy. This effect becomes less important at lower temperatures, explaining that the synclinic phases often transform to the anticlinic SmC_aP_A state on cooling or appear first in heating (Heppke *et al.*, 1997; Macdonald *et al.*, 1998). The field-induced switching between racemic and chiral states was explained based on the notion that the synclinic state is more stable (Jákli, Krüerke *et al.*, 2001). Accordingly, when a field strong enough to switch to the ferroelectric state is applied for an extended time, the material prefers to be synclinic, which is chiral. The transformation is facilitated by the application of alternating square-wave fields. After field removal this chiral state becomes antiferroelectric and anticlinic, so it can only be metastable. The more stable racemic state can reform by a nucleation process or it can be driven back to the synclinic racemic state under triangular electric fields, because during repeated switching it stays longer in the antiferroelectric than in the ferroelectric state (Jákli, Krüerke *et al.*, 2001). All these chirality transformations mean that during the switching the molecules do not strictly rotate about the layer normal on the tilt cone, but, to some extent, also rotate around their long axes (Jákli, 2002; Gorecka *et al.*, 2005; Ortega *et al.*, 2011). The rotation of the director around the tilt cone preserves the layer chirality, whereas during rotation around the long axis the chirality changes sign. This rotation is faster than the rotation around the cone and is permissible only in racemic domains. Indeed, it is usually observed that racemic switching is faster than chiral switching (Chattham *et al.*, 2010). In some examples both the opaque racemic A and the transparent chiral AF states were found to be stable and could be interchanged (Heppke *et al.*, 1999; Jákli *et al.*, 2000a), or the sign of the layer chirality could even be flipped (Martin *et al.*, 2004). This suggests their possible use in optical storage devices or multistable electronic devices, such as e books, that use energy only during retransformation between chiral and racemic states.

We note that, in addition to compounds showing ferroelectric and antiferroelectric switching, materials with multistage ferrielectriclike switching were found in bent-core 2-methyl-1,3-phenyl-enediamine derivatives (Findeisen-Tandel *et al.*, 2008; Stern, 2009; Stern *et al.*, 2009). In this case, although the field-free state is anticlinic antiferroelectric, the transition into the ferroelectric synclinic state occurs via an intermediate ferrielectric state. The layer structure of this state is characterized by a repeating three-layer unit consisting of two layers with synclinic tilt of the mesogens and parallel alignment of the molecular bows, followed by a third layer that is anticlinic and antiparallel to the two. The multistage switching mechanism is based on a frustration imposed by the competition between the long-range dipole-dipole interactions, favoring antiparallel alignment of the dipoles, and steric interactions, favoring synclinic interlayer interface (Stern, 2009). Up to now no ground state ferrielectric phases have been found in bent-core liquid crystals.

Rod-shaped molecules show optical activity (rotation of the polarization of light passing through the material) only if the material contains chiral molecules, such as in cholesteric or $SmC*$ phases. $SmCP$ phases of achiral bent-shaped materials in their homochiral layer structures however can show optical activity. By observing bent-core liquid crystal films between slightly uncrossed polarizers, it is often found that the textures split into darker and brighter domains (Imase, Kawauchi, and Watanabe, 2001; Huang *et al.*, 2002; Kumazawa *et al.*, 2004a; Liao, Stojadinovic *et al.*, 2005; Reddy *et al.*, 2011). Such optical activity might be the result of twisted or propeller shaped molecules as illustrated by Earl *et al.* (2005). An alternative model was proposed by Ortega *et al.* (2003) by modeling the SmC_aP_A with a locally achiral dielectric tensor, where the optical axis is rotating with a pitch of two layers. This model can also lead to observable optical rotation, indicating that there might be no need for the concept of conformation chirality to explain the optical activity in the fluid tilted smectic phases. On the other hand, experiments on birefringent SmC_sP_F samples (Jákli, Huang *et al.*, 2003) showed that the size of the domains with opposite optical rotation is typically in the range of 100–300 μm, whereas the size of domains with uniform layer chirality is an order of magnitude smaller, and the domain boundaries do not even correlate to those of different layer chirality. This challenges the layer-scale chirality concept or indicates another possible mechanism, such as the conformational chirality.

Chirality can also be introduced when one or more chiral carbons are incorporated in the molecules (Link *et al.*, 1997; Gorecka *et al.*, 2000; Nakata *et al.*, 2001; Jákli, 2002; Lee *et al.*, 2003; Gesekus *et al.*, 2004; Kumazawa *et al.*, 2004a; Lagerwall *et al.*, 2004; Reddy, Sadashiva, and Baumeister, 2005). In some cases the handedness of the homochiral structures was found to be very sensitive to chiral dopants (Link *et al.*, 1997) or to chiral surfaces (Jákli, Nair *et al.*, 2001). However, racemic layer structures may be formed by enantiomeric chiral molecules (Binet *et al.*, 2003), indicating that the molecular chirality has no or minor effect on the overall layer chirality and can only bias the otherwise degenerate tilt directions. Concerning polar order, in addition to the layer polarization P_l, another polarization P_c, due to the chiral and tilted molecular structure, may exist (Binet *et al.*, 2003). In the antiferroelectric racemic domains, P_l averages out but, due to the synclinic order and the molecular chirality,

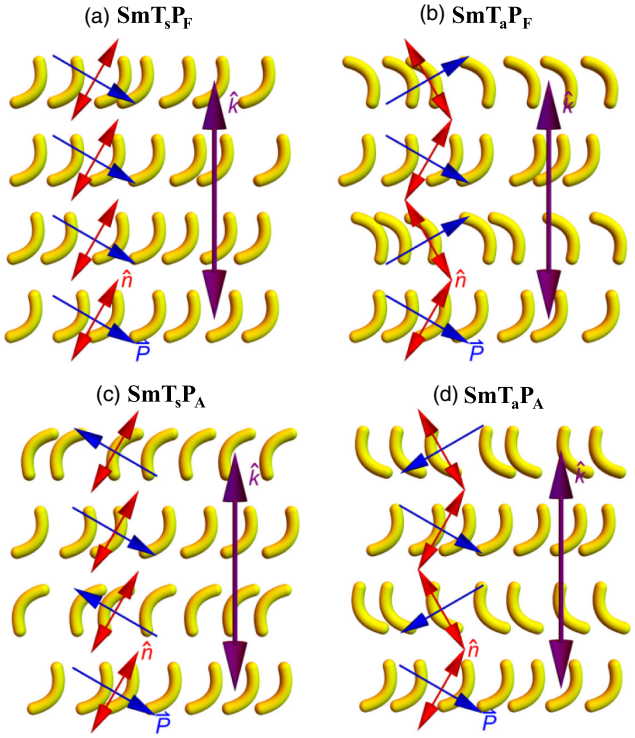

FIG. 23. Tipping (leaning), polar smectic phases of bent-core molecules. (a) SmT_sP_F, (b) SmT_aP_F, (c) SmT_sP_A, and (d) SmT_aP_A.

a P_c normal to the tilt plane, such as in the calamitic $SmC*$ phase, is possible. On the other hand, in the anticlinic ferroelectric state P_c vanishes, leaving only a P_l. For binary mixtures of an achiral and a chiral bent-shaped material, P_c has been measured and found to be an order of magnitude smaller than P_l (Jákli *et al.*, 2006). This result makes sense, since P_c is a secondary order parameter (due to tilt), whereas P_l is a primary order parameter (due to tight packing requirements).

In the case of achiral bent-core molecules, where the value of polarization is not determined by the tilt, the electric field is not expected to increase the polarization through increasing tilt (electroclinic), unlike calamitic $SmC*$ materials (Meyer and Garoff, 1977). Experimentally a high field-induced suppression of the director tilt is observed on one BCS with SmC_sP_A ground state (A. Jákli *et al.*, 2001). The metastable phase with zero director tilt relaxes back to the tilted phase only slowly.

Freely suspended smectic films are systems to study mesophase behavior of smectics and phase transitions in quasi two dimensions (Sonin, 1998). Stable films are usually formed by smectic liquid crystals. Controlling the number of smectic layers, which are parallel to the film, can precisely set the film thickness. These features make freely suspended films vital for investigation of polar order, elastic and rheological properties by using optical microscopy, ellipsometry, and x-ray diffraction. In particular, the direction of the molecular tilt and polarization can be determined by means of depolarized light microscopy at an oblique incidence. Antiferroelectric SmC_SP_A freely suspended films were found to show a strong odd-even effect (Link *et al.*, 2000), where the residual polarization was aligned along (perpendicular) the tilt director in films of an even (odd) number of layers. It was also shown that the antiferroelectric order of the layers extends down to thickness of two molecular layers followed by a breaking of layer chirality (Link *et al.*, 1997). Occasionally freestanding films have a very small residual polarization ($P_r = 1.8$ nC/cm^2), while no polarization is observed in bulk (Stannarius, Langer, and Weissflog, 2002; Stannarius, Li, and Weissflog, 2003). Because P_r does not depend on the film thickness, it cannot be explained by the surface-induced polarization typical for the antiferroelectric phases (Link *et al.*, 1997; Stannarius, Langer, and Weissflog, 2002). The origin of this weak spontaneous polarization is not yet understood.

b. SmTP phases

Another theoretical possibility for the arrangement of $\hat{\boldsymbol{n}}$, $\hat{\boldsymbol{k}}$, and $\boldsymbol{P}$ vectors is that they are all in the same plane as in all the structures shown in Fig. 23. This arrangement is normally called *leaning* or *tipping*, and it can be represented by the letter T for tipping (Zhang, Diorio *et al.*, 2012). By analogy with the previous case, we can classify phases based on whether the tipping direction is the same or alternating from layer to layer, as well as on whether the polar order is the same or alternating from layer to layer. Hence, there can be four distinct SmT_sP_F, SmT_aP_F, SmT_sP_A, and SmT_aP_A phases as shown in Figs. 23(a)–23(d). These phases are not chiral.

c. SmCTP phases

Finally, a bent-core smectic phase might have $\boldsymbol{P}$ at an oblique angle with respect to the plane of $\hat{\boldsymbol{n}}$ and $\hat{\boldsymbol{k}}$ as in Fig. 24. In that case, the phase is both tilted and tipping. Based on early predictions of de Gennes (1974), this structure is called SmC_G (for generalized). Once again, we can distinguish phases based on whether the tilt, the tipping, and the polar order are the same or alternating from layer to layer. For that reason, Fig. 24 shows eight possible phases.

Experimental evidences for the $SmCTP$ (SmC_G) phase were found both in freestanding films (Chattham *et al.*, 2010) and in bulk samples (Jákli, Krüerke *et al.*, 2001; Gorecka *et al.*, 2005; Vaupotič *et al.*, 2007). This phase is exhibited by many derivatives of 2-nitro- and 2-cyano-resorcinols (Weissflog *et al.*, 1998; Pelzl, Diele, and Weissflog, 1999; Jákli *et al.*, 2000b; Reddy and Sadashiva, 2002; Sadashiva and Amaranatha Reddy, 2003; Shreenivasa and Sadashiva, 2003a, 2003b; Umadevi and Sadashiva, 2005) that show the characteristic growth of spiral and other helical domains obtained on slow cooling of the isotropic liquid (also known as B_7 textures) (Pelzl, Diele, and Weissflog, 1999). The $SmCTP$ materials are mainly ferroelectric (Bedel *et al.*, 2000, 2001, 2002; Walba *et al.*, 2000; Rauch *et al.*, 2002), although a few examples for antiferroelectric structures were also found (Heppke, Parghi, and Sawade, 2000a, 2000b; Shankar *et al.*, 2001; Jákli, Nair *et al.*, 2003), and in some cases a transition between ferroelectric and antiferroelectric phases has been seen (Nádasi *et al.*, 2002; Rauch *et al.*, 2002; Pelzl *et al.*, 2004). In the homolog series of symmetrical bent-core compounds containing terminal n-alkyl carboxylate groups, an interesting odd-even effect was found: when n is an odd (even) number, anticlinic (synclinic) structures form. This arises from an entropic mechanism that favors out-of-layer fluctuations. For odd (even) n the end segments of the neighbor molecules are

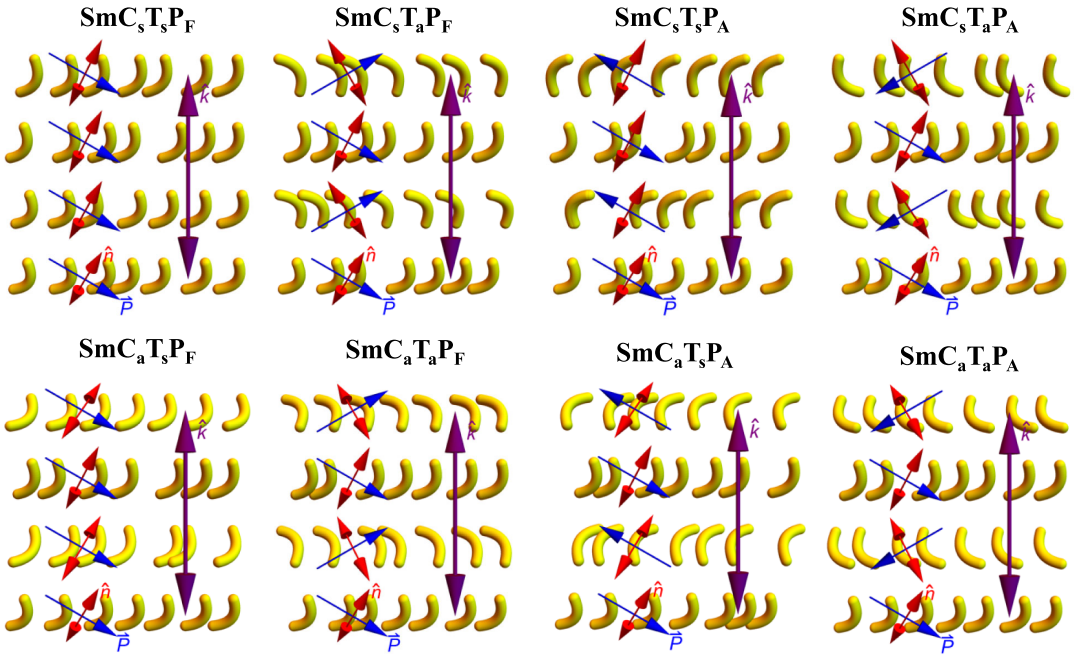

FIG. 24. Generalized smectic phases of bent-core molecules with tilt, tipping (leaning), and polar order.

parallel to each other for anticlinic (synclinic) structures (Umadevi, Jákli, and Sadashiva, 2006b).

3. Modulated smectic structures

As a full divergence term, the polarization splay affects the anchoring of the molecules at the boundaries of the liquid crystalline domains. In ferroelectric smectic $SmCP_F$ phases with large polarization ($P_o > 1$ mC/m^2), the polarization may form a splay. The resulting state is a striped domain structure formed by polarization-splayed domains separated by defect walls with reduced packing efficiency. To compensate for it, the tilt decreases at the boundaries of the stripes, resulting in a local change of the layer thickness, which drives the undulation of the smectic layers (Coleman *et al.*, 2003). Different combinations of the tilt and polarization direction in the adjacent splay stripes (see Fig. 25) yield various synclinic and anticlinic structures (Coleman *et al.*, 2008). Using this mechanism, nontilted structures are not expected to have layer undulations, since there is no local layer dilation. However, recently there have been reports about strongly asymmetric bent-shaped materials with $SmAP_F$-Sm$AP_{F\times\mathrm{mod}}$ (Zhu *et al.*, 2012) and $SmCP_{F\times\mathrm{mod}}$-$SmAP_{F\times\mathrm{mod}}$ (Zhang, Diorio *et al.*, 2012) transitions. In these cases, layer dilation might be possible due to interdigitation, or local uncorrelated tilt, or not fully stretched aliphatic chain configurations. The $SmAP_{F\times\mathrm{mod}}$ phase shows a bistable electric response, similar to that described earlier (Umadevi, Jákli, and Sadashiva, 2006a).

While nonmodulated smectic phases have one-dimensional periodicity, i.e., their x-ray pattern can be indexed by the layer spacing d only, to describe undulated layer structures in their tilted $SmCP_F$ (Heppke, Parghi, and Sawade, 2000a; Stannarius, Langer, and Weissflog, 2002; Coleman *et al.*, 2003; Umadevi, Jákli, and Sadashiva, 2006a; Zhu *et al.* 2012) or $SmCTP$ (Bailey and Jákli, 2007; Gorecka *et al.*, 2008; Pociecha *et al.*, 2008; Vaupotič, Szydlowska *et al.*, 2009; Chen, Maclennan *et al.*, 2011) phases, two lattice parameters $\boldsymbol{a}$ and $\boldsymbol{b}$, and a vertex angle γ are needed. Typical SAXS results for a completely asymmetric bent-shaped material are shown in Fig. 26(a), where the q dependence of the normalized SAXS intensity is shown for $SmCP_{F\times\mathrm{mod}}$ phase (red) and the $SmAP_{F\times\mathrm{mod}}$ phase (green) (Zhang, Diorio *et al.*, 2012). The splitting of the (1, k) and (1, $-k$) peaks ($k = 2, 3, 4$) in the $SmCP_{\mathrm{mod}}$ phase is due to the tilt of the molecular plane. It is missing in the $SmAP_{F\times\mathrm{mod}}$ phase, just showing its orthogonal nature. Figures 26(b) and 26(c) show cryo-TEM patterns in the $SmCP_{F\times\mathrm{mod}}$ and $SmAP_{F\times\mathrm{mod}}$ phases, respectively. One sees only one periodicity in both phases. They correspond to the bulk layer spacing obtained from the (1 0) x-ray peak in the $SmAP_{F\times\mathrm{mod}}$ phase. This shows that the layer undulation observed in bulk is not present in thin (~100 nm) films used for cryo-TEM measurements, i.e., it is not a robust feature of the material. The layer undulation can also be wiped out by strong enough electric fields, thus explaining why these B_7 textures are switchable electrically (Nakata *et al.*, 2005).

In freely suspended films of a synclinic layer undulated phase, the development of the long-wavelength polarization-modulated state is accompanied by the formation of labyrinthine textures formed by edge dislocations (Eremin and Jákli, 2013). As shown by SHG, this instability is preceded by an antiferroelectric-ferroelectric phase transition. The instability initiates a reversible reorganization of the edge dislocations in films of inhomogeneous thickness. This leads to an intricate maze pattern formed by terraces of the layer steps. A different type of string structure was found in films of another compound showing a uniform ferroelectric $SmCP_F$ phase (Eremin, Nemes, Stannarius, and Weissflog, 2008; Eremin, Nemes, Stannarius, Pelzl, and Weissflog, 2008). Those strings separate the regions of opposite bend deformation of the

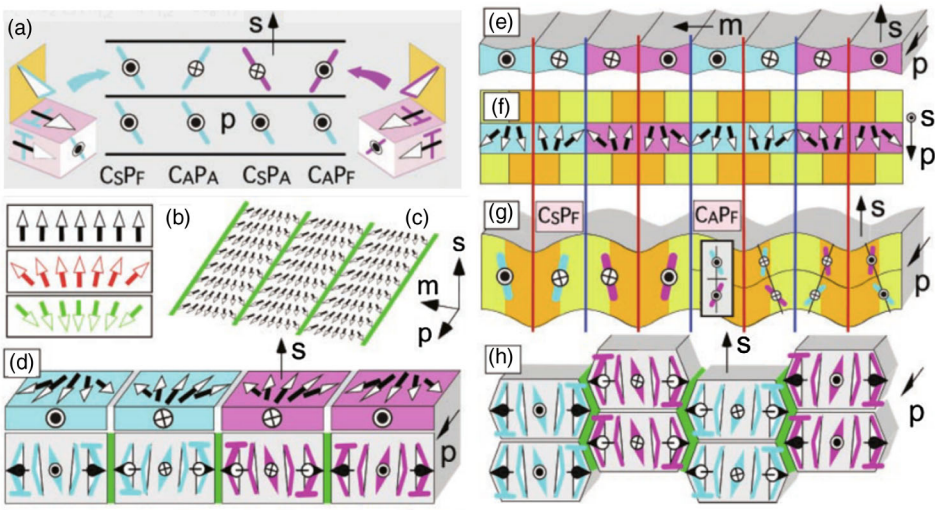

FIG. 25. Pictorial explanation of the formation and possible structures of layer undulated $SmCP_{\mathrm{mod}}$. (a) Illustration of the four possible $SmCP$ structures (for comparison, see also Fig. 22). The $SmCP$ smectic layer structure has spontaneous polar order and tilt of the bows, which makes the layers chiral, with handedness indicated by color (cyan or magenta, dark and light gray), and gives the four possible bilayer phases. Lines with end bars (T's) indicate the projection of the bent-shaped molecules so that the bar indicating the end is nearest the reader. (b) Preferred structure of a polarization field will be either positive (red, dark gray) or negative (green, light gray) splay. (c) Stripes assuming positive splay can fill space if the required defects (green lines, light gray) have sufficiently low energy. (d) Elemental splay stripe varieties, depending on handedness and orientation of P. Although everywhere we draw the polarization splay with the bent-core vertex splayed out, it may be the other way around. (e) Illustration of the layer expansion at the splay defect lines that is the mechanism driving the layer undulation. (f), (g) The layers in the intermediate regions must tilt to establish uniform layer spacing along s. This organization of P, chirality, and undulation [yellow (orange) displaced up (down)] is inferred from the optical and x-ray experiments. The handedness changes at defect lines shown in blue and does not change at lines in red. This makes the undulation crest curvature different from that of the troughs. (g) Director strain, minimized in the undulated synclinic (C_SP_F) local structure, tends to suppress the undulation in the anticlinic (C_AP_F) structure. (h) Layer interdigitation provides effective molecular packing at the polarization splay defects to produce a distinct (B_1) family of 2D ordered phases. From Coleman *et al.*, 2003.

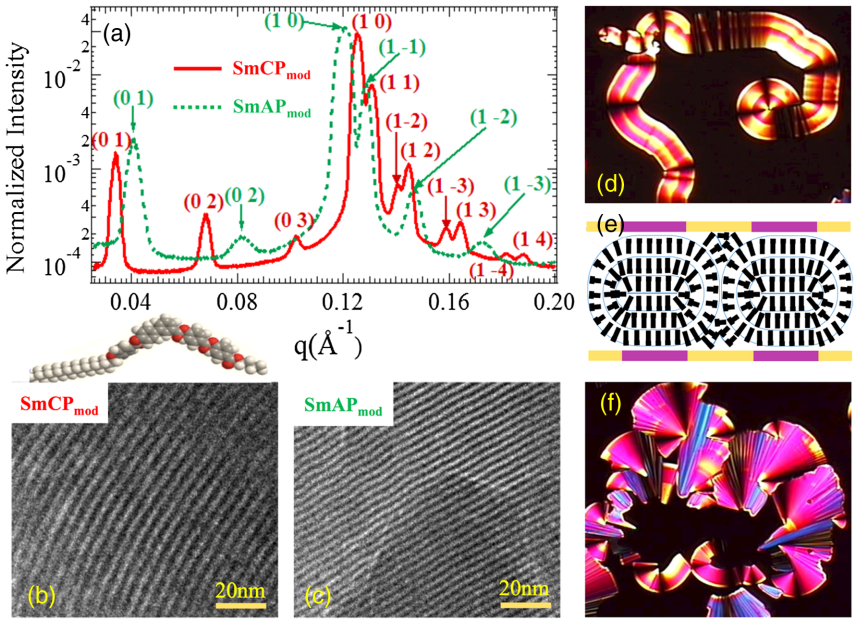

FIG. 26. Summary of experimental results on a completely asymmetric bent-core material [molecular structure shown above (b)]. (a) Scattering wave number (q) dependence of the normalized intensity of small-angle x-ray scattering. Red: $SmCP_{\mathrm{mod}}$ phase; green: $SmAP_{\mathrm{mod}}$ phase. The splitting of the (1, k) and (1, $-k$) peaks (where $k = 2, 3, 4$) in the $SmCP_{\mathrm{mod}}$ phase is due to the tilt. (b), (c) Cryo-TEM textures in the $SmCP_{\mathrm{mod}}$ and $SmAP_{\mathrm{mod}}$ phases, respectively. They show only nonmodulated smectic layering with layer spacing larger than the (1,0) peaks show in bulk x ray. (d), (f) POM textures of a 5 μm film at the isotropic-$SmCP_{\mathrm{mod}}$ transition. Textures are typical to switchable B_7 textures characterized by striped ribbon motifs as seen in (d) and in the bottom of (f). (e) Model of the layer structure explaining the formation of the striped ribbon motifs. From Zhang, Diorio *et al.*, 2012.

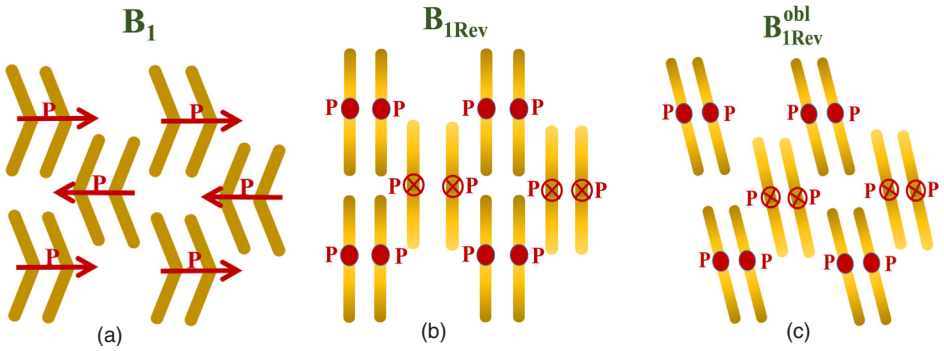

FIG. 27. Structural cartoons of three columnar phases formed by bent-core liquid crystals: (a) the B_1 phase with $p2\,mg$ symmetry. (b) Reversed orthogonal phase $B_{1\mathrm{rev}}$, and (c) tilted $B_{1\mathrm{rev}}^{\mathrm{obl}}$ phase. From Watanabe *et al.*, 1998.

molecular tilt director, while both the tilt direction and the direction of the spontaneous polarization remain continuous.

C. Columnar phases

Columnar phases of liquid crystals were discovered by Chandrasekhar, Sadashiva, and Suresh (1977). In these phases disk-shaped molecules form columns with fluid order along the columns and two-dimensional lattice normal to the columns. Based on the order along the columns and the nature of two-dimensional order there are several columnar phases (Oswald and Pieranski, 2005).

In bent-core liquid crystals there are two categories of columnar phase. One involves the two-dimensional order made up of broken layer fragments, while the other is formed by columnar stacking of disk-shaped assemblies of bent-core molecules (Takezoe and Eremin, 2017).

1. Two-dimensional order made up of broken layer fragments

Historically, columnar liquid crystals of bent-shaped molecules are denoted as the B_1 phase, referring to the fact that this was the first mesophase observed by the Tokyo group (Sekine, Takanishi *et al.*, 1997).

The first model of the B_1 phase based on the analysis of SAXS results was given by Watanabe *et al.* (1998). In this model, the bent-core mesogens form columns of frustrated blocks consisting of 4–5 molecules as shown in Fig. 27(a).

The arrangement of the blocks results in an overall antiferroelectric structure. The *p2mg* model of the B_1 phase however could not explain several features of x-ray results, such as the absence of cross reflections (2 1) and the often observed splitting of the diffuse scattering, which results from the molecular tilt (Pelz *et al.*, 2003). These discrepancies led to a model (Takanishi *et al.*, 1999; Szydlowska *et al.*, 2003), where the bows of the molecules align along the columns giving rise to a so-called reversed B_1 phase ($B_{1\mathrm{rev}}$). Actually there are several types of reversed phases: an orthogonal phase $B_{1\mathrm{rev}}$ with *pmmn* symmetry [Fig. 27(b)], and an oblique $B_{1\mathrm{rev}}^{\mathrm{obl}}$ phase with *p11n* symmetry. [Fig. 27(c)]. In contrast to the B_1 phase, the $B_{1\mathrm{rev}}$ phases show electro-optical switching in strong fields ($E > 15$ V/μm) associated with a strong polarization switching as high as 700 nC/cm^2, comparable to that of the *SmCP* phase.

The fourth columnar phase reported by C. L. Folcia *et al.* (2006) and Cesar Luis Folcia *et al.* (2006) has a splayed structure similar to that suggested by Coleman *et al.* (2003) that forms by the layer undulation mechanism [see Fig. 25(h)] when the undulation amplitude is half of the layer spacing.

Today there are a large number of reports of various bent-core materials with columnar bent-core liquid crystals with various symmetries, ferroelectric and antiferroelectric order, and electro-optical switching (Watanabe *et al.*, 1998; Szydlowska *et al.*, 2003; Gorecka *et al.*, 2004, 2008; Kishikawa *et al.*, 2005; Amaranatha *et al.*, 2007). These materials (Pelzl, Diele, and Weissflog, 1999; Pelzl *et al.*, 2006) form peculiar micrometer-scale helical patterns and slender freely suspended filaments (Jákli, Krüerke, and Nair, 2003; Eremin *et al.*, 2005, 2012; Stannarius, Nemeş, and Eremin, 2005; Nemeş *et al.*, 2006; Bailey and Jákli, 2007). Before their nanostructure was understood, they were labeled as the B_7 phase (see Fig. 28).

Now we understand that some of them have undulated layers with either *SmCP* (see Fig. 22) or *SmCTP* (see Fig. 24) local director structures (switchable B_7 or $B_{7'}$ phase), while those that cannot be switched with electric fields have the splayed columnar structure. Characteristic POM textures of the first nonswitchable B_7 material (Pelzl, Diele, and Weissflog, 1999) are shown in Fig. 28.

The optical B_7 textures attracted an intense research that led to many important findings (Pelzl, Diele, and Weissflog, 1999; Heppke, Parghi, and Sawade, 2000b; Coleman *et al.*, 2003, 2008; Zhu *et al.*, 2012; Pelzl *et al.*, 1999; Jákli, Krüerke, and Nair, 2003; Vaupotič and Čopič, 2005; Vaupotič *et al.*, 2007). SAXS (Pelzl, Diele, and Weissflog, 1999; Coleman *et al.*, 2003; Folcia *et al.*, 2005) studies revealed a number of peaks (Coleman *et al.*, 2003; Folcia *et al.*, 2005) that can be indexed by a slightly oblique monoclinic 2D unit cell with $a \sim 3$–5 nm and $b \sim 8$–20 nm periodicities. These peaks are similar to those found in switchable B_7 materials that have undulated smectic layer structure (Coleman *et al.*, 2003; Chen, Chuang *et al.*, 2011; Zhang, Diorio *et al.*, 2012), such as in that shown in Fig. 25(a).

TEM images of the nonswitchable B_7 (splayed columnar) materials are completely different from those of the switchable B_7 materials that showed no layer modulation in thin films. Cryo-TEM and freeze-fracture (FF) TEM textures of $n = 9$ and 8 members of the n-OPIMB-NO_2 homolog (see inset in Fig. 28) and the suggested packing model are shown in Fig. 29. They agree with the model based on x-ray data by Folcia *et al.* (2006) and Coleman *et al.* (2003).

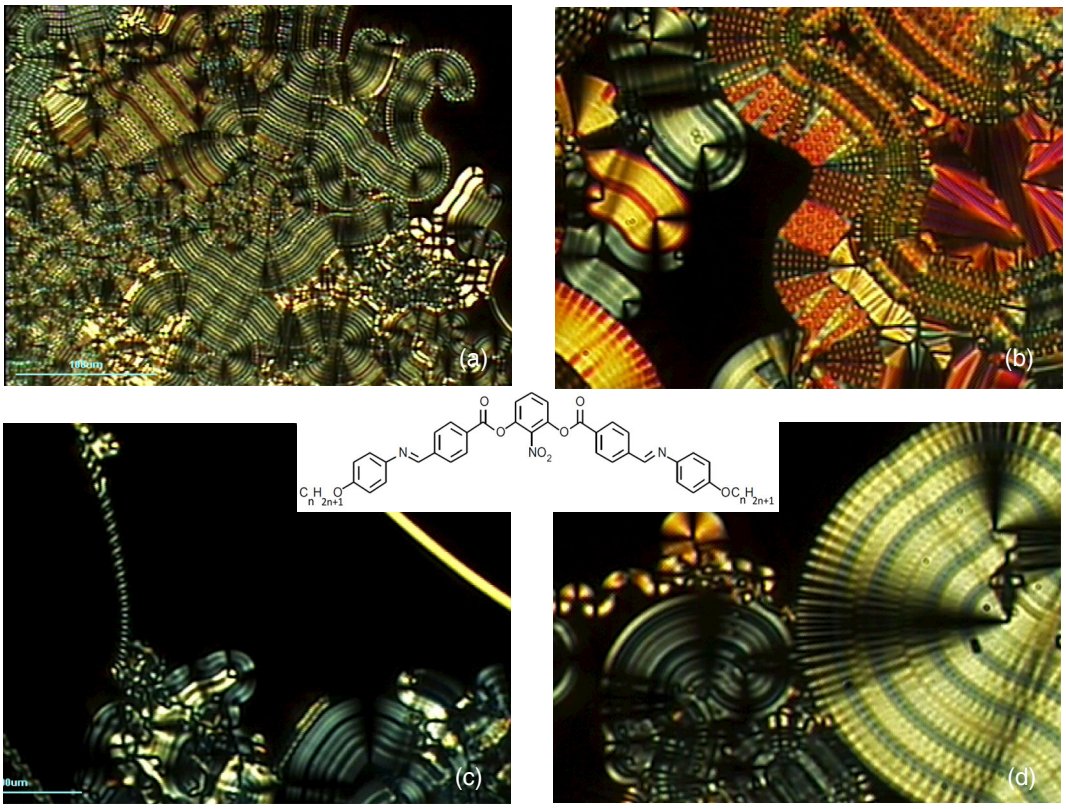

FIG. 28. Molecular structure of the prototypical B_7 material, n-OPIMB-NO_2 with $n = 7$ (inset in the middle) and typical POM texture of a 10 μm film between crossed polarizers at the isotropic B_7 transition. (a) Banded myelinic texture with director and layer structure corresponding to that shown in Fig. 25(h); (b) a combination of broken fan texture, myelinic texture, and a hexagonally patterned myelinic texture; (c) combination of spiral texture (Jákli *et al.*, 2000b) with banded myelinic texture; and (d) a combination of broken fan (right) and banded myelin textures (left).

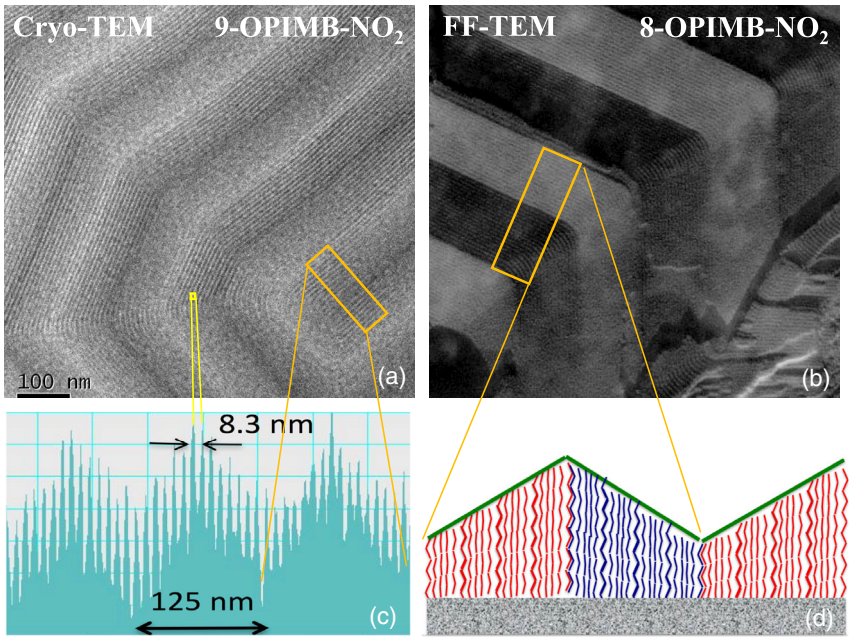

FIG. 29. Summary of TEM profiles and the suggested packing model of B_7 (splayed B_1) materials. (a) Cryo-TEM profile of 9-OPIMB-NO_2 showing modulations with $b \sim 8.3$ nm and $L \sim 125$ nm; (b) freeze-fracture (FF) TEM profile of 8-OPIMB-NO_2 showing topological features similar to that found by cryo-TEM. From N. A. Clark. (c) Histogram of the height profile and (d) suggested packing model of the molecules. From Zhang *et al.*, 2013.

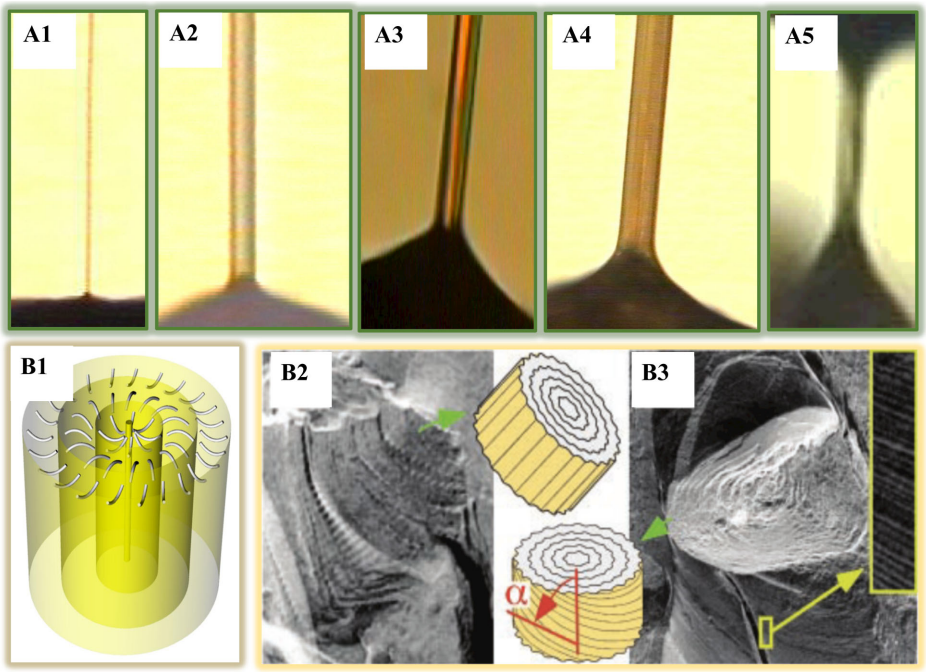

FIG. 30. Freestanding fibers of bent-core liquid crystals. (a) POM textures at the meniscus of the filaments in different phases. (a1) 8-OPIMB-NO2 in the nonswitchable B_7 (splayed B_1) phase. (a2) A material in the $SmCP_{\mathrm{mod}}$ phase; (a3), (a4) bare and chlorine substituted BCS in $SmCP$; (a5) a BCN in nematic phase. The bar indicates 10 μm. From Jákli, Krüerke, and Nair, 2003. (b1) Proposed concentric layer structure of $SmCP$ filaments; (b2), (b3) FF-TEM images of B_7 filaments with modulation direction along the filament axis (b2) and with an angle γ with respect to the filament axis (b3). (b2), (b3) From Coleman *et al.*, 2003.

Another remarkable feature of the B_7 materials is their ability to form freestanding filaments. Since surface tension minimizes the surface area and volume of a fluid, Newtonian fluids can only form freestanding filaments with length L smaller than their circumference D, i.e., their aspect ratio $S = L/D < \pi$. This is the well-known Rayleigh-Plateau instability (Rayleigh, 1880). Longer fibers can be drawn only from non-Newtonian fluids that harden during the pulling process. The hardening can be achieved either by cooling, such as in glass fibers, or by solvent evaporation, such as when spider silk loses water after spinning. Low molecular weight liquid crystals comprised of rod-shaped molecules do not form fibers, and it has been observed (Mahajan *et al.*, 1999) that nematic and smectic-A bridges collapse at aspect ratios of $S \approx \pi$ and at $S = 4.2$, respectively. Smectic liquid crystals formed by rod-shaped molecules generally form thin films (Young *et al.*, 1978). Columnar liquid crystalline phases of disk-shaped molecules were found to form stable filaments up to 0.2 mm long and as narrow as 1.5 μm diameter (Van Winkle and Clark, 1982). Their stability is due to the large compression modulus of the columnar structure.

A large number of bent-core liquid crystals were found to form stable and slender filaments [see Fig. 30(A)] (Pelzl, Diele, and Weissflog, 1999; Coleman *et al.*, 2003; Jákli, Krüerke, and Nair, 2003). The least stable and less slender filament is formed by a chlorine substituted BCN, although its slenderness ratio is $S \sim 6$ [Fig. 30(A5)], i.e., twice that of calamitic nematics. Nonmodulated $SmCP_A$ materials with no substitution in the center phenyl ring [Fig. 30(A4)], or with chlorine substitution [Fig. 30(A3)] form stable filaments with slenderness ratios $S = 60$ and 125, respectively. This is on the order of that found in disk-shaped columnar filaments. Figure 30(A2) shows a filament with $S \sim 1000$, i.e., an order of magnitude larger than of calamitic columnar LCs. Finally, Fig. 30(A1) shows a part of a filament formed by 8-OPIMB-NH_2 in the nonswitchable B_7 phase (splayed columnar) material. For this material $S \sim 4000$ was measured, although it was set only by the experimental condition (Jákli, Krüerke, and Nair, 2003). These B_7 liquid crystal filaments remain stable until the radius decreases below 1.5 μm.

The fact that filaments above the Rayleigh-Plateau limit can exist even in BCN materials is due to the non-Newtonian behavior of BCNs as shown in Fig. 13. To understand the formation of stable filaments in nonmodulated $SmCP$ materials [(A3) and (A4)], Jákli, Krüerke, and Nair (2003) proposed that the layers form concentric cylinders [see Fig. 30(B1)], which therefore provide an elastic response against variation of the filament radius. Such a structure mimics the columnar phase and stabilizes a liquid crystal cylinder against the Raleigh-Plateau instability (Link *et al.*, 1999; Pelzl, Diele, and Weissflog, 1999; Jákli, Krüerke, and Nair, 2003). Freeze-fracture TEM experiments on B_7 filaments indeed verified that the smectic layers are concentric [see Figs. 30(B2) and 30(B3)], although on those extra modulations were also seen due to the polarization splay as explained in Fig. 28 (Coleman *et al.*, 2003). The extra stability of the filaments found in the B_7 structures was explained by Eremin *et al.* (2012), as a result of the layer undulation with periodicity $b \sim 10$ nm.

In addition to single filaments, a number of larger filament bundles can be formed with diameters of 10 μm or larger with aspect ratios greater than 100 (Bailey *et al.*, 2010).

Dynamical properties of freely suspended liquid crystal filaments have been explored in Magdeburg, Germany (Stannarius, Nemeş, and Eremin, 2005; Eremin *et al.*, 2006) and Kent, Ohio (Jákli, Krüerke, and Nair, 2003; Ostapenko *et al.*, 2014; Salili, Ostapenko *et al.*, 2016) providing information on filament tensions and damping processes (Yao, Spiegelberg, and McKinley, 2000; Coleman *et al.*, 2003; Jákli, Krüerke, and Nair, 2003; Martin *et al.*, 2004; Eremin *et al.*, 2005, 2006; Stannarius, Nemeş, and Eremin, 2005; Nemeş *et al.*, 2006; Nemeş, Eremin, and Stannarius, 2006; Nemeş, 2008; Petzold *et al.*, 2009). Recently, new methods for the mechanical characterization of the filaments, based on static deformations, were proposed (Link *et al.*, 1999; Yao, Spiegelberg, and McKinley, 2000; Bauman and Phillips, 2009; Petzold *et al.*, 2009; Morys, Trittel, and Stannarius, 2012; Stannarius *et al.*, 2012). Stable BC filaments were also found to mechanically respond to electric fields (Jákli, Krüerke, and Nair, 2003): in their single strand forms they show a transversal vibration with the frequency of the electric field applied along the fiber axis, and in their multistrand bridge form they flow along the field. Both of these electromechanical effects indicate the polar nature of the fibers and offer their use as microelectromechanical devices. Finally, single B_7 filaments can also guide the light and are thus promising for novel anisotropic waveguides (Fontana *et al.*, 2009).

2. Columnar phases with cone-shaped aggregates

The other type of columnar structures formed by flat disk-shaped and conelike aggregates of several mesogens (for examples with four BC molecules as shown in Fig. 31) are denoted as Col_h and $\mathrm{Col}_h P_A$, respectively. A spontaneous dipole moment of the columns occurs in the cone-shaped configuration, due to an asymmetry of the electron-density distribution.

A transition between the disk-shaped and cone-shaped configurations gives rise to a new relaxation soft mode, where the direction of the cone tip oscillates. This mode is designated as "umbrella mode" and it yields a new switching mechanism of the columns shown in Fig. 31, which was unambiguously confirmed by SHG interferometry measurements and dielectric spectroscopy (Takezoe, Kishikawa, and Gorecka, 2006).

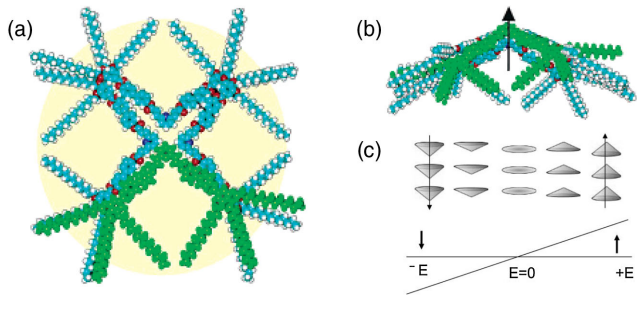

FIG. 31. (a) Schematic of the column cross section made of four bent-shaped molecules; (b) in the $\mathrm{Col}_h P_A$ phase, the molecules form a conelike structure with noncompensated dipole moment illustrated by an arrow; and (c) a schematic of the polar switching in the Col_h phase of polycatenar molecules. (a), (b) From Gorecka *et al.*, 2004. . (c) From Takezoe, Kishikawa, and Gorecka, 2006.

Recently a ferroelectric response for a columnar liquid crystal adopting a core-shell architecture that accommodates an array of polar cyano groups confined by a hydrogen-bonded amide network with an optimal strength was reported (Miyajima *et al.*, 2012). Under an applied electric field, both columns and core cyano groups align unidirectionally, thereby developing an extremely large macroscopic remnant polarization.

A columnar phase of aggregates composed of acute-angle (V-shaped) bent shape was also reported (Li *et al.*, 2010). Here each column is constructed by cylindrical layers of V-shaped molecules, so that the bend direction of the molecules is tangential and perpendicular to the column axis. This ground state therefore has no net polarization. However, when an electric field is applied along the hexagonally packed columns the bend direction of molecules turns parallel to the column axis, thus making the system polar along the electric field. Reversing the sign of the field the bend direction and the net polarization reverse, too. This model explains the lack of SHG in the field-off state, and the polarization peak under triangular field reversal and the dark texture between crossed polarizers during switching.

D. Bent-shaped liquid crystals with 3D nanostructure

In addition to the zero- (nematic), one- (smectic), and two-dimensional (columnar) positional orders, some bent-shaped liquid crystals can also possess three-dimensional periodic nanostructure. So far we distinguish two types of such structures: the "dark conglomerate" (DC) phase and the "helical nanofilament" (HNF) phase.

1. Dark conglomerate phase

A number of materials, showing local *SmCP* structure, possess a short (∼100 nm) smectic correlation length, indicating a disordered nanophase structure (Hough *et al.*, 2009b). Such a mesophase, designated as a DC phase, is optically isotropic and may show optical activity. In that case, spontaneously formed chiral domains of opposite handedness can be visualized in depolarizing microscopy with slightly uncrossed polarizers, as shown in Fig. 32(b). The twisting power of the chiral domains can be as large as $0.1°/\mu$m (Findeisen-Tandel *et al.*, 2008; Stern, 2009).

The behavior of the dark conglomerate phase was studied in detail by several groups (Dantlgraber *et al.*, 2002; Eremin *et al.*, 2003; Martínez-Perdiguero *et al.*, 2006; Zhang *et al.*, 2010; Ortega *et al.*, 2011). It was found that under the action of an electric field, or depending on the thermal history of the sample, the isotropic texture occasionally transforms into a birefringent one, which remains stable after field removal. In some cases the opposite effect occurs and a chiral isotropic state is induced by strong DC electric fields (Eremin *et al.*, 2003) or by cooling the material from the isotropic phase under square-wave ac fields (Martínez-Perdiguero *et al.*, 2006; Ortega *et al.*, 2011). The field-induced chiral isotropic phase may show a bistable switching between domains of opposite chirality (Eremin *et al.*, 2003). This switching occurs without any detectable birefringence while $P_o \sim 300$ nC/cm^2 polarization switching can be observed.

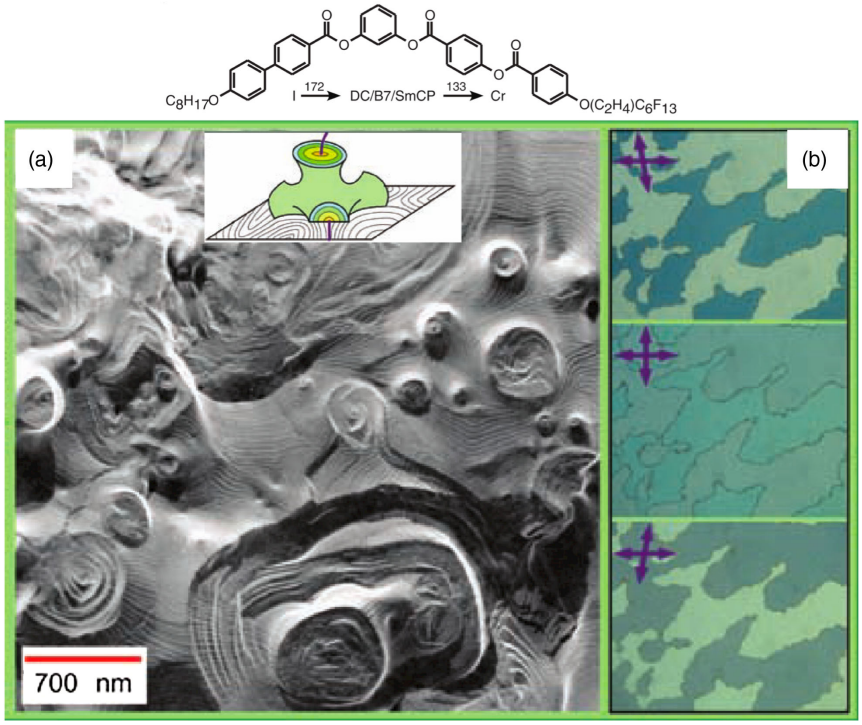

FIG. 32. Illustration of the properties of a BC mesogen W508 (molecular structure with phase sequence at the top) in the DC phase. (a) Freeze-fracture TEM image with the illustration of the formation of the sponge-type domains in the inset. (b) Optical textures of the DC phase between slightly uncrossed (top and bottom) and crossed polarizers (middle). From Hough *et al.*, 2009b.

The structure of the dark conglomerate phase was studied by several groups (Weissflog *et al.*, 2004; Liao, Pelzl *et al.*, 2005; Keith *et al.*, 2007; Hough *et al.*, 2009b; Chen, Shen *et al.*, 2011; Ortega *et al.*, 2011) by x-ray diffraction and FF-TEM. These studies revealed the presence of 20–100 nm size domains with saddle-splay-type layer structures (Fig. 32) similar to the sponge phase of lyotropic systems. A theoretical model by DiDonna and Kamien (2002) showed that the energy cost of layer deformation of a spongelike short-range polar *SmCP* structure could be compensated by the gain of the Gaussian curvature of the surfaces when the saddle-splay elastic constant K_{24} is negative. The reason for the saddle-splay defects is the mismatch of the in-plane area of the tails and cores that can be relieved by a tilt (Hough *et al.*, 2009b). The tilt creates a mismatch between the tilt planes of the two half arms, making their projections on the layer plane nearly perpendicular to each other. This situation produces a strong tendency for the negative Gaussian curvature of the layers via the coupling of the polar order and the tilt of the molecular arms to the positional order within the smectic layers. The saddle-splay curvature of the layers is believed to contribute to the large optical activity of the phase, which cannot be explained by the layer chirality of the tilted polar phase alone (Ortega *et al.*, 2003; Hough *et al.*, 2009b). The rare appearance of optically inactive DC phases (Amaranatha *et al.*, 2007; Findeisen-Tandel *et al.*, 2008) may be related to racemic structures with longer pitch racemic alternations. SHG studies (Martínez-Perdiguero *et al.*, 2006) suggest that the ground state of the DC phase is not polar and the polarity is not responsible for formation of the DC phase. Homochiral DC is realized (Ocak *et al.*, 2012) when molecular chirality is present, for example, by incorporating a chiral side chain into the bent-shaped molecules.

2. Helical nanofilament phase

Another intriguing bent-shaped liquid crystal phase with 3D nanostructure is the HNF phase (previously known as the B_4 phase). FF-TEM studies of the HNF phase revealed an assembly of twisted layers stacked to form chiral nanobundles with around $w \sim 40$ nm widths and $h \sim 100$ nm half pitch (Fig. 33) (Hough *et al.*, 2009a; Ryu *et al.*, 2015).

The hierarchical self-assembly of the nanofilament (NF) phase starts with bent-core mesogenic molecules [Fig. 33(a)] that form well-defined smectic layers with in-plane crystal or hexatic order, macroscopic polarization, and tilt of the molecular planes, which makes them chiral. In this state, the half-molecular tilt directions on either side of the layer midplane are nearly orthogonal [Fig. 33(b)], therefore the lattice structure of the projections onto the midplane of the smectic layers (yellow and violet) do not match, resulting in a local preference for saddle-splay layer curvature and driving the formation of nanofilaments [Figs. 33(c) and 33(d)]. These nanofilaments grow independently [Figs. 33(e) and 33(f)] or collectively in packs that order in the bulk into a nanoporous nanofilament structure [Fig. 33(f)] having macroscopic coherence of the phase of the NF twist.

This HNF phase is particularly interesting due to its unique hierarchical nanostructure (Niwano *et al.*, 2004) in which the individual filaments further self-organize into oriented arrays of filaments that are phase coherent with respect to their twist. The bulk HNF phase expels most guest molecules, such as rod-shaped liquid crystals (Takanishi *et al.*, 2005; Otani *et al.*,

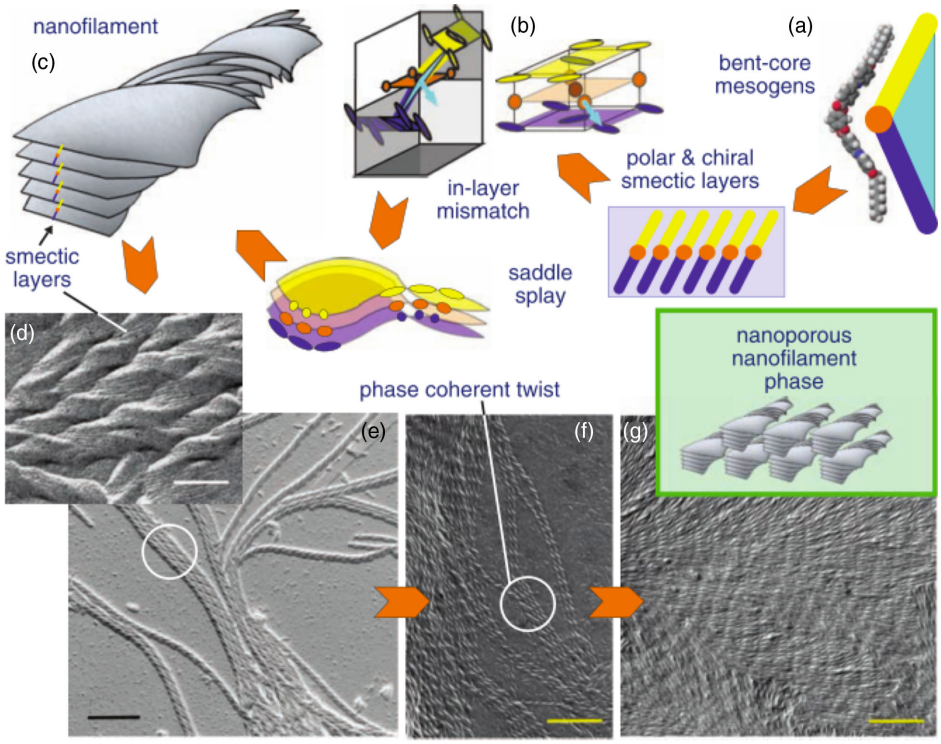

FIG. 33. Pictorial of the HNF phase. (a) Bent-core mesogenic molecules, which form well-defined smectic layers. (b) Demonstration of the projections of the lattices of the core arms (yellow and violet). (c) Sketch of an individual nanofilament. (d) FF-TEM image of NFs of the molecule shown in (a) at $T = 25$°C. (e), (f) FF-TEM images of nanofilaments growing independently or collectively in packs. (g) FF-TEM image of the bulk HNF phase exhibiting large domains of parallel, coherently twisting NFs. Scale bars, (d) 60 nm, (e), (g) 400 nm, and (f) 370 nm. From Hough *et al.*, 2009a.

2009; Chen *et al.*, 2010; Zhu *et al.*, 2010; Chen, Maclennan *et al.*, 2011; Nagayama *et al.*, 2011; Sasaki, Setoguchi *et al.*, 2011), and their unique structure makes it attractive for the design of bulk and surface structures with controlled porosity and roughness at the nanometer and micrometer scales, offering potential application of textured HNF surfaces as self-assembled super hydrophobic layers (Kim, Yi *et al.*, 2013). Other applications are envisioned in nonlinear optics, chiral separations, and photovoltaics. Solar cells require thin films in the range of 100 nm, so it is desirable to know the structure of the HNF phase in such thin films. Recent FF-TEM studies, for example, showed the formation of focal conic structures instead of the helical nanofilaments near a glass substrate (Chen *et al.*, 2012) indicating that the structure near a surface can be different than the bulk structure. While FF-TEM monitors the profile of a broken surface of a bulk (over 1 μm thick) material, cryo-TEM gives information about the inside of a thin (about 100 nm film), and provides complementary information about the structures.

Recently cryo-TEM studies have been performed on the phenylene bis (alkoxyphenyliminomethyl) benzoate (PnOPIMB) series [the molecular structure of p9OPIMB is shown in Fig. 33(a)] (Niori *et al.*, 1996; Sekine, Niori *et al.*, 1997) with $n = 7, 8, 9$, and 12 that form room-temperature HNF phases (Zhang *et al.*, 2014). It was found that for the $n = 7$ and 8 homologs the nanofilament layers stack on top of each other in a twisted configuration, where the filaments of the subsequent layers are rotated by $\beta \sim 30°$–$40°$ with respect to each other; see Fig. 34.

This angle is in the range where Chen *et al.* (2012) observed that parabolic domain walls of the HNF axes are tilted by ∼38° with respect to a periodic one-dimensional modulation imprinted in surfaces. The HNF phase thus features a double twist: One axis of twist is defined along the axis of each nanofilament; the orthogonal second axis of twist describes the rotation of the nanofilament layers. This double twisted structure explains both the observed structural blue color of some HNF materials [in fact due to their apparent blue reflection color first they were thought to be "blue phase" (BP) or twist grain boundary phase (Araoka *et al.*, 2005)] and their ambidextrous optical activity (Zhang *et al.*, 2014). When an HNF is formed by achiral bent-shaped molecules, the phase is macroscopically racemic, i.e., a conglomerate of left- and right-handed homochiral domains. Similar to DC phases, homochiral HNF phases can be formed by chiral molecules (Nakata *et al.*, 2001) or related derivatives (Lin *et al.*, 2012). Homochiral HNF phases have also been realized by taking advantage of the apparent chiral memory between the *SmCP* and HNF phases of a bent-core LC derivative with the phase sequence Iso ↔ *SmCP* ↔ HNF (Niwano *et al.*, 2004). It was also found that the addition of a chiral dopant led to the formation of diastereomeric systems with unequal amounts of left- and right-handed HNF nucleation (Chen *et al.*, 2015). Confinement in nanoporous anodic aluminum oxides was recently introduced as a means to tune the morphology (including the helical pitch, the layer spacing, and the number of layers) of confined single HNFs by adjusting the pore diameter of the confining nanopores (Kim, Lee *et al.*, 2013; Hanim Kim *et al.*, 2014, 2016).

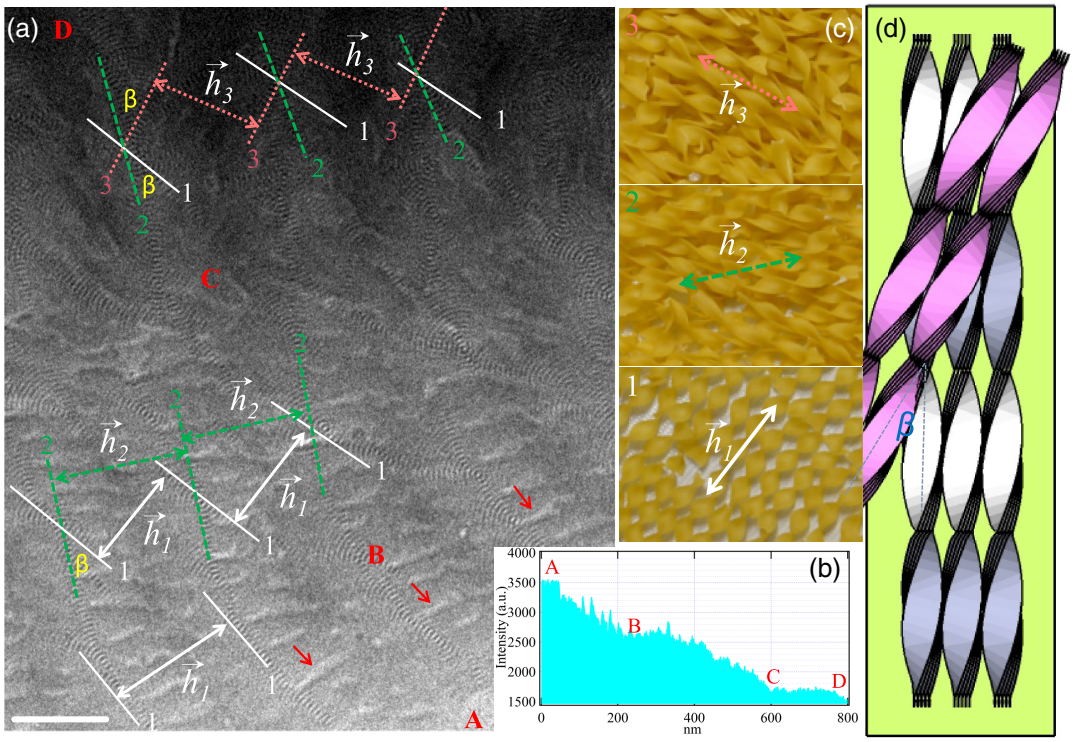

FIG. 34. TEM image and models showing double-twist structure. (a) Cryo-TEM image of an area of P8OPIMB with gradually increasing thickness from bottom right to top left. The vectors $\vec{h}_1$, $\vec{h}_2$, and $\vec{h}_3$ illustrate the direction and periodicity of the filaments. Scale bar is 100 nm. (b) Transmitted electron intensity profile along the line *ABCD*, indicating a gradual increase of the film thickness from *A* to *D*. (c) Equilibrium arrangement of different layers of helical pastas; from bottom to top are the first, second, and third layers of filament, respectively. (d) Sketch of the proposed arrangement of the helical nanofilaments. From Zhang *et al.*, 2014.

Recently modulated helical nanofilament phases (HNF_{mod} and HNF_{mod2}), characterized by additional one- and two-dimensional in-layer modulations were found as well (Tsai *et al.*, 2013; Li *et al.*, 2016). It was also shown that the enantiomeric homochiral HNF phases with opposite twist sense do not mix by forming a macroscopic conglomerate of right- and left-handed homochiral domains, but rather form an entirely different phase structure, similar to the related compound with racemic side chains (Li *et al.*, 2016).

Mixtures of the bent- and rod-shaped mesogens also attracted particular attention (Otani *et al.*, 2009; Chen *et al.*, 2010; Chen, Maclennan *et al.*, 2011; Sasaki, Nagayama *et al.*, 2011), because they show large homochiral domains, thus enabling direct observation of the filament nucleation and growth. It is found that the small rod-shaped mesogens often become segregated on a nanoscale and embedded into the network of helical nanofilaments formed by bent-core mesogens (Chen *et al.*, 2010; Sasaki, Nagayama *et al.*, 2011).

Due to their capacity to serve as porous nanotemplates with chiral surfaces that can host materials, such as low-molecular weight LCs (Araoka and Sugiyama, 2011; Wang *et al.*, 2017), LC polymers, conducting polymers, and fullerene derivatives (Chen, Zhu *et al.*, 2013). These examples show how the self-assembled, chirality-preserving 3D porous network of the HNF phase can be used to organize guest materials, by locally expelling and confining guest molecules.

IV. FLEXIBLE CORE BENT-SHAPED MATERIALS

A. Nematic phase

1. Odd-even effects in mesogenic polymers and oligomers

Active current studies of flexible bent-shaped mesogens were inspired by the development of semiflexible main-chain liquid crystal polymers in the early 1980s (Luckhurst, 1995, 2005; Imrie and Henderson, 2007). These polymers are formed by relatively rigid mesogenic units connected by flexible links, typically represented by an aliphatic chain $(CH_2)_x$ of methylene groups CH_2. The polymers forming the N_U phase exhibited a strong dependence of the clearing point (N_U-I transition) on the parity of the number x of carbon atoms in these links. Although similar odd-even effects are common in organic chemistry, the main-chain polymers showed a much stronger dependence as compared to their low-molecular counterparts in which the aliphatic chain serves as a terminal end of the molecule. An intriguing manifestation of the odd-even effect was the appearance of a mysterious uniaxial nematic N_x at the temperatures below the usual uniaxial nematic N_U, reported by Ungar, Percec, and Zuber (1992) for main-chain liquid crystalline polyethers in which semirigid units were connected by flexible spacers with $x = 5, 7, 9$ while no "secondary" nematic was detected in the materials with an even x. The secondary nematic was separated from N_U by a well-defined first-order transition and did not show any characteristics of a biaxial nematic N_B. Although the concrete structural organization of N_x remained

unknown, a remarkable observation was made that the studied polyethers are "certainly the most flexible known to exhibit a nematic phase" and that they can change conformations from straight to bent. This fact proved to be important in understanding the role of flexible spacers connecting rigid mesogenic units in the liquid crystalline ordering.

The studies of liquid crystalline polymers are challenging because of the high temperatures of mesophase existence and because of their poor ability to align. These difficulties renewed the interest to explore dimers, trimers, and other oligomers, with molecular weights intermediate between that of polymers and small molecules, as "prepolymer ptototypes" (Griffin *et al.*, 1981; Luckhurst, 1995). Vorländer (1927) synthesized dimers of 1,7-bis (4-alkyloxyphenyl-4′-azophenyl)alkane dioates and noted that the nematic-to-isotropic transition temperature depends strongly on the parity of the number x of carbon atoms in the flexible link connecting two rigid rodlike cores. Similar odd-even effects were reported for other liquid crystalline dimers by Rault, Liébert, and Strzelecki (1975) and Griffin *et al.* (1981).

The most widely explored dimers turned out to be derivatives of cyanobiphenyls (Emsley, Luckhurst, and Shilstone, 1984; Barnes *et al.*, 1993; Tuchband *et al.*, 2017). Monomeric cyanobiphenyls such as 4-pentyl-4′-cyanobiphenyl (5CB), or $CH_3(CH_2)_4\ (C_6H_4)_2CN$, first synthesized by Gray, Harrison, and Nash (1973), gained broad popularity as the prime materials for liquid crystal displays because of their chemical stability, high dielectric and optical anisotropy. Emsley, Luckhurst, and Shilstone (1984) reported on the synthesis and properties of a homologous series of dimeric cyanobiphenyls, 1,7-bis (4, 4′-cyanobiphenyloxy)alkanes, of the chemical formula $NC(C_6H_4)_2O(CH_2)_xO(C_6H_4)_2CN$, where x varied from 1 to 12. Similarly to the main-chain mesogenic polymers, the dimers demonstrated a strong odd-even effect in the temperatures of phase transitions and also in entropy of the N_U-I transition; see Fig. 35. The latter is much higher for the even x than for odd x, suggesting that the even dimers are significantly better ordered in the nematic as compared to their odd counterparts. A higher degree of orientational order in the even dimers was confirmed by NMR (Emsley, Luckhurst, and Shilstone, 1984). The dependence on parity of x in dimers was much more pronounced than in their monomeric counterparts $CH_3(CH_2)_{x-1}O(C_6H_4)_2CN$, formed by a rigid cyanobiphenyl core and an alkyl-oxy end chain with the same number of carbon atoms in the flexible link as in the corresponding dimer; see Fig. 35.

The most obvious factor that could explain the odd-even effect in Fig. 35 is the difference in the shapes of molecules, Fig. 36. Two neighboring methylene groups along the chain $(CH_2)_x$ prefer to maximally separate their hydrogen pairs from each other. The H atoms of one group are above the C-C bond, while the H atoms of the neighboring groups are below the bond, forming a "trans" conformation; the carbon "skeletons" of the $(CH_2)_x$ spacer adopt a zigzag arrangement; see Fig. 36. These transconformations are more stable than the states in which the neighboring pairs of H atoms make an angle different from 180°. It is clear then that an even x results in a nearly parallel orientation of the rigid cyanobiphenyl groups and in a rodlike overall shape of the molecule, Fig. 36(a), while

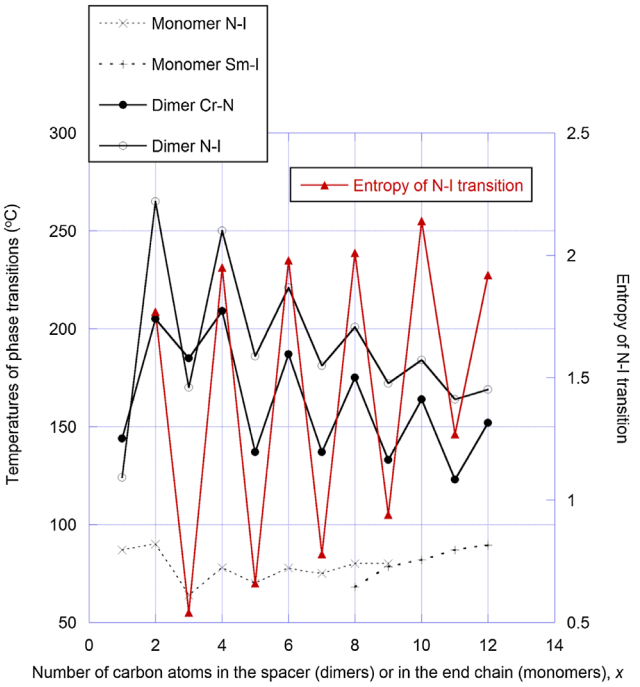

FIG. 35. Odd-even effect in the phase transition temperatures and entropy of melting for dimers with the general formula $NC(C_6H_4)_2O(CH_2)_xO(C_6H_4)_2CN$ and monomers $CH_3(CH_2)_{x-1}O(C_6H_4)_2CN$ with the same number x of carbon atoms in the alkyl-oxy end chain. Entropy changes are shown in units of the gas constant. Plotted with the data reported by Emsley *et al.* From Emsley *et al.*, 1984.

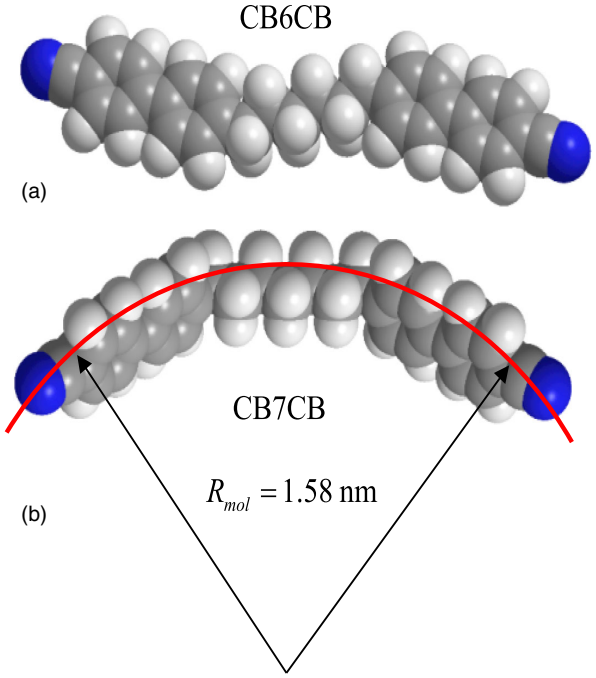

FIG. 36. Odd-even effect of the aliphatic linkers with all methylene groups in transconformations on the molecular shapes: (a) 1,7-bis (4-cyanobiphenyl-4′-yl)hexane (CB6CB), $x = 6$, shows a rodlike shape while (b) 1,7-bis (4-cyanobiphenyl-4′-yl)heptane (CB7CB), $x = 7$, is bent. The CB7CB molecular shape closely follows a circular arch of a radius as suggested by Tuchband *et al.* (2017). Chemical structure by Greta Babakhanova.

an odd x produces a bent or bananalike shape, with the two cyanobiphenyl groups making a substantial angle with each other, Fig. 36(b), according to theory (Greco, Luckhurst, and Ferrarini, 2014) and experiments (Tuchband *et al.*, 2017). The actual shape of the dimers should not be considered as rigidly fixed; the spacer is flexible and thus allows the molecules to adopt many conformational states. Taking this flexibility into account, Ferrarini *et al.* (1993), Ferrarini, Luckhurst, and Nordio (1995), and Luckhurst (1995) constructed molecular models that explain well the odd-even phenomenon qualitatively and quantitatively [especially if the rotation angle between the neighboring methylene groups is allowed to change continuously (Ferrarini, Luckhurst, and Nordio, 1995)].

2. Elastic, optical, and dielectric properties

Unusual phase behavior of odd dimers as compared to regular rodlike mesogens reveals itself in other physical properties. One of the most striking manifestations was a discovery of blue phases with an exceptionally wide temperature range (~50 °C) in a mixture of flexible dimers containing spacers with $x = 7$, 9, 11 carbon atoms, doped with a small amount of a chiral dopant (Coles and Pivnenko, 2005). This extraordinary stability of the blue phase (which usually exists within a few degrees at most) was attributed to the very high flexoelectric coefficients of the dimeric materials (Coles *et al.*, 2006). Localized flexoelectric polarization was deemed (Coles and Pivnenko, 2005) to stabilize the network of disclination lines that is required to accommodate local double-twist deformations in the blue phases. Subsequent theory by Castles *et al.* (2010) suggested that the flexoelectric polarization reduces the elastic constants of splay K_{11} and bend K_{33} and the corresponding elastic energy of disclinations of strength $-1/2$ that is proportional to both K_{11} and K_{33}; as a result, the blue phase range can expand.

The important role of the elastic constants and of their relative magnitude in stabilization of the blue phases was recognized many years ago by Kleman (1985), and then by Alexander and Yeomans (2006) and Fukuda (2012). Kleman (1985) considered the geometry of double twisted cylindrical elements of the blue phase with deformations of twist and bend and predicted that the blue phase is favored when K_{11} is larger than K_{33} and the twist constant K_{22}. Hur *et al.* (2011) found that adding rigid bent-core molecules to the chiral nematic increased K_{11}, decreased K_{33}, and expanded the range of the blue phase. Subsequent experiments (Atkinson *et al.*, 2012) on the N_U phase comprised entirely of flexible dimers demonstrated that K_{33} in an odd $x = 9$ dimer is indeed very small, 3–4 pN, an order of magnitude smaller than K_{33} measured for the even dimer with $x = 8$; in agreement with the theoretical prediction by Mirko Cestari *et al.* (2011), according to which the bent shape of the flexible dimers should decrease K_{33} but increase only slightly the corresponding flexoelectric coefficient e_{33}.

To measure all three elastic constants directly, one ideally needs to prepare two different types of cells, one with the director aligned uniformly in the plane of the cell (planar alignment) and another with the director being perpendicular to

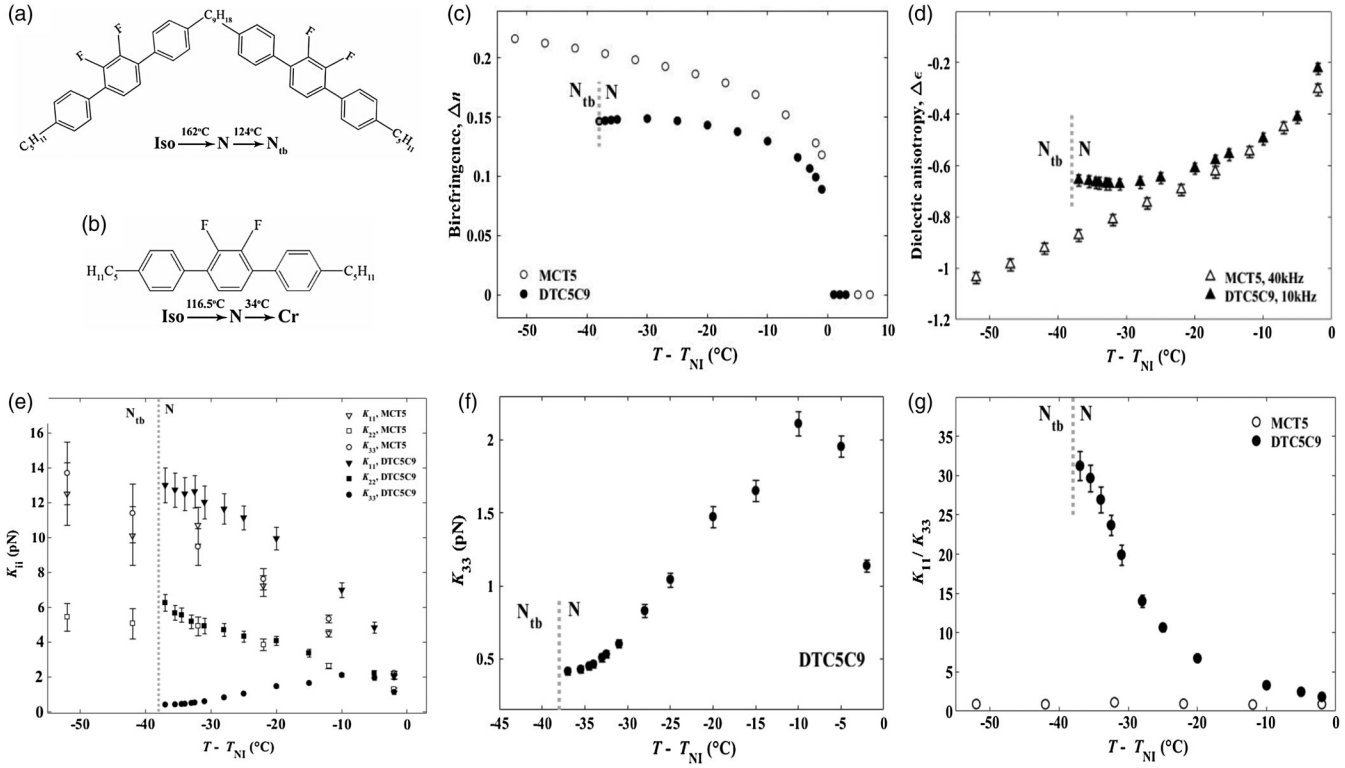

FIG. 37. Temperature dependences of physical properties of a uniaxial nematic phase formed by (a) odd dimer DTC5C9 and (b) monomer MCT5: (c) birefringence; (d) anisotropy of dielectric permittivity; (e) elastic constants of splay, twist, and bend; (f) expanded view of the temperature dependence of K_{33} in the N_U phase of DTC5C9; (g) ratio of splay and bend elastic constants K_{11}/K_{33}. From Cukrov *et al.*, 2017.

the bounding plates (homeotropic cell). So far, planar and homeotropic alignment was achieved only for dimers with a negative anisotropy of dielectric permittivity, $\Delta\varepsilon=\varepsilon_{||}-\varepsilon_{\perp}<0$, such as 1,5-bis (2′, 3′-difluoro-4″ pentyl-[1, 1′:4′1″-terphenyl]-4-yl)nonane DTC5C9, Fig. 37(b) (Borshch *et al.*, 2013). Using homeotropic and planar cells, Cukrov *et al.* (2017) measured birefringence, dielectric permittivities, scalar order parameter, and all three bulk elastic constants K_{11}, K_{22}, and K_{33} of the N_U phase formed by the dimeric molecules of DTC5C9 and compared them to the corresponding values in a monomer 2′, 3′-difluoro-4, 4″-dipentyl-*p*-terphenyl (MCT5); see Figs. 37(a) and 37(b).

The splay constant K_{11} is obtained by applying a magnetic field $\boldsymbol{B}$ perpendicularly to the director and to the bounding plates in a planar cell. Since the diamagnetic anisotropy $\Delta\chi=\chi_{\parallel}-\chi_{\perp}$ of DTC5C9 and MTC5 is positive, at some threshold value of the magnetic field B_{11}, the uniform state is no longer stable and develops splay deformation in the middle of the cell, as the molecules tend to reorient toward the direction of the field. The threshold B_{11} of this splay Frederiks transition is easy to determine by probing light transmitted through the cell and two crossed polarizers or by measuring capacitance of the cell. Provided $\Delta\chi$ is known from an independent experiment (see later), K_{11} is found from the balance (Kleman and Lavrentovich, 2009) of the destabilizing diamagnetic torque $\mu_0^{-1}\Delta\chi B^2\sin\theta\cos\theta$ and the stabilizing splay elastic torque $K_{11}\partial^2\theta/\partial z^2$ as

$$K_{11}=\left(\frac{hB_{11}}{\pi}\right)^2\frac{\Delta\chi}{\mu_o}. \tag{22}$$

Here θ is the angle of director deviation from the horizontal axis set up by the surface anchoring, z is the Cartesian coordinate perpendicular to the bounding plates, h is the cell thickness, and $\mu_o=4\pi\times10^{-7}$ H m^{-1}. K_{22} can be measured in a similar fashion, using a planar cell but applying the magnetic field perpendicularly to $\hat{\mathbf{n}}$ in the plane of the cell. Above a certain threshold B_{22}, the director twists. By testing the cell between two crossed polarizers with an obliquely directed laser beam [to avoid the so-called Mauguin regime (de Gennes and Prost, 1995) in which the polarization of light follows the local director], one determines B_{22} and thus K_{22} from an equation similar to Eq. (22). The bend constant K_{33} is determined by using a homeotropic cell with transparent electrodes at the bounding plates. Applying an ac electric field parallel to $\hat{\mathbf{n}}$, one detects the voltage threshold V_{33}, above which the molecules start to tilt away in the center of the cell and calculates K_{33} as

$$K_{33}=\frac{\varepsilon_o\Delta\varepsilon V_{33}^2}{\pi^2}. \tag{23}$$

The same homeotropic cell can be used to determine $\Delta\chi$, by measuring the magnetic Frederiks transition threshold B_{33} and using

$$\Delta\chi=\varepsilon_o\mu_o\Delta\varepsilon\left(\frac{V_{33}}{hB_{33}}\right)^2.$$

For example, $\Delta\chi=(1.1\pm0.1)\times10^{-6}$ (SI units) at $T-T_{\mathrm{NI}}=-22\,^{\circ}$C for MCT5, and $\Delta\chi=(1.4\pm0.1)\times10^{-6}$ (SI units) at $T-T_{\mathrm{NI}}=-25\,^{\circ}$C for DTC5C9 (Cukrov *et al.*, 2017). By combining the results of electric and magnetic studies, one deduces the values of the elastic constants.

Figures 37(c)–37(e) compare the properties of the rodlike monomer MTC5 and a flexible dimer DTC5C9. Anisotropic properties of MTC5 such as birefringence $\Delta n=n_e-n_o$ (n_e is the extraordinary and n_o is the ordinary refractive indices, respectively) and the absolute value of dielectric anisotropy $|\Delta\varepsilon|$ grows monotonically as the temperature is lowered, as expected for conventional rodlike nematics (de Jeu and Lathouwers, 1974; Vertogen and de Jeu, 1988); see Figs. 37(c) and 37(d). The birefringence of MTC5 (measured at the wavelength 546 nm) follows the empirical Haller's rule (Haller, 1975)

$$\Delta n=\delta n\left(1-\frac{T}{T^*}\right)^{\beta}, \tag{24}$$

with $\delta n=0.309\pm0.003$, $T^*=390.3\pm0.2$ K, and $\beta=0.178\pm0.004$. Validity of the fit in Eq. (22) allows one to approximate the temperature dependence of the order parameter as (Geppi *et al.*, 2011) $S(T)=\Delta n(T)/\delta n$ that also shows a conventional monotonous behavior in MTC5 (Cukrov *et al.*, 2017).

In contrast, the functions $\Delta n(T)$ and $|\Delta\varepsilon|(T)$ in the N_U phase of the dimer DTC5C9 are clearly nonmonotonic, with a maximum at $T\approx T_{UTB}+10\,^{\circ}$C; see Fig. 37(c). The nonmonotonic behavior of $\Delta n(T)$ with a decrease near the N_U-N$_{TB}$ transition temperature T_{UTB} is found in other dimers too (Borshch *et al.*, 2013; Meyer, Luckhurst, and Dozov, 2015; Sebastián *et al.*, 2016). Emsley *et al.* (2016) measured the scalar order parameter $S(T)$ of DTC5C9 from chemical shift anisotropies in NMR experiments and found a similar temperature dependence with a maximum at about 10 °C above T_{UTB}. The nonmonotonic behavior of $S(T)$ appears to be a rule rather than an exception for flexible dimers in which N_U exists in a broad temperature range. It was reported by Adlem *et al.* (2013) for mixtures of flexible dimers, by Burnell *et al.* (2016) for mixtures of CB9CB dimers with conventional rodlike molecules of 5CB and, most recently, by Emsley *et al.* (2017) for asymmetric dimers CB6OCB. The reason for a decrease of $\Delta n(T)$, $|\Delta\varepsilon|(T)$, and $S(T)$ within a range of about 10 °C of T_{UTB} is not entirely clear. A possible explanation is the appearance of pretransitional clusters with a structure that resembles the pseudolayered N_{TB} phase, as discussed in Sec. II.A.4. As the molecules tilt to form an oblique helicoidal structure in these clusters, the overall Δn, $|\Delta\varepsilon|$, and S should decrease. There might be other reasons. In particular, Emsley *et al.* suggested that in CBO6CB the nonmonotonic behavior of S might be caused by formation of the splay-bend nematic N_{SB} that intervenes between N_U and N_{TB} (Emsley *et al.*, 2017). Further studies are clearly in order.

The elastic constants of MCT5 follow the predictions of the mean-field models for rods, namely, $K_{ii}\propto S^2$ and $K_{33}>K_{11}>K_{22}$ (Ferrarini, 2010); see Fig. 37(e). The ratio of any two elastic constants is roughly independent of temperature, since $K_{ii}\propto S^2$; see Fig. 37(g). DTC5C9 shows a rather dramatic departure from these trends.

K_{11} of DTC5C9 is noticeably (by 40%–60%) larger than that of MCT5; see Fig. 37(e). This result correlates with the model proposed by Meyer (1982), in which K_{11} increases linearly with the length L of the molecules, $K_{11} = (k_B T/4d)L/d$, where k_B is the Boltzmann constant, T is the absolute temperature, and d is the diameter of the rodlike molecule. Splay deformations require creation of gaps between molecules. To keep the density constant, these gaps must be filled with the ends of adjacent molecules. The formula for K_{11} follows from the consideration of the entropy loss associated with rearrangements of the molecular ends assumed to behave as noninteracting particles of an ideal gas (Meyer, 1982). Such an assumption is well justified for long molecules, but is less accurate for short ones. It is worth noting that other monomer-dimer comparative studies do not show such a large difference in the values of K_{11} (Li *et al.*, 1990), and sometimes even show that K_{11} of dimers is smaller than K_{11} of a monomer. Dilisi *et al.* (1990) measured K_{11} for a monomer 4, 4′-dialkoxyphenylbenzoate [$C_5H_{11}OC_6H_4COOC_6H_4OC_5H_{11}$], its related even dimer with a spacer of ten methylene groups (Li *et al.*, 1990), and an odd dimer with nine methylene groups in the flexible bridge (Dilisi *et al.*, 1990). It turned out that the odd dimer presumably of a bent shape produced the lowest K_{11} among the three studied molecules (Dilisi *et al.*, 1990; Li *et al.*, 1990), contrary to the case of DTC5C9. One might argue that a reduced scalar order parameter of the odd dimer [which is indeed evidenced by the lower diamagnetic anisotropy (Dilisi *et al.*, 1990)] might lead to a smaller K_{11}. However, this mechanism is apparently not the main one governing K_{11} in DTC5C9 and MCT5, and the increase of the molecular length appears to be dominating.

K_{22} of DTC5C9 and MCT5 shows similar values in the upper temperature range but behaves differently at lower temperatures, as K_{22} of DTC5C9 increases noticeably near the transition into the N_{TB} phase. The measured values of K_{11} and K_{22} yield $K_{11}/K_{22} > 2$; the result agrees with Dozov's model of N_{TB} (Dozov, 2001). Interestingly, DTC5C7 with seven methyl groups in the flexible spacer shows K_{11}/K_{22} that is almost exactly equal to 2 (Sebastián *et al.*, 2016) at T_{UTB}, thus being at the border line of the theoretical criterion that separates N_{TB} from N_{SB}.

The most spectacular deviation of DTC5C9 from the classic picture of nematic elasticity and from a naïve interpretation of Dozov's model is demonstrated by K_{33}; see Figs. 37(e) and 37(f). On cooling, after reaching a maximum, K_{33} decreases to a very low but clearly nonzero value of 0.4 pN near T_{UTB}; see Fig. 37(f) (Cukrov *et al.*, 2017). The same feature was reported for a shorter homolog DTC5C7 by Sebastián *et al.* (2016) and for a mixture of dimers by Adlem *et al.* (2013). The anomalously small K_{33} is a clear result of the bent shape of the molecules, in accordance with discussion concerning rigid bent-shaped materials (Majumdar *et al.*, 2011). The shape factor also makes the ratio K_{11}/K_{33} of DTC5C9 in Fig. 37(g) strongly temperature dependent, violating the relationship $K_{ii} \propto S^2$ that often holds for rodlike nematogens (Cukrov *et al.*, 2017). The finite nonzero value of K_{33} at T_{UTB} can result from the formation of clusters with a pseudolayered N_{TB} structure. It is well known that rodlike mesogens exhibit a strong increase of K_{22} and K_{33} near the N_U—SmA phase transition, caused by the so-called cybotactic clusters with periodic density modulation that hinders deformations of twist and bend (Delaye, Ribotta, and Durand, 1973; Madhusudana and Pratibha, 1982). Similar clusters with periodic director modulations resembling N_{TB} should make twist and bend of the heliconical axis difficult. The finite K_{33} at T_{UTB} can thus be understood as a pretransitional effect.

The "drosophila fly" in the studies of flexible dimers is CB7CB, Fig. 36(b), which has positive dielectric anisotropy, $\Delta\varepsilon = \varepsilon_{\parallel} - \varepsilon_{\perp} > 0$. CB7CB can be aligned in a planar fashion, but not perpendicular to the substrates (homeotropically). Difficulties of homeotropic alignment of rigid bent-core N_U (Iglesias *et al.*, 2011; Elamain, Hegde, and Komitov, 2013) and flexible odd-dimeric N_U compounds (Borshch *et al.*, 2013) with $\Delta\varepsilon > 0$ are well documented; they might lead to surface anchoring transitions and apparent biaxial appearance of the N_U phase in materials formed by rigid bent-core and planklike molecules (Van Le *et al.*, 2009; Senyuk *et al.*, 2010, 2011; Ostapenko *et al.*, 2011; Young-Ki Kim *et al.*, 2012, 2014, 2015). So far, N_U of CB7CB has been characterized only in planar cells. The planar cell allows one to measure Δn and $\varepsilon_{\perp}$ directly (for $\varepsilon_{\perp}$, by applying a small testing electric field well below the Frederiks threshold V_{11}). The parallel component $\varepsilon_{\parallel}$ and thus $\Delta\varepsilon$, Fig. 38(b), are measured by applying a very strong field $V \gg V_{11}$ and extrapolating the measured capacitance to an infinite field limit. The functions $\varepsilon_{\perp}(T)$, $\varepsilon_{\parallel}(T)$, $\Delta\varepsilon(T)$, and $\Delta n(T)$ measured by Babakhanova *et al.* (2017) are shown in Fig. 38. Upon cooling, $\Delta n(T)$ monotonically increases, Fig. 38(a), but $\Delta\varepsilon(T)$ first briefly increases near the clearing point, and then decreases over an extended temperature range, Fig. 38(b), compare to the behavior of $|\Delta\varepsilon|$ in DTC5C9, Fig. 37(d). In the order of magnitude, $\Delta\varepsilon$ of CB7CB is 5–7 times smaller than that of typical monomeric cyanobiphenyls such as pentylcyanobiphenyl (5CB) (Kleman and Lavrentovich, 2013). In contrast, birefringence of CB7CB is similar to that of 5CB, being only slightly smaller, by about 10%–15%; see Fig. 38(a). A smaller Δn can be associated with the tilt of the cyanobiphenyl groups away from the overall director. According to the analysis by Tuchband *et al.* (Tuchband *et al.*, 2017), this tilt is substantial, about 30°. In N_{TB}, Δn decreases further because of the heliconical order (Meyer, Luckhurst, and Dozov, 2015; Tuchband *et al.*, 2017).

The difference between $\Delta\varepsilon(T)$ and $\Delta n(T)$ should not come as a surprise as these quantities reflect polarizabilities at different field frequencies (de Jeu and Lathouwers, 1974; Blinov and Chigrinov, 1994). The difference in contributing mechanisms to $\Delta\varepsilon$ and Δn is well known in the studies of rodlike mesogens (de Jeu, Goossens, and Bordewijk, 1974; de Jeu and Lathouwers, 1974).

In conventional rodlike molecules, as the temperature is lowered, $\varepsilon_{\parallel}$ increases and $\varepsilon_{\perp}$ decreases. As seen in Figs. 38(b) and 38(c), the anomalous behavior of $\Delta\varepsilon$ is caused primarily by a decrease of $\varepsilon_{\parallel}$ upon cooling. Such a behavior was found by many research groups for CB7CB and its longer homologs (M. Cestari *et al.*, 2011; Sebastián *et al.*, 2014, 2016, 2017; Robles-Hernández *et al.*, 2015, 2016; Yun *et al.*, 2015; Parthasarathi *et al.*, 2016; Babakhanova *et al.*, 2017; Trbojevic, Read, and Nagaraj, 2017).

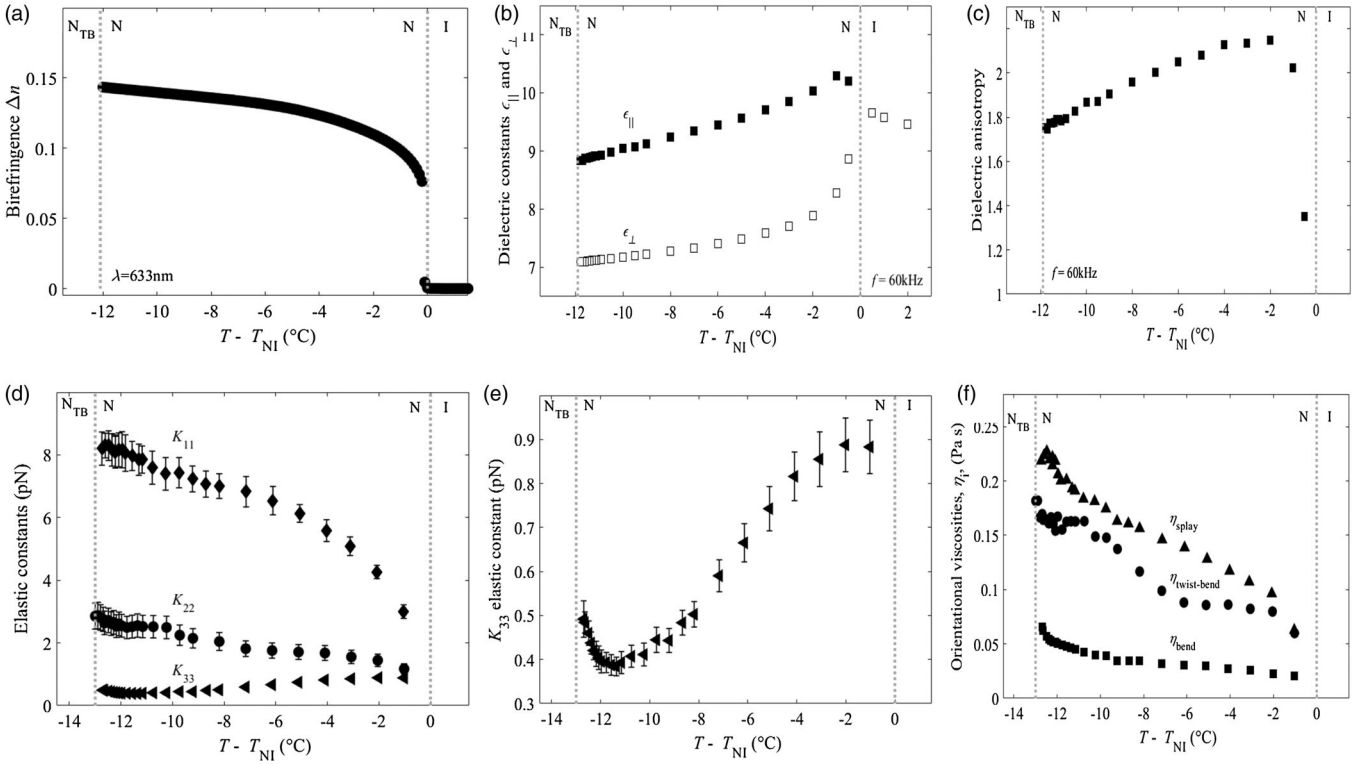

FIG. 38. Temperature dependences of material properties of CB7CB: (a) birefringence; (b) dielectric permittivities; (c) dielectric anisotropy; (d) splay K_{11}, twist K_{22}, and bend K_{33} constants; (e) detailed data for K_{33}; and (f) orientational viscosities. From Babakhanova *et al.*, 2017.

In CB7CB, the molecular net dipole moment is determined mostly by the orientation of two dipole moments located at the terminal nitrile groups (M. Cestari *et al.*, 2011; Robles-Hernández *et al.*, 2015; Sebastián *et al.*, 2017). The flexible dimers respond to changes in temperature by modifying their conformations (Ferrarini *et al.*, 1993, 1994, 1996; Ferrarini, Luckhurst, and Nordio, 1995; M. Cestari *et al.*, 2011). Theoretical models suggest that there are two main populations of conformers, extended and hairpinlike, that vary in the angle between the two cyanobiphenyl units (M. Cestari *et al.*, 2011). The hairpin conformers carry a large longitudinal dipole, while the dipole moment of the extended conformers is practically zero. In the immediate vicinity of the isotropic-to-nematic phase transition, an increase of $\Delta\varepsilon$ can be explained by a stabilization of the hairpin conformers as compared to the broad distribution of the molecular conformers in the isotropic phase (Stocchero *et al.*, 2004; Robles-Hernández *et al.*, 2016). While the hairpin conformers might contribute substantially to the overall dielectric permittivity near the clearing point, their population should diminish as the temperature is lowered and the packing density and scalar order parameter increase (Stocchero *et al.*, 2004). The prevailing extended conformers with a vanishing longitudinal dipole (Robles-Hernández *et al.*, 2015; Sebastián *et al.*, 2017) result in lowering $\varepsilon_{\parallel}$ upon cooling; see Fig. 40(b). Besides the mutual orientation of the two-nitrile group dipoles within the same molecule, their relative positions at neighboring molecules might also contribute to the unusual temperature dependence of $\varepsilon_{\parallel}$. A nonmonotonous temperature dependence of $\Delta\varepsilon$ is known for rodlike (de Jeu, Goossens, and Bordewijk, 1974; de Jeu and Lathouwers, 1974) and bent-core nematics (Avci *et al.*, 2013) near the transition of the N_U phase to the *SmA* phase. In *SmA*, the molecules are arranged in layers, with their long axes being perpendicular to these layers. The spacing between the molecules within *SmA* layers is shorter than the distance between different planes. This packing feature enhances antiparallel dipole correlations within the layers, decreasing the effective longitudinal dipole moment and thus decreasing $\varepsilon_{\parallel}$ and $\Delta\varepsilon$ (de Jeu, Goossens, and Bordewijk, 1974; de Jeu and Lathouwers, 1974).

Although the nematic phases of CB7CB do not show smectic modulations of density, enhancement of antiparallel correlations of the dipole moments located at the neighboring molecules might also contribute to the observed decrease of $\varepsilon_{\parallel}$ and $\Delta\varepsilon$.

By using planar cells, one can measure K_{11} and K_{22} by a direct Frederiks transition method, as described above. The Frederiks effect in a planar cell can yield only indirect information about K_{33}, through extrapolation. First, the electric field is applied across the cell, perpendicularly to the planar director $\hat{\mathbf{n}}$. Above the threshold voltage $V_{11} = \pi\sqrt{K_{11}/\varepsilon_0\Delta\varepsilon}$, the director in the middle of the cell starts to realign along the field, which is easily detectable optically. When the voltage is increased well above V_{11}, the director deformation, in addition to the predominant splay, acquires also some bend. By extrapolating and fitting the response function (such as capacitance of the cell or transmitted light intensity) at $V \gg V_{11}$, one deduces K_{33} (Deuling, 1972). The approach is reasonable when K_{33} is similar to K_{11} or larger, which is the case of rodlike mesogens. However, when $K_{33} \ll K_{11}$, the extrapolation is less accurate. Another

potential problem is that the strong director deformations well above the threshold voltage can produce a significant flexoelectric polarization that renormalizes the elastic response, as shown theoretically by Deuling (1974a, 1974b) and experimentally by Brown and Mottram (2003). Although the flexoelectric effect does not influence the threshold value, it does affect the values of elastic constants obtained by extrapolation to high fields. Recent experiments (Krishnamurthy, Palakurthy, and Yelamaggad, 2017; Varanytsia and Chien, 2017) suggest that the flexoelectric effect might be strong in dimers such as CB7CB. The situation is further complicated by the fact that the flexoelectric polarization can be screened by ions always present in the nematics and the extent of this screening is hard to determine (Smith, Brown, and Mottram, 2007). A significant scatter of K_{33} data reported by different research groups that used the extrapolation procedure for the splay Frederiks transition in planar cells reviewed by Babakhanova *et al.* (2017) suggests that one should use an alternative approach.

An independent and direct approach to determine elastic constants is DLS by director fluctuations (Adlem *et al.*, 2013; Babakhanova *et al.*, 2017). All three bulk elastic constants can be determined by using the same planar cell; the bend and splay-twist modes are separated from each other by using different orientation of the director with respect to the polarization of a probing laser beam. Babakhanova *et al.* (2017) applied this method to measure the temperature dependences of all three bulk elastic constants in CB7CB; see Fig. 38.

On cooling, K_{11} weakly increases in the entire N_U range; see Fig. 38(d). There is also a slight increase in K_{22}, more prominent near the N_U-N_{TB} transition. The most striking behavior is that of K_{33}; see Fig. 38(e). K_{33} decreases dramatically on cooling, approaching a value of 0.4 pN, after which there is a growth near T_{UTB}. As in DTC5C9, K_{33} never reaches a zero value near the N_U-N_{TB} transition, compare Fig. 37(f) and Fig. 38(e), which can be explained by pretransitional clusters with periodic twist-bend modulation of the director in N_U.

Besides CB7CB, the elastic properties have been determined for a number of other flexible dimers with $\Delta\varepsilon > 0$. Balachandran *et al.* (2013) explored the splay Frederiks transition in CB11CB and found that as the temperature decreases, K_{33} becomes smaller than K_{11}; namely, $K_{33} = 6$ pN, while $K_{11} = 15.5$ pN near T_{UTB}. Adlem *et al.* (2013) studied multicomponent mixtures of dimeric materials by DLS and found even more dramatic anisotropy of the elastic constants, with $K_{33} \approx 0.3$–2 pN and $K_{11} \approx 11$–14 pN in the N_U phase at the temperature about 1° above T_{UTB}; the ratio K_{11}/K_{22} was determined to be somewhat higher than 2 (Adlem *et al.*, 2013).

Another striking unusual behavior of odd dimers such as CB9CB is the anomalously large magnetic field-induced increase of the nematic-isotropic transition temperature; see Fig. 39 (Salili, Tamba *et al.*, 2016).

In the presence of a strong (22 T) magnetic field, the temperature shift of the I-N_U transition was found to be ~10 °C, which is 3 orders of magnitude larger than the shift found for rod-shaped mesogens. It was suggested that the shift is caused by a slight straightening of the bent dimer molecules in which the rigid arms have a positive diamagnetic anisotropy (Salili, Tamba *et al.*, 2016). Magnetic fields interact mainly with the delocalized electrons of the aromatic rings of the molecules, so that the free energy is minimized when the field is along the plane of the ring. When the phenyl groups are connected along the main axis of the LC molecules, the energy is minimized with the molecular long axis parallel to the field (positive diamagnetic anisotropy). This explanation of the field-induced straightening of the dimers was built on old observations made for rodlike mesogens that a 15% increase of the aspect ratio leads to the temperature shift by about 6% (Cotter, 1977). The difference in aspect ratios was used by several authors (Terentjev and Petschek, 1993; Ferrarini, Luckhurst, and Nordio, 1995) to explain the anomalously large odd-even effect of T_{NI} of the CBnCB dimers shown in Fig. 35. However, it is not yet clear whether the magnetic field can indeed cause a substantial straightening of the dimers.

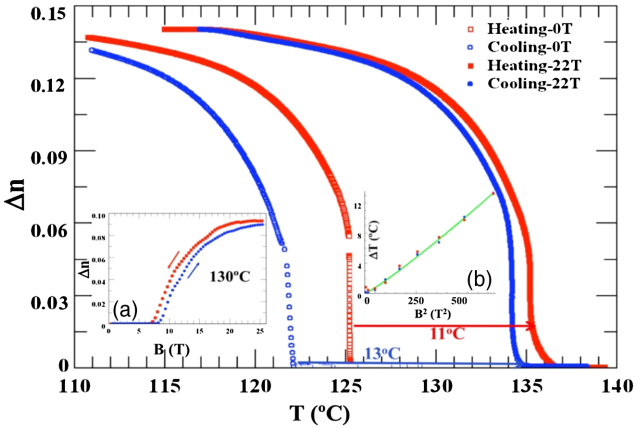

FIG. 39. Temperature dependences of birefringence of CB9CB measured in heating (red squares) and cooling (blue circles) under zero (open symbols) and 22 T magnetic fields (solid symbols). Inset (a) shows the field dependence of birefringence at 130 °C, which is above the I-N transition temperature in absence of the field. Inset (b) shows the shift of $T_{N\text{-}I}$ as a function of the square of the magnetic induction.

B. Chiral nematic phase

The ground state of a uniaxial nematic N_U is spatially uniform director $\hat{\boldsymbol{n}} = \text{const}$. When some or all of the nematic molecules are chiral, the director twists in space, following a right-angle helicoid; the molecules twist around the helicoidal axis, remaining perpendicular to it; see Fig. 40(a). The structure is called a cholesteric Ch (historically referring to the cholesterol base of the first observed liquid crystalline materials) (Planer, 1861, 2010) or sometimes a chiral nematic N^*.

The pitch P_{Ch} of a Ch is typically much larger than the nanometer size of the constituent chiral molecules, being in the range of 0.1–10 μm. The reason is that the molecules rotate around their long axes, which mitigates the chiral contribution to intermolecular interactions (Harris, Kamien, and Lubensky, 1999). The submicron and micron pitch leads to a unique effect of selective light reflection by Ch that is a part of a more general phenomenon of a structural color (Srinivasarao, 1999; Parker, 2000; Vukusic and Roy Sambles, 2003; Sharma *et al.*, 2009). Light traveling along the Ch

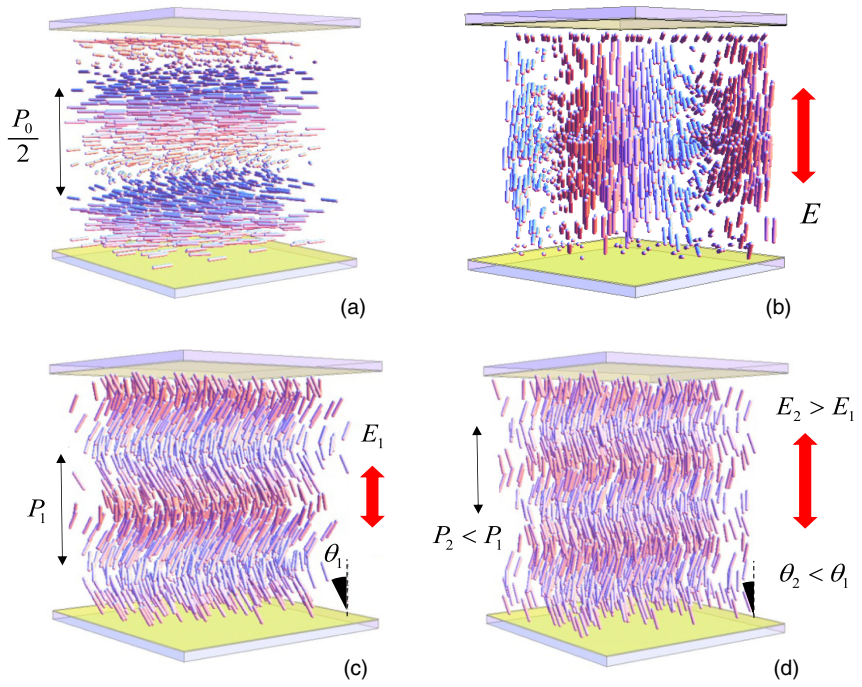

FIG. 40. Cholesterics in an external electric field: (a) right-angle helicoidal *Ch* in absence of the electric field; (b) realignment of the *Ch* with $K_{33} > K_{22}$ into a "fingerprint" texture by the electric field; (c), (d) field-induced Ch_{OH} state for $K_{33} < K_{22}$; as the electric field increases, the pitch P_{Ch} and the conical angle θ both decrease. The figures are not to scale as the experimental cell thickness is typically 20–50 times larger than the cholesteric pitch.

helicoidal axis is separated into right-handed and left-handed circularly polarized components. One component, of the same handedness as the *Ch* structure, is reflected, and the other is transmitted. For light propagating parallel to the helical axis, this Bragg reflection is observed in the spectral range $n_o P_{Ch} < \lambda < n_e P_{Ch}$ determined by the pitch and the ordinary n_o and extraordinary n_e refractive indices. The band is centered at $\lambda_p = \bar{n} P_{Ch}$, where $\bar{n}$ is the average refractive index. The selectively reflected colors are highly saturated; they add like colored lights and produce a color gamut greater than that obtained with inks, dyes, and pigments (Makow and Leroy Sanders, 1978).

The pitch P_{Ch}, and thus the wavelength λ_p of reflected light, can be controlled by exposure to a variety of stimuli (White, McConney, and Bunning, 2010), thus enabling applications, such as temperature indicators (de Gennes and Prost, 1995), sensors of minute quantities of gases (Ohzono, Yamamoto, and Fukuda, 2014), and switchable optical reflectors (De Sio *et al.*, 2013). However, the most desirable mode to control light reflection by an electric field has been elusive for many years. The reason is that the field applied parallel to the axis, instead of changing the pitch while keeping the cholesteric axis intact to reflect light, rotates this axis perpendicularly to itself, as dictated by the (locally positive) dielectric anisotropy of the LC, leading to a light scattering structure called a "fingerprint texture"; see Fig. 40(b). As a result, the use of *Ch* as materials for electrically tunable large-area smart windows, mirrors, filters, displays, and lasers is rather limited.

About 50 years ago, Meyer (1968) and De Gennes (1968) predicted that there should exist a very distinct mode of electrically induced *Ch* deformation, with the director forming an oblique helicoid. This oblique helicoidal (or "heliconical") state, which we denote as Ch_{OH}, requires the bend constant K_{33} to be smaller than the twist constant K_{22} (De Gennes, 1968; Meyer, 1968), a condition not satisfied in typical nematics formed by rodlike molecules. However, odd flexible dimers such as CB7CB and its mixtures with other dimers and 5CB do satisfy the requirement $K_{33} < K_{22}$ and thus produce the Ch_{OH} state when acted upon by the electric (Xiang *et al.*, 2014, 2015, 2016) or magnetic (Salili, Xiang *et al.*, 2016) fields. Its pitch is tunable by the electric field applied parallel to the heliconical axis in a broad range, without violating the single-mode character of the corresponding twist-bend deformations, which results in electrically controlled selective light reflection; see Fig. 41.

The field-induced Ch_{OH} mode of director deformations can be described within the framework of the Frank-Oseen free energy functional (De Gennes, 1968; Meyer, 1968). Neglecting the effects of electric field nonlocality, the energy density for *Ch* writes

$$f = \tfrac{1}{2}K_{11}(\nabla \cdot \hat{\boldsymbol{n}})^2 + \tfrac{1}{2}K_{22}(\hat{\boldsymbol{n}} \cdot \nabla \times \hat{\boldsymbol{n}} - q_{Ch})^2 + \tfrac{1}{2}K_{33}(\hat{\boldsymbol{n}} \times \nabla \times \hat{\boldsymbol{n}}) - \tfrac{1}{2}\Delta\varepsilon\varepsilon_0(\hat{\boldsymbol{n}} \cdot \boldsymbol{E})^2, \quad (25)$$

where K_{11} is the splay elastic constant, $q_{Ch} = 2\pi/P_{Ch}$, P_{Ch} is the pitch of *Ch*, $\Delta\varepsilon = \varepsilon_{\parallel} - \varepsilon_{\perp} > 0$ is the local dielectric anisotropy, representing the difference between the permittivity parallel and perpendicular to $\hat{\boldsymbol{n}}$, and $\boldsymbol{E}$ is the applied electric field. In the absence of the field, the ground state is a right-angle helicoid, such as $\hat{\boldsymbol{n}} = (\cos q_{Ch}z, \sin q_{Ch}z, 0)$. Suppose that the field is applied along the z axis, $\boldsymbol{E} = (0, 0, E)$. When the field is very high, the director is

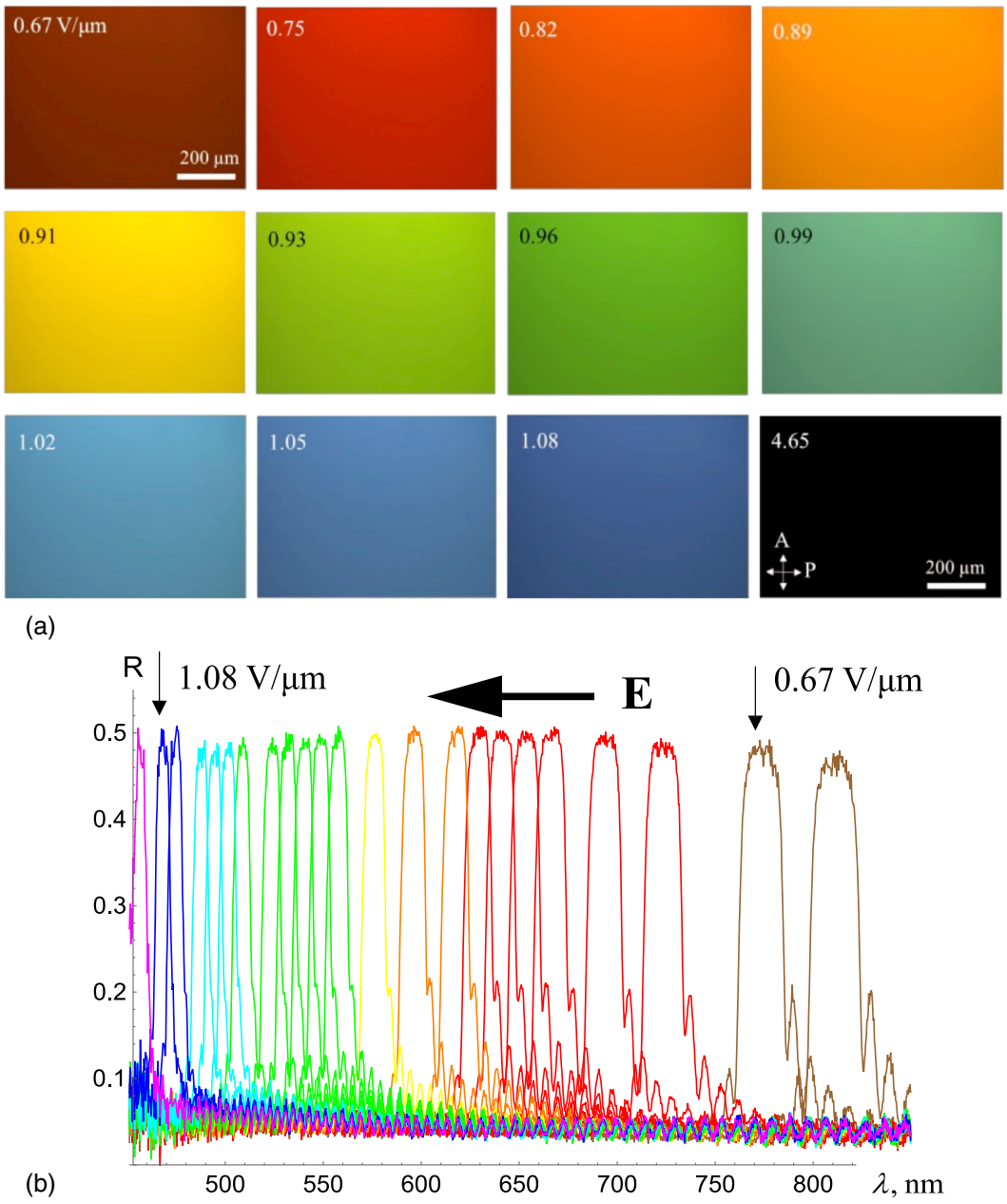

FIG. 41. Electric field-controlled colors of a cell with the Ch_{OH} structure shown as (a) polarizing optical microscope textures and (b) reflection spectra. Incident light is unpolarized. The rms amplitude of the electric field is indicated on the figures. Mixture CB7CB : CB11CB : 5CB : S811 = 49.8 : 30 : 16 : 4.2 wt%. Temperature 27.5 °C. Data by Olena Iadlovska.

parallel to it, $\hat{\boldsymbol{n}} = (0, 0, 1)$, because $\Delta\varepsilon > 0$. As the field is reduced, the tendency to twist caused by a chiral nature of molecules can compete with the dielectric torque. Below some threshold field (Meyer, 1968),

$$E_{\mathrm{UOH}} = \frac{2\pi}{P_{Ch}} \frac{K_{22}}{\sqrt{\varepsilon_0 \Delta\varepsilon K_{33}}},$$

the unwound nematic transforms into a heliconical state with the director that follows an oblique helicoid (OH), $\hat{\boldsymbol{n}} = (\sin\theta\cos\varphi, \sin\theta\sin\varphi, \cos\theta)$ with the cone angle $\theta > 0$ and the angle of homogeneous azimuthal rotation $\varphi(z) = 2\pi z/P$, Figs. 40(c) and 40(d), where the tunable heliconical pitch P is inversely proportional to the field (Meyer, 1968):

$$P = \frac{2\pi}{E}\sqrt{\frac{K_{33}}{\varepsilon_0 \Delta\varepsilon}}. \tag{26}$$

Minimization of the free energy functional based on the density (25) also relates the cone angle θ to the strength of the electric field (Xiang *et al.*, 2014):

$$\sin^2\theta = \frac{\kappa}{1-\kappa}\left(\frac{E_{\mathrm{UOH}}}{E} - 1\right), \tag{27}$$

where $\kappa = K_{33}/K_{22}$. Since $\Delta\varepsilon > 0$, it is clear, however, that the cone angle would not increase continuously to its limiting value $\theta = \pi/2$ as that would mean $\hat{\boldsymbol{n}}$ being perpendicular to $\boldsymbol{E}$

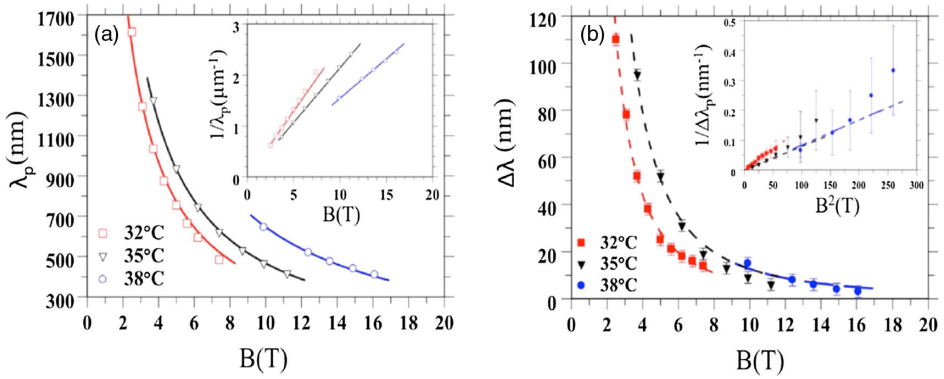

FIG. 42. (a) Magnetic field dependence of the wavelength λ_p and (b) full width at half maximum (FWHM) $\Delta\lambda = (n_e - n_0)P$ of the selective reflection peak observed at different temperatures. From Salili, Xiang *et al.*, 2016.

everywhere. One should thus expect a complete reorganization of the oblique helicoid with an axis along $\hat{\boldsymbol{x}} \| \boldsymbol{E}$ into a right-angle helicoid with the axis *perpendicular* to $\boldsymbol{E}$, at fields lower than (Xiang *et al.*, 2014):

$$E_{\mathrm{OHC}h} \approx E_{\mathrm{NOH}} \frac{\kappa[2 + \sqrt{2(1-\kappa)}]}{1+\kappa}. \tag{28}$$

The last expression is derived by balancing the energies of the right-angle and oblique helicoidal states with a small κ in the external field.

The case of the magnetic field effect is illustrated in Fig. 42 for a mixture CB9CB:CB7CB:5CB:S811 = 45:20:32:3 wt%.

For normal incidence of light, the Ch_{OH} structure reflects light with the peak wavelength $\lambda_p = \bar{n}P$, where the average refractive index for small conical angles $\theta \ll 1$ can be given as $\bar{n} \approx n_o$. Under this assumption,

$$\lambda_p = \frac{n_o}{B}\sqrt{\frac{K_{33}\mu_0}{\Delta\chi}} = a/B.$$

This relationship is indeed observed, Fig. 42(a), with the coefficient a growing at higher temperatures, apparently because of the increase of K_{33} with temperature as discussed. The width of the reflection band is $\Delta\lambda = \Delta n_{\mathrm{eff}} P$, where $\Delta n_{\mathrm{eff}} = n_{e,\mathrm{eff}} - n_o$ and the effective refractive index is

$$n_{e,\mathrm{eff}} = \frac{n_e n_o}{\sqrt{n_e^2 \cos^2\theta + n_o^2 \sin^2\theta}}.$$

Therefore,

$$\Delta n_{\mathrm{eff}} = \frac{n_o(n_e^2 - n_o^2)}{2n_e^2}\sin^2\theta$$

and

$$\Delta\lambda = \frac{\kappa^2 B_{\mathrm{th}} n_o P_0}{2(1-\kappa)B}\left(1 - \frac{n_o^2}{n_e^2}\right)\left(\frac{B_{\mathrm{UOH}}}{B} - 1\right),$$

where B_{th} is the threshold field for the oblique helix to form. For magnetic induction much smaller than B_{UOH} at which Ch_{OH} transforms into a uniformly aligned nematic (a magnetic analog of the electric field threshold E_{UOH}) the bandwidth dependence on the field can be given by $\Delta\lambda \propto 1/B^2$. The experiments indeed demonstrate $\Delta\lambda \propto 1/B^2$ for low magnetic fields; see Fig. 42(b).

As already stressed, the tuning of Ch_{OH} structure by the electric or magnetic field applied parallel to the heliconical axis changes the pitch and the conical angle but preserves the orientation of the axis itself and a single-mode periodic modulation of the director. These features are advantageous not only for an effective tuning of the selective light reflection, but also for the field-controlled lasing at the Ch_{OH} structure. By adding laser dyes to the mixture CB9CB:CB7CB:5CB:S811, Xiang *et al.* (2016) demonstrated lasing with a continuous electrical tuning of the emitting wavelength within a spectral range on the order of 100 nm.

Oblique helicoidal structures similar to Ch_{OH} can be found in the chiral smectic C ($SmC*$) phase. In $SmC*$, the value of θ is fixed by the molecular tilt within smectic layers and the structure is modulated in the sense of molecular orientation and density. Thus whenever θ changes, the thickness of smectic layers and the pitch of the pseudolayers of heliconical twist changes. The associated stresses are released either by tilt of layers or by nucleation of dislocations. The advantage of Ch_{OH} over $SmC*$ is that the molecular-scale defects are avoided when θ is changed by the electric field and in a wider range of accessible θ's. The defects associated with the pitch variations can also be mitigated by an appropriate choice of boundary conditions.

The heliconical cholesteric state can form from the field-induced homeotropic state as a transient structure when the field is removed. This transient structure quickly transforms into another transient structure that resembles a normal cholesteric with $\theta = \pi/2$, but has a pitch that is larger than the equilibrium cholesteric pitch. Yu *et al.* (2016) used CB7CB as a dopant to a cholesteric mixture and demonstrated that the decrease of the bend elastic constant in these mixtures can speed up the transition from the homeotropic to intrinsic planar cholesteric state, with a response time on the order of tens of milliseconds. Furthermore, the transient conical and planar states help to improve the quality of the resulting planar structure, avoiding defects such as dislocations and oily streaks (Yu *et al.*, 2016).

Smallness of the elastic ratio $\kappa = K_{33}/K_{22}$ should manifest itself in large-scale deformations of the cholesterics, when the typical radii of curvature are much larger than the pitch P_{Ch}. In this limit, the elastic properties of *Ch* are described in a coarse-grained Lubensky–de Gennes model (de Gennes and Prost, 1995) that treats the material as a system of flexible layers. Each layer is determined by a constant phase of the director twist; there is no density modulation. To stress the absence of density modulation, the layers in *Ch* (and N_{TB} phases) are often called "pseudolayers." In this review, while describing *Ch*, Ch_{OH} and N_{TB}, we use the term "layers" which is made unambiguous by the earlier definition through the phase.

Consider the simplest case of weak 2D deformations caused by presence of defects or external fields such as the magnetic field of induction $\boldsymbol{B}$. The layers, being originally perpendicular to the axis z, experience small displacements $u(x,z)$ along the z and x directions. The elastic free energy density writes (de Gennes and Prost, 1995; Kleman and Lavrentovich, 2009)

$$f = \frac{1}{2}K\left(\frac{\partial^2 u}{\partial x^2}\right)^2 + \frac{1}{2}C\left[\frac{\partial u}{\partial z} - \frac{1}{2}\left(\frac{\partial u}{\partial x}\right)^2\right]^2 + \frac{\Delta\chi}{2\mu_0}B^2\left(\frac{\partial u}{\partial x}\right)^2, \tag{29}$$

where K is the effective splay constant, C is the compressibility modulus, and $B = |\boldsymbol{B}|$. The quantity $\partial^2 u/\partial x^2$ describes curvatures of layers that correspond to splay of the normal $\hat{\mathbf{t}}$ to the layers. Bend and twist of the normal are prohibited by the requirements of the layers' equidistance. The nonlinear contribution $(1/2)(\partial u/\partial x)^2$ is added to the standard compression and dilation $\partial u/\partial z$ in the second term to account for the fact that when $\hat{\boldsymbol{t}}$ tilts, the separation of layers measured along the z axis is larger than their actual thickness measured along $\hat{\boldsymbol{t}}$. This correction thus eliminates a nonphysical contribution to the dilation and compression terms associated with the tilts. In the case of negative dielectric anisotropy $\Delta\chi = \chi_{\parallel} - \chi_{\perp}$, where the magnetic susceptibilities $\chi_{\parallel}$ and $\chi_{\perp}$ are measured along and perpendicularly to the local director, the field tends to realign the layers parallel to itself. In a bounded sandwich cell with the layers clamped parallel to the plates, the reorientation of layers is resisted by surface anchoring. The compromise is achieved through a periodic buckling of layers, called the Helfrich-Hurault undulation instability, in which the regions of alternating tilt are intercalated with regions of flat layers. The field-induced phenomenon has a mechanical analog as the undulations can be caused by an imposed dilation (Meyer, 1976), by increasing the cell thickness, $h \to h'$, where $h' > h$.

The effective splay constant of a coarse-grained *Ch* is related to the local bend constant $K = 3K_{33}/8$. The compressibility modulus $C = K_{22}(2\pi/P_{Ch})^2$ is determined by the twist Frank constant K_{22}. The ratio of the two elastic parameters yields a characteristic penetration length $\lambda = \sqrt{K/C} = (P_{Ch}/2\pi)\sqrt{3\kappa/8}$. When $\kappa < 1$, which is the case of bent-core materials, λ can be significantly smaller than the pitch P_{Ch}, which implies that the nonlinear correction in Eq. (29) cannot be neglected. In many problems, such as the layer distortions around the edge dislocations (Brener and Marchenko, 1999; Ishikawa and Lavrentovich, 1999; Santangelo and Kamien, 2003), or Helfrich-Hurault undulations of layers (Helfrich, 1970, 1971a; Hervet, Hurault, and Rondelez, 1973; Hurault, 1973) caused by a cell dilation (Meyer, 1976) or by an external field (Ishikawa and Lavrentovich, 2001a, 2001b), the nonlinear corrections are of prime importance. For example, the layers profile above the threshold B_{HH} of Helfrich-Hurault instability

$$u = \frac{8\lambda}{3}\left(\frac{B^2}{B_{HH}^2} - 1\right)^{1/2},$$

can be calculated only when the nonlinear term is involved. Furthermore, the nonlinear terms in Eq. (29) have been shown theoretically (Brener and Marchenko, 1999; Santangelo and Kamien, 2003) and experimentally (Ishikawa and Lavrentovich, 1999) to profoundly influence the layers profile around edge dislocations. Thus *Ch* materials with $\kappa < 1$ represent an experimentally accessible but so far unexplored model of one-dimensional periodic structures with strongly nonlinear elasticity.

An interesting example of how the small κ in *Ch* formed by flexible dimers influences the equilibrium structures in confined geometries was demonstrated recently by Salili *et al.* (2017); see Fig. 43. *Ch* was placed in flat cells of a fixed thickness $h = 5$ μm. Surface alignment was planar, with the easy axis set by rubbing of the top and bottom substrates. When the intrinsic *Ch* pitch satisfies a condition $P_{Ch} = 2h/n$, where n is an integer, then the equilibrium state represents a uniformly twisted structure with the helicoidal axis $\hat{\boldsymbol{t}}$ perpendicular to the bounding plates. However, if P_{Ch} is slightly smaller than $2h/n$, then there is a frustration between the available space and the effective thickness $nP_{Ch}/2$ that can be filled by layers of an equilibrium period $P_{Ch}/2$. In regular *Ch* with $\kappa > 1$ the frustration is resolved through pure twist deformations that bring the pitch to the value of $2h/n$ or $2h/(n+1)$; the result is the well-known Grandjean-Cano textures of *Ch* in wedge samples (de Gennes and Prost, 1995; Smalyukh and Lavrentovich, 2002).

In *Ch* with $\kappa < 1$, a better solution to accommodate the layers with a pitch that is somewhat smaller than $2h/n$ might be their periodic tilt. The effective thickness of a tilted layer measured along the normal z to the bounding plates is larger than the actual thickness measured along $\hat{\boldsymbol{t}}$. The tilt cannot be uniform since the surface anchoring sets the director parallel to the substrates. The boundary conditions thus require the tilt to be maximum in the middle of the cell and to vanish at the substrates. A natural solution is a periodic undulation of layers in the horizontal plane, similarly to the Helfrich-Hurault effect, in which the regions of tilt are intercalated with the regions of layers dilation; see Fig. 43(d). The undulations are associated with director bend, which carries a very low elastic energy price since K_{33} is small. The concrete geometry of undulations depends on the ratio $P_{Ch}/2h$. When $P_{Ch}/2h \approx 0.8$, Figs. 43(a) and 43(d), the undulation stripes are parallel to the rubbing direction, which is understandable, since the director in the middle of the cell is more or less perpendicular to the rubbing direction. When $P_{Ch}/2h \approx 0.4$, Fig. 43(b), the undulations are perpendicular

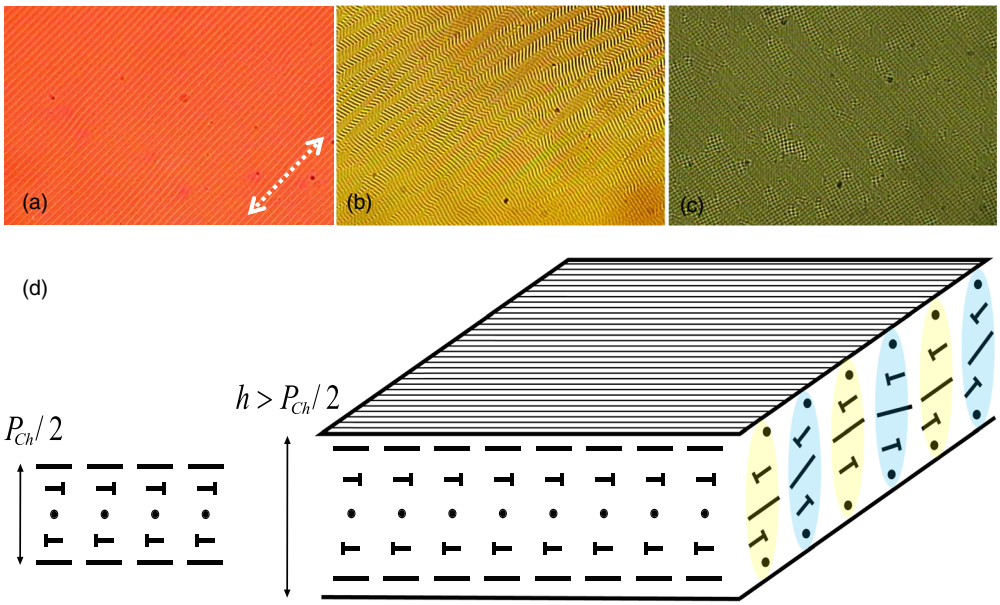

FIG. 43. Polarizing microscope textures of periodic structural deformations of a dimeric mixture KA (Adlem *et al.*, 2013) doped with (a) 1 wt%, (b) 2 wt%, and (c) 3 wt% of chiral dopant S811, respectively. Planar alignment, the rubbing direction is along the dotted arrow. Film thickness $h = 5$ μm, approximate values of the cholesteric pitch P_{Ch} are (a) 8, (b) 4, and (c) 2 μm; (d) scheme of periodic undulations with director bend that develops in a planar cell with a thickness slightly larger than the equilibrium period $P_{Ch}/2$ of *Ch* (shown on the left side). The resulting stripes are parallel to the rubbing direction. The regions of tilt are shadowed in blue, and the regions of layers dilation are shadowed in yellow.

to the rubbing direction, since the director in the middle is parallel to the rubbing direction. Finally, at shorter values of the pitch, $P_{Ch}/2h \approx 0.2$, Fig. 43(c), one observes a texture resembling the classic Helfrich-Hurault square lattice patterns (Helfrich, 1970, 1971a; Hervet, Hurault, and Rondelez, 1973; Hurault, 1973; Ishikawa and Lavrentovich, 2001a, 2001b).

C. Twist-bend nematic N_{TB} phase

The twist-bend nematic N_{TB} phase as discussed in Sec. II.2 and illustrated in Fig. 4(a) is structurally similar to the Ch_{OH} discussed in the previous section. [see Figs. 40(c) and 40(d)]. The director follows an oblique helicoid, maintaining a constant oblique angle with the helix axis and experiencing twist and bend. There are three important differences. First, the twist-bend structure in N_{TB} is thermodynamically stable in a certain temperature range (typically below the uniaxial N_U phase) and does not require any external field. Second, the N_{TB} molecules are not chiral, but have a tendency to pack with bend deformations. Third, the typical pitch of the N_{TB} phase is on the order of 10 nm, which is the molecular scale, much shorter than the supramolecular pitch in a typical *Ch*. The last difference is rooted in the fact that in the N_{TB} molecules cannot rotate freely around their long axes (local biaxiality), while in the *Ch* phase, they do (Harris, Kamien, and Lubensky, 1999). With these precautions, N_{TB} can also be considered a structural link between the usual uniaxial nematic N_U and the cholesteric *Ch*. In N_U, rodlike molecules are on average parallel to the single director $\hat{\boldsymbol{n}}$, but their centers of mass are arranged randomly. The director is a nonpolar entity, $\hat{\boldsymbol{n}} \equiv -\hat{\boldsymbol{n}}$, even if the molecules have dipole moments. In *Ch*, chiral molecules prefer to twist with respect to each other, forcing $\hat{\boldsymbol{n}}$ to follow a right-angle helicoid, either left handed or right handed. A similar structure, but with the hexatic order coupled to twist-bend deformation, was predicted by Kamien (1996).

Theoretical predictions of the N_{TB} phase as discussed in Sec. II.2 predated experimental discovery by decades. Some unusual behavior, including a first-order phase transition between two seemingly uniaxial phases, was detected in main-chain polymers (Ungar, Percec, and Zuber, 1992; Silvestri and Koenig, 1994) and then in dimers with an odd number of carbon atoms in the flexible linkers (Imrie and Henderson, 2007; Šepelj *et al.*, 2007; Panov *et al.*, 2010, 2011, 2012; M. Cestari *et al.*, 2011; Mirko Cestari *et al.*, 2011; Henderson and Imrie, 2011; Beguin *et al.*, 2012; Meyer, Luckhurst, and Dozov, 2013). While the high-temperature phase was easily identifiable as a standard uniaxial N_U, the nature of the low-temperature phase, often referred to as N_x, remained unclear. The hints about the possible nature of this mystery state depended on the experimental technique to characterize it.

1. Optical observations

Polarizing microscope observations of the low-temperature nematic N_x state often revealed the textures of so-called focal conic domains with clearly visible elliptical and hyperbolic defect lines (Barnes *et al.*, 1993; Šepelj *et al.*, 2007; M. Cestari *et al.*, 2011; Henderson and Imrie, 2011), Figs. 44(a)–44(c), and periodic stripes (Panov *et al.*, 2010; M. Cestari *et al.*, 2011; Henderson and Imrie, 2011) of width 1–100 μm; see Figs. 44(d) and 44(e).

The macroscopic stripes apparently did not represent a thermodynamically stable feature as the period depended

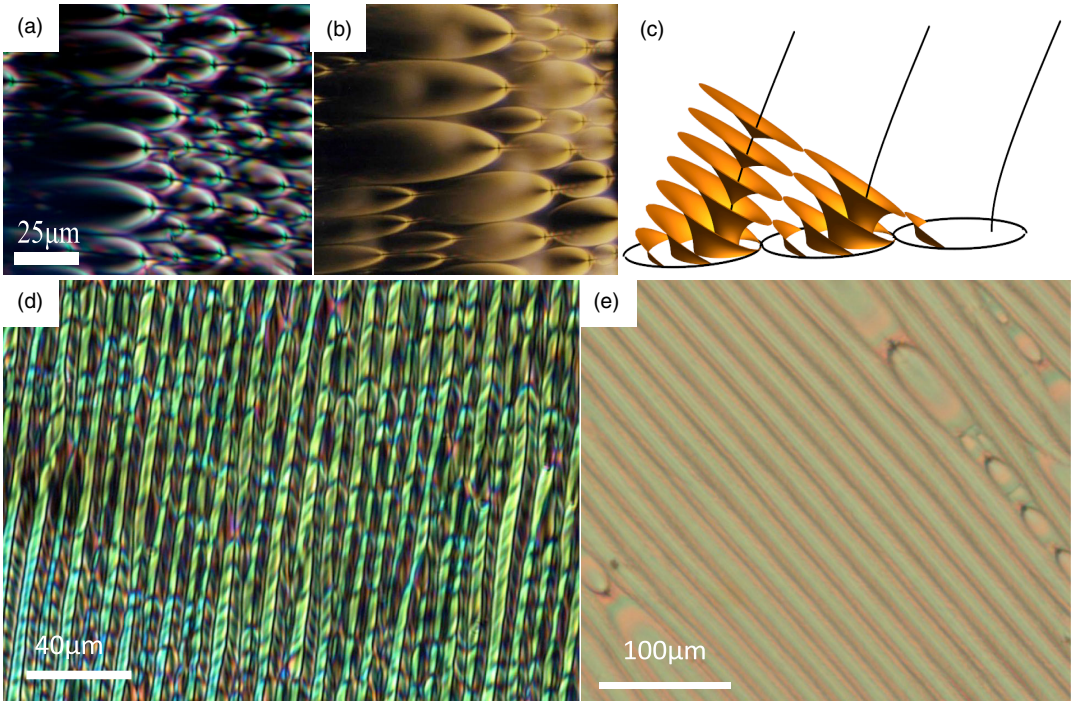

FIG. 44. Typical polarizing optical microscope textures of the N_{TB} phase (a) in a sessile droplet of N_{TB} phase of CB7CB placed on a rubbed substrate. (b) In comparison the texture in the *SmA* phase of material $CHF_2O(C_6H_4)CH=N(C_6H_4)C_4H_9$. (c) 3D scheme of layer curvatures within three focal conic domains with singularities in the shape of ellipse and hyperbolae. (d) Stripe patterns in the N_{TB} phase of CB7CB. (e) Stripe patterns in the N_{TB} phase of DTC5C9. Textures (b) and (d) from Greta Babakhanova.

strongly on the cell thickness (Panov *et al.*, 2011). Focal conics, on the other hand, provided a strong hint that the low-temperature phase is a smectic. As established by Friedel and Grandjean early in the 20th century (Friedel and Grandjean, 1910; Friedel, 1922), the presence of focal conics signals that the liquid crystal exhibits a one-dimensional positional order. This order can be caused by periodically changing density, as in smectics, or by "wave surfaces" of the director twist, as in *Ch*, with no density modulation. Unlike the case of *Ch*, in which the large micrometer-scale pitch makes it possible to trace the helicoidal packing optically, polarizing optical microscopy could not resolve the nanoscale period. Thus some earlier studies, limited by polarizing microscopy, Fig. 44, tentatively concluded that the low-temperature state was a smectic. On the other hand, when the low-temperature N_x state was characterized by x-ray diffraction, the conclusion was that it should be a nematic rather than a smectic phase as there was no signature of electron-density modulation that accompanies positional order (Ungar, Percec, and Zuber, 1992; Šepelj *et al.*, 2007; Panov *et al.*, 2010; M. Cestari *et al.*, 2011).

The optical stripes observed in mixtures with prevailing flexible dimers such as CB11CB and DTC5C11 [Figs. 44(d) and 44(e)] inspired Panov *et al.* (2010) to conclude that the materials must exhibit a new unknown nematic phase N_x. The period of the stripes, in the range 4–20 μm, was determined to be approximately twice the cell thickness h. Appearance of these stripes was attributed to the negative value of either K_{11} or K_{22}. Later studies (Borshch *et al.*, 2013; Challa *et al.*, 2014) revealed that the stripes do indeed appear in the N_{TB} samples but they are not thermodynamically stable and do not represent the natural periodic twist-bend modulation that occurs at nanoscales. Borshch *et al.* (2013) reported that the stripes can be removed by applying the electric field to the N_{TB} slabs of both $\Delta\varepsilon<0$ and $\Delta\varepsilon>0$ type. If the field is removed, the stripe pattern does not reappear. However, if the temperature is reduced, the stripes can emerge again. Similar effects were observed for the magnetic field (Challa *et al.*, 2014). Such behavior is typical for one-dimensionally periodic liquid crystals such as smectics and cholesterics and represents a variation of the Helfrich-Hurault buckling instability. As already discussed following Eq. (30), the Helfrich-Hurault undulations can be caused either by an external field or by mechanical dilations of the cell (Kleman and Lavrentovich, 2013). The latter is fully equivalent to the case when the cell thickness is fixed, but the layers shrink. If the layers shrink, they need to tilt in order to fill the space available. An alternative solution would be through nucleation and propagation of dislocation loops that increase the number of layers, but this effect is hindered by high-energy barriers and slow growth. As in other types of Helfrich-Hurault instability, the tilts of layers alternate in sign. Usually, in *SmA* and *Ch* with degenerate boundary conditions, the in-plane deformations are of a square type (Hurault, 1973). However, surface rubbing and elastic anisotropy (Salili *et al.*, 2017) might produce a preference for one-dimensional undulations; see Fig. 43.

M. Cestari *et al.* (2011) presented a comprehensive characterization of the odd dimer CB7CB [Fig. 36(b)] by using a

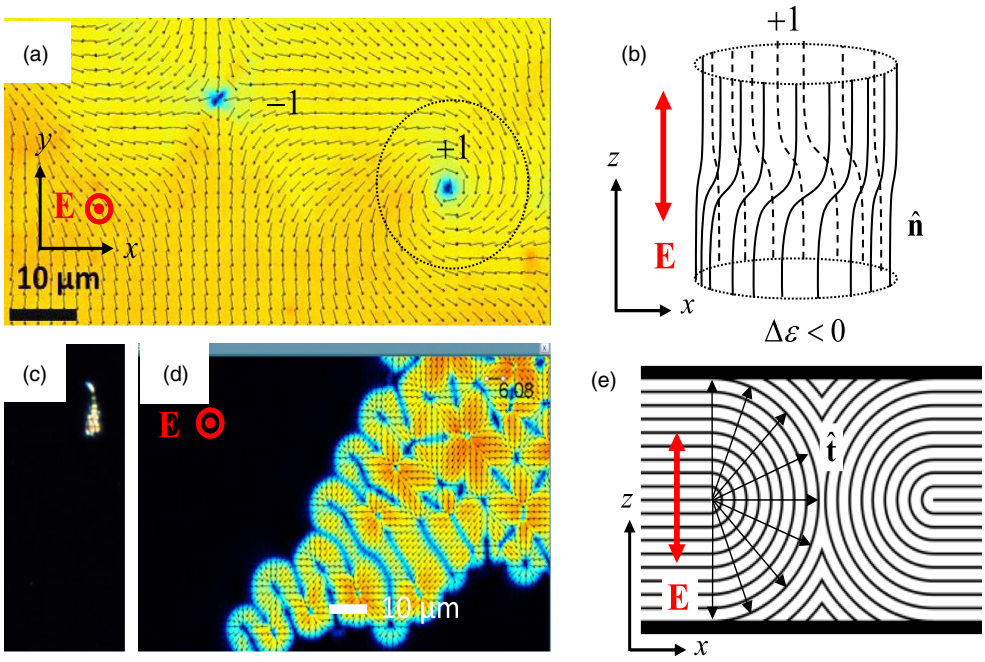

FIG. 45. Structural transitions triggered by the electric field $\boldsymbol{E} = (0, 0, E)$ in homeotropic cells of (a), (b) N_U and (c)–(e) N_{TB} materials with $\Delta\varepsilon < 0$. (a) PolScope texture showing the director projection onto the horizontal x-y plane with predominantly bend deformations, (b) 3D scheme of director deformations, (c) nucleation of a toroidal focal conic domain in N_{TB}, (d) expansion of splay and saddle-splay deformations of the helicoidal axis $\hat{\boldsymbol{t}}$ in the form of an oily streak, and (e) cross section of the oily streak; continuous lines are equidistant layers of N_{TB}. See Borshch *et al.* (2013) for more details on Frederiks transition in N_{TB}.

battery of experimental techniques, such as polarizing optical microscopy, small-angle x-ray scattering, modulated differential scanning calorimetry, dielectric spectroscopy, and magnetic resonance. Optical textures revealed focal conics, while x-ray diffraction showed no signs of density modulation. Deuterium magnetic resonance measurements indicated that the phase should be chiral either globally or locally. Combining all these features, Cestari *et al.* concluded that the low-temperature phase of CB7CB represented "a new type of uniaxial nematic phase having a nonuniform director distribution composed of twist-bend deformations," i.e., an N_{TB}. Neither of the techniques used could determine the pitch of the structure, which later turned out to be extraordinary small, on the order of 10 nm.

Periodic structure of N_{TB} imposes strong restrictions on the type of deformations of the heliconical axis as the equidistance of pseudolayers is compatible with splay but not with bend and twist. Comparison of the bend Frederiks transition in homeotropic cells filled with the N_U and N_{TB} phases in a mixture DTC5C9 (70 wt %): MTC5 (30%) provides a good illustration of the dramatic differences in the elastic behavior of these two phases. In this mixture $\Delta\varepsilon < 0$; thus the electric field applied perpendicularly to the bounding plates of a flat cell should cause a bend deformation of the director in N_U and of the heliconical axis in N_{TB}. In the N_U phase [Fig. 45(a)], once $U > U_{\mathrm{th}}$, the optic axis realigns gradually and everywhere, as in the second-order transition. Since the tilt direction is degenerate, it results in umbilics, i.e., nonsingular defects of winding numbers -1 and $+1$ (de Gennes and Prost, 1995). The $+1$ umbilics show an in-plane bend of $\hat{\boldsymbol{n}}$, which is expected, as $K_{33} \ll K_{11}$ (Borshch *et al.*, 2013; Cukrov *et al.*, 2017). The same experiment in N_{TB} reveals a completely different scenario. Reorientation of the optic axis starts only at isolated sites of the sample, associated with dust particles or surface irregularities. The nucleating regions in the shape of axisymmetric focal conic domains (Kleman and Lavrentovich, 2009) coexist with the homeotropic surrounding [Fig. 45(e)]; they expand if the voltage is higher than some threshold $\tilde{U}_{\mathrm{th}}$. The deformations of the optic axis are of splay and saddle-splay type; see Fig. 45(b). The profile of optical retardation measured across the domain of reoriented N_{TB} reaches a maximum at the center of the domain [Fig. 45(c)], indicating that the tilt of the optic axis is at a maximum in the center. The pattern is similar to the field-induced reorientation in *SmA* (Li and Lavrentovich, 1994) and *Ch* (Lavrentovich and Yang, 1998) phases with $\Delta\varepsilon < 0$, in which the layers equidistance allows splay and saddle splay, but prohibits bend and twist of the layers' normal (Clark and Meyer, 1973). The threshold voltage U_{33}^{TB} of expansion in layered liquid crystals is determined mostly by the balance of surface anchoring at the plates and the dielectric reorienting torque (Lavrentovich, Kleman, and Pergamenshchik, 1994; Li and Lavrentovich, 1994; Lavrentovich and Yang, 1998), so that

$$U_{33}^{\mathrm{TB}} = 2\sqrt{\frac{hW}{\varepsilon_0|\Delta\varepsilon|}} \propto \sqrt{h},$$

where W is the surface anchoring strength and h is the cell thickness. This result should be contrasted to the N_U phase, in which the Frederiks threshold voltage does not depend on h. The peculiar character of the dielectric response provides

another argument in favor of periodic nature of N_{TB} at the scales much shorter than the visible scales.

The first-order structural transition in N_{TB} illustrated in Fig. 45 is practically indistinguishable from the similar transition observed in *SmA* with $\Delta\varepsilon < 0$ (Kleman and Lavrentovich, 2009) and can be described by the same coarse-grained model presented by Lavrentovich and Kleman (1993) and Lavrentovich, Kleman, and Pergamenshchik (1994). The similarity extends further to the observation of focal conic domains [Fig. 44], and periodic undulations in both phases that occur either when the period of the structure shrinks because of temperature change or when the sample is acted upon by an external field. A similar nucleation process has been observed for the material abbreviated KA (0.2) (Adlem *et al.*, 2013) with $\Delta\varepsilon > 0$, where the electric field induces a planar to homeotropic transition (Ribeiro de Almeida *et al.*, 2014).

Electric polarization accompanying the heliconical structure makes the N_{TB} phase the first example of a true liquid (without any density modulation) with local polar order. Direct detection of this polarization is difficult since the polarization averages over to zero over the nanometer scales of P_{TB}. To directly demonstrate its existence, Pardaev *et al.* (2016) used light scattering at structural defects in N_{TB} textures, namely, parabolic focal domains. These domains occur well above the threshold of the Helfrich-Hurault instability when the layers shrink (or the cell is dilated) (Rosenblatt *et al.*, 1977). The layers around two parabolic line defects in these domains form conical cusps that produce an uncompensated polarization directed perpendicularly to the axis of the domain. Pardaev *et al.* (2016) observed a second harmonic signal originating from these defect regions which indicates a broken centrosymmetry and the existence of the local polar order.

The first estimate of the period of director modulations, 7 nm, came from the studies of the electroclinic effect in CB7CB by Meyer, Luckhurst, and Dozov (2013). They extend the original macroscopic model of N_{TB} to describe the electro-optic behavior of the N_{TB} phase that is driven by a flexoeffect. As discussed in Sec. II.1.a, flexoelectric polarization $\boldsymbol{P}_f$ is induced by director curvatures, namely, splay $\boldsymbol{s}=\hat{\boldsymbol{n}}\mathrm{div}\hat{\boldsymbol{n}}$ and bend $\boldsymbol{b}=\hat{\boldsymbol{n}}\times\mathrm{curl}\hat{\boldsymbol{n}}$. Flexoelectric polarization couples to the external electric field $\boldsymbol{E}$. The contribution to the free energy density is linear in $\boldsymbol{E}$ (as opposed to the dielectric term quadratic in $\boldsymbol{E}$): $f_{\mathrm{flex}} = -\boldsymbol{P}_f\cdot\boldsymbol{E} = -[e_1\hat{\boldsymbol{n}}\mathrm{div}\hat{\boldsymbol{n}} - e_3\hat{\boldsymbol{n}}\times\mathrm{curl}\hat{\boldsymbol{n}}]\cdot\boldsymbol{E}$. In N_{TB}, the vector of bend deformation $\boldsymbol{b} = q_{TB}\sin\theta_{TB}\cos\theta_{TB}(\sin q_{TB}z, -\cos q_{TB}z, 0)$ and thus the related flexoelectric polarization $\boldsymbol{P}_f = -e_3\boldsymbol{b}$ are both nonzero and directed perpendicularly to the axis $\hat{\boldsymbol{t}}$ and the director $\hat{\boldsymbol{n}}$. If an external field is applied perpendicularly to the axis $\hat{\boldsymbol{t}}$, coupling to flexoelectric polarization causes the optic axis $\boldsymbol{N}$, representing an average director, to deviate from $\hat{\boldsymbol{t}}$ along the direction of $\hat{\boldsymbol{t}}\times\boldsymbol{E}$ by some angle α, defined as (Meyer, Luckhurst, and Dozov, 2013)

$$\tan\alpha = \frac{P_{TB}(e_1 - e_3)E}{2\pi(K_{11} + K_{33})}$$

(hence the term "electroclinic effect"). By measuring this angle and assuming reasonable values of elastic constants and flexocoefficients, Meyer, Luckhurst, and Dozov (2013) arrived at the estimate $P_{TB} = 7$ nm, a remarkable achievement prior to the direct measurements by TEM (Borshch *et al.*, 2013; Chen *et al.*, 2013) and by x ray (Zhu *et al.*, 2016; Tuchband *et al.*, 2017). The described electroclinic effect is fast, with the typical response time on the order of 1 μs. A similar microsecond response, linear in the applied electric field, was observed by Panov *et al.* (2011) in cells that contained N_x materials later confirmed to be of the N_{TB} type. The textures contained macroscopic stripes [Fig. 44(d)] which made the analysis difficult, but the authors inferred that the observed electroclinic effect might be of a flexoelectric origin and related to the existence of "a very short helical pitch," again a notable achievement in absence of TEM data.

2. Transmission electron microscopy observations

In 2013, independent Colorado and Kent groups, using FF-TEM, reported direct evidence of nanoscale director modulation in CB7CB (Borshch *et al.*, 2013; Chen *et al.*, 2013) and fluorinated flexible dimers (Borshch *et al.*, 2013), with a pitch $P_{TB} \sim 8$–9 nm (Borshch *et al.*, 2013; Chen *et al.*, 2013); see Fig. 46(a). It was found that P_{TB} decreases from about 10 to 8 nm as the temperature is reduced from 100 °C to 70 °C (Zhu *et al.*, 2016; Tuchband *et al.*, 2017), which can provide a qualitative explanation of stripes. The wavelength of Helfrich-Hurault undulations immediately above the threshold is $2\sqrt{\pi\lambda h}$ when calculated under an assumption of infinitely strong surface anchoring (Ishikawa and Lavrentovich, 2001b). For a typical $h = 10$ μm and $\lambda = 30$–100 nm, the wavelength is about 2–4 μm, which is somewhat smaller than the period observed by Panov *et al.* (2010). However, the period of undulations increases a few times when the surface anchoring is finite (Ishikawa and Lavrentovich, 2001a, 2001b; Senyuk, Smalyukh, and Lavrentovich, 2006) and also when the stresses exceed the threshold (Ishikawa and Lavrentovich, 2001b; Senyuk, Smalyukh, and Lavrentovich, 2006), which might explain the discrepancy. The full theory of stripe patterns in N_{TB} requires further developments, especially because of the secondary instabilities along the stripes, clearly seen in Fig. 44(d) and analyzed experimentally by Panov *et al.* (2013, 2015, 2017) and You *et al.* (2017).

As a rule, TEM observations reveal the textures of pseudolayers that are perpendicular to the fracture plane [Fig. 46(a)], freeze-fractured N_U and *Ch*, in which the fracture plane tends to be parallel to the local director $\hat{\boldsymbol{n}}$ as it minimizes the density of molecules in the cut surface. In the N_{TB} phase, the surface with the minimum molecular density is not flat, but modulated with a period P_{TB}. This leads to a strong shadowing effect during the oblique deposition of the Pt/C film onto the freeze-fractured surfaces; the period of the replica yields the period P_{TB} of N_{TB}.

The N_{TB} structure can also be modulated in the x-y plane perpendicular to the direction of the periodic twist bend. Arrows in Fig. 46(a) indicate the regions where the regular structure of N_{TB} is broken. These regions might be either domain walls separating domains of opposite chirality or screw dislocations. Coexistence of the macroscopic (hundreds of micrometers) domains of opposite chirality have been documented by Dozov *et al.* in an electroclinic response of

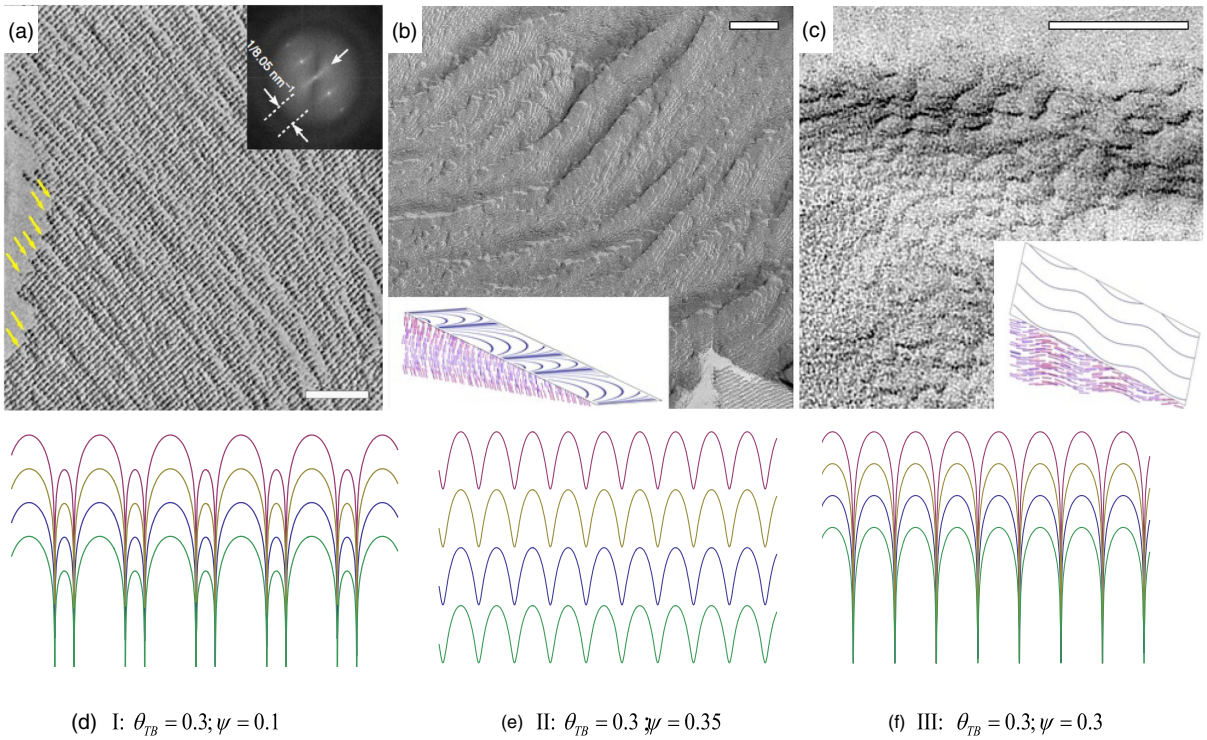

FIG. 46. FF-TEM textures of the N_{TB} phase of CB7CB (a) FF-TEM textures and corresponding fast Fourier transform (FFT) patterns with pitch $P_{TB} = 8.05$ nm viewed in the planes parallel to the optic axis. The arrows point toward domain boundaries, which are roughly perpendicular to the N_{TB} layers. The presence of domains is also revealed by a diffuse intensity pattern in FFT, marked by a white arrow. (b), (c) FF-TEM image of Bouligand arches formed as imprints of the oblique helicoidal structure onto the fracture plane that is (b) almost perpendicular and (c) almost parallel to the helicoid axis of N_{TB}. The insets show the corresponding schemes of Bouligand arches of two types in N_{TB}. All scale bars are 100 nm. (d)–(f) Three types of Bouligand arches predicted by Eq. (31): (d) type I, alternating wide and narrow arches, observed when $\psi < \theta_{TB}$; (e) type II, observed when $\psi > \theta_{TB}$; (f) type III, equidistant arches, observed for heliconical structures only when $\psi = \theta_{TB}$; in *Ch*, the equidistant arches are observed for any tilt angle $0 < \psi < \pi/2$. From Borshch *et al.*, 2013.

CB7CB to the reverse of polarity of the applied electric field (Meyer, Luckhurst, and Dozov, 2013). Archbold *et al.* (2015) reported that the addition of a chiral dopant eliminates one of the two types of domains, supporting the idea that these domains are of opposite handedness.

The periodic texture in Fig. 46(a) is obtained when the plane of the freeze fracture is parallel to the heliconical axis of N_{TB}, which is the most commonly met situation. Such a texture does not provide a direct evidence that the observed structure is indeed N_{TB}, as opposed, say, to the splay-bend nematic N_{SB} (Meyer, 1976; Dozov, 2001; Shamid, Dhakal, and Selinger, 2013; Longa and Pająk, 2016). A specific evidence of the twist-bend structure is brought about by the FF-TEM textures of periodic arches [Figs. 46(b) and 46(c)] that occur when the fracture plane is tilted away from the axis. The tilted cut planes of *Ch* structures produce a series of equidistant arches in which the director projection experiences periodic splay and bend. These are the celebrated Bouligand arches (Bouligand, Soyer, and Puiseux-Dao, 1968) of the *Ch* order. In *Ch*, each arch corresponds to a rotation of $\hat{\boldsymbol{n}}$ by π and two adjacent arches are indistinguishable from each other, as should be for a right helicoid. In the N_{TB} phase, the geometry of arches is very different. In their original paper, in addition to the equidistant *Ch* arches, Bouligand, Soyer, and Puiseux-Dao (1968) also considered asymmetric arches for a hypothetical fractured system of oblique helicoids. Their approach can be extended to the specific case of Eq. (11), written for the director field. Suppose that the plane of fracture $(x\text{-}y')$ is tilted around the axis x, by an angle ψ measured between the new axis y' and the original axis y. The director components in the fracture plane are $n_x = \cos q_{TB} z \sin\theta_{TB}$ and $n_{y'} = \sin q_{TB} z \sin\theta_{TB} \cos\psi - \cos\theta_{TB} \sin\psi$. The local orientation of the director projection in the obliquely fractured N_{TB} phase is then given by

$$\frac{dx}{dy'} = \frac{\cos(q_{TB} y' \sin\psi) \sin\theta_{TB}}{\sin(q_{TB} y' \sin\psi) \sin\theta_{TB} \cos\psi - \cos\theta_{TB} \sin\psi}, \tag{30}$$

with the solution

$$x - x_0 = \frac{\ln|2\cos\psi \sin\theta_{TB}[\sin(q_{TB} y' \sin\psi) - \tan\psi \cot\theta_{TB}]|}{q_{TB} \sin\psi \cos\psi}. \tag{31}$$

Here x_0 is the shift of one arch with respect to the other. Equation (31) distinguishes three types of the Bouligand arches expected in the N_{TB} phase, Figs. 46(d)–46(f): type I for $\psi < \theta_{TB}$, inset in Fig. 46(b), type II for $\psi > \theta_{TB}$, Fig. 46(c), and intermediate type III, with $\psi = \theta_{TB}$, that is hard to

distinguish from the classic symmetric *Ch* arches. In type I, the director imprint rotates in the entire range (0–2π) of azimuthal angles in the fracture plane, but the odd and even arches are of a different width, $l_{0,\pi} \neq l_{\pi,2\pi}$. Type II represents wavy structures extending in the direction normal to the helicoidal axis that do not explore the entire range of azimuthal orientations, Figs. 46(c) and 46(e). In type III, the odd and even arches are of the same width. Observation of type I, Fig. 46(b), and type II, Fig. 46(c), arches provide a clear evidence of the oblique helicoidal structure of the N_{TB} phase, as opposed to other potential geometries.

The nanometer scale of P_{TB} calls for a coarse-grained description of elastic and electro-optic effects in N_{TB}, in which the details of the molecular structure are replaced with macroscopic parameters. The coarse-grained free energy density functional describing any one-dimensional layered system, including N_{TB}, that experiences strong distortions (such as focal conic domains) over spatial scales much larger than the period, is generally written as a sum of a mean curvature term, Gaussian curvature term, compressibility term, and an external field term (Lavrentovich and Kleman, 1993; Lavrentovich, Kleman, and Pergamenshchik, 1994; Kleman and Lavrentovich, 2013):

$$f = \frac{1}{2}K\left(\frac{1}{R_1}+\frac{1}{R_2}\right)^2 + \bar{K}\frac{1}{R_1R_2} + \frac{1}{2}C\varepsilon^2 - \frac{1}{2\mu_0}\Delta\chi(\boldsymbol{B}\cdot\hat{\boldsymbol{t}})^2, \tag{32}$$

where $\varepsilon = 1 - P'_{\mathrm{TB}}/P_{\mathrm{TB}}$ is a dilation or compression of layers, R_1 and R_2 are the two principal radii of curvature of layers, K is the Frank modulus of splay of the normal $\hat{\boldsymbol{t}}$ to the layers, $\bar{K}$ is the saddle-splay modulus, C is the Young's modulus, and $\Delta\chi$ is the diamagnetic anisotropy determined with respect to $\hat{\boldsymbol{t}}$. To this functional, one can add a surface anchoring term (Ishikawa and Lavrentovich, 2001a) if the anchoring is not assumed to be infinitely strong. The material parameters depend on the concrete molecular structures at the scales of period, as already discussed for the case of *Ch*, in which the Young's modulus C was expressed through the twist Frank constant K_{22}. Meyer and Dozov (2016), Dozov and Meyer (2017) and later Parsouzi *et al.* (2016a, 2016b) developed coarse-grained elastic models of N_{TB} in which the material macroscopic properties K and C are expressed through the nanoscale parameters. Experimental measurements by light scattering (Parsouzi *et al.*, 2016a) yield C in the range of 10^3–10^4 Pa, which is substantially lower than the compressibility modulus in *SmA* with density modulation ($C \sim 10^6$ Pa). The splay constant K is expected (Challa *et al.*, 2014) to be close to the value of K_{11} in the N_U phase near T_{UTB}, i.e., on the order of 10 pN (Babakhanova *et al.*, 2017; Cukrov *et al.*, 2017). With $K \sim 10$ pN and $C \sim 10^3$–10^4 Pa, one finds the elastic extrapolation length $\lambda = \sqrt{K/C}$ to be in the range 30–100 nm, which is significantly larger than the period $P_{\mathrm{TB}} \sim 10$ nm. Another interesting elastic feature is that the N_{TB}'s resistance to dilations might be weaker than to compressions (Tuchband *et al.*, 2017).

The pseudolayers formed by the nanoscale heliconical periodicity render smecticlike rheological behavior of the N_{TB} materials. Specifically, Salili *et al.* (2014) found that the N_{TB} phase is strongly shear thinning. At shear stresses below 1 Pa the apparent viscosity of N_{TB} is 1000 times larger than in the nematic phase. At stresses above 10 Pa, the N_{TB} viscosity drops by 2 orders of magnitude and the material exhibits Newtonian fluid behavior. This is consistent with the heliconic axis becoming normal to the shear plane via shear-induced alignment. From measurements of the dynamic modulus the compression modulus of the pseudolayers was estimated to be $C \approx 2 \times 10^3$ Pa, close to the data in light scattering experiments (Parsouzi *et al.*, 2016a).

The quintessential feature of N_{TB} order is periodic heliconical modulation of the director in absence of any density modulations. Recent experiments by Tamba *et al.* (2015) and Abberley *et al.* (2018) demonstrate the existence of smectic phases, in which a one-dimensional density wave coexists with the heliconical modulation of the director. The important point is that achiral molecules form these phases.

As already discussed in Sec. II.2, depending on the elastic ratio K_{11}/K_{22} in the N_U phase near the transition, theoretical models (Dozov, 2001; Shamid, Dhakal, and Selinger, 2013; Longa and Pająk, 2016) predict N_{TB} with $K_{11}/K_{22} > 2$ and N_{SB}, if $K_{11}/K_{22} < 2$. Experimentally only N_{TB} is found. One of the reasons for this might be that the condition $K_{11}/K_{22} < 2$ is hard to achieve, especially when the molecules are not very short, since K_{11} typically increases with the length of molecules. Furthermore, splay deformations imply mass density variations, which might destabilize N_{SB} and favor smectic phases. Numerical simulations by Karbowniczek *et al.* (2017), based on Onsager-type excluded volume interactions for a 2D system comprised of rigid bent-core units, demonstrate that the N_{SB} phase occupies only a small region of the phase diagram constructed as a function of the angle χ between the two arms and the width-to-length or arms ratio, $\delta = D/l$. Namely, N_{SB} is stable only when the bend is relatively weak and the molecules are relatively long, $5\pi/6 \leq \chi < \pi$ and $\delta \leq 0.1$; other values of the two parameters produce smectic phases. On the other hand, N_{SB} structures can be triggered by applying a sufficiently strong electric field to the N_{TB} phase perpendicularly to the helical axis, provided that $\Delta\varepsilon < 0$ (Pająk, Longa, and Chrzanowska, 2017). Another potential instance of a forced N_{SB} occurrence has been described by Meyer, Luckhurst, and Dozov (2015), as a domain wall that separates the regions of left- and right-twisted regions of the N_{TB} phase.

The N_{TB} phase in the most-studied materials, such as CB7CB, occurs upon cooling of the uniaxial N_U phase. A direct isotropic-N_{TB} transition is also possible, as predicted by the molecular field model (Greco, Luckhurst, and Ferrarini, 2014). Recently, new materials, with a relatively short flexible spacer, have been synthesized in which N_{TB} occurs directly from the isotropic phase (Archbold *et al.*, 2015; Dawood *et al.*, 2016). The occurrence of the direct I-N_{TB} transition correlated with a decrease of the clearing temperature rather than with the increase of the temperature of the N-N_{TB} transition (Dawood *et al.*, 2016).

Currently, there are more than 100 compounds known to exhibit the N_{TB} phase. A natural question is what are the molecular factors that determine occurrences of N_{TB}. The bent shape is obviously the most important factor. Figure 47(a)

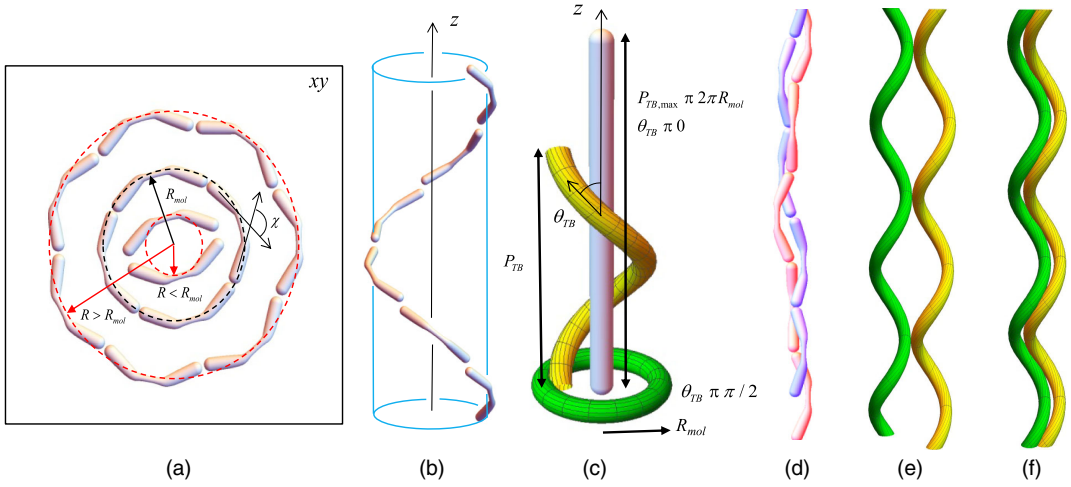

FIG. 47. Packing of bent-core molecules: (a) in a 2D x-y plane, bent-core molecules with the fixed angle χ between the rigid arms can be arranged along a circle of a certain radii R_{mol} that fits the molecular shape; see Fig. 36(b). Filling the interior $R < R_{\mathrm{mol}}$ and exterior $R > R_{\mathrm{mol}}$ of the circle with similarly bent molecules $\chi = \mathrm{const}$ is impossible; (b) bent-core molecules escape into the third z dimension along a helicoidal trajectory thus preserving a constant bend in the entire 3D space but suffering twist deformations; (c) helicoidal chain of CB7CB molecules with the pitch P_{TB}, conical angle θ_{TB}, and the contour length $2\pi R_{\mathrm{mol}}$ measured along one full turn of the helicoid. Also shown are two extreme geometries: a flat circular chain $\theta_{\mathrm{TB}} = \pi/2$ and a straight chain $\theta_{\mathrm{TB}} = 0$, both of the same contour length $2\pi R_{\mathrm{mol}}$; (d) scheme of a "duplex helical tilted chain" as a building unit of CB7CB; (e), (f) models of helicoidal flagellae studied by Barry *et al.* (2006), long before N_{TB} were observed, in out-of-phase (e) and in-phase (f) arrangements. (a), (b), and (d) From V. Borshch. (e), (f) From Barry *et al.*, 2006.

illustrates bent-core molecules with a fixed angle χ between the two rigid arms arranged onto a horizontal x-y plane. The shape suggests that the energetically favored local 2D organization would resemble a circle of a certain radius R_{mol} defined in Fig. 36(b) that fits the curved shape of the molecule; see Fig. 47(a). Unfortunately, this circular geometry cannot be extended to the rest of the x-y plane, since the molecules placed in the interior and exterior of the circle cannot have the same bent shape; χ must be either smaller (interior) or larger (exterior) than the preferred one. This 2D packing problem can be resolved if the molecules are allowed to leave the plane and escape into the third dimension, forming a helicoid in 3D that wraps around a circular cylinder under some constant angle; see Fig. 47(b).

In terms of the local director, this transition from 2D to 3D represents a transition from pure bend to a combined bend and twist. Furthermore, the helicoids can be placed next to each other, thus filling the 3D space fully. Goodby's group presented an interesting argument in favor of the decisive role of the molecular bend by noting that for many different N_{TB}-forming materials, the temperature of the N_U-N_{TB} transition is linearly proportional to the clearing temperatures of the N_U-isotropic transition (Goodby, 2017; Mandle, Stevens, and Goodby, 2017; Simpson *et al.*, 2017), concluding that the details of chemical composition of these materials are of much lesser importance than the bent shape in the formation of N_{TB}. This conclusion is supported by a large number of experimental observations on newly synthesized materials with various chemical structures (Mandle *et al.*, 2016; Mandle and Goodby, 2016a; Mandle, Stevens, and Goodby, 2017).

According to the theory by Greco, Luckhurst, and Ferrarini (2014), based on the generalized Maier-Saupe model, N_{TB} stability is very sensitive to the bend angle χ. Experimentally, Mandle *et al.* (2016) observed that the two temperatures specified before depend strongly on χ: N_{TB} in various materials is most stable when χ is in the range 110°–130°, with a maximum stability achieved at 120°–125°. The bend angles were determined by two techniques: (i) numerical minimization of conformation energy for isolated molecules at room temperature and (ii) NMR spectra recorded in dilute solutions of the dimers. These χ values should be considered only as averaged qualitative characteristics because the dimers can exist in various conformations and because in the N_{TB} phase the conformations of tightly packed molecules might be different from conformations of isolated noninteracting molecules. Because of that, the average bend angle might not be the only parameter responsible for the N_{TB} stability. And indeed, Archbold *et al.* (2017) found examples when a flexible dimer with the average bend angle close to that of CB7CB does not exhibit the N_{TB} phase. The result might be explained by a different χ distribution of molecular conformers (Archbold *et al.*, 2017) or by the fact that the bend angle of isolated molecules is substantially different from the bend angle in N_{TB}. Another direct evidence of the importance of the bend angle has been demonstrated by Paterson *et al.* (2016): flexible dimers with azobenzene groups that are capable of photoinduced trans-to-cis isomerization during which χ changes dramatically were demonstrated to exhibit a photocontrolled N_{TB} phase.

The notion that the bent shape is of prime importance implies that the N_{TB} occurrence is not restricted to dimers. Recent studies indeed confirmed appearance of the N_{TB} phase in higher oligomers. Wang *et al.* (2015) reported a room-temperature N_{TB} phase in a flexible trimer with a pitch of 19 nm. Mandle *et al.* found N_{TB} in trimers (Mandle and

Goodby, 2016c), tetramers (Mandle and Goodby, 2016b), and hexamers (Mandle, Stevens, and Goodby, 2017; Simpson *et al.*, 2017). It is expected that this list would be expanded to higher homologs and eventually to high-molecular weight macromolecules. It would be of especial interest to return to the polymers in which the low-temperature nematic phase different from N_U has been found by Ungar, Percec, and Zuber (1992) and Stevenson *et al.* (2018).

The in-depth analysis of the molecular-scale structure of N_{TB} has been recently presented on the basis of resonant x-ray studies (Zhu *et al.*, 2016; Salamończyk *et al.*, 2017; Stevenson *et al.*, 2017; Tuchband *et al.*, 2017). As already indicated, standard x-ray diffraction could not capture the periodic structure of the N_{TB} phase since the heliconical structure does not produce electron density modulation. However, resonant x-ray scattering, in which a linearly polarized x ray probes an electron cloud and produces a tensorial atomic scattering cross section for energies near the absorption edge, allows one to determine the orientation of the molecules with respect to the polarization of the beam. Zhu *et al.* (2016) used resonant soft x-ray scattering at the carbon K-edge scattering to demonstrate that the N_{TB} phase of CB7CB has indeed a bulk periodic helical modulation of molecular orientation without modulation of the electron density. The pitch of the heliconical structure was found to be 9.8 nm near the N_U-N_{TB} transition, reducing to about 7.8 nm upon cooling, similar to the results of FF-TEM (Borshch *et al.*, 2013; Chen *et al.*, 2013). The study was extended by Tuchband *et al.* (2017) to the measurements of the pitch P_{TB} and cone angle θ_{TB} in mixtures of CB7CB with 5CB as a function of concentration and temperature. The results revealed a remarkable inherent geometric relationship between the macroscopic helix and the nanometer-scale bend curvature of the CB7CB molecule. By plotting the value of the director bend in the helix, $B_H(\theta_{TB}) = q_{TB}\cos\theta_{TB}\sin\theta_{TB}$ vs $\sin\theta_{TB}$, Tuchband *et al.* (2017) found that the dependence represents a straight line of a constant slope $\sum = q_{TB}\cos\theta_{TB} = 0.64\ \mathrm{nm}^{-1}$. In other words, when the pitch and the conical angle change, the product $\sum = q_{TB}\cos\theta_{TB}$ remains the same, independent of temperature and concentration. This finding invites one to explore the limiting cases of $\theta_{TB} = 0$ and $\pi/2$; see Fig. 47(c). The first limit $\theta_{TB} = 0$ suggests that the maximum pitch $P_{TB,max}$ of N_{TB} near the transition to the N_U phase, where $\theta_{TB} = 0$ should be about 9.8 nm, which is indeed very close to the value measured experimentally (Tuchband *et al.*, 2017). The second limit $\theta_{TB} = \pi/2$ corresponds to the CB7CB molecules arranged in the plane; there is no twist. The shape of numerically equilibrated CB7CB molecules can be approximated by a circular arch with a radius of $R_{mol} \approx 1.58$ nm; Fig. 36(a). The inverse quantity, the molecular bend curvature $B_{mol} = 1/R_{mol} \approx 0.63\ \mathrm{nm}^{-1}$, is remarkably close to the slope $\sum = q_{TB}\cos\theta_{TB} = 0.64\ \mathrm{nm}^{-1}$. It means that the limiting pitch can be related to the molecular curvature $P_{TB,max} = 2\pi/\sum = 2\pi/B_{mol} = 2\pi R_{mol}$. The same quantity $2\pi R_{mol}$ defines the contour length measured along the molecular direction for a single turn of the helix for any pair P_{TB} and θ_{TB} that produces a stable N_{TB} state at a given concentration and temperature. The concept is illustrated in Fig. 47(c), which shows three possible configurations of a chain of molecules all of the same length $2\pi R_{mol}$. The flat circle corresponds to the limit $\theta_{TB} = \pi/2$. The central straight line corresponds to $\theta_{TB} = 0$. The intermediate helicoid of a single turn (one pitch) corresponds to intermediate P_{TB} and θ_{TB} that are such that the length of this helicoid is also $2\pi R_{mol}$.

The parameter $\sum$ is also related to the magnitude of the director twist $T_H = \sum \sin\theta_{TB}\tan\theta_{TB}$. The latter relationship means that the elastic cost of twist is $\propto T_H^2$, growing strongly with θ_{TB} and setting a limit on a maximum value of θ_{TB}, experimentally determined as $\theta_{TB\,max} \approx 35°$ (Tuchband *et al.*, 2017).

When the CB7CB molecules are confined to the plane, $\theta_{TB} = \pi/2$, four molecules with slightly overlapping CN groups are needed to complete the circle of circumference $2\pi R_{mol}$ (Tuchband *et al.*, 2017). This packing is similar to the sketch in Figs. 47(a) and 47(b), except that the gaps are replaced by small overlaps. Therefore, the contour length measured along the molecular direction for one turn of the helix also contains four slightly overlapping CB7CB molecules. The net result of this geometrical correspondence is that the CB7CB molecules form a chain along the helix, similar to oligomeric chains but without covalent bounds between neighboring molecules. Furthermore, the x-ray scattering data (Salamończyk *et al.*, 2017; Tuchband *et al.*, 2017) suggest that the main motif of N_{TB} structure is not a single oligomer chain, but a pair of chains wrapped around each other; see Fig. 47(d). The molecules in one chain are shifted by half-a-molecular length with respect to the other chain, so that the flexible aliphatic bridge in one chain is located closely to the cyanogroup ends of the molecules in the neighboring chain. The resulting structure resembles a brickwork-packing motif with paired adjacent chains, making this a "duplex helical tilted chain" (DHTC) of molecules the basic structural element of a N_{TB} phase formed by CB7CB. Analysis of the x-ray scattering data led Tuchband *et al.* (2017) to conclude that the bulk N_{TB} phase represents a 3D space-filling packing of DHTCs that run parallel to each other. In mixtures with rodlike molecules of 5CB, the DHTCs are formed primarily by bent-core CB7CB molecules, with 5CB filling the space between them, reducing θ_{TB} but maintaining the same value of $\sum = q_{TB}\cos\theta_{TB} = 1/R_{mol}$. A similar view on the structural elements of the N_{TB} phase as "fibers" comprised of two or more chains of molecules wrapped around each other has been expressed by Goodby and colleagues (Simpson *et al.*, 2017).

Stevenson *et al.* (2017) used resonant hard x-ray scattering at the Se K edge of the mixture containing DTC5C7 and a seleno ether flexible dimer of a molecular structure similar to that of DTC5C7. The advantage of a Se-containing mixture was that the x-ray studies could be performed on samples that are aligned by the magnetic field. The work confirmed the heliconical structure of N_{TB} with a pitch in the range of 9–12 nm (longer pitch corresponding to higher temperatures) and also demonstrated a very high degree of alignment of the helicoidal axes.

This discussion demonstrates an important role of the excluded volume interactions in the formation of N_{TB} (Greco and Ferrarini, 2015). The excluded volume mechanism was evoked by Barry *et al.* (2006), who discovered an analog of the N_{TB} phase in a lyotropic system even before the

thermotropic N_{TB} materials were characterized. The studied system represented a suspension of rigid helical flagella of a well-defined handedness isolated from *salmonella typhimurium* bacteria. These flagella are polydisperse, with an average contour length of 4 μm and a pitch of 1.1 μm. When the concentration of flagella in water increases, they pack in such a way that the tilted regions of the neighboring flagella are parallel to each other. Such packing minimizes the excluded volume and yields a layered structure in terms of the "phase" of molecular tilts rather than density; see Figs. 47(e) and 47(f) (Kolli *et al.*, 2014). The flagella can glide with respect to each other still preserving the layers of constant phase, since axial translations are coupled to rotations; this phase layering can occur without any density layering.

It is known that many polymer molecules of biological origin such as DNA (a polynucleotide), poly-γ-benzyl-L-glutamate (a polypeptide), and xanthan (a polysaccharide) form liquid crystals when dissolved in water. At low concentrations, these molecules form a stable *Ch* phase (Belli *et al.*, 2014; Dussi *et al.*, 2015; Dussi and Dijkstra, 2016). At higher concentrations, x-ray studies demonstrate a transition to the columnar phase, most likely of a hexagonal type, in which the 2D positional order propagates along the planes perpendicular to the molecular axes. Such an order is incompatible on the long length scales with twist deformations, but Livolant and Bouligand (1986) described interesting textures of DNA, poly-γ-benzyl-L-glutamate and xanthan, in which the columnar arrangement coexisted with the cholesteric twists. These materials deserve further studies as it is possible that the intermediate concentrations would reveal analogs of the N_{TB} phase in which the 2D positional order would not yet form, but the helices would be parallel to each other (rather than twisted as in the *Ch* phase at low concentrations) to minimize the excluded volume, as in Fig. 47(f).

V. CONCLUSIONS

For many decades, the interest of the liquid crystal community was focused on mesomorphic phases formed by highly symmetric rodlike and disklike molecules. These molecules upon proper averaging show rotational symmetry around the longest or shortest axis, respectively, and form three well-known major liquid crystalline states: (i) uniaxial nematics with no long-range positional order, (ii) smectics of type *A* and *C* with one-dimensional positional order, and (iii) columnar phases with two-dimensional positional order. Bent-core mesogens, intensively studied over the last two decades, expanded this picture rather dramatically by exhibiting new packing structures. The underlying mechanism is the lack of rotational symmetry of the molecular shape and appearance of a polar order. This polar order can be associated with electrostatic polarization or be of a pure steric nature. In 1969, R. B. Meyer recognized the importance of polar order in flexoelectric response of a uniaxial nematic to an externally applied electric field (Meyer, 1969) and then suggested that the deformed polarized state might occur also spontaneously as twist-bend and splay-bend structures.

Experimental exploration of newly synthesized rigid bent-core molecules in the 1990s established a plethora of new smectic, columnar, and three dimensionally modulated phases. In smectics three vector quantities, namely, the polarity vector, the normal to smectic layers, and the director form a variety of configurations and the modulation in density is accompanied by various patterns of polarization modulation. Especially interesting is the observation of layer chirality in tilted polar smectic phases consisting of achiral molecules. The overall racemic nature of these materials gives ample possibilities for new phenomena, such as electrically switching between transparent and scattering states and the formation of optically active conglomerates. Columnar structures are formed from ribbons of broken layers, or cone-shaped organizations. The most important feature of the first type is the formation of stable 1D fluid filaments that mimic the structure of neurons and can lead to special optical waveguides. Columnar liquid crystals from cone-shaped aggregates are potentially useful in ferroelectric switches. Although no commercial applications of rigid bent-core molecules exist today, these examples and many more mentioned in Sec. III makes it very likely that they will find their applications in the near future.

Recently, flexible bent-core molecules were demonstrated to form a new nematic phase, the so-called twist-bend nematic N_{TB}. N_{TB} together with rigid bent-core smectics are examples of a spontaneously broken chiral symmetry in materials formed by achiral molecules. In light of these discoveries of new phases, the absence of an experimental evidence of a highly anticipated biaxial nematic N_B represents a fundamental puzzle. The existence of a splay-bend nematic N_{SB} is another fascinating issue waiting for its experimental resolution. Exploration of the new smectic and nematic phases so far has not produced immediate wide-spread new applications, although some modes of electro-optical switching, such as electrically controlled Bragg reflection of light at Ch_{OH} structures, and large polarization effects can certainly be used in practical devices.

In this review, we focused mainly on bent-core molecules with an obtuse angle. Very little is known about mesomorphic properties of their acute-angle counterparts, in which the direction of the polar order can be parallel to the main director rather than perpendicular to it. It is safe to state that the bent-core mesogens will remain at the forefront of liquid crystal research for years to come.

ACKNOWLEDGMENTS

A. J. was supported by NSF Grants No. DMR 1307674 and No. CHE-1563087. O. D. L. acknowledges support provided to his current research by NSF Grants No. DMR-1410378, No. DMR-1507637, and No. DMREF DMS-1729509. J. V. S. was supported by NSF Grant No. DMR-1409658.

REFERENCES

Abberley, Jordan P., Ross Killah, Rebecca Walker, John M. D. Storey, Corrie T. Imrie, Miroslav Salamonzyk, Chenhui Zhu, Ewa Gorecka, and Damian Pociecha, 2018, "Heliconical Smectic Phases Formed by Achiral Molecules," Nat. Commun. **9**, 228.

Acharya, B. R., A. Primak, T. J. Dingemans, E. T. Samulski, and S. Kumar, 2003, "The Elusive Thermotropic Biaxial Nematic Phase in Rigid Bent-Core Molecules," Pramana **61**, 231–237.

Acharya, Bharat R., Andrew Primak, and Satyendra Kumar, 2004, "Biaxial Nematic Phase in Bent-Core Thermotropic Mesogens," Phys. Rev. Lett. **92**, 145506.

Addis, J., S. Kaur, D. J. Binks, M. R. Dickinson, C. Greco, A. Ferrarini, V. Görtz, J. W. Goodby, and H. F. Gleeson, 2016, "Second-Harmonic Generation and the Influence of Flexoelectricity in the Nematic Phases of Bent-Core Oxadiazoles," Liq. Cryst. **43**, 1315–1332.

Adlem, K., M. Čopič, G. R. Luckhurst, A. Mertelj, O. Parri, R. M. Richardson, B. D. Snow, B. A. Timimi, R. P. Tuffin, and D. Wilkes, 2013, "Chemically Induced Twist-Bend Nematic Liquid Crystals, Liquid Crystal Dimers, and Negative Elastic Constants," Phys. Rev. E **88**, 022503.

Akutagawa, T., Y. Matsunaga, and K. Yasuhara, 1994, "Mesomorphic Behaviour of 1, 3-Phenylene Bis[4-(4-Alkoxyphenyliminomethyl)Benzoates] and Related Compounds," Liq. Cryst. **17**, 659–666.

Alexander, G. P., and J. M. Yeomans, 2006, "Stabilizing the Blue Phases," Phys. Rev. E **74**, 061706.

Amaranatha, Reddy R., U. Baumeister, C. Keith, H. Hahn, H. Lang, and C. Tschierske, 2007, "Influence of the Core Structure on the Development of Polar Order and Superstructural Chirality in Liquid Crystalline Phases Formed by Silylated Bent-Core Molecules: Lateral Substituents," Soft Matter **3**, 558–570.

Araoka, Fumito, N. Y. Ha, Yoshitaka Kinoshita, Byougchoo Park, J. W. Wu, and H. Takezoe, 2005, "Twist-Grain-Boundary Structure in the B4 Phase of a Bent-Core Molecular System Identified by Second Harmonic Generation Circular Dichroism Measurement," Phys. Rev. Lett. **94**, 137801.

Araoka, Fumito, and Go Sugiyama, 2011, "Electric-Field Controllable Optical Activity in the Nano-Segregated System Composed of Rod-and Bent-Core Liquid Crystals," Opt. Mater. Express **1**, 27.

Archbold, Craig T., Edward J. Davis, Richard J. Mandle, Stephen J. Cowling, and John W. Goodby, 2015, "Chiral Dopants and the Twist-Bend Nematic Phase—Induction of Novel Mesomorphic Behaviour in an Apolar Bimesogen," Soft Matter **11**, 7547.

Archbold, Craig T., Richard J. Mandle, Jessica L. Andrews, Stephen J. Cowling, and John W. Goodby, 2017, "Conformational Landscapes of Bimesogenic Compounds and Their Implications for the Formation of Modulated Nematic Phases," Liq. Cryst. **44**, 2079–2088.

Atkinson, Katie L., Stephen M. Morris, Flynn Castles, Malik M. Qasim, Damian J. Gardiner, and Harry J. Coles, 2012, "Flexoelectric and Elastic Coefficients of Odd and Even Homologous Bimesogens," Phys. Rev. E **85**, 012701.

Avci, Nejmettin, Volodymyr Borshch, Dipika Debnath Sarkar, Rahul Deb, Gude Venkatesh, Taras Turiv, Sergij V. Shiyanovskii, Nandiraju V. S. Rao, and Oleg D. Lavrentovich, 2013, "Viscoelasticity, Dielectric Anisotropy, and Birefringence in the Nematic Phase of Three Four-Ring Bent-Core Liquid Crystals with an L-Shaped Molecular Frame," Soft Matter **9**, 1066–1075.

Babakhanova, Greta, Zeinab Parsouzi, Sathyanarayana Paladugu, Hao Wang, Yu. A. Nastishin, Sergij V. Shiyanovskii, Samuel Sprunt, and Oleg D. Lavrentovich, 2017, "Elastic and Viscous Properties of the Nematic Dimer CB7CB," Phys. Rev. E **96**, 062704.

Bailey, Christopher A., Katalin Fodor-Csorba, James T. Gleeson, Samuel N. Sprunt, and A. Jákli, 2009, "Rheological Properties of Bent-Core Liquid Crystals," Soft Matter **5**, 3618–3622.

Bailey, Christopher A., and Antal Jákli, 2007, "Role of Molecular Shape on Bent-Core Liquid-Crystal Structures," Phys. Rev. Lett. **99**, 207801.

Bailey, Christopher A., M. Murphy, Alexey Eremin, Wolfgang Weissflog, and Antal Jákli, 2010, "Bundles of Fluid Fibers Formed by Bent-Core Molecules," Phys. Rev. E **81**, 031708.

Balachandran, R., V. P.Panov, J. K. Vij, A. Kocot, M. G. Tamba, A. Kohlmeier, and G. H. Mehl, 2013, "Elastic Properties of Bimesogenic Liquid Crystals," Liq. Cryst. **40**, 681–688.

Barbero, G., P. Taverna Valabrega, R. Bartolino, and B. Valenti, 1986, "Evidence for the Flexo-Electric Effect in a Nematic Liquid Crystal Cell," Liq. Cryst. **1**, 483–490.

Barnes, P. J., A. G. Douglass, S. K. Heeks, and G. R. Luckhurst, 1993, "An Enhanced Odd-Even Effect of Liquid Crystal Dimers Orientational Order in the α, ω-Bis (4′-Cyanobiphenyl-4-Yl)Alkanes," Liq. Cryst. **13**, 603–613.

Barry, Edward, Zach Hensel, Zvonimir Dogic, Michael Shribak, and Rudolf Oldenburg, 2006, "Entropy-Driven Formation of a Chiral Liquid-Crystalline Phase of Helical Filaments a b c D," Phys. Rev. Lett. **96**, 018305.

Basu, Rajratan, Joel S. Pendery, Rolfe G. Petschek, Robert P. Lemieux, and Charles Rosenblatt, 2011, "Macroscopic Torsional Strain and Induced Molecular Conformational Deracemization," Phys. Rev. Lett. **107**, 237804.

Bault, P., C. Selbmann, Sebastian Rauch, Hans Sawade, and Gerd Heppke, 2002, "Biphenyl-Based Banana Shaped Compounds," *Abstract Booklet of 19th ILCC* (ILCC, Edinburgh), p. 611.

Bauman, Patricia, and Daniel Phillips, 2009, "Stability of B7 Fibers," Mol. Cryst. Liq. Cryst. **510**, 1/[1135].

Bedel, J. P., J. C. Rouillon, J. P. Marcerou, M. Laguerre, H. T. Nguyen, and M. F. Achard, 2000, "Novel Mesophases in Fluorine Substituted Banana-Shaped Mesogens," Liq. Cryst. **27**, 1411–1421.

Bedel, J. P., J. C. Rouillon, J. P. Marcerou, M. Laguerre, H. T. Nguyen, and M. F. Achard, 2001, "New Switchable Smectic Phases in Banana-Shaped Compounds," Liq. Cryst. **28**, 1285–1292.

Bedel, J. P., J. C. Rouillon, J. P. Marcerou, M. Laguerre, H. T. Nguyen, and M. F. Achard, 2002, "Influence of Fluoro Substituents on the Mesophase Behaviour of Banana-Shaped Molecules," J. Mater. Chem. **12**, 2214–2220.

Beguin, Laetitia, James W. Emsley, Moreno Lelli, Anne Lesage, Geoffrey R. Luckhurst, Bakir A. Timimi, and Herbert Zimmermann, 2012, "The Chirality of a Twist-Bend Nematic Phase Identified by NMR Spectroscopy," J. Phys. Chem. B **116**, 7940–7951.

Belli, S., S. Dussi, M. Dijkstra, and R. Van Roij, 2014, "Density Functional Theory for Chiral Nematic Liquid Crystals," Phys. Rev. E **90**, 020503(R).

Berardi, R., and C. Zannoni, 2000, "Do Thermotropic Biaxial Nematics Exist? A Monte Carlo Study of Biaxial Gay—Berne Particles Do Thermotropic Biaxial Nematics Exist? A Monte Carlo Study of Biaxial Gay—Berne Particles," J. Chem. Phys. **113**, 5971.

Berardi, Roberto, Luca Muccioli, Silvia Orlandi, Matteo Ricci, and Claudio Zannoni, 2008, "Computer Simulations of Biaxial Nematics," J. Phys. Condens. Matter **20**, 463101.

Berardi, Roberto, Luca Muccioli, and Claudio Zannoni, 2008, "Field Response and Switching Times in Biaxial Nematics," J. Chem. Phys. **128**, 024905.

Bergquist, Leah, *et al.*, 2017, "An Optically Isotropic Antiferroelectric Liquid Crystal (OI-AFLC) Display Mode Operating over a Wide Temperature Range Using Ternary Bent-Core Liquid Crystal Mixtures," ChemistryOpen **6**, 196–200.

Berreman, Dwight W., and Saul Meiboom, 1984, "Tensor Representation of Oseen-Frank Strain Energy in Uniaxial Cholesterics," Phys. Rev. A **30**, 1955–1959.

Binet, C., Sebastian Rauch, C. Selbmann, P. Bault, Gerd Heppke, Hans Sawade, and Antal Jákli, 2003, "Evidence for Molecular Chirality Induced Polarization in Banana Liquid Crystal Phases," in

Proceedings of the German Liquid Crystal Workshop (Max Planck Institute, Mainz, Germany).

Biscari, Paolo, and Maria Carme Calderer, 2005, "Telephone-Cord Instabilities in Thin Smectic Capillaries," Phys. Rev. E **71**, 051701.

Blinov, L. M., and V. G. Chigrinov, 1994, *Electrooptic Effects in Liquid Crystal Materials* (Springer, New York).

Borshch, V., *et al.*, 2013, "Nematic Twist-Bend Phase with Nanoscale Modulation of Molecular Orientation," Nat. Commun. **4**, 2635.

Borshch, Volodymyr, Sergij V. Shiyanovskii, Bing Xiang Li, and Oleg D. Lavrentovich, 2014, "Nanosecond Electro-Optics of a Nematic Liquid Crystal with Negative Dielectric Anisotropy," Phys. Rev. E **90**, 062504.

Bouligand, Y., M. O. Soyer, and S. Puiseux-Dao, 1968, "La Structure Fibrillaire et l'orientation Des Chromosomes Chez Les Dinoflagellés," Chromosoma **24**, 251–287.

Brand, H. R., and H. Pleiner, 2010, "Macroscopic Behavior of Non-Polar Tetrahedratic Nematic Liquid Crystals," Eur. Phys. J. E **31**, 37–50.

Brand, Helmut R., Harald Pleiner, and P. E. Cladis, 2005, "Tetrahedratic Cross-Couplings: Novel Physics for Banana Liquid Crystals," Physica A (Amsterdam) **351**, 189–197.

Brener, E. A., and V. I. Marchenko, 1999, "Nonlinear Theory of Dislocations in Smectic Crystals: An Exact Solution," Phys. Rev. E **59**, R4752.

Brown, C. V., and N. J. Mottram, 2003, "Influence of Flexoelectricity above the Nematic Freedericksz Transition," Phys. Rev. E **68**, 031702.

Buka, A., and N. Éber, 2012, *Flexoelectricity in Liquid Crystals: Theory, Experiments and Applications* (Imperial College Press, London).

Burnell, E. E., Z. Ahmed, C. Welch, G. H. Mehl, and R. Y. Dong, 2016, "Deuteron and Proton NMR Study of D2, p-Dichlorobenzene and 1, 3, 5-Trichlorobenzene in Bimesogenic Liquid Crystals with Two Nematic Phases," Chem. Phys. Lett. **659**, 48–54.

Carr, E. F., 1969, "Influence of Electric Fields on the Molecular Alignment in the Liquid Crystal P-(Anisalamino)-Phenyl Acetate," Mol. Cryst. **7**, 253–268.

Castles, F., S. M. Morris, and H. J. Coles, 2011, "The Limits of Flexoelectricity in Liquid Crystals," AIP Adv. **1**, 032120.

Castles, F., S. M. Morris, and H. J. Coles, 2013, "Response to 'Comment on "The Limits of Flexoelectricity in Liquid Crystals"' [AIP Advances 3, 019101 (2013)]," AIP Adv. **3**, 019102.

Castles, F., S. M. Morris, E. M. Terentjev, and H. J. Coles, 2010, "Thermodynamically Stable Blue Phases," Phys. Rev. Lett. **104**, 157801.

Cestari, M., *et al.*, 2011, "Phase Behavior and Properties of the Liquid-Crystal Dimer 1″, 7″-Bis (4-Cyanobiphenyl-4′-Yl) Heptane: A Twist-Bend Nematic Liquid Crystal," Phys. Rev. E **84**, 031704.

Cestari, Mirko, Elisa Frezza, Alberta Ferrarini, and Geoffrey R. Luckhurst, 2011, "Crucial Role of Molecular Curvature for the Bend Elastic and Flexoelectric Properties of Liquid Crystals: Mesogenic Dimers as a Case Study," J. Mater. Chem. **21**, 12303.

Chakraborty, S., J. T. Gleeson, A. Jakli, and S. Sprunt, 2013, "A Comparison of Short-Range Molecular Order in Bent-Core and Rod-like Nematic Liquid Crystals," Soft Matter **9**, 1817–1824.

Challa, P. K., V. Borshch, O. Parri, C. T. Imrie, S. N. Sprunt, J. T. Gleeson, O. D. Lavrentovich, and A. Jákli, 2014, "Twist-Bend Nematic Liquid Crystals in High Magnetic Fields," Phys. Rev. E **89**, 060501(R).

Chandrasekhar, S., B. K. Sadashiva, and K. A. Suresh, 1977, "Liquid Crystals of Disc-like Molecules," Pramana **9**, 471–480.

Chattham, Nattaporn, Eva Körblova, Renfan Shao, David M. Walba, Joseph E. Maclennan, and Noel A. Clark, 2010, "Triclinic Fluid Order," Phys. Rev. Lett. **104**, 067801.

Chen, Dong, J. E. Maclennan, R. Shao, Dong Ki Yoon, Haitao Wang, Eva Korblova, David M. Walba, Matthew A. Glazer, and Noel A. Clark, 2011, "Chirality-Preserving Growth of Helical Filaments in the B4 Phase of Bent-Core Liquid Crystals," J. Am. Chem. Soc. **133**, 12656–12663.

Chen, Dong, Michael-Scott Heberling, Michi Nakata, Loren E. Hough, Joseph E. Maclennan, Matthew A. Glaser, Eva Korblova, David M. Walba, Junji Watanabe, and Noel A. Clark, 2012, "Structure of the B4 Liquid Crystal Phase near a Glass Surface," ChemPhysChem **13**, 155–159.

Chen, Dong, Yongqiang Shen, Chenhui Zhu, Loren E. Hough, Nélida Gimeno, Matthew A. Glaser, Joseph E. Maclennan, M. Blanca Ros, and Noel A. Clark, 2011, "Interface Structure of the Dark Conglomerate Liquid Crystal Phase," Soft Matter **7**, 1879.

Chen, Dong, Michael R. Tuchband, Balazs Horanyi, Eva Korblova, David M. Walba, Matthew A. Glaser, Joseph E. Maclennan, and Noel A. Clark, 2015, "Diastereomeric Liquid Crystal Domains at the Mesoscale," Nat. Commun. **6**, 7763.

Chen, Dong, Chenhui Zhu, Richard K. Shoemaker, Eva Korblova, David M. Walba, Matthew A. Glaser, Joseph E. Maclennan, and Noel A. Clark, 2010, "Pretransitional Orientational Ordering of a Calamitic Liquid Crystal by Helical Nanofilaments of a Bent-Core Mesogen," Langmuir **26**, 15541–15545.

Chen, Dong, Chenhui Zhu, Haitao Wang, Joseph E. Maclennan, Matthew A. Glaser, Eva Korblova, David M. Walba, James A. Rego, Eduardo a. Soto-Bustamante, and Noel A. Clark, 2013, "Nanoconfinement of Guest Materials by Helical Nanofilament Networks of Bent-Core Mesogens," Soft Matter **9**, 462.

Chen, Dong, *et al.*, 2013, "Chiral Heliconical Ground State of Nanoscale Pitch in a Nematic Liquid Crystal of Achiral Molecular Dimers," Proc. Natl. Acad. Sci. U.S.A. **110**, 15931–15936.

Chen, Wei-Hong, Wei-Tsung Chuang, U-Ser Jeng, Hwo-Shuenn Sheu, and Hong-Cheu Lin, 2011, "New SmCG Phases in a Hydrogen-Bonded Bent-Core Liquid Crystal Featuring a Branched Siloxane Terminal Group," J. Am. Chem. Soc. **133**, 15674–15685.

Cinacchi, Giorgio, and Valentina Domenici, 2006, "Orientational Ordering of a Banana-Shaped Solute Molecule in a Nematic Calamitic Solvent by 2H-NMR Spectroscopy: An Indication of Glasslike Behavior," Phys. Rev. E **74**, 030701.

Cladis, P. E., and M. Kléman, 1972, "Non-Singular Disclinations of Strength $S = +1$ in Nematics," J. Phys. (France) **33**, 591–598.

Clark, N. A., and Robert B. Meyer, 1973, "Strain Induced Instability of Monodomain Smectic A and Cholesteric Liquid Crystals," Appl. Phys. Lett. **22**, 493–494.

Coleman, D. A., C. D. Jones, M. Nakata, Noel A. Clark, D. M. Walba, W. Weissflog, K. Fodor-Csorba, J. Watanabe, V. Novotna, and V. Hamplova, 2008, "Polarization Splay as the Origin of Modulation in the B1 and B7 Smectic Phases of Bent-Core Molecules," Phys. Rev. E **77**, 021703.

Coleman, D. A., *et al.*, 2003, "Polarization-Modulated Smectic Liquid Crystal Phases," Science **301**, 1204–1211.

Coles, H. J., M. J. Clarke, S. M. Morris, B. J. Broughton, and A. E. Blatch, 2006, "Strong Flexoelectric Behavior in Bimesogenic Liquid Crystals," J. Appl. Phys. **99**, 034104.

Coles, Harry J., and Mikhail Pivnenko, 2005, "Liquid Crystal 'blue Phases' with a Wide Temperature Range," Nature (London) **436**, 997–1000.

Cotter, Martha A., 1977, "Hard Spherocylinders in an Anisotropic Mean Field: A Simple Model for a Nematic Liquid Crystal," J. Chem. Phys. **66**, 1098.

Cukrov, Greta, Youssef Mosaddeghian Golestani, Jie Xiang, Yu. A. Nastishin, C. Welch, G. H. Mehl, and Oleg D. Lavrentovich, 2017, "Comparative Analysis of Anisotropic Material Properties of Uniaxial Nematics Formed by Flexible Dimers and Rod-like Monomers," Liq. Cryst. **44**, 219–231.

Dantlgraber, Gert, Alexei Eremin, Siegmar Diele, Anton Hauser, Horst Kresse, Gerhard Pelzl, and Carsten Tschierske, 2002, "Chirality and Macroscopic Polar Order in a Ferroelectric Smectic Liquid-Crystalline Phase Formed by Achiral Polyphilic Bent-Core Molecules," Angew. Chem., Int. Ed. **41**, 2408–2412.

Dawood, Alya A., Martin C. Grossel, Geoffrey R. Luckhurst, Robert M. Richardson, Bakir A. Timimi, Neil J. Wells, and Yousif Z. Yousif, 2016, "On the Twist-Bend Nematic Phase Formed Directly from the Isotropic Phase," Liq. Cryst. **43**, 2–12.

De Gennes, P. G., 1968, "Calcul de La Distorsion d'une Structure Cholesterique Par Un Champ Magnetique," Solid State Commun. **6**, 163–165.

de Gennes, P. G., and J. Prost, 1995, *The Physics of Liquid Crystals* (Claredon Press, Oxford), 2nd ed.

de Gennes, Pierre-Gilles, 1974, *The Physics of Liquid Crystals* (Clarendon Press, Oxford).

de Jeu, W. H., 1980, *Physical Properties of Liquid Crystalline Materials* (Gordon and Breach Science, New York/London/Paris).

de Jeu, W. H., and W. A. P. Claassen, 1977, "The Elastic Constants of Nematic Liquid Crystalline Terminally Substituted Azoxybenzenes The Elastic Constants of Nematic Liquid Crystalline Terminally Substituted Azoxybenzenes," J. Chem. Phys. **67**, 3705–3712.

de Jeu, W. H., W. J. A. Goossens, and P. Bordewijk, 1974, "Influence of Smectic Order on the Static Dielectric Permittivity of Liquid Crystals," J. Chem. Phys. **61**, 1985–89.

de Jeu, W. H., and Th. W. Lathouwers, 1974, "Dielectric Properties of Di-n-Heptyl Azoxybenzene in the Nematic and in the Smectic-A Phases," Phys. Rev. Lett. **32**, 40–43.

Delaye, M., R. Ribotta, and G. Durand, 1973, "Rayleigh Scattering at a Second-Order Nematic to Smectic-A Phase Transition," Phys. Rev. Lett. **31**, 443–445.

Demus, D., 1989, "Plenary Lecture: One Hundred Years of Liquid-Crystal Chemistry: Thermotropic Liquid Crystals with Conventional and Unconventional Molecular Structure," Liq. Cryst. **5**, 75–110.

Derzhanski, A., and A. G. Petrov, 1971, "A Molecular-Statistical Approach to the Piezoelectric Properties of Nematic Liquid Crystals," Phys. Lett. A **36**, 483–484.

De Sio, Luciano, Tiziana Placido, Svetlana Serak, Roberto Comparelli, Michela Tamborra, Nelson Tabiryan, M. Lucia Curri, Roberto Bartolino, Cesare Umeton, and Timothy Bunning, 2013, "Nano-Localized Heating Source for Photonics and Plasmonics," Adv. Opt. Mater. **1**, 899–904.

Deuling, H. J., 1974a, "The Piezo-Electric Effect in Nematic Layers," Mol. Cryst. Liq. Cryst. **26**, 281–284.

Deuling, H. J., 1974b, "On a Method to Measure the Flexo-Electric Coefficients of Nematic Liquid Crystals," Solid State Commun. **14**, 1073–1074.

Deuling, Heinz J., 1972, "Deformation of Nematic Liquid Crystals in an Electric Field," Mol. Cryst. Liq. Cryst. **19**, 123–131.

de Vries, Adriaan, 1970, "X-Ray Photographic Studies of Liquid Crystals I. A Cybotactic Nematic Phase," Mol. Cryst. Liq. Cryst. **10**, 219–36.

Dhakal, Subas, and Jonathan V. Selinger, 2010, "Statistical Mechanics of Splay Flexoelectricity in Nematic Liquid Crystals," Phys. Rev. E **81**, 031704.

DiDonna, B. A., and R. D. Kamien, 2002, "Smectic Phases with Cubic Symmetry: The Splay Analog of the Blue Phase," Phys. Rev. Lett. **89**, 215504.

Dilisi, Gregory A., Charles Rosenblatt, Anselm C. Griffin, and Uma Hari, 1990, "Splay Elasticity in an Oligomeric Liquid Crystal," Liq. Cryst. **8**, 437–443.

Domenici, Valentina, 2011, "Dynamics in the Isotropic and Nematic Phases of Bent-Core Liquid Crystals: NMR Perspectives," Soft Matter **7**, 1589.

Domenici, Valentina, Carlo Alberto Veracini, and Bostjan Zalar, 2005, "How Do Banana-Shaped Molecules Get Oriented (If They Do) in the Magnetic Field?" Soft Matter **1**, 408–411.

Dong, Ronald Y., K. Fodor-Csorba, J. Xu, Valentina Domenici, G. Prampolini, and C. A. Veracini, 2004, "Deuterium and Carbon-13 NMR Study of a Banana Mesogen: Molecular Structure and Order," J. Phys. Chem. B **108**, 7694–7701.

Dong, Ronald Y., and Alberto Marini, 2009, "Conformational Study of a Bent-Core Liquid Crystal:13C NMR and DFT Computation Approach," J. Phys. Chem. B **113**, 14062–14072.

Dorjgotov, E., Katalin Fodor-Csorba, James T. Gleeson, Samuel N. Sprunt, and Antal Jákli, 2008, "Viscosities of a Bent-Core Nematic Liquid Crystal," Liq. Cryst. **35**, 149–155.

Dozov, I., 2001, "On the Spontaneous Symmetry Breaking in the Mesophases of Achiral Banana-Shaped Molecules," Europhys. Lett. **56**, 247–253.

Dozov, I., and C. Meyer, 2017, "Analogy between the Twist-Bend Nematic and the Smectic A Phases and Coarse-Grained Description of the Macroscopic N TB Properties," Liq. Cryst. **44**, 4–23.

Dunmur, D. A., K. Szumilin, and T. F. Waterworth, 1987, "Field-Induced Biaxiality in Nematics," Mol. Cryst. Liq. Cryst. **149**, 385–392.

Dussi, Simone, Simone Belli, René Van Roij, and Marjolein Dijkstra, 2015, "Cholesterics of Colloidal Helices: Predicting the Macroscopic Pitch from the Particle Shape and Thermodynamic State," J. Chem. Phys. **142**, 074905.

Dussi, Simone, and Marjolein Dijkstra, 2016, "Entropy-Driven Formation of Chiral Nematic Phases by Computer Simulations," Nat. Commun. **7**, 11175.

Dussi, Simone, Nikos Tasios, Tara Drwenski, René van Roij, and Marjolein Dijkstra, 2018, "Hard Competition: Stabilizing the Elusive Biaxial Nematic Phase in Suspensions of Colloidal Particles with Extreme Lengths," Phys. Rev. Lett. **120**, 177801.

Earl, David, Mikhail Osipov, Hideo Takezoe, Yoichi Takanishi, and Mark Wilson, 2005, "Induced and Spontaneous Deracemization in Bent-Core Liquid Crystal Phases and in Other Phases Doped with Bent-Core Molecules," Phys. Rev. E **71**, 021706.

Éber, N., P. Salamon, and Á. Buka, 2016, "Electrically Induced Patterns in Nematics and How to Avoid Them," Liq. Cryst. Rev. **4**, 101–134.

Efrati, Efi, and William T. M. Irvine, 2014, "Orientation-Dependent Handedness and Chiral Design," Phys. Rev. X **4**, 011003.

Elamain, Omaima, Gurumurthy Hegde, and Lachezar Komitov, 2013, "Alignment and Alignment Transition of BC Nematics," Appl. Phys. Lett. **103**, 023301.

Emsley, J. W., M. Lelli, G. R. Luckhurst, and H. Zimmermann, 2017, "13C NMR Study of the Director Distribution Adopted by the Modulated Nematic Phases Formed by Liquid-Crystal Dimers with Odd Numbers of Atoms In," Phys. Rev. E **96**, 062702.

Emsley, J. W., G. R. Luckhurst, and G. N. Shilstone, 1984, "The Orientational Order of Nematogenic Molecules with a Flexible Core:A Dramatic Odd-Even Effect," Mol. Phys. **53**, 1023–1028.

Emsley, J. W., G. R. Luckhurst, G. N. Shilstone, and I. Sage, 1984, "The Preparation and Properties of the α, ω-Bis (4, 4′-Cyanobiphenyloxy)Alkanes: Nematogenic Molecules with a Flexible Core," Mol. Cryst. Liq. Cryst. **102**, 223–233.

Emsley, James W., M. Lelli, H. Joy, M.-G. Tamba, and G. H. Mehl, 2016, "Similarities and Differences between Molecular Order in the Nematic and Twist-Bend Nematic Phases of a Symmetric Liquid Crystal Dimer," Phys. Chem. Chem. Phys. **18**, 9419–9430.

Eremin, A., and A. Jákli, 2013, "Polar Bent-Shape Liquid Crystals—from Molecular Bend to Layer Splay and Chirality," Soft Matter **9**, 615.

Eremin, Alexey, S. Diele, G. Pelzl, and W. Weissflog, 2003, "Field-Induced Switching between States of Opposite Chirality in a Liquid-Crystalline Phase," Phys. Rev. E **67**, 020702.

Eremin, Alexey, Siegmar Diele, Gerhard Pelzl, Hajnalka Nádasi, Wolfgang Weissflog, J. Salfetnikova, and Horst Kresse, 2001, "Experimental Evidence for an Achiral Orthogonal Biaxial Smectic Phase without In-Plane Order Exhibiting Antiferroelectric Switching Behavior," Phys. Rev. E **64**, 051707.

Eremin, Alexey, Ulrike Kornek, Stephan Stern, Ralf Stannarius, Fumito Araoka, Hideo Takezoe, H. Nadasi, Wolfgang Weissflog, and A. Jakli, 2012, "Pattern-Stabilized Decorated Polar Liquid-Crystal Fibers," Phys. Rev. Lett. **109**, 017801.

Eremin, Alexey, H. Nadasi, G. Pelzl, S. Diele, H. Kresse, W. Weissflog, and S. Grande, 2004, "Paraelectric-Antiferroelectric Transitions in the Bent-Core Liquid-Crystalline Materials," Phys. Chem. Chem. Phys. **6**, 1290–1298.

Eremin, Alexey, L. Naji, Alexandru Nemeş, Ralf Stannarius, Mario Schulz, and Katalin Fodor-Csorba, 2006, "Microscopic Structures of the B7 Phase: AFM and Electron Microscopy Studies," Liq. Cryst. **33**, 789–794.

Eremin, Alexey, A. Nemes, R. Stannarius, G. Pelzl, and W. Weissflog, 2008, "Spontaneous Bend Patterns in Homochiral Ferroelectric SmCP Films: Evidence for a Negative Effective Bend Constant," Soft Matter **4**, 2186–2191.

Eremin, Alexey, Alexandru Nemes, Ralf Stannarius, Mario Schulz, Hajnalka Nádasi, and Wolfgang Weissflog, 2005, "Structure and Mechanical Properties of Liquid Crystalline Filaments," Phys. Rev. E **71**, 031705.

Eremin, Alexey, Alexandru Nemes, Ralf Stannarius, and Wolfgang Weissflog, 2008, "Ambidextrous Bend Patterns in Free-Standing Polar Smectic- CPF Films," Phys. Rev. E **78**, 061705.

Etxebarria, Jesús, César L. Folcia, Josu Ortega, and M. Blanca Ros, 2003, "Induction of Ferroelectricity in the B2 Phase of a Liquid Crystal Composed of Achiral Bent-Core Molecules," Phys. Rev. E **67**, 042702.

Ferrarini, A., 2010, "The Theory of Elastic Constants," Liq. Cryst. **37**, 811–823.

Ferrarini, A., G. R. Luckhurst, and P. L. Nordio, 1995, "Even-Odd Effects in Liquid Crystal Dimers with Flexible Spacers: A Test of the Rotational Isomeric State Approximation?" Mol. Phys. **85**, 131–143.

Ferrarini, A., G. R. Luckhurst, P. L. Nordio, and S. J. Roskilly, 1993, "Understanding the Unusual Transitional Behaviour of Liquid Crystal Dimers," Chem. Phys. Lett. **214**, 409–417.

Ferrarini, A., G. R. Luckhurst, P. L. Nordio, and S. J. Roskilly, 1994, "Prediction of the Transitional Properties of Liquid Crystal Dimers—A Molecular-Field Calculation Based on the Surface Tensor Parametrization," J. Chem. Phys. **100**, 1460–1469.

Ferrarini, A., G. R. Luckhurst, P. L. Nordio, and S. J. Roskilly, 1996, "Understanding the Dependence of the Transitional Properties of Liquid Crystal Dimers on Their Molecular Geometry," Liq. Cryst. **21**, 373–382.

Findeisen-Tandel, Sonja, Martin W. Schröder, Gerhard Pelzl, Uta Baumeister, Wolfgang Weissflog, S. Stern, Alexandru Nemes, Ralf Stannarius, and Alexey Eremin, 2008, "Multistage Polar Switching in Bent-Core Mesogens," Eur. Phys. J. E **25**, 395–402.

Folcia, C., J. Etxebarria, J. Ortega, and M. Blanca Ros, 2005, "Structure of Mesogens Possessing B7 Textures: The Case of the Bent-Core Mesogen 8-OPIMB-NO_{2}," Phys. Rev. E **72**, 041709.

Folcia, C. L., I. Alonso, J. Ortega, J. Etxebarria, I. Pintre, and M. B. Ros, 2006, "Achiral Bent-Core Liquid Crystals with Azo and Azoxy Linkages: Structural and Nonlinear Optical Properties and Photoisomerization," Chem. Mater. **18**, 4617–4626.

Folcia, Cesar Luis, J. Etxebarria, J. Ortega, and M. B. Ros, 2006, "Structural Study of a Bent-Core Liquid Crystal Showing the B1-B2 Transition," Phys. Rev. E **74**, 031702.

Fontana, Jake, Christopher A. Bailey, Wolfgang Weissflog, I. Jánossy, and Antal Jákli, 2009, "Optical Waveguiding in Bent-Core Liquid-Crystal Filaments," Phys. Rev. E **80**, 032701.

Francescangeli, Oriano, and Edward T. Samulski, 2010, "Insights into the Cybotactic Nematic Phase of Bent-Core Molecules," Soft Matter **6**, 2413–2420.

Francescangeli, Oriano, Francesco Vita, Claudio Ferrero, Theo Dingemans, and Edward T. Samulski, 2011, "Cybotaxis Dominates the Nematic Phase of Bent-Core Mesogens: A Small-Angle Diffuse X-Ray Diffraction Study," Soft Matter **7**, 895–901.

Francescangeli, Oriano, Francesco Vita, and Edward T. Samulski, 2014, "Soft Matter The Cybotactic Nematic Phase of Bent-Core Mesogens: State of the Art and Future Developments," Soft Matter **10**, 7685–7691.

Francescangeli, Oriano, *et al.*, 2009, "Ferroelectric Response and Induced Biaxiality in the Nematic Phase of Bent-Core Mesogens," Adv. Funct. Mater. **19**, 2592–2600.

Frank, F. C., 1958, "On the Theory of Liquid Crystals," Faraday Discuss. **25**, 19–28.

Freiser, M. J., 1970, "Ordered States of a Nematic Liquid," Phys. Rev. Lett. **24**, 1041–1043.

Friedel, G., 1922, "Les États Mésomorphes de La Matiére," Ann. Phys. (Paris) **9**, 273–315.

Friedel, G., and F. Grandjean, 1910, "Observations Géométriques Sur Les Liquides á Conique Focales," Bull. Soc. Fr. Minéral **33**, 409–465.

Fukuda, Jun Ichi, 2012, "Stabilization of Blue Phases by the Variation of Elastic Constants," Phys. Rev. E **85**, 020701.

Gao, Min, *et al.*, 2014, "Direct Observation of Liquid Crystals Using Cryo-TEM: Specimen Preparation and Low-Dose Imaging," Microsc. Res. Tech. **77**, 754–772.

Geppi, M., *et al.*, 2011, "Determination of Order Parameters in Laterally Fluorosubstituted Terphenyls by ^{19}F-NMR, Optical and Dielectric Anisotropies," Mol. Cryst. Liq. Cryst. **541**, 104/[342]–117/[355].

Gesekus, G., S. Gerber, M. Wulf, V. Vill, and I. Dierking, 2004, "Chiral Banana Liquid Crystals Derived from Sugars," Liq. Cryst. **31**, 145–152.

Gleeson, Helen F., Sarabjot Kaur, Verena Görtz, Abdel Belaissaoui, Stephen Cowling, and John W. Goodby, 2014, "The Nematic Phases of Bent-Core Liquid Crystals," ChemPhysChem **15**, 1251–1260.

Gomola, Kinga, Lingfeng Guo, Damian Pociecha, Fumito Araoka, Ken Ishikawa, and Hideo Takezoe, 2010, "An Optically Uniaxial Antiferroelectric Smectic Phase in Asymmetrical Bent-Core Compounds Containing a 3-Aminophenol Central Unit," J. Mater. Chem. **20**, 7944–7952.

Goodby, John W., 2017, "Free Volume, Molecular Grains, Self-Organisation, and Anisotropic Entropy: Machining Materials," Liq. Cryst. **44**, 1755–1763.

Gorecka, Ewa, Damian Pociecha, Jozef Mieczkowski, Joanna Matraszek, Daniel Guillon, and Bertrand Donnio, 2004, "Axially Polar Columnar Phase Made of Polycatenar Bent-Shaped Molecules," J. Am. Chem. Soc. **126**, 15946–15947.

Gorecka, Ewa, Damian Pociecha, Nataša Vaupotič, Mojca Čepič, Kinga Gomola, and Jozef Mieczkowski, 2008, "Modulated General Tilt Structures in Bent-Core Liquid Crystals," J. Mater. Chem. **18**, 3044.

Gorecka, Ewa, Nataša Vaupotič, Damian Pociecha, Mojca Čepič, and Jozef Mieczkowski, 2005, "Switching Mechanism in Polar Columnar Mesophases Made of Bent-Core Molecules," ChemPhysChem **6**, 1087–1093.

Gorecka, Ewa, *et al.*, 2000, "Ferroelectric Phases in a Chiral Bent-Core Smectic Liquid Crystal: Dielectric and Optical Second-Harmonic Generation Measurements," Phys. Rev. E **62**, R4524.

Görtz, Verena, and John W. Goodby, 2005, "Enantioselective Segregation in Achiral Nematic Liquid Crystals," Chem. Commun., 3262–3264.

Görtz, Verena, Christopher Southern, Nicholas W. Roberts, Helen F. Gleeson, and John W. Goodby, 2009, "Unusual Properties of a Bent-Core Liquid-Crystalline Fluid," Soft Matter **5**, 463.

Gray, G. W., K. J. Harrison, and J. A. Nash, 1973, "New Family of Nematic Liquid-Crystals for Displays," Electron. Lett. **9**, 130–131.

Greco, Cristina, and Alberta Ferrarini, 2015, "Entropy-Driven Chiral Order in a System of Achiral Bent Particles," Phys. Rev. Lett. **115**, 147801.

Greco, Cristina, Geoffrey R. Luckhurst, and Alberta Ferrarini, 2014, "Molecular Geometry, Twist-Bend Nematic Phase and Unconventional Elasticity: A Generalised Maier-Saupe Theory," Soft Matter **10**, 9318–9323.

Griffin, Anselm C., Neal W. Buckley, William E. Hughes, and David L. Wertz, 1981, "Effect of Molecular Structure on Mesomorphism.11.1 A Siamese Twin Liquid Crystal Having Two Independently Smectogenic Conformations," Mol. Cryst. Liq. Cryst. **64**, 139–144.

Gruler, Hans, 1974, "Properties," J. Chem. Phys. **61**, 5408–5412.

Guo, Lingfeng, Kinga Gomola, Ewa Gorecka, Damian Pociecha, Surajit Dhara, Fumito Araoka, Ken Ishikawa, and Hideo Takezoe, 2011, "Transition between Two Orthogonal Polar Phases in Symmetric Bent-Core Liquid Crystals," Soft Matter **7**, 2895.

Guo, Lingfeng, *et al.*, 2011, "Ferroelectric Behavior of Orthogonal Smectic Phase Made of Bent-Core Molecules," Phys. Rev. E **84**, 031706.

Haller, I., 1975, "Thermodynamic and Static Properties of Liquid Crystals," Prog. Solid State Chem. **10**, 103–118.

Harden, J., R. Teeling, J. T Gleeson, S. Sprunt, and A. Jákli, 2008, "Converse Flexoelectric Effect in a Bent-Core Nematic Liquid Crystal," Phys. Rev. E **78**, 031702.

Harden, John, Badel Mbanga, Nándor Éber, Katalin Fodor-Csorba, Samuel N. Sprunt, James T. Gleeson, and Antal Jákli, 2006, "Giant Flexoelectricity of Bent-Core Nematic Liquid Crystals," Phys. Rev. Lett. **97**, 157802.

Harris, A. B., Randall D. Kamien, and T. C. Lubensky, 1997, "Microscopic Origin of Cholesteric Pitch," Phys. Rev. Lett. **78**, 1476–1479.

Harris, A. B., Randall D. Kamien, and T. C. Lubensky, 1999, "Molecular Chirality and Chiral Parameters," Rev. Mod. Phys. **71**, 1745–1757.

Helfrich, W., 1969, "Conduction-Induced Alignment of Nematic Liquid Crystals: Basic Model and Stability Considerations," J. Chem. Phys. **51**, 4092.

Helfrich, W., 1970, "Deformation of Cholesteric Liquid Crystals with Low Threshold Voltage," Appl. Phys. Lett. **17**, 531–532.

Helfrich, W., 1971a, "A Simple Method to Observe the Piezoelectricity of Liquid Crystals," Phys. Lett. A **35**, 393–394.

Helfrich, W., 1971b, "Electrohydrodynamic and Dielectric Instabilities of Cholesteric Liquid Crystals," J. Chem. Phys. **55**, 839.

Helfrich, Wolfgang., 1974, "Inherent Bounds to the Elasticity and Flexoelectricity of Liquid Crystals," Mol. Cryst. Liq. Cryst. **26**, 1–5.

Henderson, Peter A., and Corrie T. Imrie, 2011, "Methylene-Linked Liquid Crystal Dimers and the Twist-Bend Nematic Phase," Liq. Cryst. **38**, 1407–1414.

Heppke, Gerd, Antal Jákli, Daniel Krüerke, C. Lohning, D. Lötzsch, S. Paus, Sebastian Rauch, and K. Sharma, 1997, in "Polymorphism and electro-optical properties of banana shaped molecules," *ECLC'97 Abstract Book* (Polish Academy of Sciences, Zakopane, Poland), Vol. 34.

Heppke, Gerd, Antal Jákli, Sebastian Rauch, and Hans Sawade, 1999, "Electric-Field-Induced Chiral Separation in Liquid Crystals," Phys. Rev. E **60**, 5575–5579.

Heppke, Gerd, D. D. Parghi, and Hans Sawade, 2000a, "A Laterally Fluoro-Substituted 'Banana-Shaped' Liquid Crystal Showing Antiferroelectricity," Ferroelectrics **243**, 269–276.

Heppke, Gerd, D. D. Parghi, and Hans Sawade, 2000b, "Novel Sulphur-Containing Banana-Shaped Liquid Crystal Molecules," Liq. Cryst. **27**, 313–320.

Hervet, H., J. P. Hurault, and F. Rondelez, 1973, "Static One-Dimensional Distortions in Cholesteric Liquid Crystals," Phys. Rev. A **8**, 3055–3064.

Heuer, Jana, Ralf Stannarius, Maria-Gabriela Tamba, and Wolgang Weissflog, 2008, "Longitudinal and Normal Electroconvection Rolls in a Nematic Liquid Crystal with Positive Dielectric and Negative Conductivity Anisotropy," Phys. Rev. E **77**, 056206.

Hird, M., J. W. Goodby, N. Gough, and K. J. Toyne, 2001, "Novel Liquid Crystals with a Bent Molecular Shape Containing a 1, 5-Disubstituted 2, 3, 4-Trifluorophenyl Unit. Banana-Shaped Liquid Crystals—Synthesis and Properties," J. Mater. Chem. **11**, 2732–2742.

Hird, Michael, 2005, "Banana-Shaped and Other Bent-Core Liquid Crystals," Liquid Crystals Today **14**, 9–21.

Hong, S. H., Rafael Verduzco, Jarrod C. Williams, Robert J. Twieg, Elaine DiMasi, Ronald Pindak, Antal Jákli, James T. Gleeson, and Samuel N. Sprunt, 2010, "Short-Range Smectic Order in Bent-Core Nematic Liquid Crystals," Soft Matter **6**, 4819–4827.

Hough, L. E., *et al.*, 2009a, "Helical Nanofilament Phases," Science **325**, 456–460.

Hough, L. E., *et al.*, 2009b, "Chiral Isotropic Liquids from Achiral Molecules," Science **325**, 452–456.

Huang, M. Y. M., A. M. Pedreira, O. G. Martins, A. M. Figueiredo Neto, and Antal Jákli, 2002, "Nanophase Segregation of Nonpolar Solvents in Smectic Liquid Crystals of Bent-Shape Molecules," Phys. Rev. E **66**, 031708.

Hur, Sung-Taek, Min-Jun Gim, Hyun-Jong Yoo, Suk-Won Choi, and Hideo Takezoe, 2011, "Investigation for Correlation between Elastic Constant and Thermal Stability of Liquid Crystalline Blue Phase I," Soft Matter **7**, 8800.

Hurault, J. P., 1973, "Static Distortions of a Cholesteric Planar Structure Induced by Magnetic or Ac Electric-Fields," J. Chem. Phys. **59**, 2068.

Iglesias, Wilder, Timothy J. Smith, Prem B. Basnet, Sharon R. Stefanovic, Carsten Tschierske, Daniel J. Lacks, Antal Jákli, and Elizabeth K. Mann, 2011, "Alignment by Langmuir/Schaefer

Monolayers of Bent-Core Liquid Crystals," Soft Matter **7**, 9043–9050.

Imase, T., Susumu Kawauchi, and Junji Watanabe, 2001, "Conformational Analysis of 1, 3-Benzenediol Dibenzoate as a Model of Banana-Shaped Molecules Forming Chiral Smectic Phases," J. Mol. Struct. **560**, 275–281.

Imrie, Corrie T., and Peter A. Henderson, 2007, "Liquid Crystal Dimers and Higher Oligomers: Between Monomers and Polymers," Chem. Soc. Rev. **36**, 2096–2124.

Ishikawa, T., and O. D. Lavrentovich, 1998, "Crossing of Disclinations in Nematic Slabs," Europhys. Lett. **41**, 171–176.

Ishikawa, T., and O. D. Lavrentovich, 1999, "Dislocation Profile in Cholesteric Finger Texture," Phys. Rev. E **60**, R5037.

Ishikawa, T., and O. D. Lavrentovich, 2001a, "Undulations in a Confined Lamellar System with Surface Anchoring," Phys. Rev. E **63**, 030501(R).

Ishikawa, T., and O. D. Lavrentovich, 2001b, "Defects and Undulations in Layered Liquid Crystals," in *Defects in Liquid Crystals: Computer Simulations, Theory and Experiments*, Series II: Mathematics, Physics and Chemistry, edited by O. D. Lavrentovich, P. Pasini, C. Zannoni, and S. Zumer (Kluwer Academic Publishers, Dordrecht), pp. 271–301.

Jákli, A., 2010, "Electro-Mechanical Effects in Liquid Crystals," Liq. Cryst. **37**, 825–837.

Jákli, A., 2013, "Liquid Crystals of the Twenty-First Century—Nematic Phase of Bent-Core Molecules," Liq. Cryst. Rev. **1**, 65–82.

Jákli, A., G. G. Nair, C. K. K. Lee, L. C. Chien, and A. Jakli, 2001, "Electro-Disclinic Effect in Tilted Smectic Phases of Banana-Shaped Liquid Crystal Materials," Liq. Cryst. **28**, 489–494.

Jákli, Antal, 2002, "Classification and Electro-Optical Properties of Smectic Phases of Bent-Shape Molecules," in *2nd Banana Workshop* (University of Colorado, Boulder, CO).

Jákli, Antal, 2016, "Biaxial Nematic Liquid Crystals—Theory, Simulation and Experiment," Liq. Cryst. Rev. **4**, 80–81.

Jákli, Antal, Liang-Chi Chien, Daniel Kruerke, Sebastian Rauch, Hans Sawade, Philippe Bault, Gerd Heppke, Katalin Fodor-Csorba, and Geetha G. Nair, 2003, "Light Shutters and Electro-Optical Storage Devices from Antiferroelectric Liquid Crystals of Bent-Shape Molecules," Proc. SPIE Int. Soc. Opt. Eng. **5003**, 73–80.

Jákli, Antal, Liang-Chian Chien, Daniel Kruerke, Hans Sawade, and Gerd Heppke, 2002, "Light Shutters from Antiferroelectric Liquid Crystals of Bent-Shaped Molecules," Liq. Cryst. **29**, 377–381.

Jákli, Antal, and Katalin Fodor-Csorba, 2003, "Electro-Optics of Liquid Crystals of Bent-Shape Molecules," IMID'03 Digest **03**, 1108–1111.

Jákli, Antal, Y.-M. Huang, Katalin Fodor-Csorba, Aniko Vajda, Giancarlo Galli, Siegmar Diele, and Gerhard Pelzl, 2003, "Reversible Switching Between Optically Isotropic and Birefringent States in a Bent-Core Liquid Crystal," Adv. Mater. **15**, 1606–1610.

Jákli, Antal, Daniel Krüerke, and Geetha G. Nair, 2003, "Liquid Crystal Fibers of Bent-Core Molecules," Phys. Rev. E **67**, 051702.

Jákli, Antal, Daniel Krüerke, Hans Sawade, and Gerd Heppke, 2001, "Evidence for Triclinic Symmetry in Smectic Liquid Crystals of Bent-Shape Molecules," Phys. Rev. Lett. **86**, 5715–5718.

Jákli, Antal, G. Liao, I. Shashikala, U. S. Hiremath, and C. V. Yelamaggad, 2006, "Chirality and Polarity Transfers between Bent-Core Smectic Liquid-Crystal Substances," Phys. Rev. E **74**, 041706.

Jákli, Antal, Christiane Lischka, Wolfgang Weissflog, Gerhard Pelzl, Sebastian Rauch, and Gerd Heppke, 2000a, "Structural Transitions of Smectic Phases Formed by Achiral Bent-Core Molecules," Ferroelectrics **243**, 239–247.

Jákli, Antal, Christiane Lischka, Wolfgang Weissflog, Gerhard Pelzl, and Alfred Saupe, 2000b, "Helical Filamentary Growth in Liquid Crystals Consisting of Banana-Shaped Molecules," Liq. Cryst. **27**, 1405–1409.

Jákli, Antal, Christiane Lischka, Wolfgang Weissflog, Sebastian Rauch, and Gerd Heppke, 1999, "Layer Structures of Ferroelectric Smectic Liquid Crystals Formed by Bent-Core Molecules," Mol. Cryst. Liq. Cryst. Sci. Technol., Sect. A **328**, 299–307.

Jákli, Antal, Geetha G. Nair, Chong-Kwang Lee, R. Sun, and Liang-Chy Chien, 2001, "Macroscopic Chirality of a Liquid Crystal from Nonchiral Molecules," Phys. Rev. E **63**, 061710.

Jákli, Antal, Geetha G. Nair, H. Sawade, and G. Heppke, 2003, "A Bent-Shape Liquid Crystal Compound with Antiferroelectric Triclinic-Monoclinic Phase Transition," Liq. Cryst. **30**, 265–271.

Jákli, Antal, Sebastian Rauch, D. Lötzsch, and Gerd Heppke, 1998, "Uniform Textures of Smectic Liquid-Crystal Phase Formed by Bent-Core Molecules," Phys. Rev. E **57**, 6737–6740.

Jang, Yun, Reshma Balachandran, Christina Keith, Anne Lehmann, Carsten Tschierske, and Jagdish K. Vij, 2012, "Chirality of an Achiral Bent-Core Nematic Mesogen Observed in Planar and Homeotropic Cells under Certain Boundary Conditions," Soft Matter **8**, 10479.

Jang, Yun, Vitaly Panov, A. Kocot, A. Lehmann, C. Tschierske, and J. Vij, 2011, "Short-Range Correlations Seen in the Nematic Phase of Bent-Core Liquid Crystals by Dielectric and Electro-Optic Studies," Phys. Rev. E **84**, 060701.

Jang, Yun, Vitaly P. Panov, A. Kocot, J. K. Vij, A. Lehmann, and C. Tschierske, 2009, "Optical Confirmation of Biaxial Nematic (N[Sub b]) Phase in a Bent-Core Mesogen," Appl. Phys. Lett. **95**, 183304.

Kamien, Randall D., 1996, "Liquids with Chiral Bond Order," J. Phys. II (France) **6**, 461–475.

Kang, Seung-Gon, and Jae-Hoon Kim, 2013, "Optically-Isotropic Nanoencapsulated Liquid Crystal Displays Based on Kerr Effect," Opt. Express **21**, 15719.

Karbowniczek, Paweł, Michał Cieśla, Lech Longa, and Agnieszka Chrzanowska, 2017, "Structure Formation in Monolayers Composed of Hard Bent-Core Molecules," Liq. Cryst. **44**, 254–72.

Kats, E. I., and V. V. Lebedev, 2014, "Landau Theory for Helical Nematic Phases," JETP Lett. **100**, 110–113.

Kaur, S., J. Addis, C. Greco, A. Ferrarini, V. Görtz, J. W. Goodby, and H. F. Gleeson, 2012, "Understanding the Distinctive Elastic Constants in an Oxadiazole Bent-Core Nematic Liquid Crystal," Phys. Rev. E **86**, 041703.

Kaur, S., A. Belaissaoui, John W. Goodby, Verena Görtz, and Helen F. Gleeson, 2011, "Nonstandard Electroconvection in a Bent-Core Oxadiazole Material," Phys. Rev. E **83**, 041704.

Keith, Christina, Anne Lehmann, Ute Baumeister, Marko Prehm, and Carsten Tschierske, 2010, "Nematic Phases of Bent-Core Mesogens," Soft Matter **6**, 1704–1721.

Keith, Christina, Ramaiahgari Amaranatha Reddy, Marko Prehm, Ute Baumeister, Horst Kresse, Jessie Lorenzo Chao, Harald Hahn, Heinrich Lang, and Carsten Tschierske, 2007, "Layer Frustration, Polar Order and Chirality in Liquid Crystalline Phases of Silyl-Terminated Achiral Bent-Core Molecules," Chemistry **13**, 2556–2577.

Kim, Hanim, Sunhee Lee, Tae Joo Shin, Yun Jeong Cha, Eva Korblova, David M. Walba, Noel A. Clark, Sang Bok Lee, and Dong Ki Yoon, 2013, "Alignment of Helical Nanofilaments on the Surfaces of Various Self-Assembled Monolayers," Soft Matter **9**, 6185–6191.

Kim, Hanim, Sunhee Lee, Tae Joo Shin, Eva Korblova, David M. Walba, Noel A. Clark, Sang Bok Lee, and Dong Ki Yoon, 2014, "Multistep Hierarchical Self-Assembly of Chiral Nanopore Arrays," Proc. Natl. Acad. Sci. U.S.A. **111**, 14342–14347.

Kim, Hanim, Youngwoo Yi, Dong Chen, Eva Korblova, David M. Walba, Noel A. Clark, and Dong Ki Yoon, 2013, "Self-Assembled Hydrophobic Surface Generated from a Helical Nanofilament (B4) Liquid Crystal Phase," Soft Matter **9**, The Royal Society of Chemistry: 2793–2797.

Kim, Hanim, Anna Zep, Seong Ho Ryu, Hyungju Ahn, Tae Joo Shin, Sang Bok Lee, Damian Pociecha, Ewa Gorecka, and Dong Ki Yoon, 2016, "Linkage-Length Dependent Structuring Behaviour of Bent-Core Molecules in Helical Nanostructures," Soft Matter **12**, 3326–3330.

Kim, Young-Ki, Greta Cukrov, Francesco Vita, Eric Scharrer, Edward T. Samulski, Oriano Francescangeli, and Oleg D. Lavrentovich, 2016, "Search for Microscopic and Macroscopic Biaxiality in the Cybotactic Nematic Phase of New Oxadiazole Bent-Core Mesogens," Phys. Rev. E **93**, 062701.

Kim, Young-Ki, Greta Cukrov, Jie Xiang, Sung-Tae Shin, and Oleg D. Lavrentovich, 2015, "Domain Walls and Anchoring Transitions Mimicking Nematic Biaxiality in the Oxadiazole Bent-Core Liquid Crystal C7," Soft Matter **11**, 3963–3970.

Kim, Young-Ki, Madhabi Majumdar, Bohdan I. Senyuk, Luana Tortora, Jens Seltmann, Matthias Lehmann, Antal Jákli, Jim T. Gleeson, Oleg D. Lavrentovich, and Samuel Sprunt, 2012, "Search for Biaxiality in a Shape-Persistent Bent-Core Nematic Liquid Crystal," Soft Matter **8**, 8880.

Kim, Young-Ki, Bohdan Senyuk, and Oleg D. Lavrentovich, 2012, "Molecular Reorientation of a Nematic Liquid Crystal by Thermal Expansion," Nat. Commun. **3**, 1133.

Kim, Young-Ki, Bohdan Senyuk, Sung-Tae Shin, Alexandra Kohlmeier, Georg H. Mehl, and Oleg D. Lavrentovich, 2014, "Surface Alignment, Anchoring Transitions, Optical Properties, and Topological Defects in the Thermotropic Nematic Phase of Organo-Siloxane Tetrapodes," Soft Matter **10**, 500–509.

Kishikawa, Keiki, Shoichiro Nakahara, Yohei Nishikawa, Shigeo Kohmoto, and Makoto Yamamoto, 2005, "A Ferroelectrically Switchable Columnar Liquid Crystal Phase with Achiral Molecules: Superstructures and Properties of Liquid Crystalline Ureas," J. Am. Chem. Soc. **127**, 2565–2571.

Kleman, M., 1985, "The Coexistence of Cholesteric and Two-Dimensional Orders," J. Phys. (Paris) **46**, 1193–1203.

Kleman, M., and O. D. Lavrentovich, 2009, "Liquids with Conics," Liq. Cryst., **36**, 1085–1099.

Kleman, M., and O. D. Lavrentovich, 2013, *Soft Matter Physics: An Introduction* (Springer, New York).

Kolli, Hima Bindu, Elisa Frezza, Giorgio Cinacchi, Alberta Ferrarini, Achille Giacometti, and Toby S. Hudson, 2014, "Communication: From Rods to Helices: Evidence of a Screw-like Nematic Phase," J. Chem. Phys. **140**, 081101.

Korblova, Eva, Edward Guzman, Joseph Maclennan, Matthew Glaser, Renfan Shao, Edgardo Garcia, Yongqiang Shen, Rayshan Visvanathan, Noel Clark, and David Walba, 2017, "New SmAPF Mesogens Designed for Analog Electrooptics Applications," Materials **10**, 1284.

Kramer, L., and W. Pesch, 1996, "Electrohydrodynamic Instabilities in Nematic Liquid Crystals," *In Pattern Formation in Liquid Crystals*, edited by A. Buka and L. Kramer (Springer-Verlag, New York), pp. 221–256.

Krishnamurthy, Kanakapura S., Nani Babu Palakurthy, and Channabasaveshwar V. Yelamaggad, 2017, "Confined Electroconvective and Flexoelectric Instabilities Deep in the Freedericksz State of Nematic CB7CB," J. Phys. Chem. B **121**, 5447–5454.

Kuboshita, M., Y. Matsunaga, and H. Matsuzaki, 1991, "Mesomorphic Behavior of 1, 2-Phenylene Bis[4-(4-Alkoxybenzylideneamino)Benzoates," Mol. Cryst. Liq. Cryst. **199**, 319–326.

Kumar, Pramoda, Y. G. Marinov, H. P. Hinov, Uma S. Hiremath, C. V. Yelamaggad, K. S. Krishnamurthy, and A. G. Petrov, 2009, "Converse Flexoelectric Effect in Bent-Core Nematic Liquid Crystals," J. Phys. Chem. B **113**, 9168–9174.

Kumazawa, Kazuya, Michi Nakata, Fumito Araoka, Yoichi Takanishi, Ken Ishikawa, Junji Watanabe, and Hideo Takezoe, 2004a, "Important Role Played by Interlayer Steric Interaction for the Emergence of Ferroelectric Phase in Bent-Core Mesogens," J. Mater. Chem. **14**, 157–164.

Kundu, B., 2009, "Experimental Investigations on Physical Properties of Some Novel Liquid Crystals with Banana-Shaped and Rodlike Molecules," Ph.D. dissertation (Raman Research Institute, Bangalore, India).

Kundu, Brindaban, R. Pratibha, and N. V. Madhusudana, 2007, "Anomalous Temperature Dependence of Elastic Constants in the Nematic Phase of Binary Mixtures Made of Rodlike and Bent-Core Molecules," Phys. Rev. Lett. **99**, 247802.

Kundu, Brindaban, Arun Roy, R. Pratibha, and N. V. Madhusudana, 2009, "Flexoelectric Studies on Mixtures of Compunds Made of Rodlike and Bent-Core Molecules," Appl. Phys. Lett. **95**, 081902.

Lagerwall, Jan P. F., Frank Giesselmann, Michael D. Wand, and David M. Walba, 2004, "A Chameleon Chiral Polar Liquid Crystal: Rod-Shaped When Nematic, Bent-Shaped When Smectic," Chem. Mater. **16**, 3606–3615.

Lansac, Yves, Matthew A. Glaser, Prabal K. Maiti, and Noel A. Clark, 2003, "Phase Behavior of Bent-Core Molecules," Phys. Rev. E **67**, 011703.

Larson, Ronald G., 1999, *The Structure and Rheology of Complex Fluids. Topics in Chemical Engineering Series*, Vol. 10 (Oxford University Press, New York).

Lavrentovich, O. D., and M. Kleman, 1993, "Field-Driven First-Order Structural Transition in Restricted Geometry of a Smectic-A Cell," Phys. Rev. E **48**, R39.

Lavrentovich, O. D., and D. Yang, 1998, "Cholesteric Cellular Patterns with Electric-Field-Controlled Line Tension," Phys. Rev. E **57**, R6269.

Lavrentovich, O. D, M. Kleman, and V. M. Pergamenshchik, 1994, "Nucleation of Focal Conic Domains in Smectic A Liquid Crystals," J. Phys. II (France) **4**, 377–404.

Lee, Chong-Kwang, Soon-Sik Kwon, Tae-Sung Kim, E-Joon Choi, Sung-Tae Shin, Wang-Cheol Zin, Dae-Cheol Kim, Jae-Hoon Kim, and Liang-Chy Chien, 2003, "Synthesis and Properties of New Materials with Banana-Shaped Achiral Cores and Chiral End Groups," Liq. Cryst. **30**, 1401–1406.

Lehmann, Matthias, 2011, "Biaxial Nematics from Their Prediction to the Materials and the Vicious Circle of Molecular Design," Liq. Cryst. **38**, 1389–1405.

Leslie, Frank M., 1968, "Theory of Flow Phenomena in Nematic Liquid Crystals," Arch. Ration. Mech. Anal. **28**, 265.

Li, Jian-Feng, Ch. Rosenblatt, O. D. Lavrentovich, and V. Percec, 1994, "Biaxiality in a Cyclic Thermotropic Nematic Liquid Crystal," Europhys. Lett. **25**, 199–204.

Li, Lin, Miroslaw Salamonczyk, Antal Jákli, and Torsten Hegmann, 2016, "A Dual Modulated Homochiral Helical Nanofi Lament Phase with Local Columnar Ordering Formed by Bent Core Liquid Crystals: Effects of Molecular Chirality," Small **12**, 3944–3955.

Li, Xiaodong, Sungmin Kang, Seng Kue Lee, Masatoshi Tokita, and Junji Watanabe, 2010, "Unusual Formation of Switchable Hexagonal Columnar Phase by Bent-Shaped Molecules with Low Bent-Angle Naphthalene Central Core and Alkylthio Tail," Jpn. J. Appl. Phys. **49**, 121701.

Li, Zili, Gregory A. Di Lisi, Rolfe G. Petschek, and Charles Rosenblatt, 1990, "Nematic Electroclinic Effect," Phys. Rev. A **41**, 1997–2004.

Li, Zili, and Oleg D. Lavrentovich, 1994, "Surface Anchoring and Growth Pattern of the Field-Driven First-Order Transition in a Smectic-A Liquid Crystal," Phys. Rev. Lett. **73**, 280–283.

Liao, G., G. Pelzl, W. Weissflog, S. Sprunt, A. Jakli, and S. Stojadinovic, 2005, "Optically Isotropic Liquid-Crystal Phase of Bent-Core Molecules with Polar Nanostructure," Phys. Rev. E **72**, 021710.

Liao, G., S. Stojadinovic, Gerhard Pelzl, Wolfgang Weissflog, Samuel N. Sprunt, and Antal Jákli, 2005, "Optically Isotropic Liquid-Crystal Phase of Bent-Core Molecules with Polar Nanostructure," Phys. Rev. E **72**, 021710.

Lin, Shih Chieh, Rong Ming Ho, Chin Yen Chang, and Chain Shu Hsu, 2012, "Hierarchical Superstructures with Control of Helicity from the Self-Assembly of Chiral Bent-Core Molecules," Chemistry **18**, 9091–9098.

Link, D. R., L. Radzihovsky, G. Natale, J. E. Maclennan, N. A. Clark, M. Walsh, S. S. Keast, and M. E. Neubert, 2000, "Ring-Pattern Dynamics in Smectic-C* and Smectic-C*A Freely Suspended Liquid Crystal Films," Phys. Rev. Lett. **84**, 5772–5775.

Link, Darren R., Nattaporn Chattham, Noel A. Clark, Eva Körblova, and David M. Walba, 1999, "Optical and X-Ray Obsercations of Freely Suspended Filaments of a Smectic Liquid Crystal," in *Proceedings of the 7th International Conference on Ferroelectric Liquid Crystals* (University of Darmstadt, Darmstadt, Germany).

Link, Darren R., Giorgio Natale, Renfan Shao, Joseph E. Maclennan, Noel A. Clark, Eva Körblova, and David M. Walba., 1997, "Spontaneous Formation of Macroscopic Chiral Domains in a Fluid Smectic Phase of Achiral Molecules," Science **278**, 1924–1927.

Livolant, F., and Y. Bouligand, 1986, "Liquid Crystalline Phases given by Helical Biological Polymers (DNA, PBLG and Xanthan). Columnar Textures," J. Phys. France **47**, 1813–1827.

Longa, Lech, and Grzegorz Pająk, 2016, "Modulated Nematic Structures Induced by Chirality and Steric Polarization," Phys. Rev. E **93**, 040701.

Longa, Lech, Grzegorz Pająk, and Thomas Wydro, 2009, "Chiral Symmetry Breaking in Bent-Core Liquid Crystals," Phys. Rev. E **79**, 040701.

Lorman, V. L., and B. Mettout, 2004, "Theory of Chiral Periodic Mesophases Formed from an Achiral Liquid of Bent-Core Molecules," Phys. Rev. E **69**, 061710.

Lubensky, T. C., and L. Radzihovsky, 2002, "Theory of Bent-Core Liquid-Crystal Phases and Phase Transitions," Phys. Rev. E **66**, 031704.

Luckhurst, G. R., 1995, "Liquid Crystal Dimers and Oligomers: Experiment and Theory," Macromol. Symp. **96**, 1–26.

Luckhurst, G. R., 2001, "Biaxial Nematic Liquid Crystals: Fact or Fiction?" Thin Solid Films **393**, 40–52.

Luckhurst, Geoffrey R., 2004, "Liquid Crystals: A Missing Phase Found at Last?" Nature (London) **430**, 413–414.

Luckhurst, Geoffrey R., 2005, "Liquid Crystals: A Chemical Physicist's View," Liq. Cryst. **32**, 1335–1364.

Macdonald, R., P. Warnick, G. Heppke, and F. Kentischer, 1998, "Antiferroelectricity and Chiral Order in New Liquid Crystals of Nonchiral Molecules Studied by Optical Second Harmonic Generation," Phys. Rev. Lett. **81**, 4408–4411.

Madhusudana, N. V., and R. Pratibha, 1982, "Elasticity and Orientational Order in Some Cyanobiphenyls: Part IV. Reanalysis of the Data," Mol. Cryst. Liq. Cryst. **89**, 249–257.

Madsen, L. A., T. J. Dingemans, M. Nakata, and E. T. Samulski, 2004, "Thermotropic Biaxial Nematic Liquid Crystals," Phys. Rev. Lett. **92**, 145505.

Mahajan, M. P., M. Tsige, P. L. Taylor, and C. Rosenblatt, 1999, "Liquid Crystal Bridges," Liq. Cryst., **26**, 443–448.

Majumdar, Madhabi, Péter Salamon, Antal Jákli, James T. Gleeson, and Samuel N. Sprunt, 2011, "Elastic Constants and Orientational Viscosities of a Bent-Core Nematic Liquid Crystal," Phys. Rev. E **83**, 031701.

Makow, David M., and C. Leroy Sanders, 1978, "Additive Colour Properties and Colour Gamut of Cholesteric Liquid Crystals [4]," Nature (London) **276**, 48–50.

Mandle, Richard J., Craig T. Archbold, Julia P. Sarju, Jessica L. Andrews, and John W. Goodby, 2016, "The Dependency of Nematic and Twist-Bend Mesophase Formation on Bend Angle," Sci. Rep. **6**, 36682.

Mandle, Richard J., and John W. Goodby, 2016a, "Does Topology Dictate the Incidence of the Twist-Bend Phase? Insights Gained from Novel Unsymmetrical Bimesogens," Chemistry **22**, 18456–18464.

Mandle, Richard J., and John W. Goodby, 2016b, "A Liquid Crystalline Oligomer Exhibiting Nematic and Twist-Bend Nematic Mesophases," ChemPhysChem **17**, 967–970.

Mandle, Richard J., and John W. Goodby, 2016c, "Progression from Nano to Macro Science in Soft Matter Systems: Dimers to Trimers and Oligomers in Twist-Bend Liquid Crystals," RSC Adv. **6**, 34885–34893.

Mandle, Richard J., Matthew P. Stevens, and John W. Goodby, 2017, "Developments in Liquid-Crystalline Dimers and Oligomers," Liq. Cryst. **44**, 2046–2059.

Marino, Lucia, Andrei Th. Ionescu, Salvatore Marino, and Nicola Scaramuzza, 2012, "Dielectric Investigations on a Bent-Core Liquid Crystal," J. Appl. Phys. **112**, 114113.

Martin, W. Schroder, Gerhard Pelzl, Wolfgang Weissflog, and Siegmar Diele, 2004, "Field-Induced Switching of the Layer Chirality in SmCP Phases of Novel Achiral Bent-Core Liquid Crystals and Their Unusual Large Increase in Clearing Temperature under Electric Field Application," ChemPhysChem **5**, 99–103.

Martínez-Perdiguero, J., I. Alonso, C. Folcia, J. Etxebarria, and J. Ortega, 2006, "Some Aspects about the Structure of the Optically Isotropic Phase in a Bent-Core Liquid Crystal: Chiral, Polar, or Steric Origin," Phys. Rev. E **74**, 031701.

Matsunaga, Y., and S. Miyamoto, 1993, "Mesomorphic Behavior of 2, 4-Bis-(4-Alkoxybenzylidene)Cyclopentanones and Related Compounds," Mol. Cryst. Liq. Cryst. Sci. Technol., Sect. A **237**, 311–317.

Matsuzaki, H., and Y. Matsunaga, 1993, "New Mesogenic Compounds with Unconventional Molecular Structures 1, 2-Phenylene and 2, 3-Naphthylene Bis [4-(4-Alkoxyphenyliminomethyl) Benzoates] and Related Compounds," Liq. Cryst. **14**, 105–120.

Memmer, R., 2002, "Liquid Crystal Phases of Achiral Banana-Shaped Molecules: A Computer Simulation Study," Liq. Cryst. **29**, 483–496.

Meyer, C., and I. Dozov, 2016, "Local Distortion Energy and Coarse-Grained Elasticity of the Twist-Bend Nematic Phase," Soft Matter **12**, 574–580.

Meyer, C., G. R. Luckhurst, and I. Dozov, 2013, "Flexoelectrically Driven Electroclinic Effect in the Twist-Bend Nematic Phase of Achiral Molecules with Bent Shapes," Phys. Rev. Lett. **111**, 067801.

Meyer, C., G. R. Luckhurst, and I. Dozov, 2015, "The Temperature Dependence of the Heliconical Tilt Angle in the Twist-Bend

Nematic Phase of the Odd Dimer CB7CB," J. Mater. Chem. C **3**, 318–328.
Meyer, R. B., 1973, "Existence of Even Indexed Disclinations in Nematic Liquid Crystals," Philos. Mag. **27**, 405–424.
Meyer, R. B., 1976, "Structural Problems in Liquid Crystal Physics," in *Molecular Fluids*, Les Houches Summer School in Theoretical Physics, edited by R. Balian and G. Weill (Gordon and Breach, New York), pp. 271–343.
Meyer, R. B., 1982, "Macroscopic Phenomena in Nematic Polymers," in *Polymer Liquid Crystals*, edited by A. Ciferri, W. R. Krigbaum, and R. B. Meyer (Academic Press, Inc., New York/London), pp. 133–185.
Meyer, Robert B., 1968, "Effects of Electric and Magnetic Fields on the Structure of Cholesteric Liquid Crystals," Appl. Phys. Lett. **12**, 281–282.
Meyer, Robert B., 1969, "Piezoelectric Effects in Liquid Crystals," Phys. Rev. Lett. **22**, 918–921.
Meyer, Robert B., and Stephen Garoff, 1977, "Electroclinic Effect at the A—C Phase Change in a Chiral Smectic Liquid Crystal," Phys. Rev. Lett. **38**, 848–851.
Miyajima, Daigo, Fumito Araoka, Hideo Takezoe, Jungeun Kim, Kenichi Kato, Masaki Takata, and Takuzo Aida, 2012, "Ferroelectric Columnar Liquid Crystal Featuring Confined Polar Groups Within Core—Shell Architecture," Science **336**, 209–214.
Morys, Michael, Torsten Trittel, and Ralf Stannarius, 2012, "Measurement of the Tension of Freely Suspended Liquid Crystal Filaments," Ferroelectrics **431**, 129.
Nádasi, Hajnalka, Wolfgang Weissflog, Alexey Eremin, Gerhard Pelzl, Siegmar Diele, Banani Das, and Siegbert Grande, 2002, "Ferroelectric and Antiferroelectric 'Banana Phases' of New Fluorinated Five-Ring Bent-Core Mesogens," J. Mater. Chem. **12**, 1316–1324.
Nagayama, Hiroki, Yuji Sasaki, Fumito Araoka, Kenji Ema, Ken Ishikawa, and Hideo Takezoe, 2011, "Discrete and Sequential Formation of Helical Nanofilaments in Mixtures Consisting of Bent- and Rod-Shaped Molecules," Soft Matter **7**, 8766.
Nair, Geetha G., Christopher A. Bailey, Stefanie Taushanoff, Katalin Fodor-Csorba, Aniko Vajda, Zoltán Varga, Attila Bóta, and Antal Jákli, 2008, "Electrically Tunable Color by Using Mixtures of Bent-Core and Rod-Shaped Molecules," Adv. Mater. **20**, 3138–3142.
Nakata, M., *et al.*, 2005, "Electric-Field-Induced Transition in Polarization Modulated Phase Studied Using Microbeam X-Ray Diffraction," Phys. Rev. E **71**, 011705.
Nakata, Michi, Darren R. Link, Fumito Araoka, Jirakorn Thisayukta, Yoichi Takanishi, Ken Ishikawa, Junji Watanabe, and Hideo Takezoe, 2001, "A Racemic Layer Structure in a Chiral Bent-Core Ferroelectric Liquid Crystal," Liq. Cryst. **28**, 1301–1308.
Nakata, Michi, Yoichi Takanishi, Junji Watanabe, and Hideo Takezoe, 2003, "Blue Phases Induced by Doping Chiral Nematic Liquid Crystals with Nonchiral Molecules," Phys. Rev. E **68**, 041710.
Nemeş, Alexandru, 2008, "Liquid Crystal Filaments Formed by Bent Shaped Mesogens," Ph.D. thesis University of Magdeburg.
Nemeş, Alexandru, Alexey Eremin, and Ralf Stannarius, 2006, "Mechanical Properties of Freely Suspended LC Filaments," Mol. Cryst. Liq. Cryst. **449**, 179–189.
Nemeş, Alexandru, Alexey Eremin, Ralf Stannarius, Mario Schulz, Hajnalka Nádasi, and Wolfgang Weissflog, 2006, "Structure Characterization of Free-Standing Filaments Drawn in the Liquid Crystal State," Phys. Chem. Chem. Phys. **8**, 469–476.
Niori, Teruki, Tomoko Sekine, Junji Watanabe, Tomoo Furukawa, and Hideo Takezoe, 1996, "Distinct Ferroelectric Smectic Liquid Crystals Consisting of Banana Shaped Achiral Molecules," J. Mater. Chem. **6**, 1231–1233.
Niori, Teruki, J. Yamamoto, and H. Yokoyama, 2004, "Dynamics of the Nematic Phase Formed by Achiral Banana-Shaped Materials," Mol. Cryst. Liq. Cryst. **409**, 475–482.
Niwano, Hiroko, Michi Nakata, Jirakorn Thisayukta, Darren R. Link, Hideo Takezoe, and Junji Watanabe, 2004, "Chiral Memory on Transition between the B2 and B4 Phases in an Achiral Banana-Shaped Molecular System," J. Phys. Chem. B **108**, 14889–14896.
Ocak, Hale, Belkız Bilgin-Eran, Marko Prehm, and Carsten Tschierske, 2012, "Effects of Molecular Chirality on Superstructural Chirality in Liquid Crystalline Dark Conglomerate Phases," Soft Matter **8**, 7773.
Ohzono, Takuya, Takahiro Yamamoto, and Jun Ichi Fukuda, 2014, "A Liquid Crystalline Chirality Balance for Vapours," Nat. Commun. **5**, Nature Publishing Group: 3735.
Olivares, J., S. Stojadinovic, Theo J. Dingemans, Samuel N. Sprunt, and Antal Jákli, 2003, "Optical Studies of the Nematic Phase of an Oxazole-Derived Bent-Core Liquid Crystal," Phys. Rev. E **68**, 041704.
Ortega, J., C. L. Folcia, J. Etxebarria, J. Martínez-Perdiguero, J. A. Gallastegui, P. Ferrer, Nélida Gimeno, and M. Blanca Ros, 2011, "Electric-Field-Induced Phase Transitions in Bent-Core Mesogens Determined by x-Ray Diffraction," Phys. Rev. E **84**, 021707.
Ortega, Josu, C. L. Folcia, Jesús Etxebarria, N. Gimeno, and M. B. Ros, 2003, "Interpretation of Unusual Textures in the B2 Phase of a Liquid Crystal Composed of Bent-Core Molecules," Phys. Rev. E **68**, 011707.
Ostapenko, T., S. M. Salili, Alexey Eremin, Antal Jákli, and R. Stannarius, 2014, "Stress-Driven Dynamic Behavior of Free-Standing Bent-Core Liquid Crystal Filaments," Ferroelectrics **468**, 101–113.
Ostapenko, Tanya, Cuiyu Zhang, Samuel N. Sprunt, Antal Jákli, and James T. Gleeson, 2011, "Magneto-Optical Technique for Detecting the Biaxial Nematic Phase," Phys. Rev. E **84**, 021705.
Oswald, Patrick, and Pawel Pieranski, 2005, *Smectic and Columnar Liquid Crystals* (Taylor and Francis, Boca Raton), 1st ed.
Otani, Taketo, Fumito Araoka, Ken Ishikawa, and Takezoe Hideo, 2009, "Enhanced Optical Activity by Achiral Rod-like Molecules Nanosegregated in the B4 Structure of Achiral Bent-Core Molecules," J. Am. Chem. Soc. **131**, 12368–12372.
Pająk, Grzegorz, Lech Longa, and Agnieszka Chrzanowska, 2017, "Nematic Twist—Bend Phase in an External Field," arXiv: 1801.00027.
Palffy-Muhoray, P., 2013, "Comment on 'The Limits of Flexoelectricity in Liquid Crystals' [AIP Advances 1, 032120 (2011)]," AIP Adv. **3**, 019101.
Panarin, Y. P., M. Nagaraj, S. P. Sreenilayam, J. K. Vij, Anne Lehmann, and Carsten Tschierske, 2011, "Sequence of Four Orthogonal Smectic Phases in an Achiral Bent-Core Liquid Crystal: Evidence for the SmAP (α) Phase," Phys. Rev. Lett. **107**, 247801.
Panarin, Y. P., M. Nagaraj, J. K. Vij, C. Keith, and C. Tschierske, 2010, "Field-Induced Transformations in the Biaxial Order of Non-Tilted Phases in a Bent-Core Smectic Liquid Crystal," Europhys. Lett. **92**, 26002.

Pang, Jinzhong, and Noel A. Clark, 1994, "Observation of a Chiral-Symmetry-Breaking Twist-Bend Instability in Achiral Freely Suspended Liquid-Crystal Films," Phys. Rev. Lett. **73**, 2332–2335.

Panov, V., M. Nagaraj, J. Vij, Yu. Panarin, A. Kohlmeier, M. Tamba, R. Lewis, and G. Mehl, 2010, "Spontaneous Periodic Deformations in Nonchiral Planar-Aligned Bimesogens with a Nematic-Nematic Transition and a Negative Elastic Constant," Phys. Rev. Lett. **105**, 167801.

Panov, V. P., R. Balachandran, M. Nagaraj, J. K. Vij, M. G. Tamba, A. Kohlmeier, and G. H. Mehl, 2011, "Microsecond Linear Optical Response in the Unusual Nematic Phase of Achiral Bimesogens," Appl. Phys. Lett. **99**, 261903.

Panov, V. P., R. Balachandran, J. K. Vij, M. G. Tamba, A. Kohlmeier, and G. H. Mehl, 2012, "Field-Induced Periodic Chiral Pattern in the Nx Phase of Achiral Bimesogens," Appl. Phys. Lett. **101**, 234106.

Panov, V. P., M. C. M. Varney, I. I. Smalyukh, J. K. Vij, M. G. Tamba, and G. H. Mehl, 2015, "Hierarchy of Periodic Patterns in the Twist-Bend Nematic Phase of Mesogenic Dimers," Mol. Cryst. Liq. Cryst. **611**, 180–185.

Panov, Vitaly P., Sithara P. Sreenilayam, Yuri P. Panarin, Jagdish K. Vij, Chris J. Welch, and Georg H. Mehl, 2017, "Characterization of the Sub-Micrometer Hierarchy Levels in the Twist-Bend Nematic Phase with Nanometric Helices via Photopolymerization. Explanation for the Sign Reversal in the Polar Response," Nano Lett. **17**, 7515–7519.

Panov, Vitaly P., Jagdish K. Vij, Reshma Balachandran, Volodymyr Borshch, Oleg D. Lavrentovich, Maria G. Tamba, and Georg H. Mehl, 2013, "Properties of the Self-Deforming Ntb Phase in Mesogenic Dimers," Proc. SPIE Int. Soc. Opt. Eng. **8828**, 88280X.

Pardaev, Shokir A., S. M. Shamid, M. G. Tamba, G. H. Mehl, J. T. Gleeson, D. W. Allender, J. V. Selinger, B. Ellman, A. Jakli, and S. Sprunt, 2016, "Second Harmonic Light Scattering Induced by Defects in the Twist-Bend Nematic Phase of Achiral Liquid Crystal Dimers," Soft Matter **12**, 4472–4482.

Parker, Andrew Richard, 2000, "515 Million Years of Structural Colour," J. Opt. A **2**, R15–R28.

Parsouzi, Z., *et al.*, 2016a, "Light Scattering Study of the 'Pseudo-Layer' Compression Elastic Constant in a Twist-Bend Nematic Liquid Crystal," Phys. Chem. Chem. Phys. **18**, 31645.

Parsouzi, Z., *et al.*, 2016b, "Fluctuation Modes of a Twist-Bend Nematic Liquid Crystal," Phys. Rev. X **6**, 021041.

Parthasarathi, Srividhya, D. S. Shankar Rao, Nani Babu Palakurthy, C. V. Yelamaggad, and S. Krishna Prasad, 2016, "Binary System Exhibiting the Nematic to Twist-Bend Nematic Transition: Behavior of Permittivity and Elastic Constants," J. Phys. Chem. B **120**, 5056–5062.

Patel, J. S., and Hiroshi Yokoyama., 1993, "Continuous Anchoring Transition in Liquid Crystals," Nature (London) **362**, 525–527.

Paterson, Daniel A., *et al.*, 2016, "Reversible Isothermal Twist–Bend Nematic–Nematic Phase Transition Driven by the Photoisomerization of an Azobenzene- Based Nonsymmetric Liquid Crystal Dimer," J. Am. Chem. Soc. **138**, 5283–5289.

Peláez, Jorge, and Mark R. Wilson, 2006, "Atomistic Simulations of a Thermotropic Biaxial Liquid Crystal," Phys. Rev. Lett. **97**, 267801.

Pelz, K., W. Weissflog, U. Baumeister, and S. Diele, 2003, "Various Columnar Phases Formed by Bent-Core Mesogens," Liq. Cryst. **30**, 1151–1158.

Pelzl, G., S. Diele, A. Jákli, and W. Weissflog, 2006, "The Mysterious B7 Phase: From Its Discovery up to the Present Stage of Research," Liq. Cryst. **33**, 1513–1523.

Pelzl, G., I. Wirth, and W. Weissflog, 2001, "The First 'banana Phase' Found in an Original Vorlander Substance," Liq. Cryst. **28**, 969–72.

Pelzl, Gerhard, Siegmar Diele, Antal Jákli, Christiane H. Lischka, Ina Wirth, and Wolfgang Weissflog, 1999, "Preliminary Communication Helical Superstructures in a Novel Smectic Mesophase Formed by Achiral Banana-Shaped Molecules," Liq. Cryst. **26**, 135–139.

Pelzl, Gerhard, Siegmar Diele, and Wolfgang Weissflog, 1999, "Banana-Shaped Compounds—A New Field of Liquid Crystals**," Adv. Mater. **11**, 707–724.

Pelzl, Gerhard, Alexey Eremin, Siegmar Diele, Horst Kresse, and Wolfgang Weissflog, 2002, "Spontaneous Chiral Ordering in the Nematic Phase of an Achiral Banana-Shaped Compound," J. Mater. Chem. **12**, 2591–2593.

Pelzl, Gerhard, and Wolfgang Weissflog, 2007, "Mesophase Behavior at the Borderline between Calamitic and 'Banana-Shaped' Mesogens," in *Thermotropic Liquid Crystals: Recent Advances*, edited by Ayyalusamy Ramamoorthy (Springer, Dordrecht), 1st ed., pp. 1–58.

Pelzl, Gerhard, *et al.*, 2004, "The First Bent-Core Mesogens Exhibiting a Dimorphism B 7-SmCP A," J. Mater. Chem. **14**, 2492–2498.

Petzold, J., Alexandru Nemeş, Alexey Eremin, Christopher A. Bailey, Nicholas J. Diorio, Antal Jákli, Ralf Stannarius, and A. Nemes, 2009, "Acoustically Driven Oscillations of Freely Suspended Liquid Crystal Filaments," Soft Matter **5**, 3120–3126.

Planer, J., 1861, "Notiz Über Das Cholestearin," Annalen Der Chemie Und Pharmacie **118**, 25–27.

Planer, J., 2010, "Note about Cholesterol," Condens. Matter Phys. **13**, 37001.

Pociecha, Damian, Mojca Čepič, Ewa Gorecka, Jozef Mieczkowski, Ewa Gorecka, and Mojca Cepic, 2003, "Ferroelectric Mesophase with Randomized Interlayer Structure," Phys. Rev. Lett. **91**, 185501.

Pociecha, Damian, Nataša Vaupotič, Ewa Gorecka, Jozef Mieczkowski, Kinga Gomola, and Mojca Čepič, 2008, "2-D Density-Modulated Structures in Asymmetric Bent-Core Liquid Crystals," J. Mater. Chem. **18**, 881.

Querciagrossa, L., R. Berardi, and C. Zannoni, 2018, "Can Off-Centre Mesogen Dipoles Extend the Biaxial Nematic Range?" Soft Matter **14**, 2245–2253.

Radzihovsky, Leo, and Noel A. Clark, 2016, personal communication.

Ramos, A., N. G. Green, A. Castellanos, and H. Morgan, 1998, "Ac Electrokinetics: A Review of Forces in Microelectrode Structures," J. Phys. D **31**, 2338–2353.

Rauch, Sebastian, P. Bault, Hans Sawade, Gerd Heppke, Geetha G. Nair, and Antal Jákli, 2002, "Ferroelectric-Chiral–Antiferroelectric-Racemic Liquid Crystal Phase Transition of Bent-Shape Molecules," Phys. Rev. E **66**, 021706.

Rault, J., L. Liébert, and L. Strzelecki, 1975, "Sur La Synthèse de Quelques Mésogènes dimérisés," B. Soc. Chim. Fr. II Ch. **5**, 1175–1178.

Rayleigh, Lord, 1880, "On the Stability or Instability of Certain Fluid Motion," Proc. London Math. Soc. **10**, 57–82.

Reddy, R. Amaranatha, and B. K. Sadashiva, 2002, "Helical Superstructures in the Mesophase of Compounds Derived from 2-Cyanoresorcinol," Liq. Cryst. **29**, 1365–1367.

Reddy, R. Amaranatha, B. K. Sadashiva, and Ute Baumeister, 2005, "Liquid Crystalline Properties of Unsymmetrical Bent-Core Compounds Containing Chiral Moieties," J. Mater. Chem. **15**, 3303–3316.

Reddy, R. Amaranatha, *et al.*, 2011, "Spontaneous Ferroelectric Order in a Bent-Core Smectic Liquid Crystal of Fluid Orthorhombic Layers," Science **332**, 72–77.

Reinitzer, Friedrich, 1888, "Beiträge zur Kenntniss des Cholesterins," Monatshefte für Chemie und verwandte Teile anderer Wissenschaften **9**, 421–441.

Ribeiro de Almeida, R. R., Cuiyu Zhang, O. Parri, S. N. Sprunt, and A. Jákli, 2014, "Nanostructure and Dielectric Properties of a Twist-Bend Nematic Liquid Crystal Mixture," Liq. Cryst. **41**, 1661–1667.

Robinson, W. K., C. Carboni, P. Kloess, S. P. Perkins, and H. J. Coles, 1998, "Ferroelectric and Antiferroelectric Low Molar Mass Organosiloxane Liquid Crystals," Liq. Cryst. **25**, 301–307.

Robles-Hernández, Beatriz, Nerea Sebastián, M. Rosario de la Fuente, David O. López, Sergio Diez-Berart, Josep Salud, M. Blanca Ros, David A. Dunmur, Geoffrey R. Luckhurst, and Bakir A. Timimi, 2015, "Twist, Tilt, and Orientational Order at the Nematic to Twist-Bend Nematic Phase Transition of 1″, 9″-Bis (4-Cyanobiphenyl-4′-Yl) Nonane: A Dielectric, H 2 NMR, and Calorimetric Study," Phys. Rev. E **92**, 062505.

Robles-Hernández, Beatriz, Nerea Sebastián, Josep Salud, Sergio Diez-Berart, David A. Dunmur, Geoffrey R. Luckhurst, David O. López, and M. Rosario De La Fuente, 2016, "Molecular Dynamics of a Binary Mixture of Twist-Bend Nematic Liquid Crystal Dimers Studied by Dielectric Spectroscopy," Phys. Rev. E **93**, 062705.

Rosenblatt, Ch. S., R. Pindak, N. A. Clark, and R. B. Meyer, 1977, "The Parabolic Focal Conic?: A New Smectic a Defect," J. Phys. France **38**, 1105–1115.

Rudquist, P., *et al.*, 1999, "The Case of Thresholdless Antiferroelectricity: Polarization-Stabilized Twisted SmC* Liquid Crystals Give V-Shaped Electro-Optic Response," J. Mater. Chem. **9**, 1257–1261.

Ryu, Seong Ho, *et al.*, 2015, "Nucleation and Growth of a Helical Nanofilament (B4) Liquid-Crystal Phase Confined in Nanobowls," Soft Matter **11**, 7778–7782.

Sadashiva, B. K., and R. Amaranatha Reddy, 2003, "Occurrence of the B7 Mesophase in Two Homologous Series of Seven-Ring Achiral Compounds Composed of Banana-Shaped Molecules," Liq. Cryst. **30**, 273–283.

Sadashiva, B. K., R. Amaranatha Reddy, R. Pratibha, and N. V. Madhusudana, 2002, "Biaxial Smectic A Phase in Homologous Series of Compounds Composed of Highly Polar Unsymmetrically Substituted Bent-Core Molecules," J. Mater. Chem. **12**, 943–950.

Salamon, P., N. Eber, J. Seltmann, M. Lehmann, J. T Gleeson, S. Sprunt, and A. Jákli, 2012, "Dielectric Technique to Measure the Twist Elastic Constant of Liquid Crystals: The Case of a Bent-Core Material," Phys. Rev. E **85**, 061704.

Salamon, Péter, Nándor Éber, Ágnes Buka, James T. Gleeson, Samuel Sprunt, and Antal Jákli, 2010, "Dielectric Properties of Mixtures of a Bent-Core and a Calamitic Liquid Crystal," Phys. Rev. E **81**, 031711.

Salamończyk, Mirosław, Nataša Vaupotič, Damian Pociecha, Cheng Wang, Chenhui Zhu, and Ewa Gorecka, 2017, "Structure of Nanoscale-Pitch Helical Phases: Blue Phase and Twist-Bend Nematic Phase Resolved by Resonant Soft X-Ray Scattering," Soft Matter **13**, 6694–6699.

Salili, S. M., C. Kim, S. Sprunt, J. T. Gleeson, O. Parri, and Antal Jákli, 2014, "Flow Properties of a Twist-Bend Nematic Liquid Crystal," RSC Adv. **4**, 57419–57423.

Salili, S. M., T. Ostapenko, O. Kress, C. Bailey, W. Weissflog, K. Harth, A. Eremin, R. Stannarius, and A. Jákli, 2016, "Rupture and Recoil of Bent-Core Liquid Crystal Filaments," Soft Matter **12**, 4725–4730.

Salili, S. M., R. R. Ribeiro de Almeida, P. K. Challa, S. N. Sprunt, J. T. Gleeson, and A. Jakli, 2017, "Spontaneously Modulated Chiral Nematic Structures of Flexible Bent-Core Liquid Crystal Dimers," Liq. Cryst. **44**, 160–64.

Salili, S. M., M.-G. Tamba, S. N. Sprunt, C. Welch, G. H. Mehl, A. Jákli, and J. T. Gleeson, 2016, "Anomalous Increase in Nematic-Isotropic Transition Temperature in Dimer Molecules Induced by Magnetic Field," Phys. Rev. Lett. **116**, 217801.

Salili, S. M., J. Xiang, H. Wang, Q. Li, D. A. Paterson, C. T. Imrie, O. D. Lavrentovich, S. N. Sprunt, J. T. Gleeson, and A. Jakli, 2016, "Magnetically Tunable Selective Reflection of Light by Heliconical Cholesterics," Phys. Rev. E **94**, 042705.

Salter, P. S., C. Tschierske, S. J. Elston, and E. P. Raynes, 2011, "Flexoelectric Measurements of a Bent-Core Nematic Liquid Crystal," Phys. Rev. E **84**, 031708.

Santangelo, C., and Randall Kamien, 2003, "Bogomol'nyi, Prasad, and Sommerfield Configurations in Smectics," Phys. Rev. Lett. **91**, 045506.

Sasaki, Y., H. Nagayama, F. Araoka, and H. Yao, 2011, "Distinctive Thermal Behavior and Nanoscale Phase Separation in the Heterogeneous Liquid-Crystal B_{4}Matrix of Bent-Core Molecules," Phys. Rev. Lett. **107**, 237802.

Sasaki, Y., Y. Setoguchi, H. Nagayama, H. Yao, H. Takezoe, and K. Ema, 2011, "Calorimetric Studies on Isotropic-B4 Phase Transition in the Mixture of Bent-Shaped and Rod-like Molecules," Physica E (Amsterdam) **43**, Elsevier: 779–781.

Sathyanarayana, P., and Surajit Dhara, 2013, "Antagonistic Flexoelectric Response in Liquid Crystal Mixtures of Bent-Core and Rodlike Molecules," Phys. Rev. E **87**, 012506.

Sathyanarayana, P., M. Mathew, Q. Li, V. S. S. Sastry, B. Kundu, K. V. Le, H. Takezoe, and Surajit Dhara, 2010, "Splay Bend Elasticity of a Bent-Core Nematic Liquid Crystal," Phys. Rev. E **81**, 010702(R).

Sathyanarayana, P., V. S. R Jampani, M. Skarabot, I. Musevic, K. V. Le, H. Takezoe, and S. Dhara, 2012, "Viscoelasticity of Ambient-Temperature Nematic Binary Mixtures of Bent-Core and Rodlike Molecules," Phys. Rev. E **85**, 011702.

Sathyanarayana, Paladugu, Tatipamula Arun Kumar, Vanka Srinivasa Suryanarayana Sastry, Manoj Mathews, Quan Li, Hideo Takezoe, and Surajit Dhara, 2010, "Rotational Viscosity of a Bent-Core Nematic Liquid Crystal," Appl. Phys. Express **3**, 091702.

Scharf, Toralf, 2007, *Polarized Light in Liquid Crystals and Polymers* (John Wiley & Sons, Hoboken, NJ).

Sebastián, N., B. Robles-Hernández, S. Diez-Berart, J. Salud, G. R. Luckhurst, D. A. Dunmur, D. O. López, and M. R. de la Fuente, 2017, "Distinctive Dielectric Properties of Nematic Liquid Crystal Dimers," Liq. Cryst. **44**, 177–190.

Sebastián, Nerea, David Orencio López, Beatriz Robles-Hernández, María Rosario de la Fuente, Josep Salud, Miguel Angel Pérez-Jubindo, David A. Dunmur, Geoffrey R. Luckhurst, and D. J. B. Jackson, 2014, "Dielectric, Calorimetric and Mesophase Properties of 1″-(2′, 4-Difluorobiphenyl-4′-Yloxy)-9″-(4-Cyanobiphenyl-4′-Yloxy) Nonane: An Odd Liquid Crystal Dimer with a Monotropic Mesophase Having the Characteristics of a Twist-Bend Nematic Phase," Phys. Chem. Chem. Phys. **16**, 21391–21406.

Sebastián, Nerea, *et al.*, 2016, "Mesophase Structure and Behaviour in Bulk and Restricted Geometry of a Dimeric Compound Exhibiting a Nematic-Nematic Transition," Phys. Chem. Chem. Phys. **18**, 19299–19307.

Sekine, Tomoko, Teruki Niori, Masato Sone, Junji Watanabe, Suk-Won Choi, Yoichi Takanishi, and Hideo Takezoe, 1997, "Origin of Helix in Achiral Banana-Shaped Molecular Systems," Jpn. J. Appl. Phys. **36**, 6455–6463.

Sekine, Tomoko, Yoichi Takanishi, Teruki Niori, Junji Watanabe, and Hideo Takezoe, 1997, "Ferroelectric Properties in Banana-Shaped Achiral Liquid Crystalline Molecular Systems," Jpn. J. Appl. Phys. **36**, L1201–L1203.

Selinger, Jonathan V., 2003, "Chiral and Antichiral Order in Bent-Core Liquid Crystals," Phys. Rev. Lett. **90**, 165501.

Selinger, Jonathan V., Zhen-Gang Wang, Robijn F. Bruinsma, and Charles M. Knobler, 1993, "Chiral Symmetry Breaking in Langmuir Monolayers and Smectic Films," Phys. Rev. Lett. **70**, 1139–1142.

Seltmann, Jens, Alberto Marini, Benedetta Mennucci, Sonal Dey, Satyendra Kumar, and Matthias Lehmann, 2011, "Nonsymmetric Bent-Core Liquid Crystals Based on a 1, 3, 4-Thiadiazole Core Unit and Their Nematic Mesomorphism," Chem. Mater. **23**, 2630–2636.

Senyuk, B., Y.-K. Kim, L. Tortora, S.-T. Shin, S. V. Shiyanovskii, and O. D. Lavrentovich, 2011, "Surface Alignment, Anchoring Transitions, Optical Properties and Topological Defects in Nematic Bent-Core Materials C7 and C12," Mol. Cryst. Liq. Cryst. **540**, 20–41.

Senyuk, B., Hugh Wonderly, Manoj Mathews, Quan Li, S. Shiyanovskii, and Oleg Lavrentovich, 2010, "Surface Alignment, Anchoring Transitions, Optical Properties, and Topological Defects in the Nematic Phase of Thermotropic Bent-Core Liquid Crystal A131," Phys. Rev. E **82**, 041711.

Senyuk, B. I., I. I. Smalyukh, and O. D. Lavrentovich, 2006, "Undulations of Lamellar Liquid Crystals in Cells with Finite Surface Anchoring near and Well above the Threshold," Phys. Rev. E **74**, 011712.

Šepelj, Maja, Andreja Lesac, Ute Baumeister, Siegmar Diele, H. Loc Nguyen, and Duncan W. Bruce, 2007, "Intercalated Liquid-Crystalline Phases Formed by Symmetric Dimers with an α, ω-Diiminoalkylene Spacer," J. Mater. Chem. **17**, 1154–1165.

Shamid, Shaikh M., David W. Allender, and Jonathan V. Selinger, 2014, "Predicting a Polar Analog of Chiral Blue Phases in Liquid Crystals," Phys. Rev. Lett. **113**, 237801.

Shamid, Shaikh M., Subas Dhakal, and Jonathan V. Selinger, 2013, "Statistical Mechanics of Bend Flexoelectricity and the Twist-Bend Phase in Bent-Core Liquid Crystals," Phys. Rev. E **87**, 052503.

Shankar, Rao, Doddamane S., Geetha G. Nair, S. Krishna Prasad, S. Anita Nagamani, and C. V. Yelamaggad, 2001, "Experimental Studies on the B7 Phase of a Banana-Shaped Achiral Mesogen," Liq. Cryst. **28**, 1239–1243.

Shanker, G., M. Prehm, M. Nagaraj, J. K. Vij, and Cartsen Tschierske, 2011, "Development of Polar Order in a Bent-Core Liquid Crystal with a New Sequence of Two Orthogonal Smectic and an Adjacent Nematic Phase," J. Mater. Chem. **21**, 18711–18714.

Shanker, Govindaswamy, Marko Prehm, Mamatha Nagaraj, Jagdish K. Vij, Marvin Weyland, Alexey Eremin, and Carsten Tschierske, 2014, "1, 2, 4-Oxadiazole-Based Bent-Core Liquid Crystals With Cybotactic Nematic Phases," ChemPhysChem **15**, 1323–1335.

Sharma, Vivek, Matija Crne, Jung Ok Park, and Mohan Srinivasarao, 2009, "Structural Origin of Circularly Polarized," Science **325**, 449–452.

Shen, Yongqiang, Tao Gong, Renfan Shao, Eva Körblova, Joseph E. Maclennan, David M. Walba, and Noel A. Clark, 2011, "Effective Conductivity Due to Continuous Polarization Reorientation in Fluid Ferroelectrics," Phys. Rev. E **84**, 020701.

Shimbo, Yoshio, Ewa Gorecka, Damian Pociecha, Fumito Araoka, Masanao Goto, Yoichi Takanishi, Ken Ishikawa, Jozef Mieczkowski, Kinga Gomola, and Hideo Takezoe, 2006, "Electric-Field-Induced Polar Biaxial Order in a Nontilted Smectic Phase of an Asymmetric Bent-Core Liquid Crystal," Phys. Rev. Lett. **97**, 113901.

Shimbo, Yoshio, Yoichi Takanishi, Ken Ishikawa, Ewa Gorecka, Damian Pociecha, Jozef Mieczkowski, Kinga Gomola, and Hideo Takezoe, 2006, "Ideal Liquid Crystal Display Mode Using Achiral Banana-Shaped Liquid Crystals," Jpn. J. Appl. Phys. **45**, L282–284.

Shreenivasa, Murthy H. N., and B. K. Sadashiva, 2002, "Banana-Shaped Mesogens: Effect of Lateral Substituents on Seven-Ring Esters Containing a Biphenyl Moiety," Liq. Cryst. **29**, 1223–1234.

Shreenivasa, Murthy H. N., and B. K. Sadashiva, 2003a, "Observation of a Transition from Non-Switchable B7 Mesophase to an Antiferroelectric Sub-Phase in Strongly Polar Bent-Core Compounds," J. Mater. Chem. **13**, 2863–2869.

Shreenivasa, Murthy H. N., and B. K. Sadashiva, 2003b, "Banana-Shaped Mesogens: A New Homologous Series of Compounds Exhibiting the B7 Mesophase," Liq. Cryst. **30**, 1051–1055.

Silvestri, Regan L., and Jack L. Koenig, 1994, "Spectroscopic Characterization of Trans-Gauche Isomerization in Liquid Crystal Polymers with t w o Nematic States," Polymer **35**, 2528–2537.

Simpson, Frank P., Richard J. Mandle, John N. Moore, and John W. Goodby, 2017, "Investigating the Cusp between the Nano- and Macro-Sciences in Supermolecular Liquid-Crystalline Twist-Bend Nematogens," J. Mater. Chem. C **5**, 5102–5110.

Smalyukh, I. I., and O. D. Lavrentovich, 2002, "Three-Dimensional Director Structures of Defects in Grandjean-Cano Wedges of Cholesteric Liquid Crystals Studied by Fluorescence Confocal Polarizing Microscopy," Phys. Rev. E **66**, 051703.

Smalyukh, I. I., O. D. Lavrentovich, A. N. Kuzmin, A. V. Kachynski, and P. N. Prasad, 2005, "Elasticity-Mediated Self-Organization and Colloidal Interactions of Solid Spheres with Tangential Anchoring in a Nematic Liquid Crystal," Phys. Rev. Lett. **95**, 157801.

Smith, A. A. T., C. V. Brown, and N. J. Mottram, 2007, "Theoretical Analysis of the Magnetic Freedericksz Transition in the Presence of Flexoelectricity and Ionic Contamination," Phys. Rev. E **75**, 041704.

Sonin, A. A., 1998, *Freely Suspended Liquid Crystalline Films* (John Wiley & Sons, Inc., New York), 1st ed.

Srigengan, S., M. Nagaraj, A. Ferrarini, R. Mandle, S. J. Cowling, M. A. Osipov, G. Pająk, J. W. Goodby, and H. F. Gleeson, 2018, "Anomalously Low Twist and Bend Elastic Constants in an Oxadiazole-Based Bent-Core Nematic Liquid Crystal and Its Mixtures; Contributions of Spontaneous Chirality and Polarity," J. Mater. Chem. C **6**, 980–988.

Srinivasarao, Mohan, 1999, "Nano-Optics in the Biological World: Beetles, Butterflies, Birds, and Moths," Chem. Rev. **99**, 1935–1962.

Srivastava, Anoop Kumar, Jongyoon Kim, Sunggu Yeo, Jinyoung Jeong, E-Joon Choi, Vijay Singh, and Ji-Hoon Lee, 2017, "Anomalously High Dielectric Strength and Low Frequency Dielectric Relaxation of a Bent-Core Liquid Crystal with a Large Kink Angle," Curr. Appl. Phys. **17**, 858–863.

Stannarius, Ralf, Alexey Eremin, Kirsten Harth, Michael Morys, Andrew DeMiglio, Christian Ohm, and Rudolf Zentel, 2012, "Mechanical and Optical Properties of Continuously Spun Fibres of a Main-Chain Smectic A Elastomer," Soft Matter **8**, 1858.

Stannarius, Ralf, Alexey Eremin, M.-G. Tamba, Gerhard Pelzl, and Wolfgang Weissflog, 2007, "Field-Induced Texture Transitions in a Bent-Core Nematic Liquid Crystal," Phys. Rev. E **76**, 061704.

Stannarius, Ralf, Christian Langer, and Wolfgang Weissflog, 2002, "Electro-Optic Study of Antiferroelectric Freely Suspended Films of Bent-Core Mesogens in the B2 Phase," Phys. Rev. E **66**, 031709.

Stannarius, Ralf, Jianjun Li, and Wolfgang Weissflog, 2003, "Ferroelectric Smectic Phase Formed by Achiral Straight Core Mesogens," Phys. Rev. Lett. **90**, 025502.

Stannarius, Ralf, Alexandru Nemeş, and Alexey Eremin, 2005, "Plucking a Liquid Chord: Mechanical Response of a Liquid Crystal Filament," Phys. Rev. E **72**, 020702.

Stern, Stephan, 2009, "Polare Ordnung in Smektischen Phasen Gewinkelter Mesogene: Elektro-Optische Und Nichtlinear-Optische Untersuchungen," Otto-von-Guericke University Magdeburg.

Stern, Stephan, Ralf Stannarius, Alexey Eremin, and Wolfgang Weissflog, 2009, "A Model for a Field-Induced Ferrielectric State in a Bent-Core Mesogen," Soft Matter **5**, 4136–4140.

Stevenson, W. D., *et al.*, 2017, "Molecular Organization in the Twist–Bend Nematic Phase by Resonant X-Ray Scattering at the Se K-Edge and by SAXS, WAXS and GIXRD," Phys. Chem. Chem. Phys. **19**, 13449–13454.

Stevenson, Warren D., Jianggen An, Xiang-bing Zeng, Min Xue, Heng-xing Zou, Yong-song Liu, and Goran Ungar, 2018, "Twist-Bend Nematic Phase in Biphenylethane-Based Copolyethers," Soft Matter **14**, 3003.

Stocchero, M., A. Ferrarini, G. J. Moro, D. A. Dunmur, and G. R. Luckhurst, 2004, "Molecular Theory of Dielectric Relaxation in Nematic Dimers," J. Chem. Phys. **121**, 8079.

Stojadinovic, Strahinja, Anthony Adorjan, Samuel N. Sprunt, Hans Sawade, and Antal Jákli, 2002, "Dynamics of the Nematic Phase of a Bent-Core Liquid Crystal," Phys. Rev. E **66**, 060701.

Szydlowska, Jadwiga, *et al.*, 2003, "Bent-Core Liquid Crystals Forming Two- and Three-Dimensional Modulated Structures," Phys. Rev. E **67**, 031702.

Tadapatri, Pramod, Uma S. Hiremath, C. V. Yelamaggad, and K. S. Krishnamurthy, 2010a, "Patterned Electroconvective States in a Bent-Core Nematic Liquid Crystal," J. Phys. Chem. B **114**, 10–21.

Tadapatri, Pramod, Uma S. Hiremath, C. V. Yelamaggad, and K. S. Krishnamurthy, 2010b, "Permittivity, Conductivity, Elasticity, and Viscosity Measurements in the Nematic Phase of a Bent-Core Liquid Crystal," J. Phys. Chem. B **114**, 1745–1750.

Tadapatri, Pramod, K. Krishnamurthy, and W. Weissflog, 2010, "Multiple Electroconvection Scenarios in a Bent-Core Nematic Liquid Crystal," Phys. Rev. E **82**, 031706.

Takanishi, Yoichi, Tatsuya Izumi, Junji Watanabe, Ken Ishikawa, Hideo Takezoe, and Atsuo Iida, 1999, "Field-Induced Molecular Reorientation Keeping a Frustrated Structure in an Achiral Bent-Shaped Liquid Crystal," J. Mater. Chem. **9**, 2771–2774.

Takanishi, Yoichi, Gyo Jic Shin, Jin Chul Jung, Suk-Won W. Choi, Ken Ishikawa, Junji Watanabe, Hideo Takezoe, and Pierre Toledano, 2005, "Observation of Very Large Chiral Domains in a Liquid Crystal Phase Formed by Mixtures of Achiral Bent-Core and Rod Molecules," J. Mater. Chem. **15**, 4020–4024.

Takezoe, H., K. Kishikawa, and E. Gorecka, 2006, "Switchable Columnar Phases," J. Mater. Chem. **16**, 2412–2416.

Takezoe, Hideo, and Alexey Eremin, 2017, *Bent-Shaped Liquid Crystals—Structures and Physical Properties* (Taylor & Francis, Boca Raton), 1st ed.

Takezoe, Hideo, and Yoichi Takanishi, 2006, "Bent-Core Liquid Crystals: Their Mysterious and Attractive World," Jpn. J. Appl. Phys. **45**, 597–625.

Tamba, M. G., S. M. Salili, C. Zhang, A. Jakli, G. H. Mehl, R. Stannarius, and A. Eremin, 2015, "A Fibre Forming Smectic Twist–Bent Liquid Crystalline Phase," RSC Adv. **5**, 11207–11211.

Tanaka, Shingo, Hideo Takezoe, Nandor Eber, Katalin Fodor-Csorba, Aniko Vajda, and Agnes Buka, 2009, "Electroconvection in Nematic Mixtures of Bent-Core and Calamitic Molecules," Phys. Rev. E **80**, 021702.

Taushanoff, Stefanie, Khoa Van Le, Jarrod Williams, Robert J. Twieg, B. K. Sadashiva, Hideo Takezoe, and Antal Jákli, 2010, "Stable Amorphous Blue Phase of Bent-Core Nematic Liquid Crystals Doped with a Chiral Material," J. Mater. Chem. **20**, 5893.

Terentjev, Eugene, and Rolfe G. Petschek, 1993, "Properties of Uniaxial Nematic Liquid Crystal of Semiflexible Even and Odd Dimers," J. Phys. II (France) **3**, 661–680.

Thisayukta, Jirakorn, Hiroko Niwano, Hideo Takezoe, and Junji Watanabe, 2002, "Enhancement of Twisting Power in the Chiral Nematic Phase by Introducing Achiral Banana-Shaped Molecules," J. Am. Chem. Soc. **124**, 3354–3358.

To, T. B. T., T. J. Sluckin, and G. R. Luckhurst, 2013, "Biaxiality-Induced Magnetic Field Effects in Bent-Core Nematics: Molecular-Field and Landau Theory," Phys. Rev. E **88**, 062506.

Toulouse, G., 1977, "For Biaxial Nematics," J. Phys. Lett. **38**, L67–68.

Toulouse, G., and M. Kleman, 1976, "Principles of a Classification of Defects in Ordered Media," J. Phys. (Orsay, Fr.) **37**, L149–151.

Trbojevic, Nina, Daniel J. Read, and Mamatha Nagaraj, 2017, "Dielectric Properties of Liquid Crystalline Dimer Mixtures Exhibiting the Nematic and Twist-Bend Nematic Phases," Phys. Rev. E **96**, 052703.

Tsai, Ethan, Jacqueline M. Richardson, Eva Korblova, Michi Nakata, Dong Chen, Yongqiang Shen, Renfan Shao, Noel A. Clark, and David M. Walba, 2013, "A Modulated Helical Nanofilament Phase," Angew. Chem. **52**, 5254–5257.

Tuchband, Michael R., *et al.*, 2017, "Double-Helical Tiled Chain Structure of the Twist-Bend Liquid Crystal Phase in CB7CB," arXiv:1703.10787v1.

Umadevi, S., Antal Jákli, and B. K. Sadashiva, 2006a, "Bistable Linear Electro-Optical Switching in the $B7'$ Phase of Novel Bent-Core Molecules," Soft Matter **2**, 215.

Umadevi, S., Antal Jákli, and B. K. Sadashiva, 2006b, "Odd-Even Effects in Bent-Core Compounds Containing Terminal n-Alkyl Carboxylate Groups," Soft Matter **2**, 875.

Umadevi, S., and B. K. Sadashiva, 2005, "New Five-Ring Symmetrical Bent-Core Mesogens Exhibiting the Fascinating B7 Phase," Liq. Cryst. **32**, 1233–1241.

Ungar, G., V. Percec, and M. Zuber, 1992, "Liquid Crystalline Polyethers Based on Conformational Isomerism. 20. Nematic-Nematic Transition in Polyethers and Copolyethers Based on 1-(4-Hydroxyphenyl)2-(2-R-4-Hydroxyphenyl)Ethane with $R =$ Fluoro, Chloro and Methyl and Flexible Spacers Containing An," Macromolecules **25**, 75–80.

Van Le, K., *et al.*, 2011, "Liquid crystalline amorphous blue phase and its large electrooptical Kerr effect," J. Mater. Chem. **21**, 2855.

Van Le, Khoa, Fumito Araoka, Katalin Fodor-Csorba, Ken Ishikawa, and Hideo Takezoe, 2009, "Flexoelectric Effect in a Bent-Core Mesogen," Liq. Cryst. **36**, 1119–1124.

Van Le, Khoa, Manoj Mathews, Martin Chambers, John Harden, Quan Li, Hideo Takezoe, and Antal Jákli, 2009, "Electro-Optic Technique to Study Biaxiality of Liquid Crystals with Positive Dielectric Anisotropy: The Case of a Bent-Core Material," Phys. Rev. E **79**, 030701(R).

Van Winkle, D. H., and N. A. Clark, 1982, "Freely Suspended Strands of Tilted Columnar Liquid Crystal Phases: One Dimensional Nematics with Orientational Jumps," Phys. Rev. Lett. **48**, 1407–1410.

Varanytsia, Andrii, and Liang-Chy Chien, 2017, "Giant Flexoelectro-Optic Effect with Liquid Crystal Dimer CB7CB," Sci. Rep. **7**, 41333.

Vaupotič, N., J. Szydlowska, M. Salamonczyk, A. Kovarova, J. Svoboda, M. Osipov, D. Pociecha, and E. Gorecka, 2009, "Structure Studies of the Nematic Phase Formed by Bent-Core Molecules," Phys. Rev. E **80**, 030701.

Vaupotič, Nataša, and Martin Čopič, 2005, "Polarization Modulation Instability in Liquid Crystals with Spontaneous Chiral Symmetry Breaking," Phys. Rev. E **72**, 031701.

Vaupotič, Nataša, Martin Čopič, Ewa Gorecka, and Damian Pociecha, 2007, "Modulated Structures in Bent-Core Liquid Crystals: Two Faces of One Phase," Phys. Rev. Lett. **98**, 247802.

Vaupotič, Nataša, Damian Pociecha, Mojca Čepič, Kinga Gomola, Jozef Mieczkowski, and Ewa Gorecka, 2009, "Evidence for General Tilt Columnar Liquid Crystalline Phase," Soft Matter **5**, 2281.

Vertogen, G., and W. H. de Jeu, 1988, *Thermotropic Liquid Crystals, Fundamentals* (Springer-Verlag, Berlin).

Volovik, G. E., and O. D. Lavrentovich, 1983, "Topological Dynamics of Defects: Boojums in Nematic Drops," Sov. Phys. JETP **58**, 1159–1166.

Volovik, G. E., and V. P. Mineyev, 1977, "Investigation of Singularities in Superfluid He-3 and Liquid-Crystals by Homotopic Topology Methods," Zh. Eksp. Teor. Fiz. **72**, 2256–2274.

Vorländer, D., 1927, "Über die Natur der Kohlenstoffketten in kristallin-flüssigen Substanzen," Z. Phys. Chem. **126U**, 126–449.

Vorländer, D., 1929, "Die Richtung der Kohlenstoff-Valenzen in Benzol-Abkommlingen," Ber. Dtsch. Chem. Ges. B **62**, 2831.

Vorländer, D., and A. Apel, 1932, "Die Richtung der Kohlenstoff-Valenzen in Benzolabkömmlingen (II)," Ber. Dtsch. Chem. Ges. B **65**, 1101.

Vukusic, Pete, and J. Roy Sambles, 2003, "Photonic Structures in Aquatic Systems," Nature (London) **424**, 852.

Wahlstrom, E. E., 1969, *Optical Crystallography* (Wiley, New York).

Walba, David M., Eva Körblova, Renfan Shao, Joseph E. Maclennan, Darren R. Link, Matthew A. Glaser, Noel A. Clark, and Eva Korblova., 2000, "A Ferroelectric Liquid Crystal Conglomerate Composed of Racemic Molecules," Science **288**, 2181–2184.

Wang, Junren, Leah Bergquist, Jung Im Hwang, Kyeong Jin Kim, Joun Ho Lee, Torsten Hegmann, and Antal Jákli, 2018, "Wide Temperature-Range, Multi-Component, Optically Isotropic Antiferroelectric Bent-Core Liquid Crystal Mixtures for Display Applications," Liq. Cryst. **45**, 333.

Wang, Junren, Antal Jákli, Yu Guan, Shaohai Fu, and John West, 2017, "Developing Liquid-Crystal Functionalized Fabrics for Wearable Sensors," Information Display **33**, 16–20.

Wang, Yuan, Gautam Singh, Dena M. Agra-Kooijman, Min Gao, Hari Krishna Bisoyi, Chenming Xue, Michael R. Fisch, Satyendra Kumar, and Quan Li, 2015, "Room Temperature Heliconical Twist-Bend Nematic Liquid Crystal," CrystEngComm **17**, 2778–2782.

Watanabe, Junji, Teruki Niori, Tomoko Sekine, and Hideo Takezoe, 1998, "Frustrated Structure Induced on Ferroelectric Smectic Phases in Banana-Shaped Molecular System," Jpn. J. Appl. Phys. **37**, L139.

Weissflog, Wolfgang, Heinz Dehne, Banani Das, Siegbert Grande, Martin W. Schroder, Alexey Eremin, Siegmar Diele, Gerhard Pelzl, Siegmar Sokolowski, and Horst Kresse, 2004, "Chiral Ordering in the Nematic and an Optically Isotropic Mesophase of Bent-Core Mesogens with a Halogen Substituent at the Central Core," Liq. Cryst. **31**, 923–933.

Weissflog, Wolfgang, Ulrike Dunemann, Martin W. Schroder, Siegmar Diele, Gerhard Pelzl, Horst Kresse, and Siegbert Grande, 2005, "Field-Induced Inversion of Chirality in SmCPA Phases of New Achiral Bent-Core Mesogens," J. Mater. Chem. **15**, 939–946.

Weissflog, Wolfgang, Christiane Lischka, I. Benne, T. Scharf, Gerhard Pelzl, Siegmar Diele, and H. Kruth, 1998, "New Banana-Shaped Mesogens," Proc. SPIE Int. Soc. Opt. Eng., **3319**, 14.

White, Timothy J., Michael E. McConney, and Timothy J. Bunning, 2010, "Dynamic Color in Stimuli-Responsive Cholesteric Liquid Crystals," J. Mater. Chem. **20**, 9832.

Wiant, D., and James T. Gleeson, Nandor Eber, Katalin Fodor-Csorba, Antal Jákli, and T. Toth-Katona, 2005, "Nonstandard Electroconvection in a Bent-Core Nematic Liquid Crystal," Phys. Rev. E **72**, 041712.

Wild, Janine H., Kevin Bartle, Nicola T. Kirkman, Stephen M. Kelly, Mary O'Neill, Tom Stirner, and Rachel P. Tuffin, 2005, "Synthesis and Investigation of Nematic Liquid Crystals with Flexoelectric Properties," Chem. Mater. **17**, 6354–6360.

Williams, Richard, 1963, "Domains in Liquid Crystals," J. Chem. Phys. **39**, 384–388.

Xiang, Jie, Yannian Li, Quan Li, Daniel A. Paterson, John M. D. Storey, Corrie T. Imrie, and Oleg D. Lavrentovich, 2015, "Electrically Tunable Selective Reflection of Light from Ultraviolet to Visible and Infrared by Heliconical Cholesterics," Adv. Mater. **27**, 3014–3018.

Xiang, Jie, Sergij V. Shiyanovskii, Corrie Imrie, and Oleg D. Lavrentovich, 2014, "Electrooptic Response of Chiral Nematic Liquid Crystals with Oblique Helicoidal Director," Phys. Rev. Lett. **112**, 217801.

Xiang, Jie, Andrii Varanytsia, Fred Minkowski, Daniel A. Paterson, John M. D. Storey, Corrie T. Imrie, Oleg D. Lavrentovich, and Peter Palffy-Muhoray, 2016, "Electrically Tunable Laser Based on Oblique Heliconical Cholesteric Liquid Crystal," Proc. Natl. Acad. Sci. U.S.A. **113**, 12925–12928.

Xiang, Ying, J. W. Goodby, V. Görtz, and H. F. Gleeson, 2009, "Revealing the Uniaxial to Biaxial Nematic Liquid Crystal Phase Transition via Distinctive Electroconvection," Appl. Phys. Lett. **94**, 193507.

Xu, Jianling, Robin L. B. Selinger, Jonathan V. Selinger, and R. Shashidhar, 2001, "Monte Carlo Simulation of Liquid-Crystal Alignment and Chiral Symmetry-Breaking," J. Chem. Phys. **115**, 4333.

Yao, Minwu, Stephen H. Spiegelberg, and Gareth H. McKinley, 2000, "Dynamics of Weakly Strain-Hardening Fluids in Filament Stretching Devices," J. Non-Newtonian Fluid Mech. **89**, 1–43.

Yelamaggad, Channabasaveshwar V., Indudhara Swamy Shashikala, Guangxun Liao, Doddamane S. Shankar Rao, Subbarao Krishna Prasad, Quan Li, and Antal Jakli, 2006, "Blue Phase, Smectic Fluids, and Unprecedented Sequences in Liquid Crystal Dimers," Chem. Mater. **18**, 6100–6102.

Yoon, HyungGuen, Shin-Woong Kang, Matthias Lehmann, Jung Ok Park, Mohan Srinivasarao, and Satyendra Kumar, 2011, "Homogeneous and Homeotropic Alignment of Bent-Core Uniaxial and Biaxial Nematic Liquid Crystals," Soft Matter **7**, 8770.

You, Ra, Daniel A. Paterson, John M. D. Storey, Corrie T. Imrie, and Dong Ki Yoon, 2017, "Formation of Periodic Zigzag Patterns in the Twist- Bend Nematic Liquid Crystal Phase by Surface Treatment," Liq. Cryst. **44**, 168–176.

Young, C. Y., R. Pindak, N. A. Clark, and Robert B. Meyer, 1978, "Light Scattering Study of Two-Dimensionalmolecular Orientation

Fluctuations in a Freely Suspended Ferroelectric Liquid Crystal Film," Phys. Rev. Lett. **40**, 773.

Yu, L. J., and Alfred Saupe, 1980, "Observation of a Biaxial Nematic Phase in Potassium Laurate-1-Decanol-Water Mixtures," Phys. Rev. Lett. **45**, 1000–1004.

Yu, Meina, Xiaochen Zhou, Jinghua Jiang, Huai Yang, and Deng-Ke Yang, 2016, "Matched Elastic Constants for a Perfect Helical Planar State and a Fast Switching Time in Chiral Nematic Liquid Crystals," Soft Matter **12**, 4483–4488.

Yun, Chang-Jun Jun, M. R. Vengatesan, Jagdish K. Vij, and Jang-Kun Kun Song, 2015, "Hierarchical Elasticity of Bimesogenic Liquid Crystals with Twist-Bend Nematic Phase," Appl. Phys. Lett. **106**, 173102.

Zhang, C., N. Diorio, O. D. Lavrentovich, and A. Jákli, 2014, "Helical Nanofilaments of Bent-Core Liquid Crystals with a Second Twist," Nat. Commun. **5**, 3302.

Zhang, C., B. K. Sadashiva, O. D. Lavrentovich, and A. Jákli, 2013, "Cryo-TEM Studies of Two Smectic Phases of an Asymmetric Bent-Core Material," Liq. Cryst. **40**, 1636–1645.

Zhang, Cuiyu, Nicholas Diorio, S. Radhika, B. K. K. Sadashiva, Samuel N. Sprunt, and Antal Jákli, 2012, "Two Distinct Modulated Layer Structures of an Asymmetric Bent-Shape Smectic Liquid Crystal," Liq. Cryst. **39**, Taylor & Francis: 1149–57.

Zhang, Cuiyu, Min Gao, Nicholas J. Diorio, Wolfgang Weissflog, Ute Baumeister, Samuel N. Sprunt, James T. Gleeson, and Antal Jákli, 2012, "Direct Observation of Smectic Layers in Thermotropic Liquid Crystals," Phys. Rev. Lett. **109**, 107802.

Zhang, Yongqiang, Ute Baumeister, Carsten Tschierske, Michael J. O'Callaghan, and Christopher Walker, 2010, "Achiral Bent-Core Molecules with a Series of Linear or Branched Carbosilane Termini: Dark Conglomerate Phases, Supramolecular Chirality and Macroscopic Polar Order," Chem. Mater. **22**, 2869–2884.

Zhu, Chenhui, Dong Chen, Yongqiang Shen, Christopher D. Jones, Matthew A. Glaser, Joseph E. Maclennan, and Noel A. Clark, 2010, "Nanophase Segregation in Binary Mixtures of a Bent-Core and a Rodlike Liquid-Crystal Molecule," Phys. Rev. E **81**, 011704.

Zhu, Chenhui, Michael R. Tuchband, Anthony Young, Min Shuai, Alyssa Scarbrough, David M. Walba, Joseph E. Maclennan, Cheng Wang, Alexander Hexemer, and Noel A. Clark, 2016, "Resonant Carbon K-Edge Soft X-Ray Scattering from Lattice-Free Heliconical Molecular Ordering: Soft Dilative Elasticity of the Twist-Bend Liquid Crystal Phase," Phys. Rev. Lett. **116**, 147803.

Zhu, Chenhui, *et al.*, 2012, "Topological Ferroelectric Bistability in a Polarization-Modulated Orthogonal Smectic Liquid Crystal," J. Am. Chem. Soc. **134**, 9681–9687.